EXPERIMENTAL AND NUMERICAL STUDY OF SOLUTE TRANSPORT THROUGH SATURATED FRACTURED POROUS AQUIFER

NELSON AMOAH

INFORMATION TO USERS

This manuscript has been reproduced from the microfilm master. UMI films the text directly from the original or copy submitted. Thus, some thesis and dissertation copies are in typewriter face, while others may be from any type of computer printer.

The quality of this reproduction is dependent upon the quality of the copy submitted. Broken or indistinct print, colored or poor quality illustrations and photographs, print bleedthrough, substandard margins, and improper alignment can adversely affect reproduction.

In the unlikely event that the author did not send UMI a complete manuscript and there are missing pages, these will be noted. Also, if unauthorized copyright material had to be removed, a note will indicate the deletion.

Oversize materials (e.g., maps, drawings, charts) are reproduced by sectioning the original, beginning at the upper left-hand corner and continuing from left to right in equal sections with small overlaps. Each original is also photographed in one exposure and is included in reduced form at the back of the book.

Photographs included in the original manuscript have been reproduced xerographically in this copy. Higher quality 6" x 9" black and white photographic prints are available for any photographs or illustrations appearing in this copy for an additional charge. Contact UMI directly to order.

UMI

EXPERIMENTAL AND NUMERICAL STUDY OF

SOLUTE TRANSPORT THROUGH SATURATED

FRACTURED POROUS AQUIFER

By

NELSON AMOAH, B.Sc. (Hons), M.Eng.

A thesis submitted to the School of Graduate

Studies in partial fulfilment of the

requirements for the degree of

Doctor of Philosophy

Faculty of Engineering and Applied Science

Memorial University of Newfoundland

April 1997

St John's   **Newfoundland**   **Canada**

0-612-25764-9

Canadä

This thesis is dedicated to my

father (late Opanin Kwaku Adu)

mother (Madam Akua Afiriyie)

&

Wife and Children

Esther, Michael and Emmanuel

Abstract

The evaluation of groundwater pollution in different subsurface media has always been a challenging task. The knowledge required for the conceptual basis for analysis is often insufficient. Site specific data are usually not available. In fractured formations further difficulties arise since contaminant migration patterns are influenced in a complex way by the variability of fracture characteristics. In addition many numerical models have been found to be inefficient in handling the equations governing subsurface contaminant transport. This means that the investigator is confronted with several sources of uncertainties arising from both the input data and the numerical model itself.

This thesis presents a field experiment and numerical study of solute transport through a saturated fractured aquifer located in St. John's, Newfoundland, Canada. The aquifer at the test site consists of a thin glacial till overlying a fractured bedrock. The investigation comprised two parts. The first part involved several months of groundwater level monitoring, in situ tests for hydraulic conductivity and study of the groundwater chemistry. High spatial variability of hydraulic conductivity in the bedrock aquifer was observed. The second part involved two natural gradient tracer tests. Experimental results indicate that there is limited hydraulic communication between the overlying till and the fractured bedrock. Tracer migration patterns in the bedrock suggest a dense network of highly interconnected fractures which cannot be represented on individual scale. Tracer migration in the bedrock showed no evidence of flow channelling. The concentration distribution has been represented by breakthrough curves.

Knowledge from the field study has been used to develop an efficient numerical model for solute transport based on the advection-dispersion equation. The numerical model was based on the dual reciprocity boundary element method (DRBEM). A new approach in the application of this technique to a class of non-linear, nonhomogeneous equations has been proposed. Several numerical experiments to test the accuracy and efficiency of the

new model have been performed. Numerical results showed that the new approach improves the accuracy of the DRBEM. Good agreement was obtained between model results and the analytical solutions for several theoretical test problems. The ability of the DRBEM to handle the dual nature of the advection-dispersion equation was also recognized by achieving accurate results at high Peclet numbers. The efficiency of the DRBEM compared with other numerical solution techniques was also observed.

The DRBEM model was applied to a practical field situation by using the results from a tracer test. Numerically simulated breakthrough curves were compared with the experimental results obtained from the tracer test. Aquifer parameters optimized for a reasonable match between the numerically simulated and the experimental results have been estimated. Simulation results suggest that the advection-dispersion model is highly suitable for solute transport analysis in this aquifer. Sensitivity analysis has been performed by computing sensitivity coefficients for the various aquifer parameters. The field experiment and the numerical study have provided considerable insights into the processes controlling solute transport in this fractured aquifer.

Acknowledgements

v

I am sincerely grateful to my dear wife Esther and my two sons Michael and Emmanuel for all the efforts, encouragement and prayers they have put in to assist me in reaching this goal. The patience in tolerating an absentee husband and father was very instrumental for the success of this work. I also thank our families in Ghana for their prayers and encouragement.

Behind all these was the consistent spiritual support and nourishment provided by our Lord Jesus Christ through the brothers and sisters at Faith Bible Chapel, 43 Kenmount Road, St. John's. Their constant prayers, encouragement, and support were a great source of strength for the completion of my studies.

I must make a special mention of Gerry and Donna Stapleton and their entire family who have consistently supported and encouraged me and my family throughout my student life in St. John's.

I would also like to thank Dr Ranjith Liyanapathirana of the Univerrsity of Western Australia and Mr Michael Rokich (Consulting Architect) in Perth, Western Australia for their persistent encouragement throughout my graduate studies.

Finally I would like to thank many other graduate students in the Faculty of Engineering at Memorial University especially Mr Andrew Tomilson (my office mate) who helped me a great deal in arranging the figures.

Contents

List of Figures

xi

xii

List of Tables

List of Symbols

Λ	Aquifer thickness (L)
$|V|$	Average linear groundwater velocity (L/T)
ρ_b	Bulk density of soil (M/L^3)
Γ	Boundary of the domain
C_r	Courant number (dimensionless)
c_o	Concentration at input source (M/L^3)
c	Concentration distribution the global coordinate system (M/L^3)
c	Concentration distribution in the transformed coordinate system (M/L^3)
D_x	Dispersion coefficient in x-direction (L^2/T)
D_y	Dispersion coefficient in x-direction (L^2/T)
Ω	Domain
n_x , n_y	Direction cosines
Δ_i	Dirac delta function
ρ_w	Density of water (M/L^3)
K_d	Distribution coefficient (dimensionless)
ϵ	Effective porosity (dimensionless)
δ	Kronecker delta
w	Fracture width (L)
λ	First order decay constant (L^{-1})
c^*	Fundamental solution
x , y	Global Cartesian cordinates (L)
g	Gravitational acceleration (L/T^2)
K	Hydraulic conductivity (L/T)
i	Hydraulic gradient (dimensionless)
M	Injected solute mass (M)
α_L	Longitudinal dispersivity (L)
D_L	Longitudinal dispersion coefficient (L^2/T)

∇	Laplacian operator
c	Particular solution
P_e	Peclet number (dimensionless)
R	Retardation factor (dimensionless)
ξ	Size of fracture aperture (L)
S_s	Specific storage of aquifer (L^{-1})
v	Specific discharge or Darcy velocity (L/T)
M_o	Solute mass per unit aquifer thickness (M/L)
Δ_x	Spatial grid dimension in x-direction (L)
Δ_y	Spatial grid dimension in y-direction (L)
D_o	Solute free diffusion coefficient (L^2/T)
σ	Standard deviation
D_T	Transverse dispersion coefficient (L^2/T)
τ	Tortuosity factor of the soil medium (dimensionless)
t	Time (T)
D^*	Transport diffusion coefficient (L^2/T)
α_T	Transverse dispersivity (L)
x_l , y_l	Transformed Cartesian cordinates (L)
V_x	Velocity in x-direction (L/T)
V_y	Velocity in y-direction (L/T)
Q	Volumetric flow rate or fluid injection/withdrawal rate (L^3/T)
υ	Viscosity (poise)

Chapter 1

Introduction

1.1 Groundwater pollution

Potable water for human use is one of the most limited natural resources in our world today. It has been shown (Murray and Reeves 1977) that the oceans represent 97.2 % of the world's total water supply while 2.14 % is contained in ice caps and glaciers, groundwater to the depth of 400 meters account for 0.61 %, saline lakes, 0.008%, soil moisture, 0.005%, freshwater lakes, 0.009% and rivers, 0.0001 %. It follows that only a small quantity (approximately 0.62%) of the total water resources is available as potable water. Since about 98% of this fresh usable water is found underground, any activity that renders the groundwater unwholesome is a direct threat to the survival of mankind. Unfortunately pollution of groundwater resources owing to the migration of contaminants has become common in many countries. Over the years, poor waste disposal practices and the use of inefficient subsurface waste containment facilities have resulted in mass leakage of both domestic and industrial wastes, polluting the limited groundwater resources.

The concern over groundwater pollution has therefore attracted great attention in many countries during the past two decades. Intensive research has attempted to understand the behaviour of contaminants in different subsurface media. Physical investigations of groundwater contaminant transport have been carried out using laboratory and field methods to understand the conceptual basis of the problem. Although many influencing factors are still under debate, it can be said that the theories underlying solute transport in saturated porous media are quite well developed at the moment. Mathematical conceptualizations have also been proposed to describe the physical and chemical processes involved. In recent years the availability of computers has facilitated the mathematical simulation of the contaminant transport process. This has led to many solute transport codes in the literature based on analytical and numerical techniques commonly termed 'analytical and numerical models'.

1.2 Difficulties Involved in Groundwater Pollution Studies

The past two decades has witnessed a significant improvement in groundwater pollution studies in different subsurface media. However there are still many existing sites and needs which require detailed understanding of the groundwater hydrology and hydrogeology and their influence on contaminant transport processes. An increasing emphasis is also being placed on the use of predictive computer models in regulatory and

clean up activities but this requires more economical, accurate and robust groundwater numerical models. Many difficulties still exist in modelling subsurface solute transport but the major ones that are related to this work may be classified as:

● problem misconceptualization and limited availability of data

● inefficient and inaccurate numerical solution techniques

Groundwater pollution problems are site specific and therefore require a detailed understanding and reliable data pertaining to a given geological and geochemical setting. Such understanding is also a basic requirement for determining the type of theoretical concept applicable for the use of a numerical model. However such information is usually not available. In the few cases where field data are available, some have been obtained by earlier studies for different purposes. Beljin (1988) observed that such data are usually subject to inaccuracies, interpretive bias, and loss of information. As a result of a lack of carefully obtained field data, current numerical modelling test procedures usually involve the verification with analytical solutions and code inter-comparison.

An illustration of data shortage can be given by examining subsurface contaminant transport mechanisms in the aquifers found in the province of Newfoundland. On many sites the geological structure consists of a thin compact glacial till overlying fractured bedrock (Figure 1) A surface impoundment in the till could be a potential source of contamination if leakage occurs. Depending on the hydraulic communication between the overlying glacial till and the bedrock, contaminant plume may form in the till and in the

bedrock or somewhere between these two layers. The contribution of the thin overlying till and the effects of the fractured bedrock on the down-gradient migration of solutes has not been investigated by field experiments. To date no specific conceptual basis has been proposed for solute transport analysis. No quantitative values of aquifer solute transport parameters have been determined even though reports of groundwater contamination have been published in the literature (Dominie 1992, Guzzwell 1996).
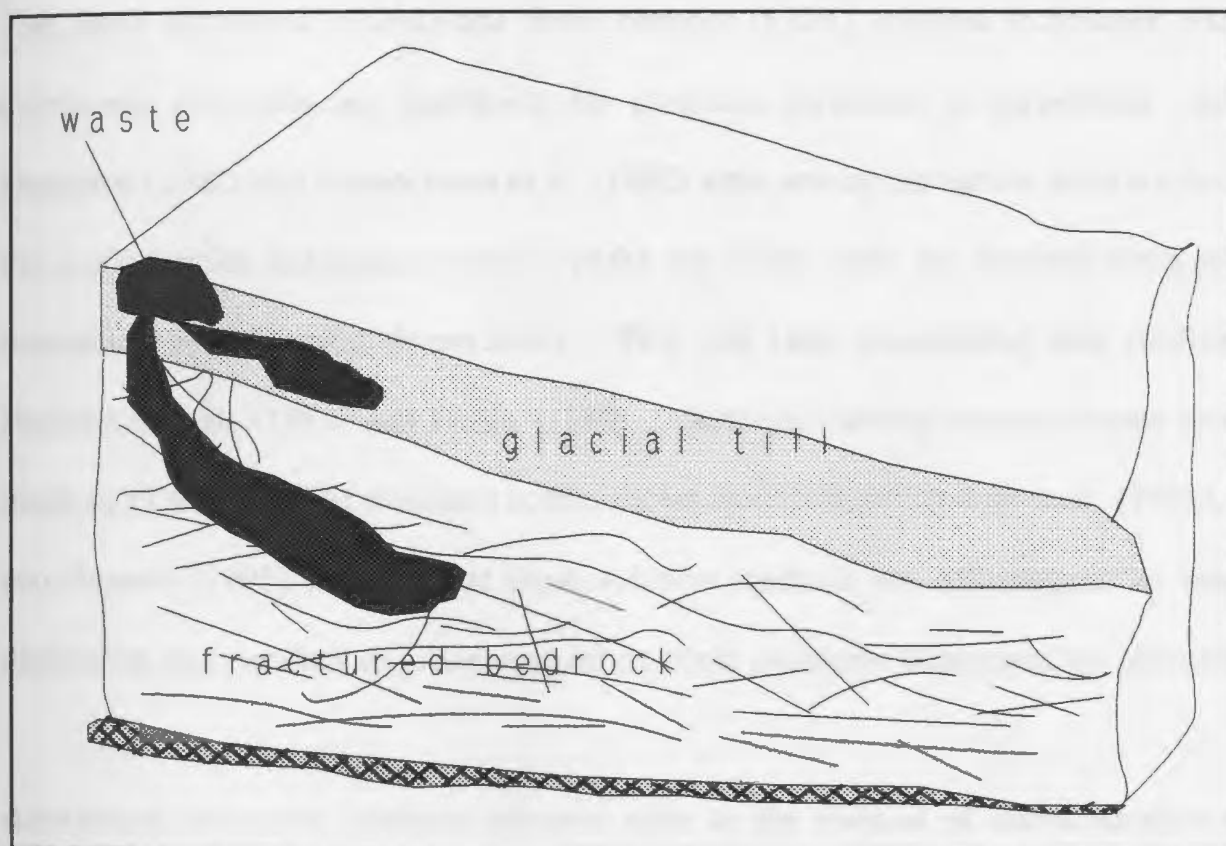
Figure 1.1: Typical geological scenario and subsurface solute migration pattern in an aquifer.

The second difficulty relates to the performance of the mathematical solution techniques commonly employed in solute transport analysis. The implementation of the classical equations governing subsurface contaminant transport still poses unresolved problems for all the commonly used numerical techniques. The mathematical nature of the governing equations may change from parabolic to hyperbolic and vice versa depending on whether advection (the transport of dissolved contaminants by moving ground water) or dispersion (the spreading of contaminants in different directions) dominates in the transport process. The finite difference (FDM) and finite element (FEM) solution techniques which are commonly employed are inefficient for problems governed by hyperbolic equations. Hamilton (1982) and Sophocleous et al. (1982) were among the earlier workers to observe the inefficiencies and inaccuracies of FDM and FEM codes for practical field problems dominated by advection (hyperbolic). This was later investigated and confirmed by Huyakorn et al. (1984) and Beljin (1988). Although several improvements have been made in FDM and FEM transport codes, recent studies by Moltyaner et al. (1993), Zheng and Bennett (1995) confirm that these solution methods are still plagued by numerical dispersion and oscillations when applied to field problems dominated by advection.

Alternative numerical solution schemes such as the method of characteristics (MOC, Konikow and Bredehoeft 1978) and the method of random walk (RNDWK, Prickett et al. 1981) that use particle tracking techniques have been developed and improved over the years (Walton 1989, Zheng 1992, 1993, Koch and Prickett 1993) to handle advection dominated problems successfully. However these techniques have consistently proved less

efficient when advection is low or dispersion is dominant in the solute transport process (Zheng and Bennett 1995). A number of workers (Celia et al. 1990, Healy and Russel 1992) have recently employed the finite volume method to handle advection-dominated problems and also achieve mass conservation. However this method has proved very cumbersome for simple one-dimensional theoretical problems.

The boundary element method (BEM) has recently been recognized as an efficient numerical solution technique for similar boundary value problems in other areas of engineering e.g., time dependent problems (Wrobel et al. 1986), thermal problems (Brebbia and Wrobel 1987, Partridge et al. 1992). The advantage of the BEM is its increased accuracy as shown by many workers (Liu and Liggett 1978, Partridge et al. 1992, and Haie et al. 1996). In addition to this the BEM requires only the boundary of the domain to be defined and discretized therefore reducing the dimensionality of the problem by one. This is a major advantage over other domain methods (FDM, FEM, MOC and RNDWK) since the amount of work for the modeller is reduced in terms of data preparation and computational efficiency. However, the BEM has not gained wide recognition in solute transport analysis. In a detailed review of the recent groundwater software catalog published by the international groundwater modelling centre (IGWMC–USA, van der Heijde 1994) it was revealed that none of the solute transport codes currently used in the industry is based on the BEM. Although this list is not exhaustive it indicates that the mathematical resources available for improvement in our modelling approach have not been fully exploited.

As a summary, modelling methodologies must be improved if we expect to meet the challenging demands for groundwater quality. More site specific studies on different subsurface media are needed to enhance our understanding of the problem. The mathematical approaches should take full advantage of more efficient schemes. An integrated approach which combines physical and numerical investigation should also be followed in groundwater pollution studies.

1.3 The Objectives and Scope of this Work

The main goal of this research is to investigate the solute transport mechanisms in the type of fractured bedrock aquifer found around St. John's, Newfoundland. To accomplish this task a field experiment was conducted and data from this was used in a numerical model. This will demonstrate the practical application of a boundary element numerical model in subsurface contaminant transport. It will also provide a conceptual understanding and hydraulic parameters pertaining to these aquifers.

The field work included a detailed review of the available data on site geology and an experimental study of the site hydrogeology and groundwater hydrology over a period of two years. During this time the background chemistry and groundwater levels were monitored and in situ tests for hydraulic conductivity were performed. Two natural gradient tracer experiments have also been performed to supplement data obtained from in situ tests and also to provide calibration and validation data for the numerical model.

Since the primary objective of the field tests was to obtain qualitative and quantitative insights of the physical solute transport mechanisms in this aquifer, greater attention was focused on the analysis of conservative solutes during the tracer tests. Based on the available literature on groundwater pollution investigation in Newfoundland this is the first time that such a systematic and comprehensive study has been performed to obtain insights of aquifer hydraulic behaviour and quantitative estimates for the purpose of solute transport analysis.

A numerical implementation of the solute transport equation is presented using the dual reciprocity boundary element approach (Nardini and Brebbia 1982). We have proposed a solution procedure which involves series of transformations and mathematical manipulations to transform the governing equation to a simpler form for a more efficient application of the dual reciprocity method (DRM). This procedure eliminates some of the difficulties known with the DRM in its application to such types of problems. A computer implementation of the method has been developed and verified by the analytical techniques for a certain class of problems. Furthermore the accuracy and efficiency of the method has been verified by comparing the results with other numerical solution schemes. The numerical model was applied to field problems by calibration with data obtained from field tracer tests. Such an integrated approach is not usually employed in studies of subsurface contaminant transport.

It must be emphasized that this work does not attempt to develop new theories or mathematical concepts underlying solute transport analysis but rather, employs the classical theories and equations in current use. It is an attempt to combine physical site investigation with numerical modelling by exploiting the potential advantages of the boundary element method for subsurface contaminant transport analysis. This challenging task is obviously limited by constraints such as time and financial support and the present work is therefore based on a small scale study.

1.4 Organization of the Thesis

In this section a brief description of the materials covered in the various chapters is outlined. The study emphasizes an integration of physical and numerical modelling and the results obtained.

In Chapter 2, the theoretical background of solute transport in porous and fractured media are provided. The chapter reviews the main processes involved in subsurface solute transport and theoretical concepts that have been proposed to examine flow and mass transport through different subsurface media. The major parameters that are needed for qualitative and quantitative analysis of solute migration are identified. Finally the classical equations governing groundwater flow and subsurface solute transport are also presented and explained.

Chapter 3 concentrates on a detailed review of the mathematical methods which are commonly employed in solving the classical equations. These include analytical and numerical techniques. However greater emphasis is placed on the numerical methods such as the finite difference method, finite element method, method of characteristics, method of random walk and the boundary element method. A detailed description of the application of these methods in solute transport analysis, the progress that has been made over the years to overcome the various difficulties involved and the current difficulties that still require attention and improvement are presented. A section is also devoted to some of the recent field investigations in different subsurface media that have employed tracer experiments. The level of understanding and the need for further studies have also been pointed out in this chapter.

Chapter 4 describes the field study with the location of the experimental site, its geology and hydrogeology. The experimental procedures, the qualitative and quantitative observations of groundwater, the in situ tests and the tracer plume movement are presented. Estimates of solute transport parameters and conclusions drawn from the field study which are needed for theoretical conceptualization of the solute transport process in the type of aquifer under consideration are also presented. This chapter provides the necessary background for the development and calibration of the numerical model.

In Chapter 5, the boundary element formulation for the solute transport equation is presented. The dual reciprocity method (DRM) is reviewed and its general application is explained. A series of transformations and mathematical manipulations of the governing classical equation of solute transport are performed so that current difficulties in the application of the method are circumvented. The DRM is then employed in an efficient way which provides a boundary only formulation of the classical advection-dispersion equation. The standard boundary element discretization procedure is further employed to complete the development.

Chapter 6 concerns the verification of the boundary element numerical model which is implemented in a FORTRAN 77 code. The model was first applied to a heat transport problem proposed and solved by Partridge et al. (1992) by using the traditional DRM procedure for these types of problems. This was used to verify the efficiency and accuracy of the new approach we have taken. The model was then applied to three different types of solute transport problems commonly encountered in the field: (i) continuous migration of solute from a strip source (patch source problem); (ii) continuous migration of solute from a point source; and (iii) instantaneous release of solute from a point source. The results from the BEM model are compared with their analytical solutions by using realistic input parameters. During the verification process the parameters were selected such that the accuracy of the model with respect to advection and dispersion dominated transport was tested. The performance of the model was also tested against other numerical solution techniques by using case studies proposed in the literature.

Chapter 7 presents the application of the boundary element model to field data. The information and knowledge obtained from the field studies are used to calibrate the numerical model. Numerically derived breakthrough curves are compared with those obtained from tracer tests. An attempt has been made to estimate aquifer parameters from optimal input values that produced reasonable breakthrough curves. Sensitivity analysis is also performed by computing sensitivity coefficients for the various aquifer parameters.

Finally, Chapter 8 highlights the contribution of this work to both industry and academia as well as the limitations of the study. The chapter also presents a summary, conclusions and recommendations for future studies on solute transport, especially in the type of aquifers found in Newfoundland.

Chapter 2

Solute Transport in Saturated Porous and Fractured Media

2.1 Solute Transport in Saturated Porous media

Contaminant transport through saturated porous and fractured formations is usually explained in the context of the advection-dispersion theory for saturated porous media flow. In the analysis of solute transport through saturated porous media, a representative elementary volume (REV), (Bear 1972) is defined whereby the individual microscopic parameters are averaged over the bulk volume to obtain macroscopic parameters representing the porous medium. This is usually termed continuum (porous medium) approach. A mass balance analysis is then employed to describe how solute concentrations change in space and with time according to the main processes such as advection, dispersion and diffusion. This chapter reviews some of the basic processes underlying solute transport through porous and fractured formations and also the basic equation that have been developed to analyze these processes.

2.1.1 Solute Transport by Advection

Advection is the process whereby moving groundwater carries dissolved solute with it (Bear 1972, Fetter 1988). The advective transport of subsurface conservative contaminants follow Darcy's law for laminar groundwater flow which is given as:

$$|V| = \frac{K}{\epsilon} i \tag{2.1}$$

where, $|V|$ is the average linear velocity, K is the hydraulic conductivity tensor of the medium, i is the hydraulic gradient, and ϵ is the effective porosity. The effective porosity is defined as the ratio of volume of the interconnected pore spaces available for flow to the total volume of the aquifer material. In solute transport analysis, effective porosity is that porosity required to achieve a reasonable agreement between calculated travel time and the observed travel time of a conservative tracer. It can therefore be estimated by taking the ratio of the Darcy velocity to the observed tracer velocity (Zheng and Bennett 1995).

2.1.2 Solute Transport by Mechanical Dispersion

As groundwater moves through microscopic pore spaces the molecules travel at different rates, some travel through different sizes of pore spaces and branch through tortuous pathways. Due to the complexity of microscopic flow analysis, subsurface flow and solute transport are analyzed at the macroscopic scale. At the macroscopic scale the inhomogeneity of subsurface materials result in spatial variations in velocity. Velocity is not constant in the center of the channel, and its local direction varies significantly around the average value direction. As the solute advects through tortuous pathways with varying velocities in the porous medium (Figure 2.1), it undergoes spatial spreading in the longitudinal and transverse directions of flow and mixes with uncontaminated water. This process is termed mechanical dispersion and causes dilution of the solute in space and in time. Mechanical dispersion occurring in the direction of the bulk movement of the solute (longitudinal dispersion) will cause some the solute to move and spread ahead of the advective front. Similarly, mechanical dispersion occurring in the transverse direction (transverse dispersion) will cause some of the solute to spread in this direction. Normally in field problems longitudinal dispersion is stronger than transverse dispersion (Freeze and Cherry 1979). Figure 2.2, shows the mechanical mixing and dilution process that causes solute concentration to reduce.
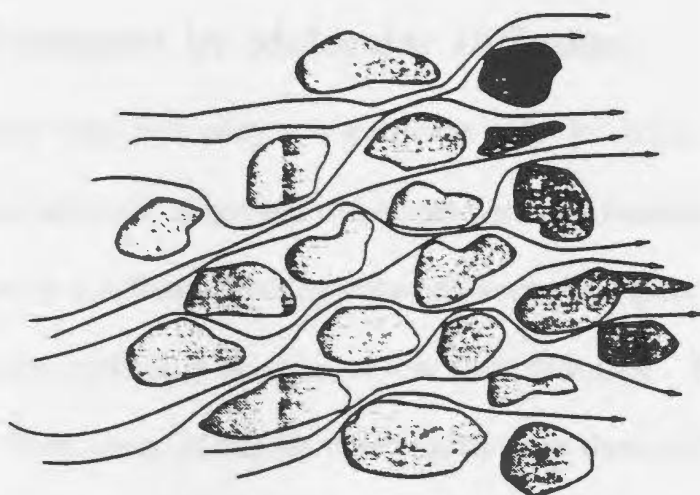
Figure 2.1 Tortuous branching of solutes in a porous medium (after Zheng and Bennet, 1995)

Continuous injection of tracer

Direction of average flow

Schematic representation of the dilution process caused by mechanical dispersion in granular porous media.

Mixing in individual pores

Mixing of pore channels

Mixing by molecular diffusion
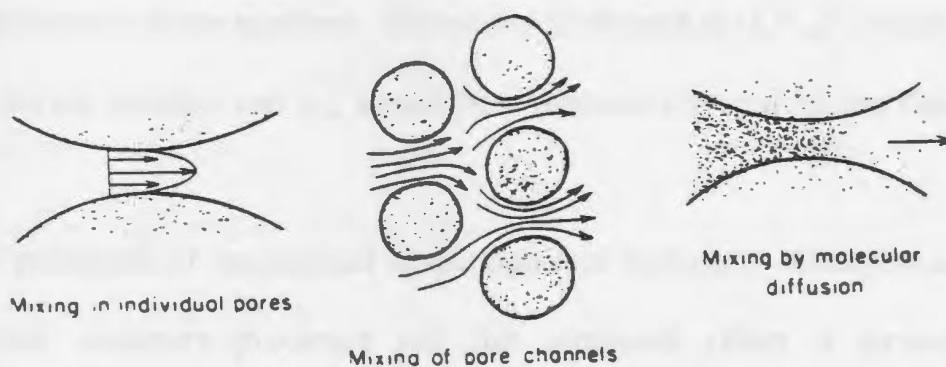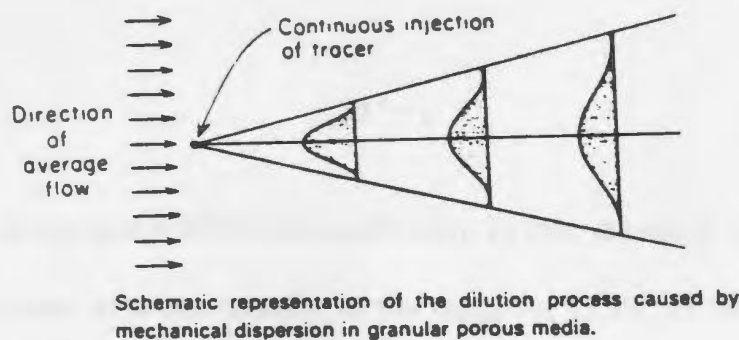
Figure 2.2: Mechanical dispersion and molecular diffusion processes in porous media (after Freeze and Cherry, 1979)

2.1.3 Solute Transport by Molecular Diffusion

Another mechanism that can play a significant role in solute transport is molecular diffusion. As solute advects, disperses and mixes with uncontaminated water in the porous media, concentration gradients develop between areas of higher concentration and those of low concentration especially in areas of low fluid mobility. This causes contaminants to be transferred from areas of higher concentration to those of low concentration by a process termed molecular diffusion of solutes. It is purely a chemical process which is predominant in areas of low groundwater flow velocities such as dead ends. Bear (1972) has described the amount of diffusion through the tortuous microscopic paths in porous media by the term effective diffusion coefficient (D*) which is expressed as:

$$D^* = \tau \ D_o \qquad\qquad (2.2)$$

where D_o (L^2/t) is the solute diffusion coefficient in free standing water (D_o is well known for many electrolytes in water usually in the range of 1×10^{-9} to 2×10^{-9}, Fetter 1988) and τ is the tortuosity of the medium. Tortuosity is defined as $(L/L_e)^2$, where L is the shortest possible travel distance and L_e, actual flow distance covered by the fluid.

The two processes of mechanical dispersion and molecular diffusion are inseparable in most solute transport processes and the combined effect is termed hydrodynamic dispersion. This causes solutes to spread over a wider area both in the longitudinal and transverse directions than it would have been for advection only. In solute transport

analysis, hydrodynamic dispersion is represented by the dispersion coefficients in the longitudinal (D_L) and transverse (D_T) directions respectively.

2.1.4 Chemical and Biological Processes Affecting Solute Transport

There are other processes that alter the rate of solute movement, the spatial spreading and magnitude of concentrations suggested by advection and dispersion processes. The solute may undergo radioactive or biological decay during transport in the form of:

$$\frac{\partial c}{\partial t} = -\lambda\, c \qquad\qquad (2.3)$$

where λ is calculated based on the half life ($t_{1/2}$) of the radioactive solute as $\lambda = (\ln 2)/t_{(1/2)}$. and c is the concentration of the solute. Other solutes also may undergo chemical reactions that result in sorption on surfaces of the mineral grains or sorption by organic carbon present, undergo chemical precipitation, be subject to abiotic as well as biodegradation or participate in oxidation-reduction reactions (Fetter 1993). Solutes that are affected by these processes are termed reactive or non-conservative (reactive) solutes. All these processes can cause advance rate of the solute front to be retarded (attenuation of contaminants). In one dimension, retardation will cause the non conservative solute to travel behind the front of a conservative solute. In two dimensions the retarded plume is less spread out and exhibit high concentrations. The exact interaction of different

contaminants with different subsurface materials still lack behind required knowledge and has been a subject of intense research in recent years. The effects are usually accounted for by inclusion of a retardation (attenuation) factor R which is defined as (Freeze and Cherry 1979)

$$R = 1 + \frac{\rho_b}{\epsilon} K_d \qquad (2.4)$$

where ρ_b is the dry bulk mass density of the soil, ϵ the porosity and K_d the distribution coefficient. The distribution coefficient is usually determined from laboratory experiments that establishes the relationship between the mass adsorbed per mass of solid and the concentration of the constituent in solution at constant temperature (isotherms). The commonly used isotherms are linear, Freundlich and Langmuir isotherms (Freeze and Cherry 1979).

2.2 The Dispersion Coefficient

One of the most elusive parameters to determine in practice is the dispersion coefficient. The classical relationship between the flow velocity, the dispersion coefficient and the nature of the porous medium have been studied by Scheidegger (1961), Bachmat and Bear (1964), and Bear (1972). These workers observed that the influence of geometry of the

void space on the dispersion of solutes can be represented by a coefficient termed dispersivity of the porous medium which in saturated flow is a property of the geometry of the solid matrix. In an isotropic medium, Bachmat and Bear (1964), Bear (1972) have shown that the medium's dispersivity is related to two constants α_L, (longitudinal dispersivity) and α_T (transverse or lateral dispersivity). Over the past decade field and laboratory experiments have been conducted to quantify dispersivity in different media. All these studies have shown that dispersivity values measured in the laboratory are several times smaller than in the field. Hence dispersivity increases with the scale of measurement. This has been termed the scale effect (Anderson 1979). Higher values of dispersivity obtained from field tests are attributed to heterogeneity and anisotropy. However Gelhar and Axness (1983) have observed an upper limit of dispersivity as solutes travel longer distances over several hundreds of meters.

Bear (1979), derived a general expression for the dispersion coefficient as:

$$D_{ij} = \alpha_T |V| \delta_{ij} + (\alpha_L - \alpha_T)\frac{V_i V_j}{|V|} \qquad (2.5)$$

where D_{ij} is the dispersion coefficient, $|V|$ is the magnitude of the velocity vector, V_i, V_j are the linear velocities in their respective directions and δ_{ij} is the Kronecker delta. In two dimensional form the components of the dispersion coefficient are given as

$$D_{11} = \alpha_T |V| + \frac{(\alpha_L - \alpha_T)V_1^2}{|V|} = \frac{\alpha_L V_1^2 + \alpha_T V_2^2}{|V|}$$

$$D_{12} = D_{21} = \frac{(\alpha_L - \alpha_T)V_1 V_2}{|V|} = (\alpha_L - \alpha_T)\frac{(V_1 V_2)}{|V|} \tag{2.6}$$

$$D_{22} = \alpha_T |V| + \frac{(\alpha_L - \alpha_T)V_2^2}{|V|} = \frac{\alpha_T V_1^2 + \alpha_L V_2^2}{|V|}$$

where $|V|^2 = V_1^2 + V_2^2$. The dispersion coefficients can then be expressed in the form:

$$[D_{ij}] = \begin{bmatrix} D_{11} & D_{12} \\ D_{21} & D_{22} \end{bmatrix} \tag{7}$$

Furthermore, Bear (1979) has shown that in an isotropic medium the components of the dispersivity do not change with the rotation of the coordinate axis, hence it is convenient to define the coordinate axis to coincide with the principal axis of dispersion. In many practical field cases where the Cartesian coordinate system is employed, it is possible to define one of the axis (say x) to coincide with the principal direction of the dispersion tensor. Hence $D_x = D_{11} = D_L$, and $D_y = D_{22} = D_T$ become the principal values of dispersion and $D_{xy} = D_{yx} = D_{11} = D_{12} = D_{21}$, where D_x and D_y are the dispersion coefficients in the x and y directions respectively. Then the components of D_{ij} (including molecular diffusion) can be expressed as:

$$D_x = \alpha_L \frac{v_x^2}{|V|} + \alpha_T \frac{v_y^2}{|V|} + D^* \qquad (2.8)$$

$$D_y = \alpha_T \frac{v_x^2}{|V|} + \alpha_L \frac{v_y^2}{|V|} + D^* \qquad (2.9)$$

$$D_{xy} = (\alpha_L - \alpha_T)\frac{v_x v_y}{|V|} + D^* \qquad (2.10)$$

where $|V|$ is the average linear velocity. For a uniform flow in (say) x-direction the components of dispersion reduce to only the principal values as:

$$[D_{ij}] = \begin{bmatrix} D_x & 0 \\ 0 & D_y \end{bmatrix} \qquad (2.11)$$

which are now expressed as:

$$D_x = \alpha_L|V| + D^*$$

$$(2.12)$$

$$D_y = \alpha_T|V| + D^*$$

In a nonuniform flow field the coordinate system will not always coincide with the principal axis of flow. Wang and Anderson (1984) have suggested a transformation approach by defining a counterclockwise rotation angle θ, $(\theta = v_y/v_x)$ which represents the deviation from the principal direction. The components of the dispersion coefficient now becomes (Wang and Anderson 1984):

$$D_{11} = D_L\cos^2\theta + D_T\sin^2\theta$$
$$D_{22} = D_L\sin^2\theta + D_T\cos^2\theta \qquad (2.13)$$
$$D_{12} = D_{21} = (D_L - D_T)\ \sin\theta\ \cos\theta$$

2.3 Solute Transport in Saturated Fractured Formations

The theories on subsurface solute transport were first developed from studies on granular porous media. As in porous media, the advection, dispersion and diffusion mechanisms also govern solute transport in fractured formations. However the occurrence of fractures alter these mechanisms of solute transport and the conceptual basis of analysis. For example the fractures create secondary porosities which provide more or less tortuous pathways for solute transport. While a representative elementary volume (Bear 1972) can be conveniently defined to treat a porous medium as a single continuum, the same cannot always be said for a fractured medium. Heterogeneities that occur in fractured aquifers

may be due to several factors including variations of material properties within the rock matrix; spatial variations of the fracture characteristics such as, lengths, spacings, opening sizes (apertures), orientations etc. Depending on the number of fractures per unit area and their degree of interconnectivities a small or large portion of the planar area may contribute to flow. If the rock matrix is porous, advection and dispersion mechanisms may transport contaminants with most of the advection occurring in the fractures. Hydrodynamic dispersive transport of solutes in fractured formations is mainly attributed to mixing at fracture intersections, variations in aperture across the width and along the longitudinal axis of the fracture, molecular diffusion into the microfractures penetrating the inter-fracture block and those into the inter-fracture porous matrix blocks (Palmer and Johnson 1989). In a single fracture however dispersion may be due to variability in fracture aperture which develops as a result of roughness of the fracture walls (Domenico and Schwartz 1990). Figure 3.3 shows various ways in which fractures influence dispersive and advective transport.

(a) Diffusion into the Matrix

Diffusion

Source

Rock block

Fracture

Advection and dispersion

Tracer distribution

Closed fracture

--- Fracture aperture (μm)

(b) Variability in Velocity due to Fracture Roughness

Source

(c) Mixing at Fracture Intersections

(d) Variability in Velocity due to Differing Scales of Fracturing

(e) Variability in Velocity due to Variable Fracture Density

Figure 3.3: Illustration of the difference causes of hydrodynamic dispersion in fractured formations (after Domenico and Schwartz, 1990)

Early studies in flow through fractured media used the analogy of flow through parallel plates to derive a relationship between the flow and the fracture characteristics by what is commonly termed as the cubic law. The cubic law states that, flow through a fracture is proportional to the cube of the fracture aperture (Domineco and Schwartz 1990). For a laminar flow between two parallel plates, Romm (1966) used the expression:

$$Q = \frac{\rho_w \, g \, \xi^2}{12v}(\xi \ w)\frac{dh}{dl} \tag{2.14}$$

where Q is the volumetric flow rate, ρ_w is the density of water, g is the acceleration due to gravity, v is the viscosity, ξ is the aperture opening, w is the fracture width perpendicular to the flow direction, and dh/dl is the gradient in the flow direction. By relating this equation to Darcy's law the hydraulic conductivity for the fractured medium is expressed as

$$K = \frac{\rho_w \, g \, \xi^2}{12v} \tag{2.15}$$

Although the validity of the cubic law and many influencing factors has been a subject of debate since the 1980s, the general agreement is that the basis for determining flow parameters in a fractured formation is necessarily different from that of granular porous

medium (Berkowitz et al. 1988). In practice the evaluation of solute transport through fractured formation poses a great challenge especially in determining the conceptual basis of the analysis. Some workers have recently used laboratory and field experiments to propose three main theoretical concepts for analyzing solute transport in fractured formations. These are, continuum, discrete fracture and channel concepts.

The continuum or an equivalent porous medium approach is applied when the number of fractures per volume of the aquifer is high and the inter-connectivity of these fractures is also high. In such cases treating the individual effect of fractures becomes impossible therefore the spatial varying parameters are averaged over a representative elementary volume defined to represent the system. The system is then treated as an equivalent porous medium. It is important to recognize that a representative elemental volume (REV, Bear 1972) can be defined for a fractured media only when evidence exist that the fracture density and interconnectivity are high. The continuum approach for fractured porous media analysis may be applied in two ways; either by considering the media as single porosity or a double porosity (Barenblatt et al. 1960, Berkowitz et al. 1988). The single porosity models are employed in the analysis of crystalline fractured rocks which have very low primary porosity therefore the fractures provide the main source of porosity. The dual porosity concept assumes that fractured porous media can be represented by two interacting continua: the primary porosity blocks of low permeability and some storage capacity and secondary porosity fractures with high permeability and some storage capacity. The two systems are linked by a leakage term representing the fluid exchange

between them. This concept is usually applied in the analysis of transport in permeable rocks such as shales and sandstones. The equations used for the analysis of fractured medium as single continuum are similar to the classical equations of granular porous media transport. However, the derivation of the material parameters (e.g., hydraulic conductivity, porosity, etc.) used to describe the fractured media are totally different. Since the 1980s, many workers including Bibby (1981), Pankov et al. (1986), Berkowitz et al. (1988) etc., have investigated this concept in the analysis of ground water flow and solute transport. For example Pankov et al. (1986) concluded that the equivalent porous media concept is effective in the case of small fracture spacing, high fracture inter-connectivity and high block porosity. A systematic investigation of the conditions under which the continuum approach is justified in fractured formations was conducted by Berkowitz et al. (1988). They observed that for highly fractured formations with interconnected network, an equivalent porous medium is justified. However the application of this concept to actual field situation requires a knowledge of the equivalent aquifer parameters. Such parameters must be determined by analysis of breakthrough curves obtained from field tracer tests (Berkowitz et al. 1988). To date the main difficulty in the application of the continuum approach lies in the definition of the REV or in determining the main fracture characteristics such as high density per area and high inter connectivity that will justify the definition of a REV.

The discrete fracture concept involves a detailed characterization of flow through individual fractures. It has been recognized that a representative elementary volume can

not always be defined especially in aquifers where the fractures are sparsely distributed, have different characteristics (different families for fractures) and are sparsely connected. The use of the discrete fracture approach require adequate knowledge of the fracture properties like the apertures, orientations, length and spacings and their spatial variations within the aquifer. Workers including Grisak and Pickens (1980, 1981), Sudicky and Frind (1982), Tang et al. (1981) have investigated this approach theoretically and reported its validity. However the difficulty in characterizing the fracture properties of an aquifer in such detail poses a severe limitation for the practical application of this concept. It becomes virtually impossible to determine the precise locations and characteristics of all fractures (Berkowitz et al. 1988).

The channel approach was first proposed by Tsang and Tsang (1987). The idea originated from the laboratory observations and the results from Whitherspoon et al. (1980) and the field tracer tests conducted by Neretnieks (1987) and Abelin et al. (1991). These experiments indicated that flow through fractured formations occur in paths of least resistance in small fingers or localized channels. Neretnieks (1987) observed that, approximately one-third of flow entered from approximately 2% of the fractured rocks during a filed tracer experiment. Tsang et al. (1991) also observed that under certain circumstances the hydraulic conductivity of the fracture can be controlled by constrictions along the flow paths which cause flow to be confined to narrow channels instead of the entire fracture plane. Rasmusson and Neretnieks (1986) have also observed that, in some cases, as little as 20% of the total planar area of the fracture may contribute to flow.

Mathematical conceptualizations describing this phenomena were developed and solved analytically by Tsang et al. (1991). Although this concept is not disputed in the literature, sufficient laboratory and field tracer tests have not been performed to provide more insights for its specific applications and the concept is still under investigation.

All the above concepts are valid in different field situations but their applicability require a detailed understanding of the hydraulic behaviour of the aquifer in question. Due to this any groundwater quality assessment model for such aquifers should be preceded by adequate field investigation to evaluate the specific theoretical concept upon which the formulation is based.

2.4 Governing Equations of Groundwater Flow and Solute Transport

In contaminant transport modelling, it is customary to combine two separate equations of flow and mass transport. The groundwater flow equation is first solved to provide the hydraulic head distribution in the system from which average groundwater velocity and flux fields are obtained as inputs in the solute transport model. The solute transport equation is then solved to obtain the changes in concentration distribution in the domain.

2.4.1 Groundwater Flow Equations

The partial differential equations governing groundwater flow are based on the principles of conservation of fluid mass and momentum. For the flow equation, Darcy's law is combined with the mass balance to relate the net mass flux of water and the gain or loss of water due to sources and sinks to the net rate of storage within an elemental volume of an aquifer. The governing equation can be written in tensorial form as (Bear, 1972)

$$\frac{\partial}{\partial x_i}\left(K_{ij}\frac{\partial h}{\partial x_j}\right) = S_s\,\frac{\partial h}{\partial t} - Q \qquad (2.16)$$

where h is the hydraulic head (L), S_s is the specific storage of the aquifer (1/L), Q is the general source/sink term (L/T), K_{ij} (i,j=1,2,3) denotes the component of the hydraulic conductivity (L/T) tensor and x_i (i=1,2,3) denotes the spatial coordinates. When the principal directions of the hydraulic conductivity tensor coincide with the Cartesian coordinate axes equation (2.16) can be written as (Bear 1972):

$$\frac{\partial}{\partial x}\left(K_{xx}\frac{\partial h}{\partial x}\right) + \frac{\partial}{\partial y}\left(K_{yy}\frac{\partial h}{\partial y}\right) + \frac{\partial}{\partial z}\left(K_{z}\frac{\partial h}{\partial z}\right) + Q = S_s\frac{\partial h}{\partial t} \qquad (2.17)$$

where K_{xx}, K_{yy}, and K_{zz} are the hydraulic conductivities in their respective directions.

2.4.2 Solute Transport Equations

The concept of mass balance is traditionally used to examine pollutant migration in space and time. The assumption is generally made that the contaminant is miscible with the groundwater and that there is no significant density difference between the groundwater with and without the dissolved solute. By using these concepts, the classical partial defferential equation describing the advection and dispersion mechanisms can be written in tensorial form as (Bear 1972, 1979) :

$$\frac{\partial}{\partial x_i}\left(D_{ij}\frac{\partial c}{\partial x_j}\right) - \frac{\partial}{\partial x_i}(v_i\ c) + Q = \frac{\partial c}{\partial t} \qquad (2.18)$$

Where D_{ij} and v_i are the components of hydrodynamic dispersion tensor and specific discharge respectively, c is the concentration of the solute and Q is the source/sink term. The general form of this equation in two-dimensions can be written as (Bear 1972, 1979):

$$\frac{\partial}{\partial x}\left(D_{11}\frac{\partial c}{\partial x} + D_{12}\frac{\partial c}{\partial y}\right) + \frac{\partial}{\partial y}\left(D_{21}\frac{\partial c}{\partial x} + D_{22}\frac{\partial c}{\partial y}\right)$$

$$-\frac{\partial}{\partial x}(c\ v_x) - \frac{\partial}{\partial y}(c\ v_y) + Q = \frac{\partial c}{\partial t} \qquad (2.19)$$

Similarly, in a Cartesian coordinate system where one of the axis (say x) is defined to coincide with the principal axis of dispersion the explicit form of the advection dispersion equation including sources/sinks, effects of retardation and decay is written (Bear 1979) as:

$$\frac{\partial}{\partial x}\left(D_x\frac{\partial c}{\partial x}\right) + \frac{\partial}{\partial y}\left(D_y\frac{\partial c}{\partial y}\right) - v_x\frac{\partial c}{\partial x} - v_y\frac{\partial c}{\partial y} - R\lambda c + Q = R\frac{\partial c}{\partial t} \qquad (2.20)$$

where D_x and D_y are the principal components of the dispersion tensor, λ is a first order decay constant for solutes that undergo radioactive decay (1/T) and R is a retardation factor.

2.4.3 The Nature of the Solute Transport Equation

The advection-dispersion equation (ADE) has two main components. On the left hand side (LHS) of equation (2.20) the dispersion components are described by the first two terms; the advection components are described by the third and fourth terms; the last two terms denote the solid-solute interactions and reactions. At any time either dispersion or advection is dominant in the transport process which changes the mathematical nature of

the equation. When dispersion dominates over advection in the transport process, the equation tends to be more parabolic in nature. On the other hand when transport process shifts from dispersion-dominated to advection-dominated the fundamental nature of the equation is modified and the equation changes from parabolic to a first order hyperbolic equation. This means that, mathematically it is required to treat both hyperbolic terms and parabolic terms. The dual nature of this equation poses a great challenge to all the mathematical solution techniques in current use. In practice a dimensionless quantity termed Peclet number (P_e) is usually defined to describe the character of the (ADE) as it varies from parabolic (advection dominated) to hyperbolic (dispersion dominated). The Peclet number is defined as (Bear 1979):

$$P_e = \frac{VL}{D} \qquad\qquad (2.21)$$

where V is the velocity, L is a characteristic length and D is the dispersion coefficient. High Peclet numbers ($P_e > 4.0$, Voss 1984) indicate advection dominated transport.

2.5 Initial and Boundary Conditions for Flow and Transport Problems

In order to obtain a unique solution for the flow and transport problems it is necessary to define initial and boundary conditions. For groundwater flow problems the initial

conditions may be described as the hydraulic heads at a reference time (say t=0). The boundary flow conditions describe the behaviour of flow at the boundary. Three main boundary flow conditions that are usually used are (a) a specified value of hydraulic head along a boundary or part of it (Dirichlet or first type), (b) a specified flux of water along the boundary (Neuman or second type) expressed as $q_n = K \, dh/dn$ where n defines the direction normal to the boundary; (c) a specified relationship between the flux rate and the head difference across a boundary (Cauchy or third type).

In solute transport problems the initial conditions describe the concentration distribution at all locations in the domain at an initial time (t=0). A zero initial concentration may be assumed throughout the domain. The general form is then given as:

$$c(x,y,z,t=0) = 0 \qquad\qquad (2.22)$$

For the solute boundary conditions, three types are usually employed (Javandel et al. 1984, Huyakorn et al. 1984). The first type (Dirichlet) consist of a prescribed concentration $c_o(x,y,z)$ for a particular portion of the boundary (Dirichlet type) given as:

$$(2.23)$$

$$c = c_o(x,y,z,t)$$

Typical examples are, a zero concentration prescribed on the boundary far from the contaminant source, or a specified value of concentration at injection wells.

The second type of boundary condition (flux or Neuman type) is given as:

$$\left(D_{ij}\frac{\partial c}{\partial x_j}\right)n_i = q(x,y,z,t) \tag{2.24}$$

where $q(x,y,z,t)$ is a known function and n_i is the components of the unit vector normal to the boundary in the i direction. Practical examples are a zero normal concentration gradient on impervious boundaries and a normal concentration gradient at outflow boundaries.

The third-type boundary conditions (Cauchy type) specifies the total advective and dispersive fluxes at the boundary and usually expressed as:

$$\left(D_{ij}\frac{\partial c}{\partial x_j} - c\ V\right)n_i = q\ c_0(x,y,z,t) \tag{2.25}$$

where $q\ c_0$ is the solute flux. The first term on the left hand side of equation (2.25) represent the flux due to dispersion and the second term represents the effects of advection. A notable example of the application of this type of boundary condition is a

specified mass flux of contaminant at injection wells in which case q (L/T) corresponds to the volumetric fluid injection rate per unit area of aquifer (L/T) and c_0 is the concentration of the injected fluid (M/L^3). A second example could be a specified mass flux of contaminant at the boundary receiving influx of contaminant from sources such as landfills, disposal ditches etc. (Huyakorn et al. 1984).

Chapter 3

Previous Mathematical and Field Investigations of Subsurface Solute Transport

This chapter presents a review of the commonly used mathematical solution methods in solute transport analysis and some of their limitations. The main methods reviewed here are analytical and numerical methods. A section is also devoted to some recent field studies conducted to enhance the understanding of the solute transport process and provide data for mathematical simulation.

3.1 Analytical Methods in Solute Transport Analysis

Analytical methods have long been used in solute transport analysis. A major advantage of analytical approach is its ability to provide a close form or exact solution which are free from computational errors. Currently analytical solutions of equations for solute transport through porous and fractured media have been developed by Bear (1972), Ogata and Banks (1961), Neretnieks et al. (1982) etc. Many workers including Tang et al. (1981),

have provided analytical solutions for transport through a single fracture while Sudicky and Frind (1982) provided a similar one for a system of parallel fractures. There are several analytical groundwater flow and solute transport codes available in the literature (e.g., Bear 1972, Cleary and Ungs 1978, Van Genuchten and Alves 1982, Beljin 1985, Neville 1994). Rowe and Booker (1988) have also provided semi-analytical solutions for solute transport analysis.

The practical application of analytical models are limited due to simplifying assumptions that are required to obtain the exact solution. For problems with complex boundary conditions and heterogeneous material behaviour, analytical methods do not provide reliable results. Nevertheless, analytical methods have proved useful for verifying numerical models. It is currently a standard practice to verify a numerical model by comparing the results with the analytical solution for a simplified case. Moreover in some practical field cases, analytical models have proved more economical to obtain a preliminary idea of the extent of groundwater contamination.

3.2 Numerical Methods in Groundwater Flow and Solute Transport Analysis

The materials characterizing different subsurface media are nonuniform and actual boundaries are usually irregular. Numerical methods have the ability to represent field

problems in a realistic way by discretizing the domain into zones or elements to reflect the changing parameter field that may occur due to material heterogeneities. Different numerical techniques have been proposed to investigate groundwater flow and contaminant transport in many geologic media. It must however be noted that numerical methods only provide an approximate solution to the governing equations. The numerical solution techniques used for solute transport analysis may be classified into three, based on the methods of simulation and spatial discretization or a combination thereof. These classifications are: non-particle tracking domain methods (the finite difference (FDM) and finite element (FEM) approaches); the particle tracking domain approach (the method of characteristics and the method of random walk); and non particle tracking boundary approach (the boundary integral technique). Section 3.2.1 reviews the previous applications of the first group (FDM and FEM) in solute transport analysis. Section 3.2.2 introduces the particle tracking techniques. Finally section 3.2.3 presents a review of the boundary integral method which is employed in this thesis. A summary of the commonly used analytical and numerical codes currently used in groundwater flow and solute transport analysis is also presented .

3.2.1 Non-particle Tracking Techniques in Solute Transport Analysis (the Finite Difference and Finite Element Methods)

The finite difference method (FDM) is the simplest and most popular of all the available numerical methods used in groundwater flow and solute transport analysis. The method

being conceptually straightforward and easy to understand, many groundwater flow and solute transport analysis codes in current use employ it. By discretizing the domain into elements (usually rectangular) the FDM can be easily used to compute required parameters by using simple mathematical concepts. Over the years, the FDM code have been advanced with different modifications. Well documented and powerful FDM computer codes now exist for 2-D and 3-D analysis. The 3-D finite difference groundwater flow code (MODFLOW) developed by U.S. Geological Survey (McDonald and Harbaugh 1988) and 2-D finite difference code (PLASM) developed by Prickett and Lonnquist (1971) are among the most widely used in the groundwater industry. However a major weakness of FDM is that it is restricted to rectangular grids (Figure 3.1). When the boundary of the domain is very irregular, cumbersome interpolations and extrapolations are required for accurate solution along the boundaries. Alternatively mesh sizes may be reduced to accommodate such irregular boundaries at the expense of computational cost.

The finite element technique was employed to overcome some of the weaknesses of the FDM. It was quickly realized that the FEM can handle media heterogeneity and irregular boundaries more efficiently than the FDM. By using different element types, mesh sizes and shapes (Figure 3.2) the domain can be conveniently discretized to reflect the changing parameter field and an irregular boundary. This leads to more flexibility and improved accuracy. Such advantages have attracted FEM application in contaminant transport analysis by many workers. Grisak and Pickens (1980) used the finite element method to model transport through both fractured and porous media. Bibby (1981) analyzed a two-

dimensional contaminant transport with the Galerkin FEM and showed its higher accuracy over FDM. The works of Huyakorn (1983), Voss (1984), Sudicky (1989), have demonstrated further advantages of FEM over FDM. with computer codes for 2-D and 3-D analysis of actual field problems.

The main disadvantages of both the FDM and FEM are that they are domain methods and therefore their application to even simple non-elliptic equations require the domain to be discretized. Domain methods do not reduce the dimensionality of the problem and therefore their computational implementation can be cumbersome especially for some 2-D and 3-D problems. The main disadvantage of these methods in their application to solute transport problems, is their inability to handle the dual nature of the governing equations efficiently. It has been found by many field and theoretical application of FDM and FEM codes that (Hamilton 1982, Sophocleous et al. 1982, Huyakorn et al. 1984, Beljin 1988) when the transport process is dominated by advection the methods are plagued by numerical difficulties such as artificial oscillations and numerical dispersion especially when Peclet numbers exceed 2 (in FDM codes) and 4 (in FEM codes). Beljin (1988) observed that the finite element techniques can produce superior accuracy in field conditions but the fine mesh sizes required to achieve this will be impractical for many large scale field studies. Although consistent efforts have been made to improve the accuracy and performance of these techniques over the years (e.g., Noorishad et al. 1992), recent field studies by Moltyaner et al. (1993) and theoretical works by Zheng and Bennett (1995) still confirm the existence of such difficulties.
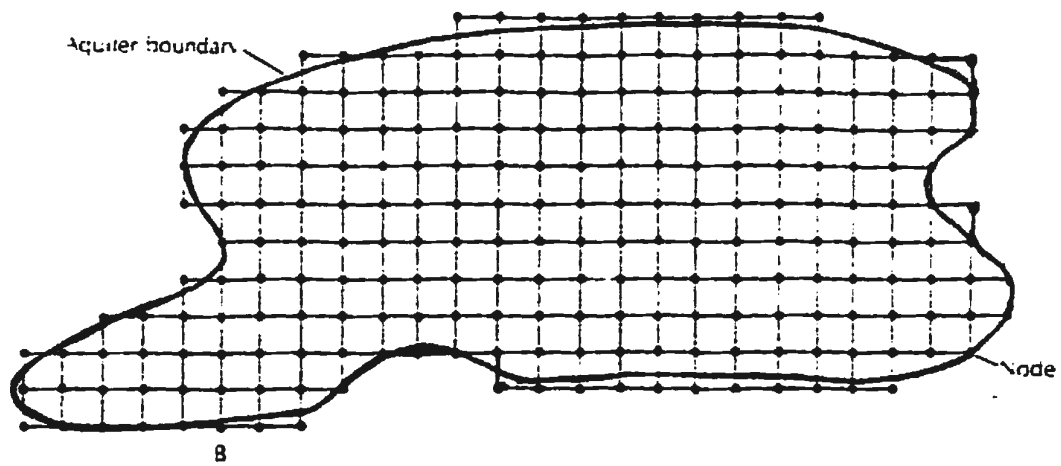
Figure 3.1: Domain discretization by the finite difference method (after Fetter 1988)
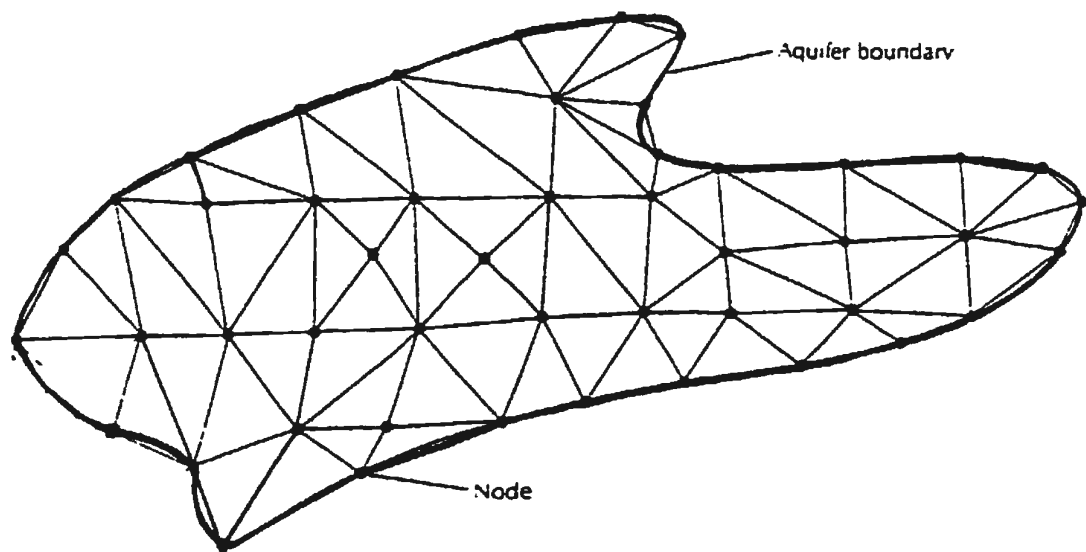
Figure 3.2: Domain discretization by the finite element method (after Fetter 1988)
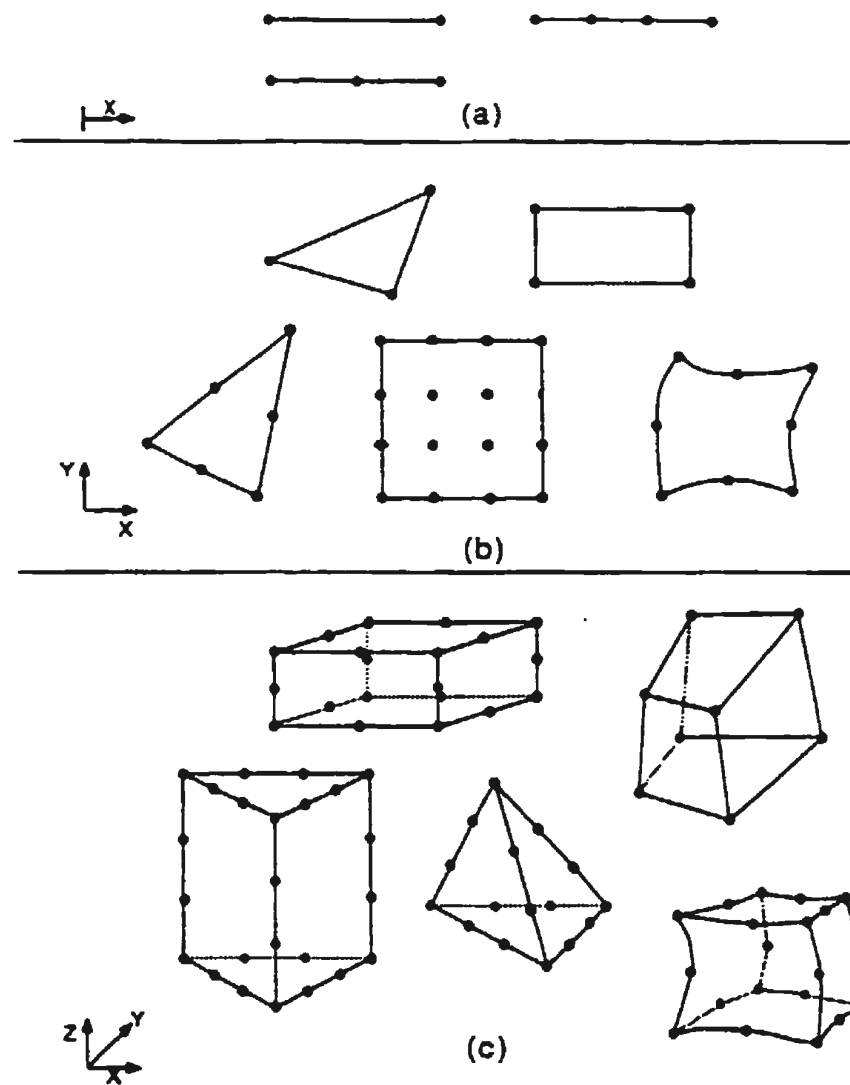
Figure 3.3 Different kinds of finite elements (a) 1-D, (b) 2-D, and (c) 3-D (after Bedient et al. 1994)

3.2.2 Particle Tracking Techniques in Solute Transport Analysis (the Method of Characteristics and the Method of Random Walk)

Alternative numerical solution techniques have been developed to overcome the difficulties encountered in advection dominated problems. Currently the most successful approach employs particle tracking to simulate the advective transport and a finite difference method to handle the dispersion process. Two of the most widely used particle tracking solution techniques based on the method of characteristics and the method of random walk are reviewed in this section.

The application of the method of characteristics (MOC) for transport in porous media was first proposed by Gardner et al. (1964) to overcome the numerical dispersion problems encountered by using the finite difference method. Since that time, MOC has been successfully used by many workers to simulate the transport of miscible compounds in groundwater (Bredehoeft and Pinder (1973), Konikow and Bredehoeft 1978). To efficiently handle the parabolic nature of the ADE when advection dominates, the method of characteristics splits the governing partial differential equation into simplified forms of ordinary differential equations by separating the advection part from the dispersion part. The procedure can be illustrated by considering the one dimensional form of the ADE as:

$$D_x \frac{\partial^2 c}{\partial x^2} - v_x \frac{\partial c}{\partial x} = \frac{\partial c}{\partial t} \qquad (2.26)$$

The approach employed by MOC is to split equation (2.26) into the following system of ordinary differential equations:

$$\frac{dx}{dt} = v_x \qquad (2.28)$$

$$\frac{dc}{dt} = D_x \frac{\partial^2 c}{\partial x^2} \qquad (2.27)$$

These two simplified equations are termed the characteristic differential equations of equation (2.26) and their solutions are called the characteristic curves. The mathematical development of this technique for transport problems in porous media can be found in Pinder and Cooper (1970), Bredehoeft and Pinder (1973) etc. By its mathematical nature it is efficient in solving parabolic problems and therefore is more compatible with advective dominated problems in solute transport (Konikow and Bredehoeft 1978).

In the numerical implementation of the solute transport equation, MOC employs a finite difference grid and a set of moving points or representative fluid particles moving at the average linear groundwater velocity (Figure 3.3). The initial procedure involves placing a number of traceable fluid particles in each of the reference finite difference grid. These form a set of points that are distributed in a geometrically uniform pattern throughout the zone of interest (Konikow and Bredehoeft 1978). The location of each moving point is specified by its coordinate in the finite difference grid and the number of fluid particles per grid simulates the concentration. The concentration at any location and time step is determined by the number of fluid particles in the element. MOC has achieved greater success in solute transport analysis in both theoretical and field scale applications to advection dominated transport problems. The U.S. Geological Survey two-dimensional code based on MOC (Konikow and Bredehoeft 1978) is perhaps the most widely used solute transport code in the groundwater industry (Beljin 1988). Due to its success in practical field problems, MOC codes have undergone tremendous improvement over the years, for example the modified method of characteristics (MMOC), (Chiang et al. 1989, Yeh 1990, Yeh et al. 1992) and the hybrid modified method of characteristics (HMOC) which is implemented in the solute transport code MT3D (Zheng 1990, 1993). The computational implementation of the traditional MOC code can however be cumbersome due to large number of particles generated in all the finite difference cells and also the fact that new concentrations must be assigned for every time step.
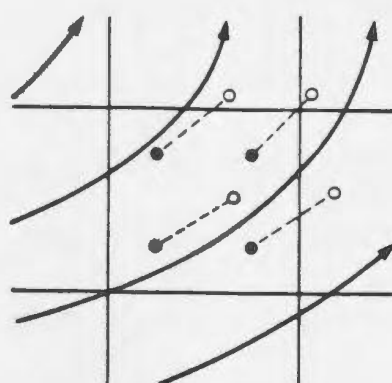
(a)

EXPLANATION

● Initial location of particle
○ New location of particle
➜ Flow line and direction of flow
--- Computed path of particle
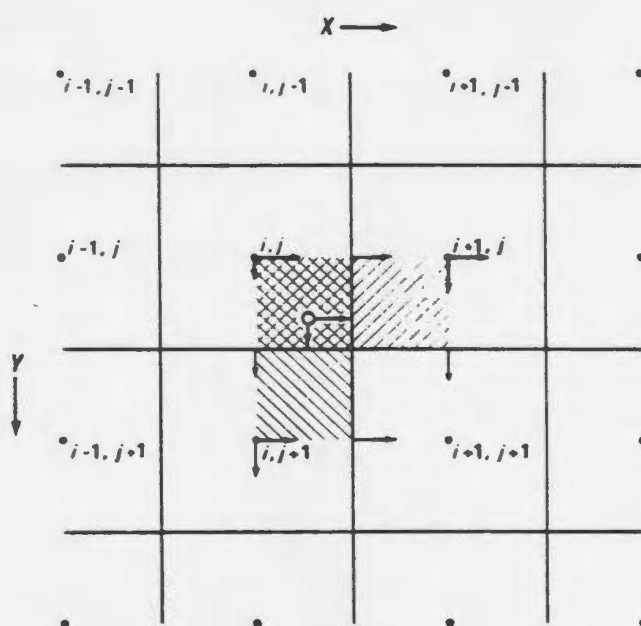
(b)

EXPLANATION

● Node of finite-difference grid
○ Location of particle p
➜ X or Y component of velocity

▨ Area of influence for interpolating velocity
in X direction at particle p

▨ Area of influence for interpolating velocity
in Y direction at particle p

Figure 3.4: Particle tracking process in MOC, (a) relation of flow field to movement of points, (b) finite difference grid (after Konikow and Bredehoeft 1978)

The method of random walk was proposed to improve the efficiency of the MOC. The technique is based on the concept that dispersion in porous media is a random process (Prickett et al. 1981). A finite difference grid is also employed in the particle tracking process. The advection term in the solute transport equation is simulated by particle tracking which moves with the average linear velocity. Unlike the MOC approach where each particle is assigned a concentration, the random walk assigns a fixed particle mass that represents a fraction of the total mass of solute injected. These particles are only assigned to the portions in the domain where concentrations are required to be computed. The hydrodynamic dispersion component is treated as a random process by using the procedure proposed by Bear (1972). The rationale behind this approach is illustrated by comparing the density function of a normally distributed random variable and the analytical solution of the one dimension solute transport equation (equation 2.26). The probability density function f(x) is given as:

$$f(x) = \frac{1}{(2\pi\sigma)^{1/2}} \exp\left[-\frac{(x-\mu)^2}{2\sigma^2}\right] \qquad (2.29)$$

where μ and σ are the mean and standard deviation of the distribution respectively. The analytical solution of the one dimensional solute transport equation is also given as (Bear 1972):

$$c(x,t) = \frac{1}{(4\pi \ D \ t)^{1/2}} \ \exp\left[-\frac{(x-V \ t)^2}{4 \ D \ t}\right] \qquad (2.30)$$

where $c(x,t)$ is the solute concentration, D is the hydrodynamic dispersion coefficient and V is the average linear velocity and t is the time. Prickett et al. (1981) observed that equations (2.29) and (2.30) are identical if $\mu = V \ t$ and $\sigma^2 = 2 \ D \ t$.

In the numerical simulation, particles in the finite difference cells are first moved by advection and then random displacements in the longitudinal or transverse direction are added to represent dispersion (Figure 3.4). Particle distributions around the mean are made to follow the normal distribution by use of random number generator. The locations of such particles can be up to six standard deviations of the mean. The concentration at a node (i,j) is computed by using the relation;

$$c_{i,j,k} = \frac{\Delta M \ N_{i,j,k}}{N \ \epsilon \ \Lambda_{i,j} \ \Delta x \ \Delta y} \qquad (2.31)$$

where ΔM is the total solute mass injected, N is the total number of particles, $N_{i,j,k}$ is the number of particles in the grid block (i,j) at the time k, and $\Lambda_{i,j}$ is the average saturated thickness of the block and ϵ is the effective porosity. By this technique no separate

dispersion equation is solved thus improving the efficiency greatly. This solution technique has been employed in solute transport analysis with success (e.g., Prickett et al. 1981, Moltyaner et al. 1993) especially for advection dominated solute transport problems. The TRANS model developed by Prickett et al. (1981), RAND3D (Koch and Prickett 1993) are all based on this technique.

According to Prickett et al. (1981) the random walk approach has several advantages over MOC. Some of these are that only one finite difference grid is involved in solving the advective portion and the particle movement takes place in a continuous space; concentration distribution is calculated only when needed and particles are specified only in areas of interest. A major weakness of this approach is that, it may require a large number of particles to achieve an acceptable result. However, Prickett et al. (1981) has suggested that up to 5,000 particles are sufficient to produce the accuracy required for many engineering problems.

In a recent application of different numerical solute transport codes to field problems Moltyaner et al. (1993) confirmed the accuracy of these particle tracking methods over the finite element method especially for advection dominated problems. The random walk method for example was found to be free from numerical dispersion (Figure 3.5) showing the remarkable improvements in subsurface solute transport modelling. However, these particle tracking approaches also have the disadvantage of domain methods and require significant input data preparation time and high computational effort. In addition, the

particle tracking methods have been found inefficient when it becomes necessary to track large number of particles (low advective transport or dispersion dominant flow) and usually lead to mass balance errors. Zheng and Bennett (1995) explained that such difficulties arise because this approach is not based entirely on conservation of mass. They also observed that since the random walk method is based entirely on moving particles it gives numerical difficulties in the presence of irregular spatial discretization.

Recently some workers have attempted the use of finite volume method to achieve mass conservation and and at the same time handle advection dominated transport efficiently. The method is also a domain approach which may be implemented on a finite difference or finite element setting. An important component of this aproach is that the integral representing the mass-storage term is evaluated numerically at the current time level. Intergration points and the mass associated with this are then forward-tracked up to the next level and it is able to achieve accurate results at low and high Peclet numbers. Celia et al. (1990) employed this technique for a theoretical study of the advection-diffusion equation. Healy and Russel (1992), proposed a finite volume Eulerian-Lagrangian adjoint method for solving a one dimensional advection dispersion equation.

A major disadvantage of this technique is that it is cumbersome for even a one-dimension problem. The number of integration points required to reach a specified level of accuracy increases as the problem dimension increases and its effciency is also problem-dependent hence not suitable for many field problems.

$$d_L > 0$$
$$d_T = 0$$

Old particle position xx,yy

$$DY = V_y \cdot DELP$$

$$DD = \sqrt{DX^2 + DY^2}$$

$$DX = V_x \cdot DELP$$

CONVECT

σ_L

$$\sigma_L = \sqrt{2d_L DD}$$

DISPERSE RL·DD

RL·DY

RL·DX

New particle position xx,yy

Where:

$$RL \cdot DD = \sqrt{2d_L DD} \ ANORM \ (0)$$
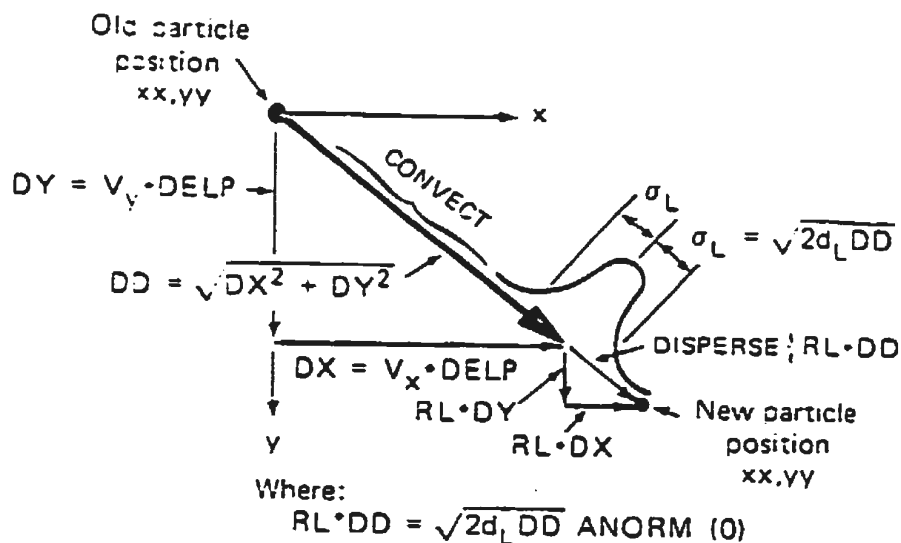
New position	=	Old position	+	Convection	+	Dispersion
xx	=	xx	+	DX	+	RL·DX
yy	=	yy	+	DY	+	RL·DY

(B) TRANSVERSE DISPERSION

$d_L = 0$ (to avoid a zero divide in code —
$$DISPL = 10^{-30})$$
$$d_T > 0$$

Old particle position

$$DX = V_x \cdot DELP$$

CONVECT

$$DY = V_y \cdot DELP$$

DISPERSE RT·DD

—RT·DX

$$DD = \sqrt{DX^2 + DY^2}$$

RT·DY

$$\sigma_T = \sqrt{2d_T DD}$$

σ_T

Where:

$$RT \cdot DD = \sqrt{2d_T DD} \ ANORM \ (0)$$
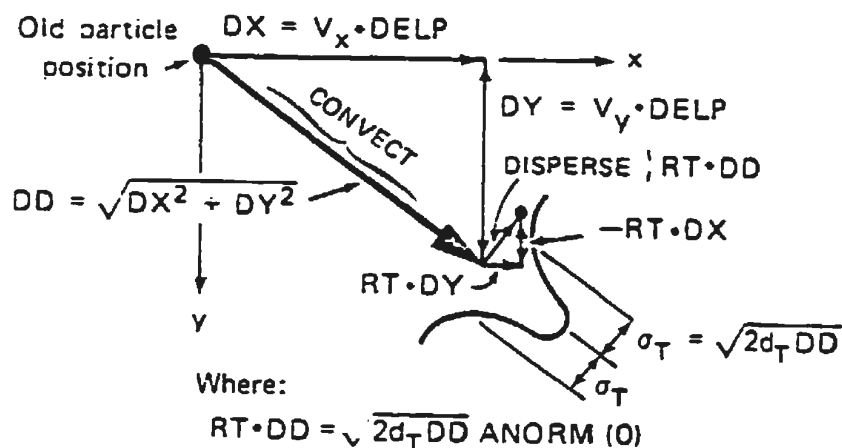
New position	=	Old position	+	Convection	+	Dispersion
xx	=	xx	+	DX	+	RT·DY
yy	=	yy	+	DY	−	RT·DX

Figure 3.5: Particle movement due to advective displacement and random displacement in the longitudinal and transverse directions in the Random Walk method (after Prickett et al. 1981)
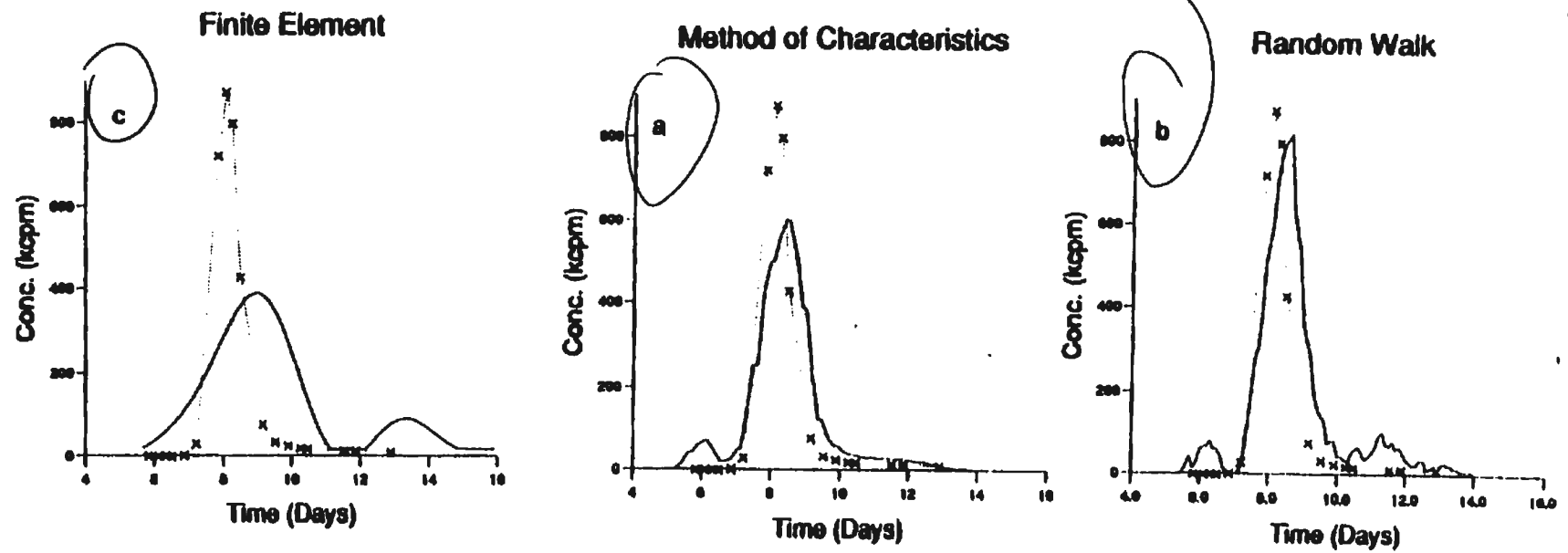
Figure 3.6: Comparison of measured breakthrough curves (dotted lines) and numerically

simulated results (solid lines) from MOC, Random walk and FEM numerical codes for

field problem (after Moltyaner et al. 1993)

3.2.3 Non-Particle Tracking Boundary Only Techniques in Flow and Transport Analysis (the Boundary Integral Equation Method)

An alternative numerical solution technique that has not gained much attention in contaminant transport analysis is the boundary integral equation method (BIEM, also known as boundary element method (BEM)). BEM has been used in many engineering applications and model studies involving complex boundary value problems. The BEM possess many of the useful advantages listed under the FDM, FEM and MOC in addition to other advantages. First, by modelling only the boundary (Γ) of the system domain (Ω) (Figure 3.7), BEM reduces the dimensionality of the basic problem by one. Second, the accuracy of this method has been found to be higher (Liu and Liggett 1978, Taigbenu and Liggett 1986, Haie et al. 1993, 1996) than FDM and FEM for solution of similar problems. Some of the previous applications of BEM in flow and solute transport analysis are reviewed in this section.
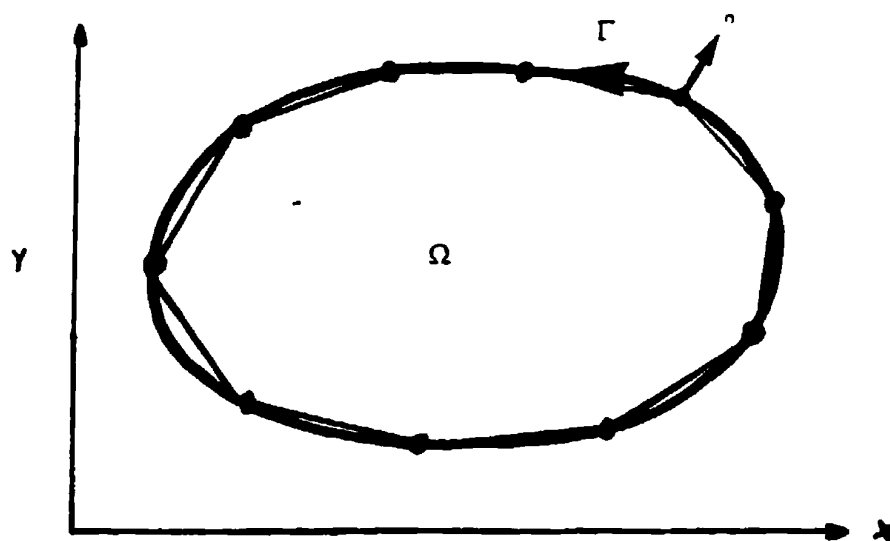
Figure 3.7: Descretization of problem domain with linear boundary elements

The first application of the boundary integral method to flow in a porous medium was carried out by Liggett (1977). The method was used to solve two-dimensional free surface problems that were governed by Laplace equations. It was especially found to be convenient for free surface problems since the nodal points could be made to represent the surface as desired. Liu and Liggett (1979a, 1979b) extended the study to model unsteady flow in confined aquifers by proposing two solution approaches: the Laplace transform solution and the direct Green's function solution. Following their convincing results some workers directed attention to this numerical technique for various groundwater flow problems.

Lennon et al. (1979a, 1979b) proposed a method for solving axisymetric potential flow problems based on BEM. The numerical technique was first used to compute uniform potential flow in a circular pipe and then the method was extended to solve both steady and transient axisymetric recharge flows and well flows in porous media. The results from this method compared well with the analytical solutions of Dagan (1967).

Lennon et al. (1980) extended this idea to formulate a boundary integral equation method for solving three dimensional potential flow problems in a porous media for three different cases: groundwater recharge in an aquifer of infinite depth and horizontal extent; an aquifer of finite depth; and a steady state flow from a pond through a homogeneous porous material. The BEM results from these were also found to be in close agreement with their

analytical solutions.

Taigbenu (1985) employed BEM to solve confined and unconfined flows in aquifers by proposing a modified formulation termed the Poisson formulation. The method used the fundamental solution of the highest order derivative terms and cast them into boundary integral using Green's second identity while the remaining terms remain as domain integrals. Several advantages over FEM were observed in terms of accuracy, computer time and data preparation.

Cheng and Lafe (1991) applied the integral equation technique for solving the stochastic boundary value problem in groundwater flow. The aquifer parameters like hydraulic conductivity was considered to be deterministic while the boundary conditions and domain recharge were assumed to be random. The application of the techniques to two examples produced good results that compared well with their exact solutions. The applications of the BEM approach to groundwater flow have demonstrated the efficiency of the method, however fewer applications have been made to solute transport analysis which are discussed next.

Fodgen et al. (1988) made a specific application of boundary element method to solve a steady state transport of reactive solutes through a fractured porous medium. The two dimensional model was based on the assumption of steady vertical groundwater flow through the fracture and in the porous matrix. Contaminant diffusion was however

assumed to occur in both vertical and horizontal directions. Corresponding Green's functions were constructed for both matrix and fractured regions. By applying the appropriate boundary conditions, the flux at the fracture matrix interface was obtained in the form of a Fredholm integral equation of the first kind. The numerical solution then involved the discretization of the domain and its boundary. While their approach was a very useful effort in the boundary element formulation, their overall procedure as admitted by the authors was cumbersome and computationally expensive.

A two dimensional BEM model was proposed by Leo and Booker (1993), to analyze contaminant transport in fractured media having a two or three dimensional orthogonal fracture network. The formulation was based on the assumption that contaminant transport occurred through the fractures while diffusion occurred through the low permeable matrix. In their approach, a series of Laplace and Fourier transformations were employed and the governing equation was transformed to a modified Helmholtz type. The fundamental solution satisfying the self adjoint modified Helmholtz equation was then derived and used. The concentrations in the time domain were obtained by using a special inversion technique. The solution technique was tested with two idealized examples and the results were compared with a semi-analytic solutions proposed by Rowe and Booker (1990). This procedure was then extended to a parametric study of contaminant behaviour in a deeply buried rectangular repository. Although their theoretical study demonstrated several advantages and the accuracy of the BEM, they failed to extend it to field problems.

Several theoretical applications of BEM to a variety of problems in other areas of engineering have demonstrated the efficiency of the method. For example Brebbia and Wrobel (1987), Partridge et al. (1992), have obtained convincing results at higher Peclet numbers for heat conduction problems. The potential success of the method in handling the dual nature of the equation was also demonstrated. The boundary element method can now be used to solve problems successfully at Peclet numbers over 20 (Brebbia 1996, personal communication). In spite of the advantages of BEM over other numerical techniques its conventional application to many engineering problems pose some difficulties. In general, the mathematical procedure is more involving than the FDM and FEM. In its application to non-elliptic equations the luxury of employing Green's identities to cast the equations into boundary only integrals is lost due to the non homogeneous terms (body forces). Fundamental solutions have to be derived to provide a boundary only solution which are very cumbersome and may not even be possible for some non-linear problems. The traditional approach for dealing with body forces is to discretize both the boundary and the interior of the domain (Figure 3.8) and then employ a finite element type of technique to evaluate internal solutions. Such approach has been employed by workers including Lennon et al. (1980), Lafe et al. (1981). Although accuracy of the results remain high the use of internal cells reduces its major advantage over domain methods such as FDM and FEM. In the application of BEM to contaminant transport problems the body forces result from the temporal derivatives and the advective terms. There has been recent efforts to improve the efficiency of the BEM by using simpler approaches and also to avoid domain integration. Some of these are reviewed next.
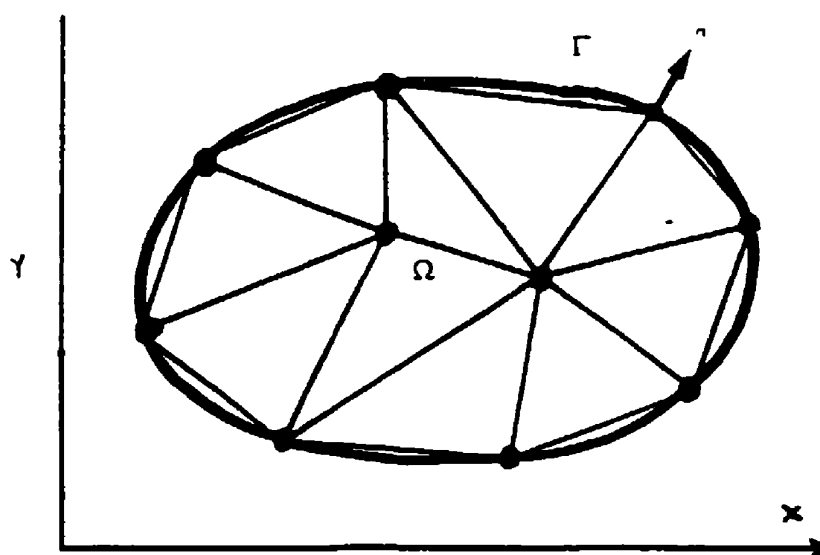
Figure 3.8: Discretization of problem domain with boundary elements and internal cells

3.2.4 Recent Improvements in the Boundary Element Technique

Matsumoto et al. (1990), employed the boundary element method for the transient analysis of scalar wave equation by first transforming it to a modified Helmholtz type. The BEM formulation then employed an approximate fundamental solution corresponding to the Laplacian part of the equation and the extra terms were treated as domain integral. The method was applied to two problems (wave propagation problems in a square plate and transient vibration of a circular membrane) with convincing results. A useful feature in their approach was the use of the simpler fundamental solution of the Laplace equation instead of deriving a more cumbersome fundamental solution. In spite of this their approach involved domain discretization.

Ingber and Phan-Thien (1992) proposed a boundary element approach for parabolic differential equations using a class of particular solutions. Their method generally avoided domain integration by use of particular solutions. In their approach a generalized forcing function was selected and then expressed in terms of radial basis functions. Two methods were proposed in solving time-dependent problems. The first method combines the forcing function with the time derivative term into a generalized forcing function. Then " using a transformation of variables involving an approximate particular solution the original problem was transformed into solving a sequence of Laplace equations" (Ingber and Phan-Thien 1992). In their second approach the problem was transformed into a sequence of modified Bessel equations that can be cast into boundary integrals using BEM.

The two methods were tested alongside with the conventional domain integral method by applying to sample problems. The inaccuracies observed in their results were attributed to the difficulty of selecting the radial basis functions.

Nowak and Brebbia (1989) proposed a more efficient procedure called the multiple reciprocity method (MRM) to convert domain integrals to the boundary in order to fulfil the boundary only formulation required of the BEM. The method generally treats the non Laplacian terms of the governing equation as a generalized body force. The resulting domain integration is then converted to the boundary by using higher order fundamental solutions. The combination of higher order fundamental solutions and a sequence of body force Laplacians lead to an exact form of boundary only formulation. Nowak and Brebbia (1989) employed this technique to solve thermal problems and other problems governed by Helmholtz equations with great success. A major disadvantage of this approach for general application is the need to derive higher order fundamental solution for the particular problem at hand. The derivation of higher order fundamental solution can be very tedious for many problems.

The most general approach to avoid domain integral was proposed by Nardini and Brebbia (1982) called the Dual Reciprocity Method (DRM). The method was first proposed for solution of elastodynamic problems and later extended to time dependent problems by Wrobel et al. (1986). The approach is essentially a generalized way of constructing particular solutions. In this approach an approximating function F is sought such that its

Laplacian is equal to a set of selected interpolation functions. The nonhomogeneous term is then written as a linear combination of approximating functions F_j which are linked by series of particular solutions. By choosing a suitable radial basis function for F_j, the particular solution can be evaluated. Thus a nonhomogeneous equation can be transformed to a homogeneous one which can be discretized on the boundary alone by using a standard BEM discretization procedure. The major advantage over MRM and other hybrid approaches is that, any suitable fundamental solution can be employed. DRM has been applied successfully to many engineering problems in heat transfer and recently to groundwater flow analysis in porous media by El Harrouni et al. (1992). Haie et al. (1993) made a theoretical comparison between DRM and FEM in solute transport analysis and obtained closed agreement in results. Another theoretical comparison of DRM, FEM and FDM was made by Haie et al. (1996) and the DRM approach was claimed to give the most convincing results in terms of accuracy and efficiency. However, this study only compared two theoretical problems and did not demonstrate the full potential of the method over a wide range of problems or field application. As a result of its flexibility the DRM approach will be employed in this thesis to demonstrate both the theoretical and practical potential of the BEM in solute transport analysis.

3.4 Summary of the Mathematical Solution Methods Used in Previous Studies

This section has reviewed the mathematical solution techniques commonly used in groundwater flow and contaminant transport analysis. A brief discussion was given on the application of analytical techniques. The numerical solution methods so far discussed are the finite difference method, the finite element method, the method of characteristics, the method of random walk and the boundary element method. In general, the numerical solution of the groundwater flow equation does not pose problems to any of the solution schemes discussed. The accuracy and efficiency of any of these techniques is satisfactory but perhaps the finite difference method which is the simplest may also be the easiest to use for such analysis. However the solution of the solute transport equation poses a great challenge to all the numerical techniques discussed.

The solution methods for the solute transport equation were classified into three groups based on their simulation technique and method of discretization. The non particle tracking techniques are efficient for dispersion dominated problems and less efficient for advection dominated problems. The particle tracking techniques are efficient for simulation of advection dominated problems and less efficient for dispersion dominated problems. It must be pointed out that all the particle tracking techniques also employ the finite difference technique. The boundary element technique although have not been

widely employed in solute transport analysis, seem to be a balance between these two groups in terms of handling the dual nature of the equation. The numerical schemes in the first two categories are all domain methods and their solution involves the discretization of both interior and the boundary of the domain and this makes their application computationally intensive. Only the BEM has the ability to simplify the dimensionality of the problem with increased computational advantage. All of these techniques are however under intensive research to improve their accuracy and overcome the difficulties involved in their application.

Beljin (1988) made a systematic comparison of numerical solute transport codes based on three numerical solution schemes; FEM, MOC and random walk. He observed that although the finite element method produced superior accuracy in dispersion dominated problems, the fineness of mesh sizes required to achieve this may not always be feasible for many practical problems. MOC and random walk have superior practical application over FEM for advection dominated problems. In general the MOC model proved superior to all the others solution techniques for most of the theoretical and practical applications. The random walk model was accurate in determining the concentration front but less accurate in computing the magnitude of the concentration at a point in the domain. In recent application of numerical models to field studies, Moltyaner et al. (1993) observed a better results from MOC and Random walk than the FEM codes. Zheng and Bennett (1995) have also observed that although MOC and Randomwalk approaches offer significant improvements, they are still not very efficient when advection is low or

dispersion is dominant. The authors explained that such difficulties are due to the fact that these particle tracking methods are not fully based on the mass balance concept .

The literature on current numerical solution codes on solute transport frequently used in the industry was reviewed by using manuals and catalogues obtained from the international ground water modelling centre (IGWMC-USA). It was observed that none of the widely used codes is based on the boundary element method in spite of its known advantages. Although this list is not exhaustive it points to the fact that the few applications of the BEM in this area have been restricted to theoretical analysis and hence the full potential of the available numerical techniques has not been exploited. Table 1 is a summary of some analytical and numerical codes extracted from the IGWMC software catalogue (Van der Heijde 1994).

Table 3.1: Summary of some commonly used groundwater flow and solute transport codes

(after IGWMC- Van der Heijde 1994)

Code name	Problem type	Solution method	Author(s)/developer(s)
MODFE	flow	FEM	Cooley R.L. & Torak L.J. (USGS-USA)
GWFLOW	flow	analytical	Van der Heijde, P.K.M. (USGS)
VERTPAK-1	flow/transport	analytical	Intera Enivron. Inc. (USA)
TRAFRAP-WT	flow/transport	FEM	Huyakorn et al. (IGWMC-USA)
AGU-10	flow/transport	analytical	Javandel et al., and Beljin, M.S., (USA)
FLONET	flow	FEM	Waterloo Hydrogeol. Software-Canada
FLOWPATH	flow	FDM	Waterloo hydrogeol Software-Canada
MODFLOW	flow	FDM	McDonald, M.G. & Harbough, A.W. (USGS-USA)
PLASM	flow	FDM	Prickett, T.A. & Lonnquist, C.G. (USA)
SUTRA	flow/transport	FEM	Voss, C.I. (USGS-USA)
FLOWCAD	flow	FDM	Waterloo Hydrogeol Software Canada
SOLUTE	transport	analytical	Beljin, M.S. (IGWMC-USA)
PLUME2D	transport	analytical	Van der Heijde, P.K.M (USA)
AT123D	transport	analytical	Yeh, G.T. (-USA)
HST3D	flow/transport	FDM	Kipp, K.L. (USGS-USA)
MOC	flow/transport	MOC	Konikow, L.F. & Bredehoeft,J.D.(USGS USA)
MT3D	transport	MOC	Zheng, Z (Papadopulos & Assoc. - USA)
RANDOM WALK	flow/transport	random walk	Prickett T.A. et. al., (Illinois State Water Survey-USA)
MOCDENSE	flow/transport	MOC	Sanford, W.E. and Konikow, L.F. (USGS-USA)

3.5 Some Field Studies on Subsurface Solute Transport

The common approach in the physical modelling of contaminant transport in groundwater is by laboratory experiments. Most of the theories developed for the understanding of solute transport processes were based on laboratory studies. In recent years the demand for improved modelling methodology has led to the extension of laboratory investigation methods to the field. In fact proper field studies on the contaminant transport process is indispensable for the theoretical and mathematical understanding required to meet our current demand for groundwater quality assessment. The literature is still deplete of physical modelling involving field experiments in this area. In a comprehensive review of the literature on field scale transport studies around the world, Gelhar et al. (1985) observed that, out of 55 sites where dispersive studies have been conducted, only five yielded dispersivity values that could be considered reliable. They further noted that, among these five, only one, Sudicky et al. (1983) involved a natural gradient tracer test. Since 1985, there has been an increase in field studies (Gelhar et al. 1992) and some of the successful ones that have provided useful results are reviewed next.

One of the most successful field tracer experiments to date was conducted by Mackay et al. (1986) at a site in Borden, Ontario, Canada. The experiment was conducted in an unconfined sandy and gravel aquifer underlained by a thick silty clay deposit. The primary aim was to assemble a database for developing and validating mathematical models. Sutton and Barker (1986) also conducted a similar experiment in the same type

of aquifer close to the Borden site. In another comprehensive field study Leblanc et al. (1991) conducted a natural gradient tracer experiment in an abandoned gravel pit in Cape Cod, Massachussetts, U.S.A. to examine the transport mechanisms of solutes. A similar large scale experiment was also conducted by Boggs et al. (1992) in an alluvial deposit in Columbus, Mississippi-USA.

All these are well known successful large scale field experiments that have provided significant insights in to the solute transport process and a large database that are still used in numerical investigations. However, they all have one thing in common. They have been conducted in aquifers made up of glacio-fluvial deposits and sands therefore their findings may be only significant to such aquifers. Their findings are usually not applicable to aquifers located in other types of subsurface media such as fractured formations.

To date the most comprehensive field study of solute transport in fractured formations involved a natural gradient tracer experiments performed by Neretnieks (1987), Abelin et al. (1991) in the Stripa mine in Sweden. Several findings on the flow behaviour in fractures were revealed which led to the concept of channel flow model (Tsang et al. 1991). However these experiments have been conducted in very deep formations over 100 meters with the primary aim of exploiting such areas for the storage of radioactive waste. The behaviour of fractures under such conditions may not be similar to those in shallow aquifers usually of interest to potable groundwater assessment. There has also been field tracer experiments in shallow aquifers reported in the literature, Raven et al., (1988),

Novakowski and Lapcevic (1994, 1996). However these workers have also employed induced-gradient or forced advection tests. While this approach is very economical, it does not mimic the natural transport behaviour of solutes that are observed with time and in space. Raven et al. (1988) observed that induced gradient tests were likely to underestimate dispersive characteristics of fractures under natural flow conditions. At the moment knowledge of solute transport in shallow fractured aquifers severely lack behind required knowledge. The need for comprehensive field studies on different subsurface media especially those in fractured porous formations that supply potable water has been a major recommendation by many authors.

Chapter 4

The Field Experimental Study

4.1 Introduction

This chapter presents the experimental field study of the hydraulic behaviour and solute transport mechanisms in a typical aquifer in the vicinity of St. John's, Newfoundland. The various sections present a detailed description of the experimental site, the site geology and hydrogeology and the experimental procedures involving in situ permeability testing, groundwater level monitoring, and two natural gradient tracer experiments. The conceptual, qualitative and quantitative insights obtained from this investigation are also presented. The site investigation was thought necessary to help understand the mechanisms that contribute to the transport of contaminants in groundwater. Practical field data will also be available for testing numerical models for solute transport analysis in this type of aquifer.

4.2 General Location and Description of the Test Site

A detailed description of the experimental site can be found in Ivany (1994), but will be summarized here for completeness. The site is located on 47° 31 north and 52° 47 west of St. John's, in the Avalon Peninsula of the province of Newfoundland, Canada (Figure 4.1). The site is part of the Agriculture Canada Research Station situated within the Waterford River basin (approximately 61 km^2 in area) and on the eastern boundary of the city of Mount Pearl. The test site covering an area of approximately 1.6 hectares has been previously used by Ivany (1994) for the study of agricultural waste infiltration into the groundwater. The surface grades gently towards the Waterford River Valley and hence surface drainage flows in that direction. Figure 4.2 shows location maps of the site and test area marked plot 7B.

The climate of the Avalon Peninsular is very much influenced by the cold Labrador current from the Arctic circle and to a lesser extent by the warm Atlantic drift. The local weather pattern is controlled by the numerous bays and inlets with little evaporation and general cooling effects caused by the prevailing westerly and south easterly winds in the region. Solar and terrestrial radiation is greatly reduced by frequent cloud cover and fog in many times of the year. Mean annual temperatures are about 5°C with average yearly precipitation of 1595 mm (Ivany 1994).
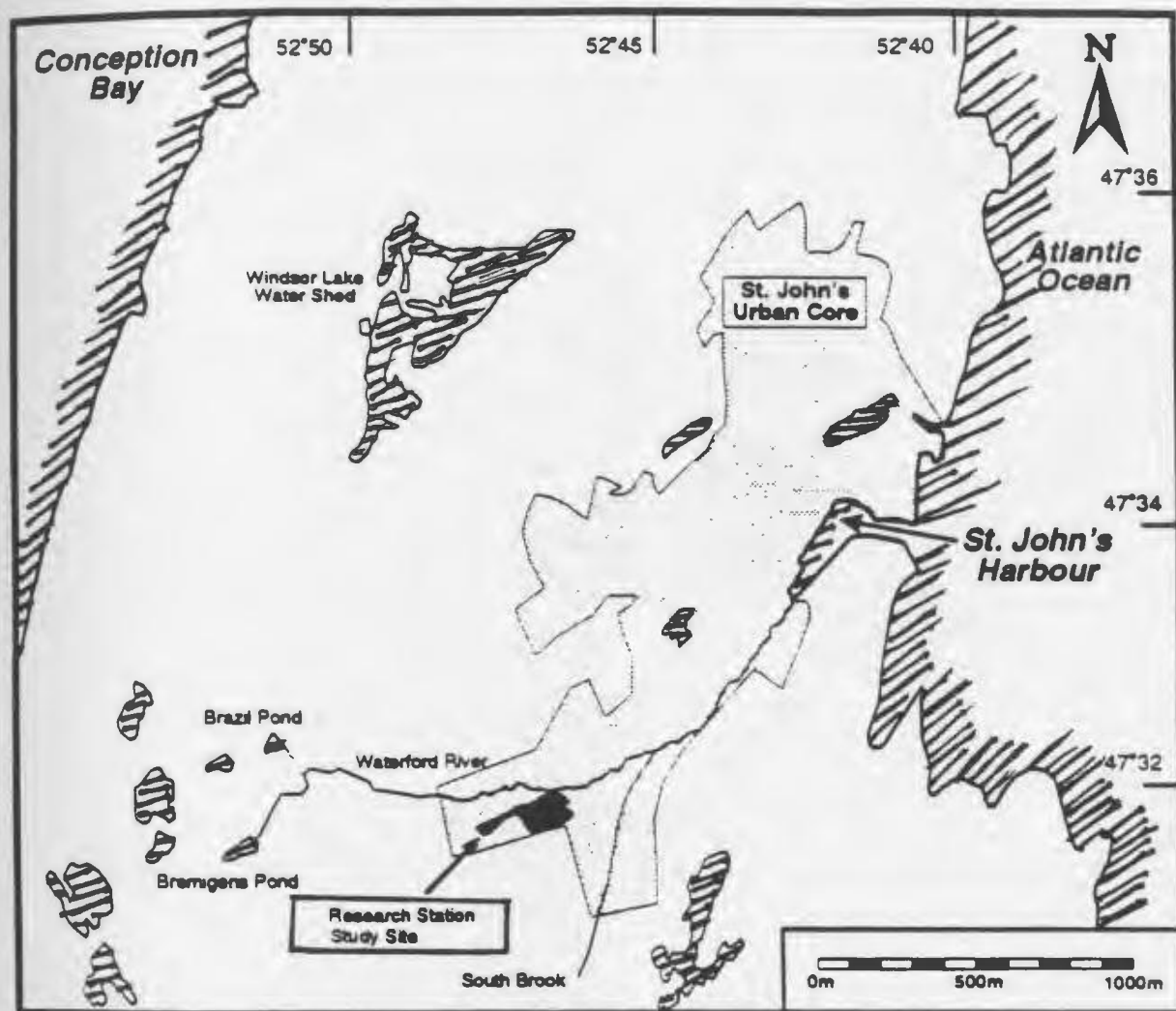
Figure 4.1: General location of the experimental site (after Ivany 1994)
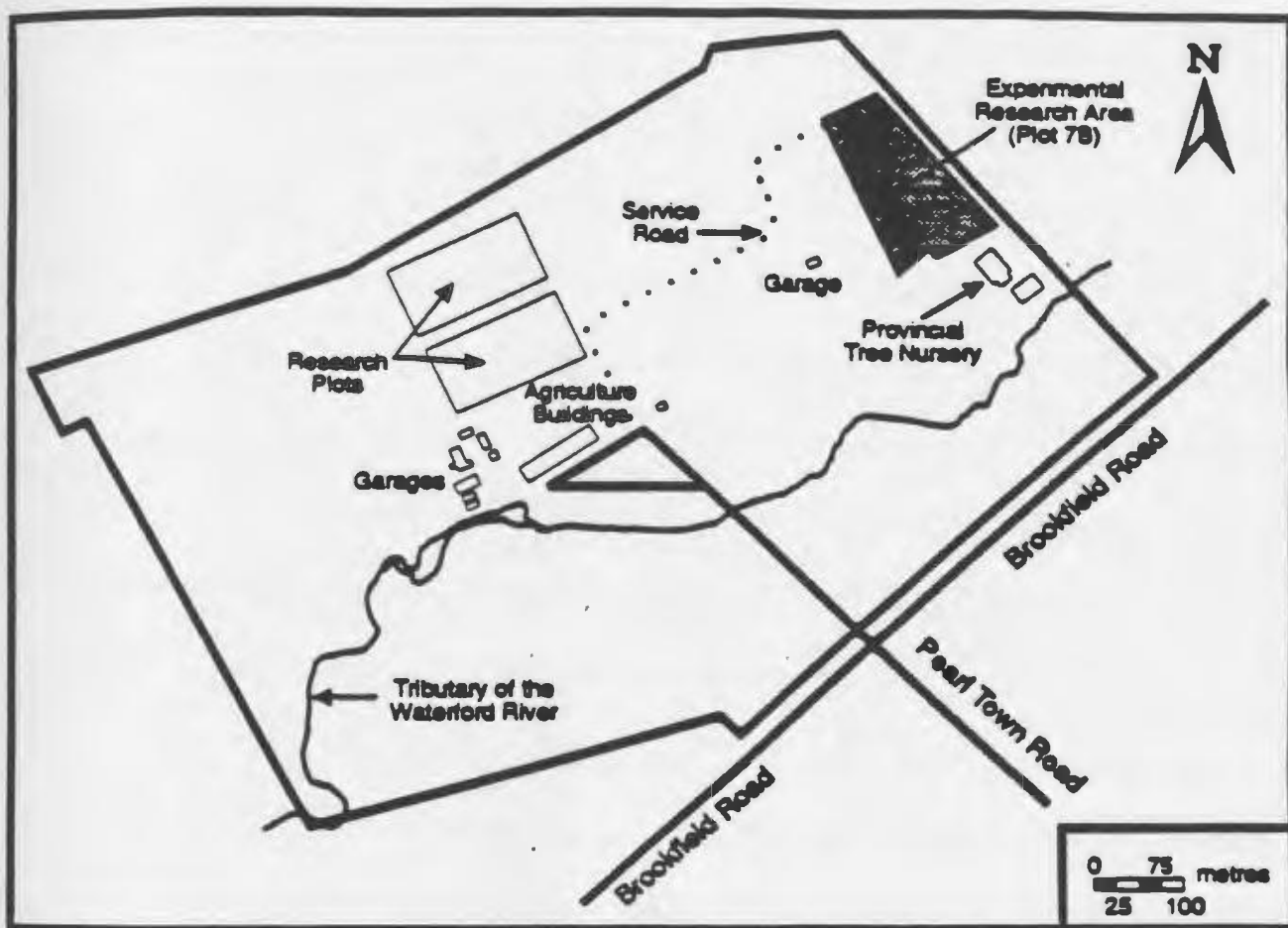
Figure 4.2 Layout of the experimental site (after Ivany 1994)

4.2 Surficial and Bedrock Geology

The surficial and bedrock geology of the Avalon Peninsula has been a subject of intensive study over the past twenty years (Batterson 1984, King 1990). The general geological structure consists of a thin overburden underlain by fractured sedimentary bedrock. The surface mantle overlying the bedrock is of glacial origin. Batterson (1984) has observed that in general the overburden is dense and poorly sorted with very little clay content. Glacial loading is known to have caused the overconsolidation of this layer resulting in hydraulic conductivity values lower than similar tills. The thickness of the overburden is less than three meters in many places. In a detailed geotechnical investigation conducted on the overlying glacial till at the test site Ivany (1994) obtained average values of specific gravity of 2.63 and in place bulk densities of 1.69 g/cm^3 respectively. Analysis of particle distribution suggested that the overlying till material is poorly sorted with little or no fines. Such findings confirmed the general observations reported by Batterson (1984) and King (1990).

The bedrock geology in the Avalon Peninsula has also been studied in detail by King (1990). The underlying bedrock is known to consist of a thick sequence of precambrian volcanic and sedimentary rocks and trace fossils forming a typical feature of the Atlantic realm. The bedrock geological structure consists of thick relatively unmetamorphosed precambrian succession. The St. John's area is located in one of the four main geological

classifications called the St. John's group. This constitutes a continuous conformable sequence of grey to black cleaved shales and grey buff sandstones throughout the Avalon Peninsula (King 1990). The St. John's group has sub-classifications according to local variation of their internal structure. The experimental site is located in one of these called the Fermeuse formation which is generally composed of grey to black shales, sandstones and siltstones. Numerous sedimentary and tectonic faults are known to complicate the internal structure of the Fermeuse formation . The bedrock is characterized by major plumbing folds, bedding planes and fracture zones with slaty cleavage (King 1990). Observations from road cut surfaces and rock outcrops near the site show the extent of fracturing and the random nature of the fracture orientations. The mineralogical composition of the Fermeuse formation consist of albite and quartz with traces of calcite and dolomite (King 1990).

4.3 General Site Hydrogeology

The site hydrogeology is influenced by the surficial and bedrock geology described above. The thin, compact, poorly sorted overburden with little clay content in general does not exert critical influence on the ground water regime in the area except for local hydraulic recharge. However, the well cemented bedrock characterized by slaty cleavage controls the hydrogeologic pattern by acting as the main conduits for groundwater movement. The primary porosity of the bedrock material in this area is very low. Gale et al. (1984) noted that sedimentary bedrock units in this area are very well cemented giving rise to low

giving rise to low primary porosity and permeability values close to those of metamorphic and granitic rocks. In general, the hydraulic characteristics are highly influenced by the inter-connection of the different joints and open bedding planes which form conduits for groundwater movement. An aquifer pumping test was conducted in wells located very close to the site by Gale (1993, personal communication). Using well log and drawdown data the fractured bedrock aquifer at the test site was classified as confined with little K value. It was noted that the fractured aquifer is sandwiched between low permeable basal till on top and impermeable black argillite rocks at the base. The thickness of the aquifer at the pumping location was estimated to be 3.6 m thick. As a result of the lesser influence of the overburden on the general hydrogeology of the area most of the present study reported in this thesis was focused on the solute transport behaviour in the bedrock.

4.4 In Situ Assessment of Site Hydraulic Characteristics

4.4.1 Hydrogeologic Testing and Monitoring

A preliminary assessment of the hydraulic characteristics of the test site was conducted using in situ tests in monitoring wells. There were twenty five standing pipes installed at the site as part of the study performed by Ivany (1994). This initial study involved in situ testing for hydraulic conductivity, groundwater level monitoring and study of background chemistry of the existing groundwater. The purpose of this was to provide an estimate of

aquifer parameters that will help to predict the rate and direction of tracer movement and also understand the groundwater chemistry. A number of falling head permeability tests were performed. Data from these tests were analyzed using conventional Hvorslev shape factors and the direct method proposed by Chapuis et al. (1981). Hydraulic conductivities obtained for the overburden glacial till ranged from 1.5×10^{-4} to 5.5×10^{-4} cm/s. However estimates of hydraulic conductivities obtained by using the piezometers installed in the bedrock was found to vary over a range of 3 orders of magnitude (from 10^{-4} to 10^{-7} cm/s). Statistical analysis were performed and the hydraulic conductivities were found to follow a lognormal distribution. The geometric mean of 6.0×10^{-5} cm/s was obtained and the coefficient of variation was found to be greater than 1.0. There were distinct variations in hydraulic conductivity values measured in the fractured bedrock across the site. Based on the hydraulic conductivity distribution the site was divided into two parts, the northern part and the southern part (Figure 4.3). The values from northern part were consistently higher than southern part. A geometric mean of 2.6×10^{-4} cm/s was obtained for the north compared to 1.0×10^{-5} cm/s for the south. However one monitoring well (#13) located on the northern part indicated a hydraulic conductivity value (1.1×10^{-5} cm/s) close to the average value for the southern part. A summary of the hydraulic conductivity distribution across the site can be found in Appendix A, (Table A1).
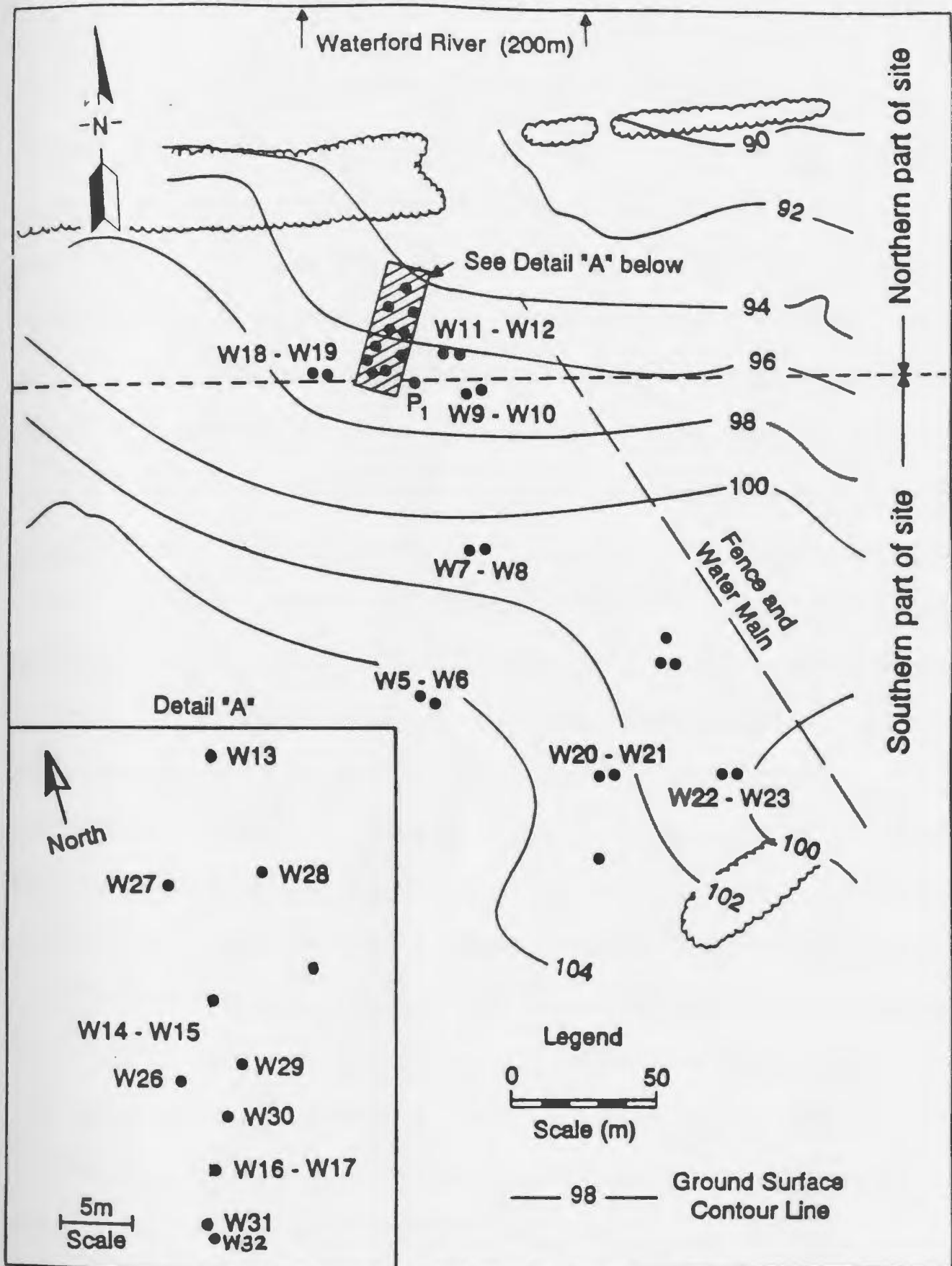
Figure 4.3: Layout of the experimental site showing the northern and southern parts (after Amoah and Morin 1996a)

The surface topography of the northern part was found to be more uniform with gentle gradient and was selected to be the location of the natural gradient tracer experiment. The northern part was therefore monitored more frequently for hydraulic heads during the period of the study. Groundwater levels obtained between October 1994 and December 1995 were analyzed. Hydrographs were constructed and compared with those obtained by Ivany (1994) for the year 1992. The potentiometric surface was found to fluctuate due to the seasonal variations in precipitation and recharge. It was observed that most of the recharge occurred in late fall in response to higher precipitation and in the early Spring in response to snow melt from the winter season (Figure 4.4). The potentiometric surface drops in the summer months and reaches a minimum in August. In Fall, the potentiometric surface rises again after high precipitation recharge in October-November and temporarily stabilizes in the winter months. However, this pattern can change from year to year according to changes in seasonal precipitation. A wet summer (e.g., 1992) will temporarily recharge the aquifer as shown by a distinct peak in July on the hydrograph for that particular year. Average annual hydraulic heads in the North part of the site is shown in a tabular format in Appendix A (Table A2) together with the range (maximum minus minimum recorded values) for the year 1994. The hydraulic heads were found to fluctuate within a range of 1.63 m but the coefficient of variation was less than 0.40. The longitudinal movement of the groundwater did not appear to change direction seasonally. General groundwater flow was observed to be in the northwestern direction and seemed to be maintained throughout the year.
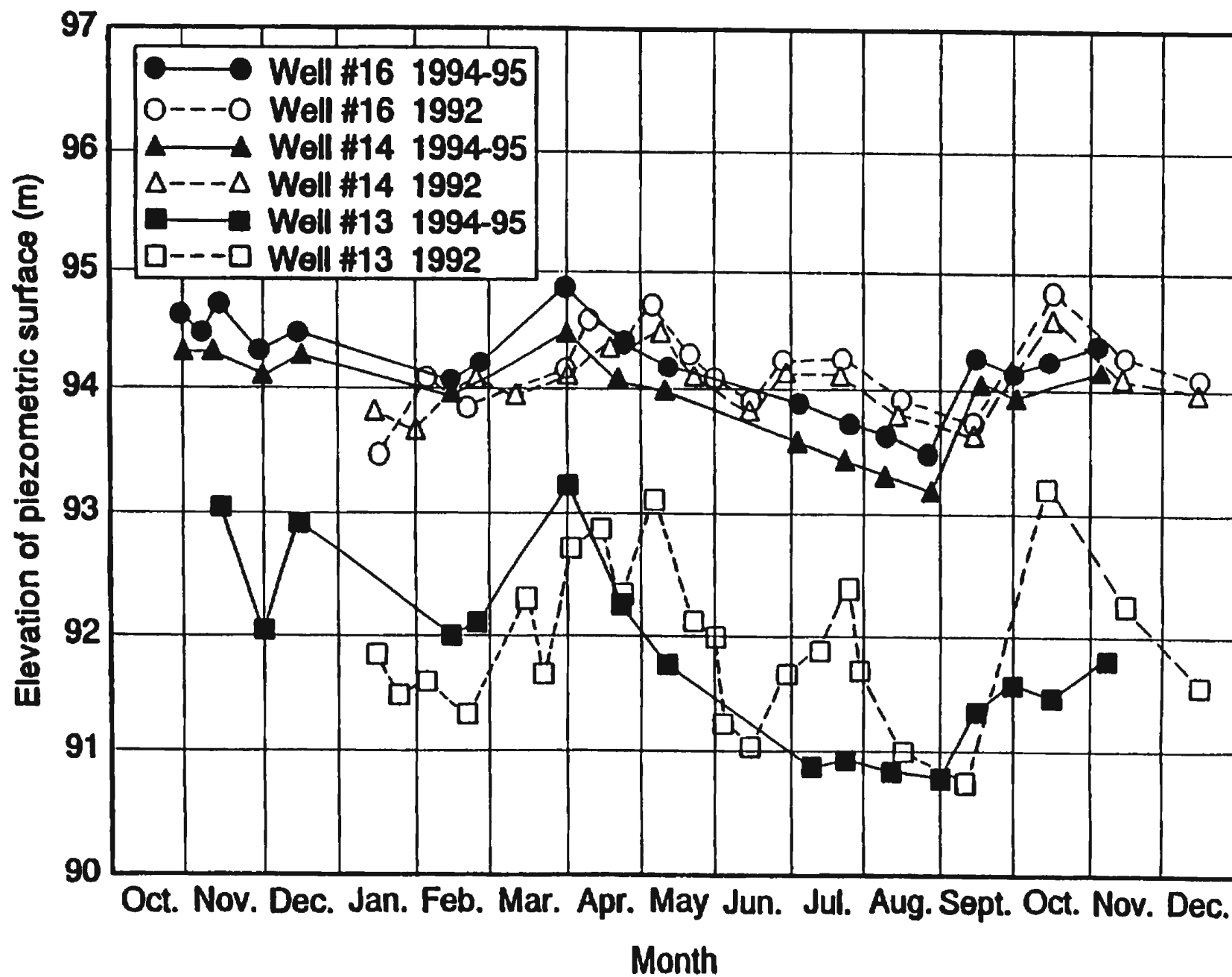
Figure 4.4: Comparison of 1992 and 1994-95 hydrographs for some wells in the bedrock

(after Amoah and Morin 1996a)

Figure 4.5 shows a cross section of the site along the Northern part which shows how the potentiometric surfaces for different wells varied along the surface and bedrock topographies. There was evidence of temporal variations in the hydraulic gradient in response to the seasons. However the spatial changes in hydraulic gradients were observed to follow the changes in bedrock slope. Values of the hydraulic gradients along the predicted flow path for the year 1994 have been plotted (Figure 4.6) and they show the seasonal variations of the above described pattern. Hydraulic gradients computed by using well #31 as the reference are shown in Appendix A (Table A3) The hydraulic gradient data were found to be normally distributed (Appendix A, Figures A2.1 to A2.3). Although the hydraulic heads and gradients exhibit spatial and temporal variability, the hydraulic conductivity was considered to be the major source of parameter uncertainty in this aquifer (Amoah and Morin 1996a).

A mean hydraulic gradient of 0.08 was computed for the northern part and combined with the geometric mean of the hydraulic conductivity, to estimate a mean specific discharge of 1.8 cm/day for bedrock and 3.11 cm.day for till respectively. An important parameter that could not be estimated at this stage was the effective porosity for this fractured aquifer. It was expected that the effective porosity will be greatly influenced by the secondary porosity produced by the network of fractures and could only be estimated by more detailed methods such as tracer tests.
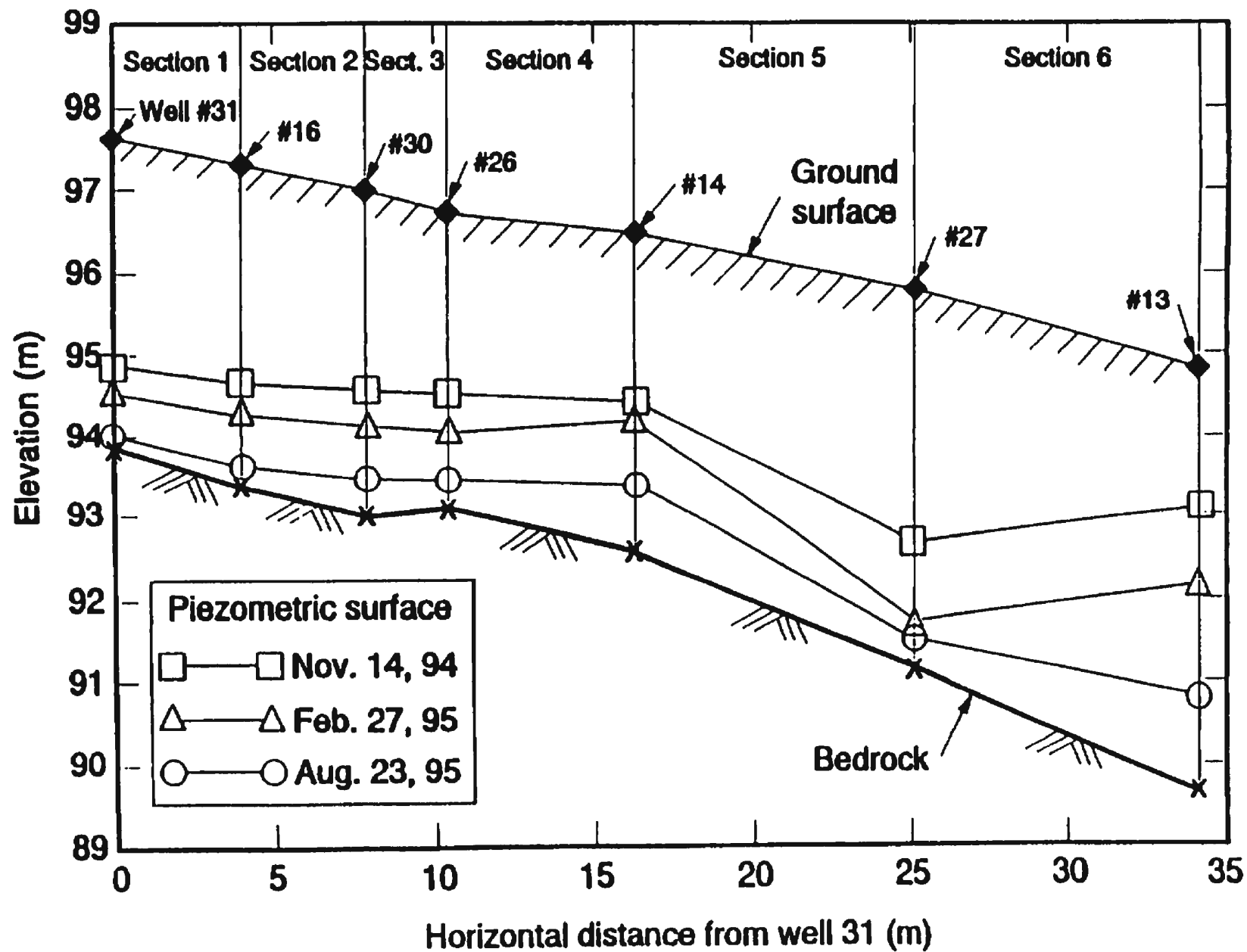
Figure 4.5: Cross section and potentiometric surface in the north part of the site (after Amoah and Morin 1996a)
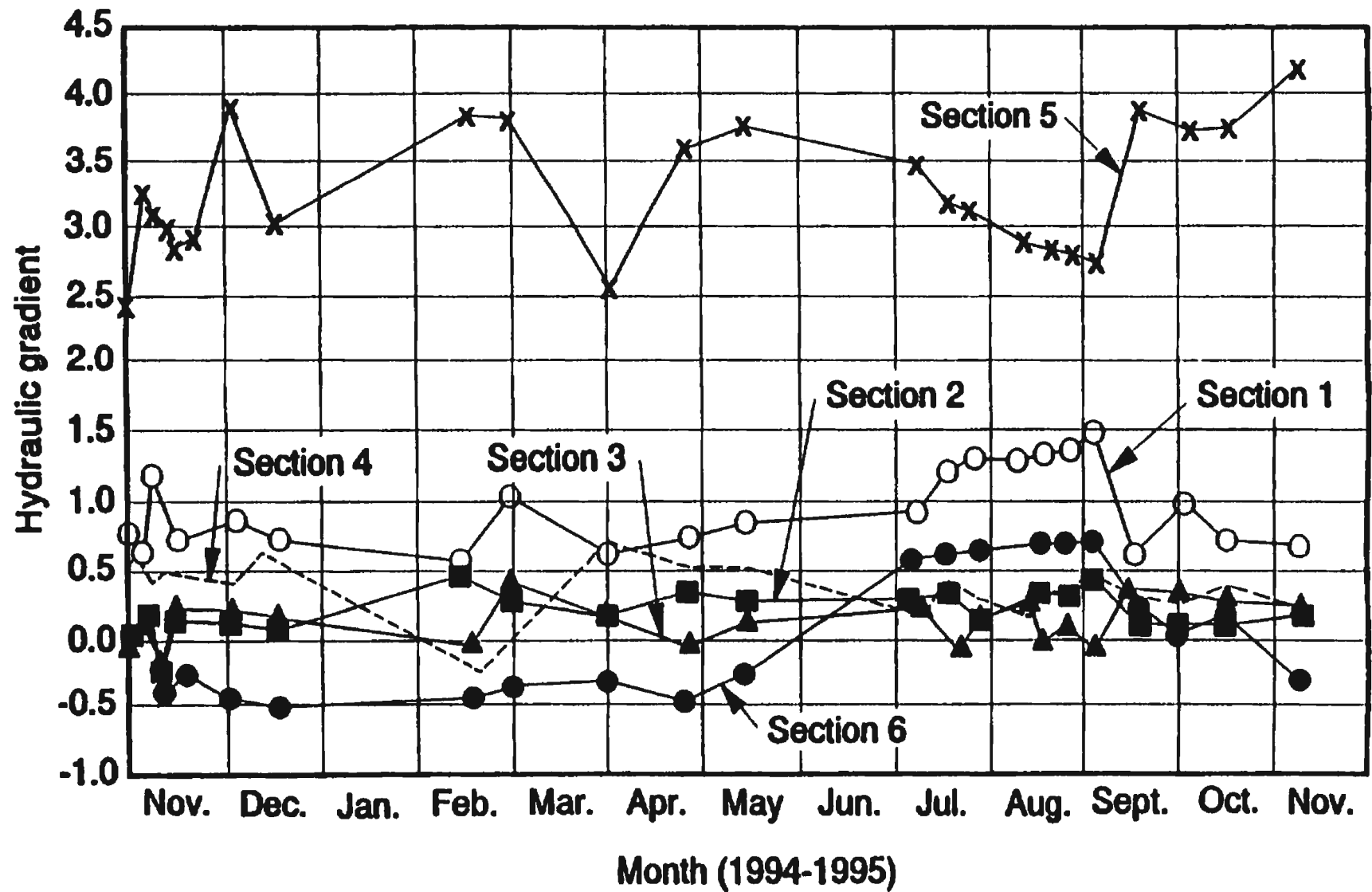
Figure 4.6: Hydraulic gradients over the period 1994-1995 (after Amoah and Morin 1996, for section location, refer to figure 4.5)

4.4.2 Background Chemistry of the Site Groundwater

The background levels of certain chemical species in the site groundwater were established by Ivany (1994) for the two year period preceding the test. Chemical monitoring was continued from September 1993, to August 1994, during which time other species of interest were also measured. The primary aim of the background chemical study was to guide the selection of tracers for the experiment. Proper selection of tracers for field scale experiments is very important for the successful interpretation of results but is sometimes challenging due to chemical interaction. It was also important to know the initial conditions of concentrations that are required for the numerical simulation of tracer movement. Since we had certain tracers already in mind, the study was limited to background concentration levels of selected chemical species. The groundwater was found to have very low total dissolved solids (0.08-0.25 mg/L) and consequently exhibited low conductance (0.2-0.5 mS/cm). The pH ranged between 6.0-8.4. However the ionic composition of the groundwater on the northern part was dominated by Chloride (18-40 mg/L) mainly due to a Sodium Chloride tracer test performed in the area (Ivany, 1994). However, background concentrations of compounds such as Bromide, Lithium, and some fluorescent dyes were all below detection limit and were approximated to be zero for the sake of determining an initial condition. Details of some of the chemical characteristics are shown in Appendix A (Table A5).

4.5 The Natural Gradient Tracer Experiment-Phase I

Two natural gradient tracer experiments were performed to supplement the in situ tests and hydraulic monitoring. The tracer tests were conducted in two phases. Phase I was aimed at providing a conceptual knowledge of the solute transport behaviour of the aquifer to assist in the development of the numerical model. Based on the results of phase I a second test was designed to complement the data and improve the field verification. The sections that follow present details of the experimental procedure and results.

4.5.1 Main Objectives of Tracer Test Phase I

The primary objectives of the tracer test phase I were to;

● understand the hydraulic interaction between the overlying glacial till and the underlying fractured bedrock,

● determine the intensity of fracturing and degree of fracture inter-connectivity in the bedrock in order to estimate the most applicable of the three major theoretical concepts in solute transport analysis,

● obtain more reliable field data and combine with the above objectives for the formulation and calibration of the boundary element numerical model for solute transport.

4.5.2 Test Location and Installation of Additional Wells

As pointed out earlier the north side of the site was selected for the tracer test after a careful study of the surface and bedrock topographies. At this location nine wells were already installed (Ivany 1994). Six of these wells were in the fractured bedrock while the other three were in the overlying till. Additional wells were drilled in early October 1994 (Figure 4.7). Drilling of the new wells provided an opportunity for physical examination of the bedrock type, fractured surfaces, bedding planes and for testing primary porosity. During the drilling process, rock samples were collected from boreholes at different depths. Primary porosity was determined by using the water volume displacement method. Several drill samples were soaked in water for three days and their individual volumes were obtained by recording the volume of water displaced in a graduated cylinder. The samples were then placed in an oven for another three days and put back into water to determine the volume of water soaked up which will represent the volume of voids. The porosity was then estimated by the ratio of volume of voids to the total volume of the sample. Primary porosity of the rock matrix ranged between 0.7 and 6 % with an average of 2.9 %. This falls in the lower range of expected porosity for the type of rock encountered (black shales, argillite etc.) and confirm the findings of Gale et al. (1984). Visual observations of the rocks obtained from different boreholes at depths below 3 meters revealed old fractured surfaces similar to what is usually observed in rock outcrops in many areas around St. John's.

Figure 4.7: Well drilling activities at the site

4.5. 3 Tracer Selection

The tracers for the experiment were selected based on the information on the background chemistry, the primary aim of the test and facilities available for chemical analysis and above all suitability for regulatory practice in the province of Newfoundland. Generally fluorescent dye tracers have been found to be suitable because they are less toxic (except those in the rhodamine family, e.g., Rhodamine B, Sulforhodamine B and G Rhodamin WT etc.) and can be measured at very low concentrations levels (Gaspar 1987a).

A detailed review of the literature on some tracers was made. In a comprehensive study of eight dyes used as tracers, Smart and Laidlaw (1977) observed that the fluorescence of Pyranine is strongly affected by pH levels. Amino G acid is very stable within pH range of 5 and 11. Amino G acid, Photine CU, Pyranine and Uranine all have high photochemical decay rates. Pyranine, Lissamine FF, Amino G acid are the dyes most resistant to adsorption but rhodamine WT, Uranine and Sulpho rhodamine B also have moderately high resistance while Rhodamine is easily adsorbed. Lissamine FF was the most costly of the dyes. Some important characteristics of these dyes are shown in Appendix A (Table A6).

Two of these fluorescent dyes, Amino G acid and Uranine were selected. Uranine (Sodium Fluorescein, Acid Yellow 73) $C_{20}H_1O_5Na_5$ appears in anionic form with a molecular weight of 376.15. Its solubility in water is 25 g/l and appears as characteristic bright

yellowish-green in dilute concentrations. It is however said to be the oldest fluorescent dye tracer used in hydrology (Gaspar 1987). Amino G acid (7-amino 1,3 naphthalene disulphonic acid) also appears in anionic form with characteristic bluewish in colour under dilute concentrations. Its high resistance to adsorption makes it an ideal tracer. In addition to their specific characteristics their previous performance in tracer tests (Smart and Laidlaw 1978, Novakowski and Lapcevic 1988) and the ability to visually observe their appearance in a withdrawn sample before chemical analysis made the choice of these dyes more suitable.

In order to trace both the overlying till and the underlying bedrock simultaneously, other tracers were selected. Lithium Bromide was selected based on its performance in previous studies. Bromide (conservative anion) and Lithium (reactive cation) proved very successful in previous tests (Mackay et al. 1986, Boggs et al. 1987). Although Chloride is a good competitor, the high background levels encountered in the site groundwater made it use unsuitable.

4.5.4 Tracer Injection

The first tracer test was performed in both the overlying glacial till and the underlying fractured bedrock. Two injection wells, each with 75 mm inside diameter PVC pipes (Figure 4.8) were used to introduce the tracers into the ground.

● The first injection well (#32) was installed in the overlying glacial till (shallow well). A total of 2000 litres of solution with concentrations of 100 mg/l for each of the two dyes (Amino G acid and Uranine) was injected into the shallow well.

● The second injection well (#31) was installed in the bedrock (deep well). Another 2000 litres of solution containing Lithium Bromide with injection concentrations of 575mg/l Bromide and 50 mg/l Lithium was also injected into this well.

The tracers were injected in the form of a pulse release of the solution into the aquifer. An injection flow rate of 3.5 l/min was used for the shallow well. However this injection rate was found too high for the deep well due to its low yield. A flow rate of 2.65 l/min was found to be suitable during the injection period. The dyes were purposely injected into the overlying till to study the hydraulic interaction between these two different media. It is suspected that the thin overburden plays very little role in groundwater regime but the actual interaction between these two media (especially how the overburden acts as a recharge medium) is unknown. It was expected that the appearance of dye (which was injected in the shallow well) in deep wells in the bedrock will give some idea of the hydraulic communication between them. This will also give an idea of source/sink terms.

injection wells

GL.

glacial till

monitoring wells

fractured bedrock
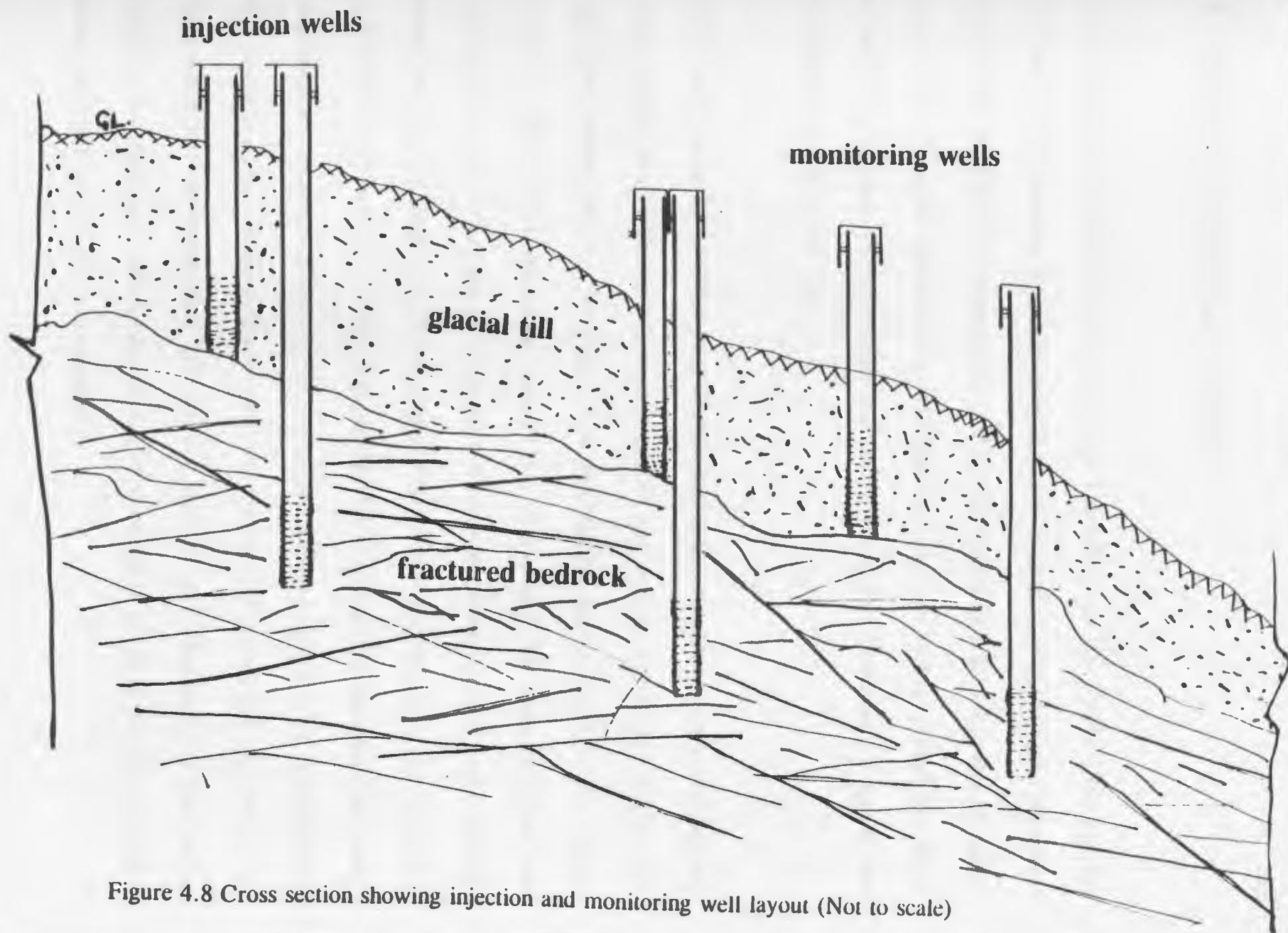
Figure 4.8 Cross section showing injection and monitoring well layout (Not to scale)

4.5.5 Sample Collection and Analysis

The tracer plume was monitored for a period of 9 months from late Fall of 1994 through the Winter and Spring-thaw periods to early Summer of 1995. During this period samples were collected periodically for laboratory analysis and hydraulic heads were also measured (Figure 4.9). The water samples were collected by using two bailers consisting of PVC pipe with 25.4 mm and 100 mm (inside diameters) Devlin foot valves with stainless steel balls respectively (Figure 4.10).

Several quality control procedures were adopted during the sampling process. A minimum of three samples were withdrawn from each well to obtained representative samples. To avoid cross contamination, the bailer was thoroughly washed after every sample withdrawal. Moreover, a sampling procedure was adopted such that those wells that were suspected to be least contaminated at the time of sampling were sampled first. Another approach was that the deep wells were sampled first usually with one particular bailer and then the shallow wells were sampled with another bailer. Collected samples were stored in polyethylene containers (Figure 4.10), which had been labelled to store samples from particular wells only. The containers were wrapped in aluminium foil and kept in an opaque container to be transported for chemical analysis in the laboratory. The opaque container minimizes light contact and reduces photochemical decay of the dyes in case it was not possible to analyze them immediately.

Figure 4.9: Groundwater level monitoring activities on site

Figure 4.10: Groundwater sampling activities on site

Water samples were analyzed for Lithium using Atomic Absorption Spectrophotometer and Bromide characteristics were measured using ion chromatography. Calibration of these machines for the measurement of these chemical species had been done earlier. Dye concentrations were analyzed using a spectrofluorimeter. This instruments identifies several flourescent dyes mixed in water. Measurements are done with small sample volume (approximately 5 ml) and when the maximum excitation and emission of the particular dye (Appendix A, Table A6) is given the instrument measures the concentration in terms of its fluorescence which is them converted to ppm or ppb. During calibration it was found that the instrument could detect up to 1.0 ppb).

Every effort was made to analyze the samples within 24 hours after collection from the site. Before chemical analysis was began for any sample collected in a particular day, standard solutions with known concentrations that were used for the calibration were measured first to check the accuracy of the spectrofluorimeter. Three samples were then taken from each container and analyzed to check the consistency of results. Figures 4.11 and 4.12 show breakthrough curves at different distances from the injection well. Figure 4.13 and 4.14 also show 2-D and 3-D contour plots for bromide plume at different times after tracer injection into the bedrock.
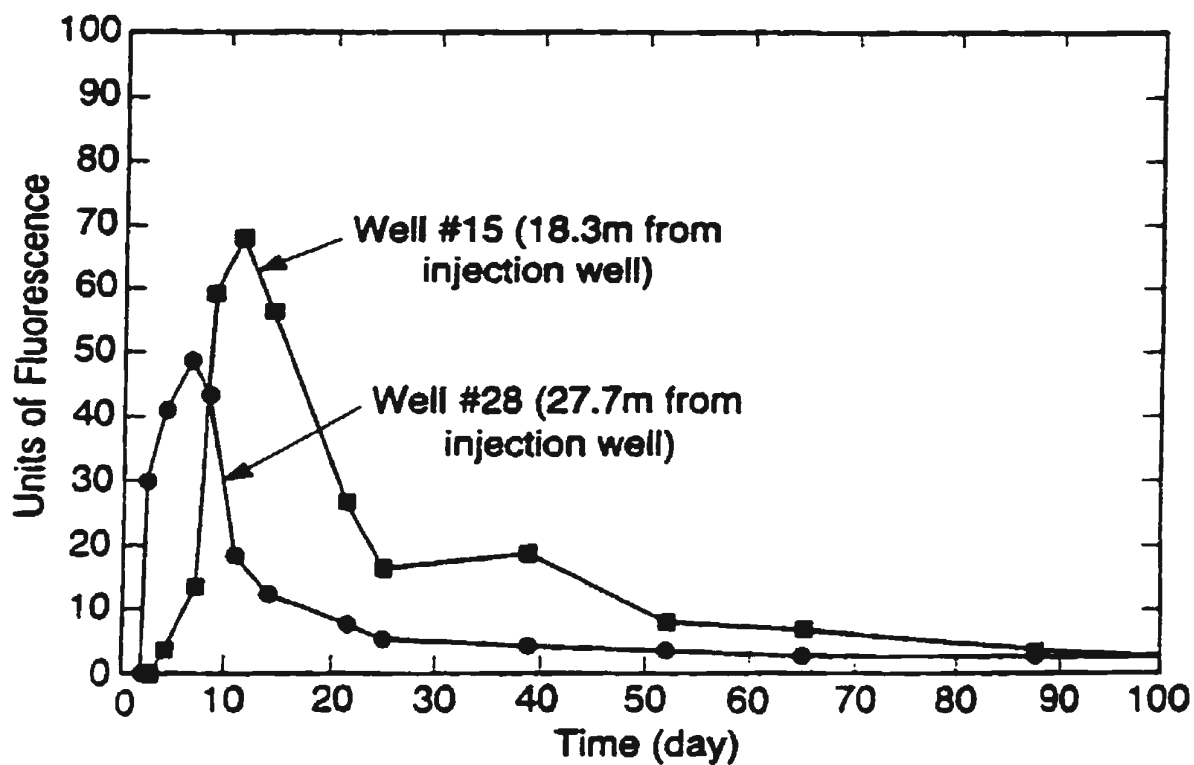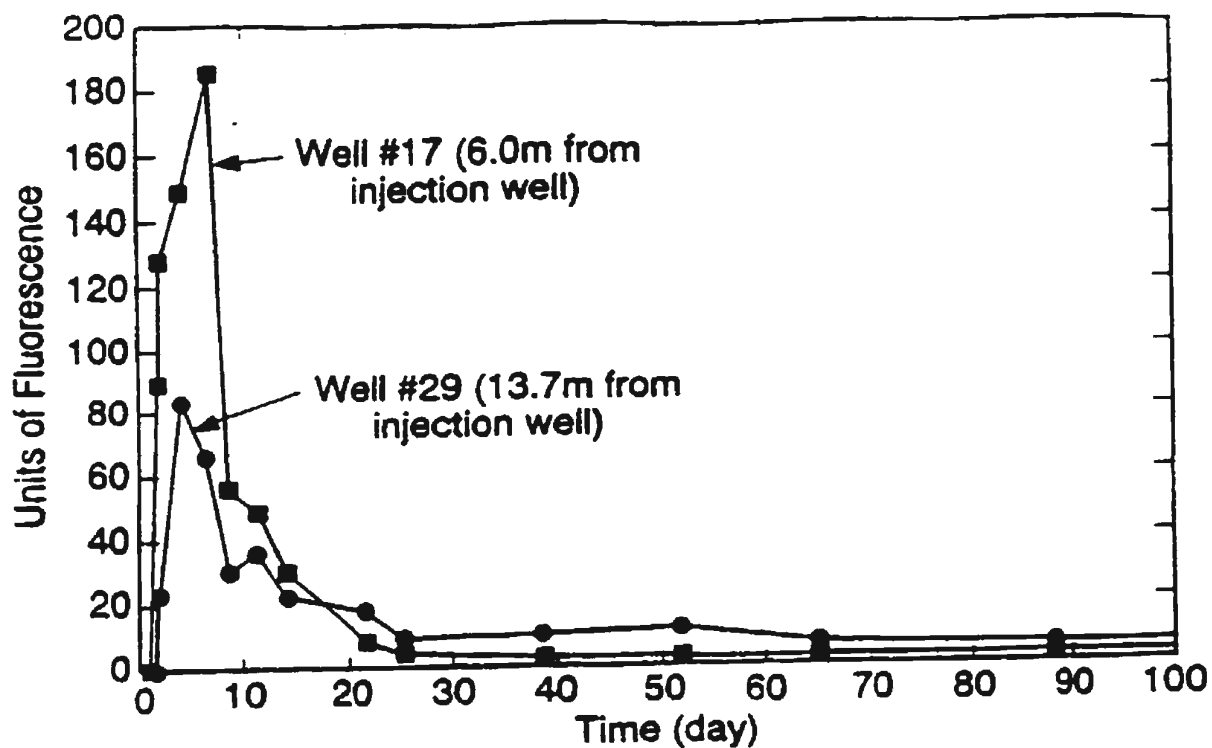
Figure 4.11: Tracer breakthrough curves for uranine in the overlying glacial till
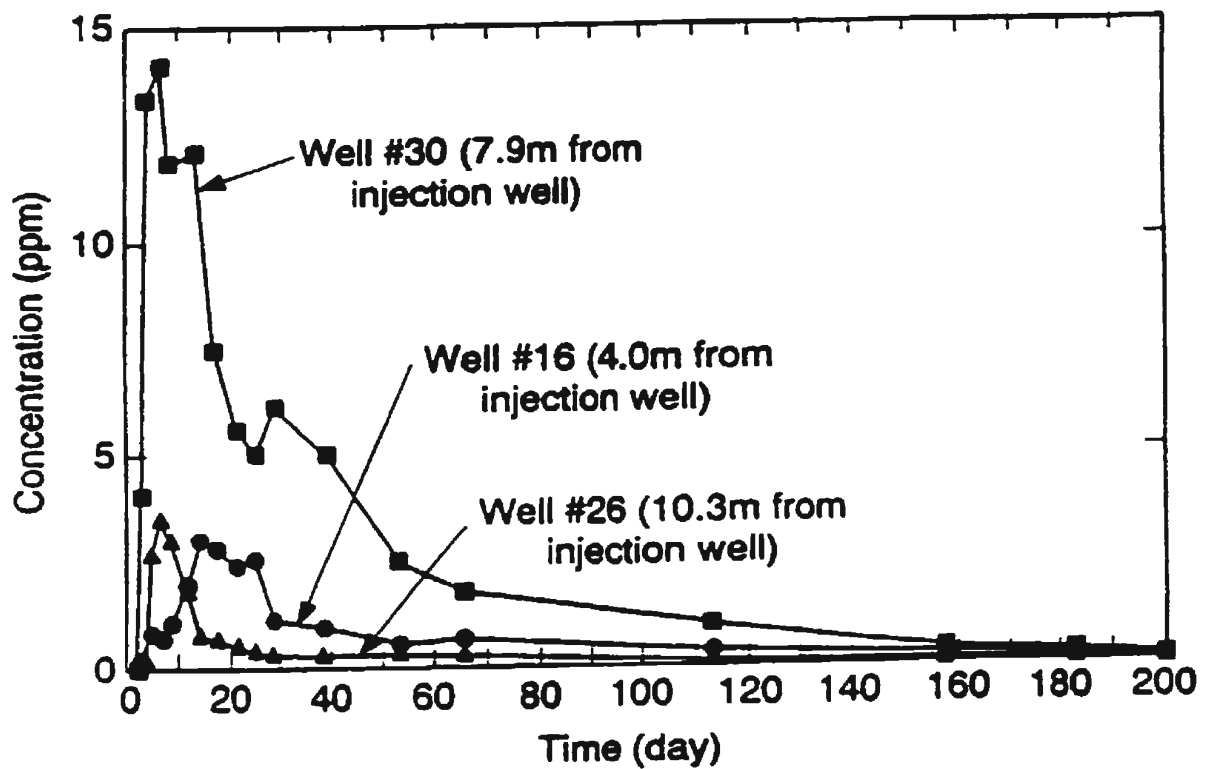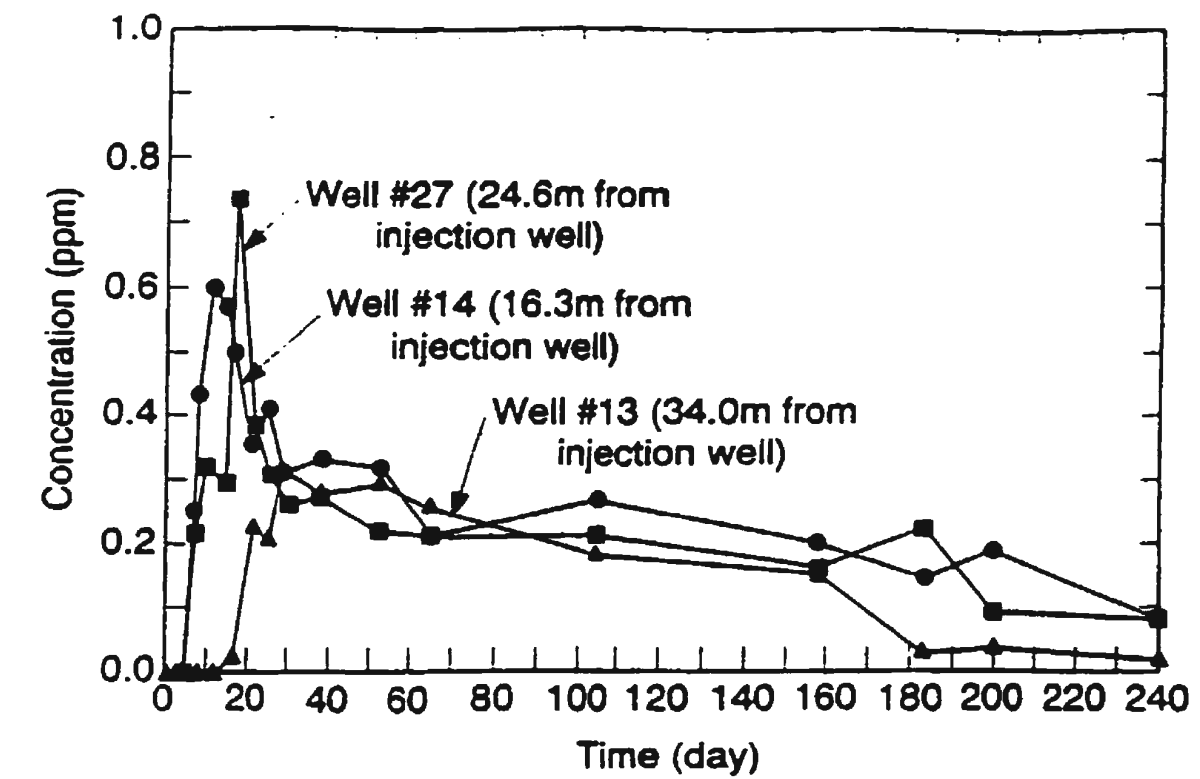
Figure 4.12: Tracer breakthrough curves for bromide in the fractured bedrock

Distance from injection well (source, (m))
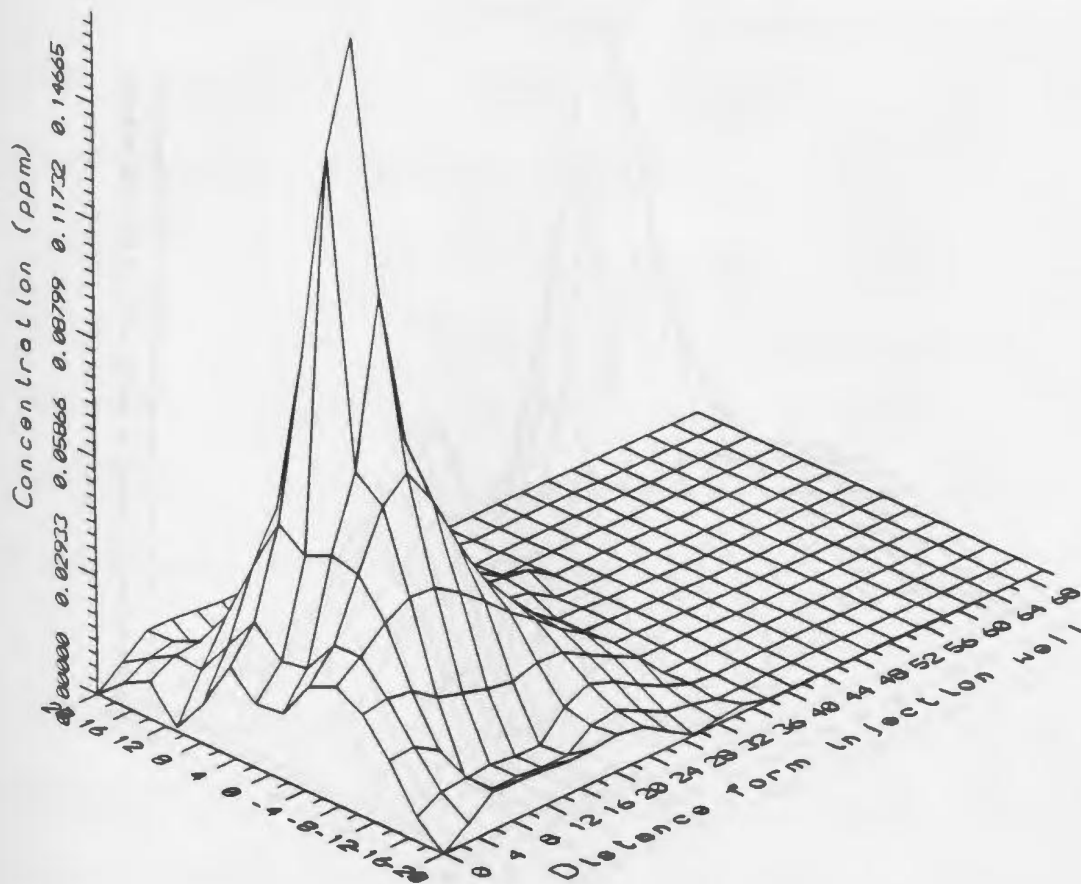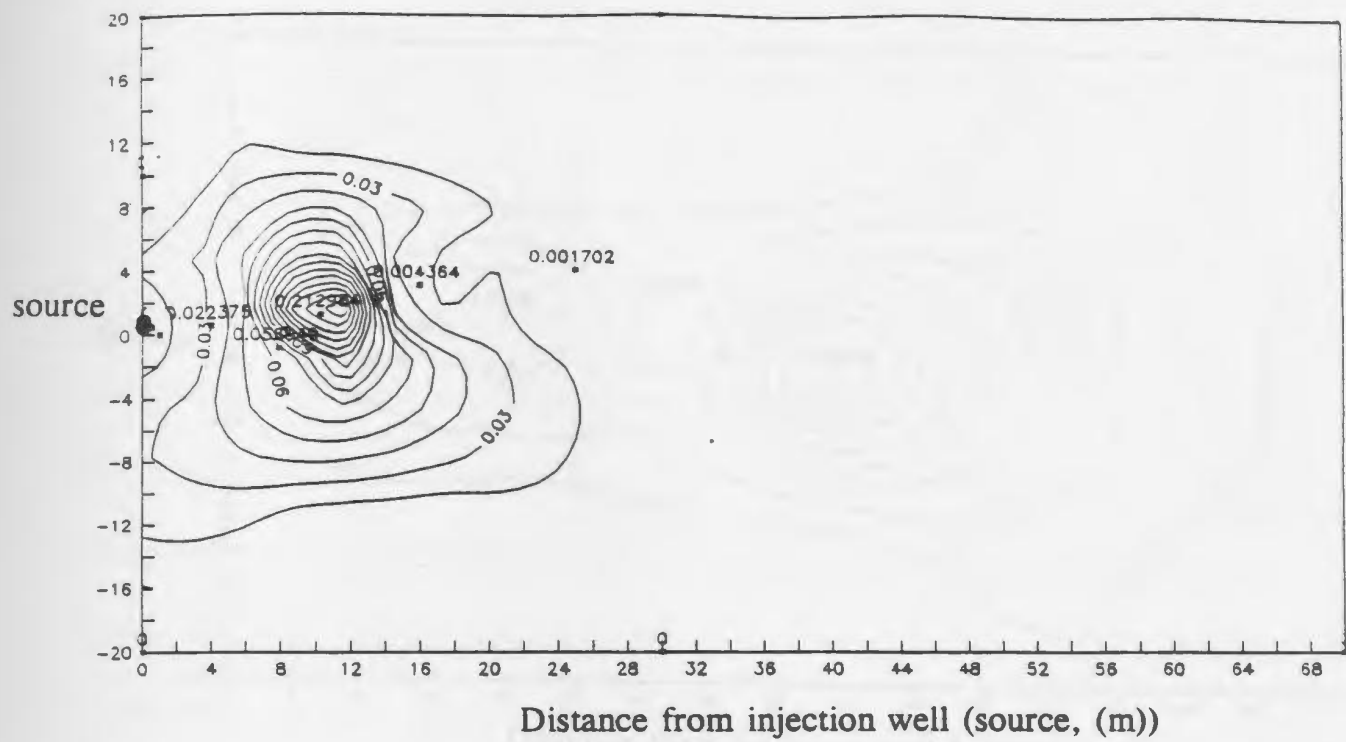
Figure 4.13: 2-D and 3-D isoconcentration contour plot of Bromide plume, 7 days after tracer injection.
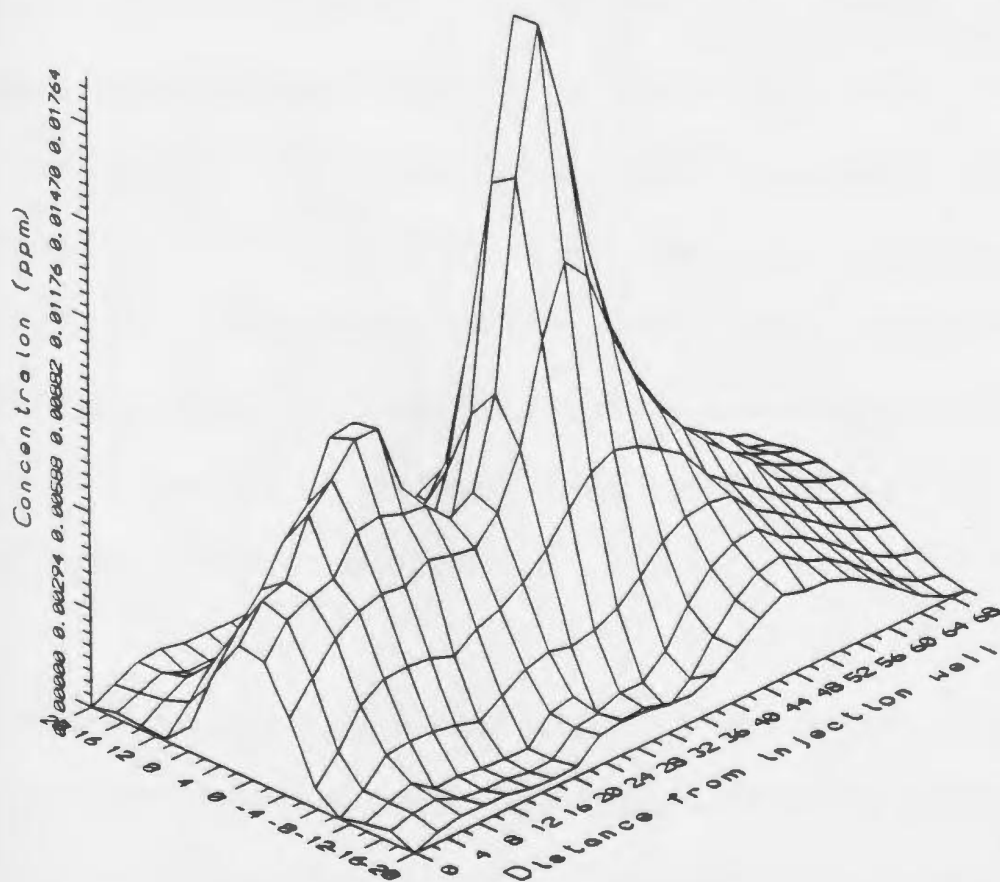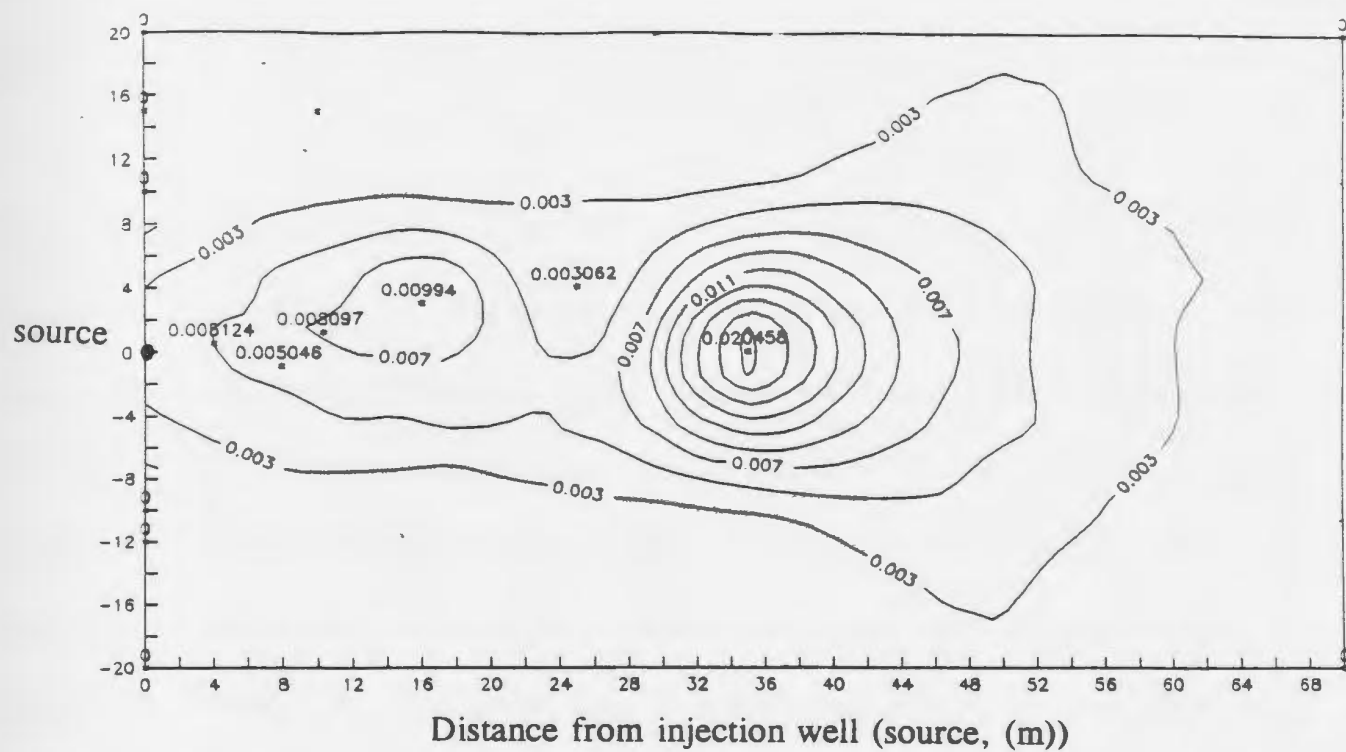
Figure 4.14: 2-D and 3-D isoconcentration contour plot of Bromide plume, 23 days after tracer release.

4.5.6 Tracer Migration Pattern in the Overlying Glacial Till

The first arrival of the dye was noticed in well #17 (4 meters down-gradient) two hours after the injection has started. The tracer plume quickly moved down gradient in the north easterly direction following the groundwater flow path predicted earlier from the hydraulic head data. Peak concentration values obtained from wells off the predicted flow path were consistently lower than those on the expected path. This down-gradient migration was accompanied by significant spreading in longitudinal and transverse directions. The appearance of both dyes were observed in all the down-gradient wells located in the surface glacial till. Sixty days after the injection, it was observed that dye concentrations in all the wells located within 40 m of the injection well had almost reached background levels. There were no differences between the first arrival times for Uranine and Amino G Acid. Similarly the peak arrival times for these two dyes were the same for all the wells monitored. This seems to suggest that uranine proved to be an equally conservative tracer as amino G acid in this type of medium. However, Amino G acid was found to be more diluted than Uranine. The breakthrough curves (Figure 4.11) are all characterized by steep fronts and long trailing tails.

Throughout the monitoring period, no dye was found in the deep wells in the underlying bedrock. While a firm conclusion could not be drawn on the fluid interaction between these two different layers due to the spatial scale of the test, this finding seem to suggest that at least in the short term hydraulic communication between the overlying surface till

and the underlying fractured bedrock is limited although recharge of the bedrock may occur in certain locations.

4.5.7 Tracer Migration Patterns in the Fractured Bedrock

There were many inconsistencies in the concentration values obtained from Lithium due to the limitations of the Atomic Absorption Spectrophotometer. Since only the physical transport mechanisms were of prime interest, measurements for Lithium was discontinued at an earlier stage and attention was focused on Bromide migration patterns which are reported here.

The first arrival times of the bromide in the fractured bedrock were slower than the dyes in the overlying till. The bromide plume followed the same trajectory observed for the dyes in the overlying layer and appeared in all wells located down gradient in the direction of groundwater flow. This seems to confirm the evidence of significant fracture inter-connectivity. Peak bromide concentrations measured on the predicted tracer pathway along the main flow direction were higher than those in the transverse directions. This is the effect of transverse dispersion due to mixing at fracture intersections. In general the bromide migration pattern in the fractured bedrock was similar to the dyes in the overlying porous till. The breakthrough curves (Figure 4.12) are also characterized by steep front and long trailing tails.

Another intriguing observation was made. The first tracer arrival time in well #16 located 4 meters from the injection well was later than in well #14 located 16 meters away although both are located on the predicted pathway of the tracer. This illustrates the complicated nature of flow through fractured formations. It is suspected that the closer well is located on tributary fracture zones which have smaller apertures. Reduced mixing occurs at such fracture intersections resulting in smaller volume and rate of contaminant movement through them. In spite of this observation, the appearance of tracer in longitudinal and transverse lateral directions is an evidence of the absence of localized channel flow. Assuming observation is valid for the areas beyond the test area, it is reasonable to assume that an equivalent porous media conceptualization may be the closest conceptual basis for analyzing solute transport mechanisms in this fractured aquifer.

4.5.8 Estimates of Aquifer Parameters from Tracer Test data

The computation of parameters such as solute transport velocities, and porosity was done following the procedure suggested by Sudicky et al. (1983), and Zou and Parr (1994). Tracer velocities were estimated by assuming that the location of peak concentration coincides with the position of the advective front. The arrival times of peak concentrations (t_{max}) were estimated from longitudinal profiles of concentration breakthrough curves for various wells in the direction of flow. Relating this to the distance L from the injection well, the average linear velocity ($|V|$) is computed by using the relation $|V| = L/t_{max}$. Values of $|V|$ were computed for various travel distances and they range from 1.1 m/day to 1.5 m/day for the bedrock and 2.0 m/day to 4.3 m/day for the overlying glacial till. These values suggest that the average tracer migration rates in the till are nearly three times greater than that in the bedrock. The low range of velocity variations in the bedrock suggests uniform migration rates of solutes. However, such findings may not be obtained for the entire site due to the higher spatial variability of hydraulic conductivity. By using the specific discharge (v) values computed for the bedrock in earlier work (Amoah and Morin 1996a), effective porosity ϵ for the upper till and fractured bedrock were computed from the relation $\epsilon = v/|V|$. An average effective porosity of 0.014 (bedrock) and 0.0089 (upper till) were computed for the test area.

Dispersivities were estimated by using the analytical formulas proposed by Zou and Parr (1994). Different approaches for estimating dispersivities from tracer test data have been

reported in the literature. Sauty (1980), developed dimensionless type curves to estimate dispersivity and porosity. Sudicky et al. (1983), Mackay et al. (1986), Freyberg (1986) Gerabedian et al. (1991) used spatial moment analysis to compute the tracer dispersivity by using the first moment (mean) and second moment (variance) of the concentration distribution of the tracer measured at sampling points. The spatial moment analysis assume tracer concentration distribution to be Gaussian. Wang et al. (1987) and Jiao (1993) have also employed graphical methods to estimate dispersivity from tracer test data. Zou and Parr (1994) proposed two approaches for estimating dispersivities. Their methods use the concentration versus time data obtained from tracer test.

In determining a suitable approach for estimating dispersivity from this work, it was observed that the spatial scale and data density was not high enough for spatial moment analysis to provide accurate results. Moreover statistical analysis of the concentration data did not indicate that the data follows a Gaussian distribution. It was therefore considered useful to employ the analytical approach following the procedure proposed by Zou and Parr (1994). These workers used the analytical solution of the advection dispersion equation governing an instantaneous release of conservative solute into a 2D domain under uniform flow which is given as (Wilson and Miller 1978, Hunt 1978):

$$c(x,y,t) = \frac{M}{4 \pi |V| t \Lambda \epsilon (\alpha_L \alpha_T)^{1/2}} \exp\left(-\frac{(x-|V| t)}{4\alpha_L t} - \frac{y^2}{4\alpha_T t}\right) \qquad (4.1)$$

where Λ is the aquifer thickness, ϵ is the effective porosity, t, is the elapsed time after solute release, x and y are the spatial coordinates of the sampling point, M is the solute mass, α_L and α_T are the dispersivities in their respective directions and c is the concentration. By differentiating this equation and relating it to the concentration versus time data, Zou and Parr (1994) derived two expressions for the longitudinal and transverse dispersivities as:

$$\alpha_L = \frac{|V| \, \Delta t_1^2}{4(t_1 \, \ln(R_1) - \Delta t_1)} \tag{4.2}$$

$$\alpha_T = \frac{y^2 \, |V| \, \Delta t_1^2}{4B_1 - A_1} \tag{4.3}$$

where the parameters are defined as:

$$A_1 = 4t_1(x^2 - |V|^2 \, t_{max}^2)\ln(R_1)$$

$$B_1 = x^2 \Delta t_1 - |V|^2 \, t_{max} t_1 \Delta t_1 \tag{4.4}$$

$$R_1 = \frac{c_{max} \, t_{max}}{c_1 t_1}, \quad \Delta t_1 = t_{max} - t_1$$

c_{max} is the maximum concentration obtained from tracer breakthrough curve, t_{max} is the corresponding time of its arrival, c_1, is half of the peak concentration value and t_1 is its corresponding time of arrival. By using these expressions, dispersivities were estimated from the different breakthrough curves. The longitudinal dispersivities computed for the bedrock ranged from 1.31 m to 7.23 m. The transverse dispersivities also ranged from 0.014 m^2/day to 0.305 m^2/day. For the overlying glacial till, longitudinal dispersivity values ranged from 0.7 m^2/day to 15 m^2/day. These values of dispersivities will also be as input parameters during the calibration of the numerical model .

4.6 Tracer Test Phase II

The second tracer test was conducted in the bedrock only with purpose of complementing the understanding of the first test. The procedure for second test was the same as the first except that 1600 litres of Uranine was used in place of Bromide. Tracer injection coincided with the summer of 1995 and solute migration patterns in the fractured bedrock

were also monitored through the fall and winter periods of 1996. Data on tracer concentration distribution in the bedrock at different well locations are shown in Appendix B (Table B1). Although a different well was used, the breakthrough curves are similar to those obtained from the first test. They are all characterized by steep fronts and long trailing tails. Tracer migration rates were also similar and velocities ranged from 1.2 to 1.7 cm/day. Uranine concentrations were measured in all the wells in which bromide appeared in the first test confirming the hydraulic connectivity of the different wells.

4.7 Summary of the Field Study

This chapter has presented the details of the field investigation on the hydraulic characteristics and solute transport mechanisms in a fractured bedrock aquifer overlain by a thin glacial till at a test site in St. John's, Newfoundland. In situ tests for hydraulic conductivity of the underlying fractured bedrock indicate a very high spatial variability and was found to follow a lognormal distribution. Hydraulic heads and gradients also exhibit some form of spatial and temporal variability. However because of the higher variability of hydraulic conductivity compared to other parameters, it was assumed to be the major cause of uncertainty for solute transport analysis. All of these findings together with information on initial groundwater chemistry were used as guidelines to perform two natural gradient tracer experiments at the site.

Results from the experiments have given good indications of contaminant migration

patterns in the overburden glacial till and the underlying bedrock. Observations from the test indicated that tracer migration rates in the overlying glacial till are about three times faster than in the bedrock. Estimates of longitudinal and transverse dispersivities in the porous till were also found to be larger. It was observed that all the tracers both in the overlying till and bedrock followed the same direction predicted by hydraulic head data and underwent spatial spreading. Tracers injected in the overlying till were not measured in any of the wells installed in the bedrock. This unique observation suggests that in certain areas of the aquifer and at least in the short term, there is limited hydraulic communication between the overlying glacial till and the underlying bedrock. The long term hydraulic communication between these two layers and the general validity of this finding outside the area of the test will require further studies to be performed. However this information seem to confirm the findings of Gale (1993), that the aquifer at the test site may be confined. It is therefore reasonable to assume at least within the test location that the aquifer is confined for the purpose of numerical analysis.

Observations from tracer migration patterns in the bedrock and the appearance of the tracer in all the deep wells down-gradient suggest high density of fractures, significant fracture inter connectivity and non uniform nature of fracture orientations. Assuming that such observations apply beyond the boundaries of the test area, an equivalent porous medium conceptualization seems appropriate for analyzing contaminant migration in this aquifer. Tracer migration patterns and rates observed in the second test confirmed all the findings of the first test in the bedrock.

Although further studies will be needed to confirm these findings, the test has provided a good understanding of the solute transport behaviour of a typical aquifer found in the St. John's area. This has also provided a conceptual understanding and field data for the development and field verification of a boundary element numerical model for solute transport. To the best of our knowledge, this is the first known field test to characterize an aquifer for the purpose of contaminant transport analysis in the province of Newfoundland.

Chapter 5

Mathematical Formulation by the Boundary Integral Equation Method

5.1 The Boundary Element Method

The boundary integral equation method (also known as boundary element method (BEM)) has been recognized as a powerful numerical solution technique for many complex boundary value problems. The recent improvements of the BEM, for example the dual reciprocity method (DRM) which avoids domain discretization in the solution of non-homogeneous equations makes it more attractive for solute transport analysis. However to demonstrate the full potential of the BEM and the DRM in solute transport analysis we have taken an alternative approach in the DRM application to such types of problems. In this chapter a review of the dual reciprocity boundary element method given and then present a more efficient DRM formulation of the advection dispersion equation governing solute transport in saturated porous media.

5.1.1 The Dual Reciprocity Boundary Element Method

As a starting point in the BEM model development, the mathematical basis of the DRM will be illustrated through an example application to the solution of a Poisson type equation by following the procedure proposed by Partridge and Brebbia (1990) and Partridge et al. (1992). Consider the Poisson equation

$$\nabla^2 c = b \qquad (5.1)$$

where $b(x,y)$ is a known function of position and ∇^2 is the Laplace operator. In the conventional BEM approach, a weighted residual statement can be written using a special type of weighting function called the fundamental solution (c^*) as:

$$\int_\Gamma c^* (\nabla^2 c - b) \, d\Omega = 0 \qquad (5.2)$$

where Ω is the domain and Γ represents the boundary of the domain. The fundamental solution in this case satisfies the Poisson equation

$$\nabla^2 c^* + \Delta_i = 0 \qquad (5.3a)$$

where Δ_i is the Dirac delta function which is infinity at the point $x = x_i$ and is equal to zero everywhere else. An important integral property of the Dirac delta function is termed the sifting property which is given as:

$$\int_{-\infty}^{\infty} f(x)\Delta(x-s)dx = f(s)$$

(5.3b)

Hence

$$\int_{\Omega} c(\nabla^2 c^*) \, d\Omega = \int_{\Omega} c(-\Delta_i) \, d\Omega = -c_i$$ (5.4)

The fundamental solution for Laplace's equation is given as:

$$c^* = \frac{1}{2\pi}\ln\left[\frac{1}{r}\right] \qquad \text{for} \quad 2D$$

$$c^* = \frac{1}{4\pi r} \qquad \text{for} \quad 3D \qquad (5.5)$$

where $r^2 = (x-x_i)^2 + (y-y_i)^2$ for any (x,y) in the domain (Ω). If the Laplacian part of equation (5.2) is integrated by parts twice and terms rearranged, a boundary domain equation will result in the form:

$$a_i c_i + \int_{\Gamma} qc^* \, d\Gamma - \int_{\Gamma} cq^* \, d\Gamma = -\int_{\Omega} bc^* \, d\Omega$$

(5.6)

where the q's are the normal derivatives given as $q = \partial c/\partial n$, $q^* = \partial c^*/\partial n$ and n is the outward normal to the boundary. In equation (5.6), whether the function b is known or not, the traditional application of the boundary element method will require the interior of the domain

to be discretized in addition to the boundary therefore losing an important advantage of a boundary only formulation. This is the main weakness of the boundary element approach for solution of such types of problems. The dual reciprocity method (Nardini and Brebbia 1982) is an efficient way of overcoming this problem. The method proposes the use of approximation functions F_j to expand the function b in terms of its nodal values. A series of particular solutions $\hat{c}_j$ is used, the number of which is equal to the number of nodes defined in the problem. For example, (see Figure 5.1) N nodes are specified on the boundary and L interior nodes are also defined such that the total number of nodes is $N+L$. Particular solutions are then sought at these nodes by selecting a suitable radial basis function for F_j. The internal nodes are usually needed to provide a convenient way of mapping the function b over the entire domain and can be defined at the points where internal solutions are needed for the sake of convenience.
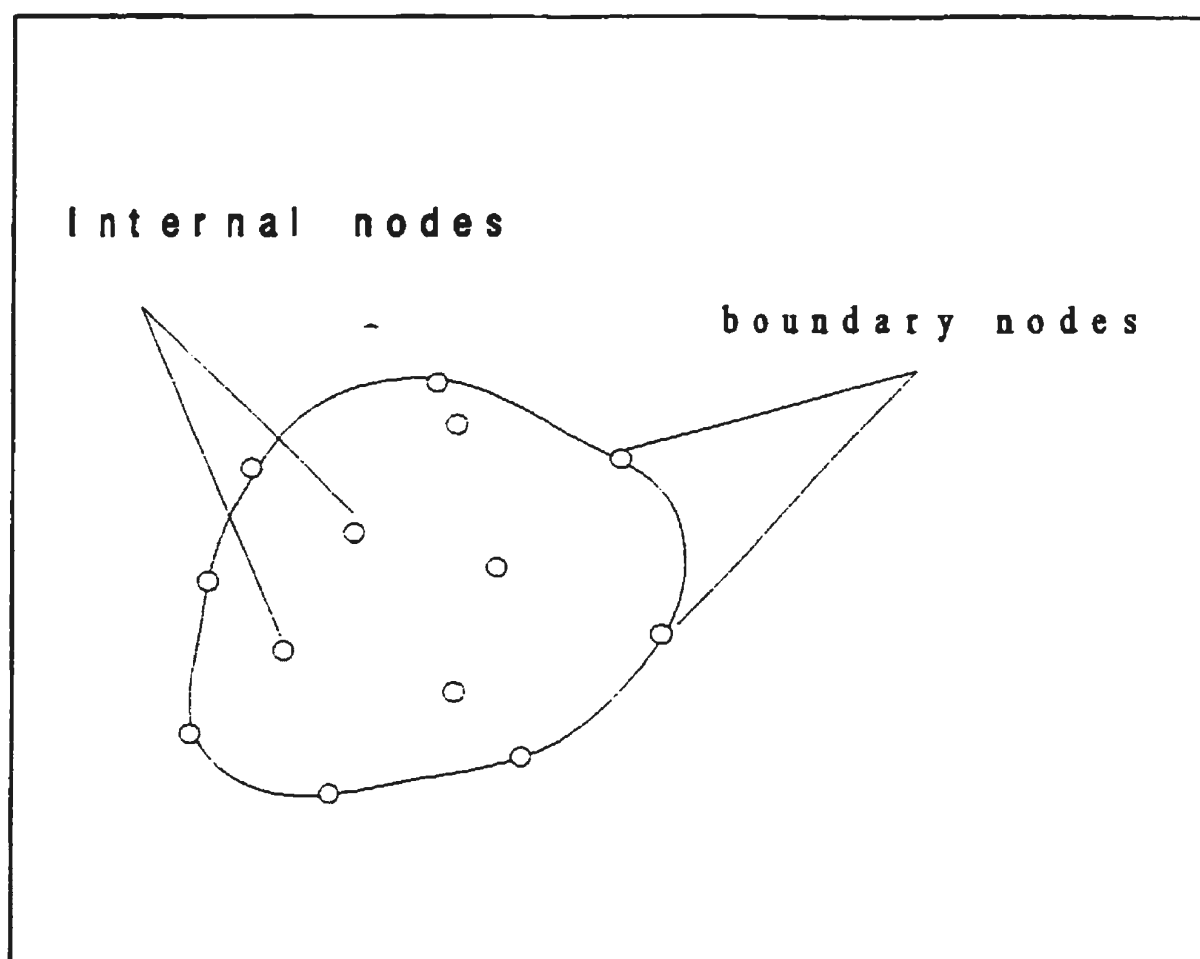
Figure 5.1: Boundary and DRM (internal) nodes

The function b is approximated as:

$$b \simeq \sum_{j-1}^{N+L} \phi_j \, F_j \qquad (5.7)$$

where ϕ_j are a set of unknown coefficients and F_j are approximating functions which depend only on the geometry. A particular solution $\hat{c}_j$ is sought to the following Poisson equation:

$$\nabla^2 \hat{c}_j - F_j \qquad (5.8)$$

Note that since F_j will be a function of r it follows that $\hat{c}_j = \hat{c}_j(r)$. Equation (5.1) is then written as:

$$\nabla^2 c - \sum_{j-1}^{N+L} \phi_j \left(\nabla^2 \hat{c}_j\right) \qquad (5.9)$$

which in a more compact form is written as:

$$\nabla^2 \left[c - \sum_{j=1}^{N+L} \phi_j \hat{c}_j \right] = 0 \qquad (5.10)$$

By using the divergence theorem or integration by parts a boundary only equation can be written for each node i (i=1...N) as:

$$a_i c_i + \int_\Gamma q^* c \, d\Gamma - \int_\Gamma c^* q \, d\Gamma = \sum_{j=1}^{N+L} \phi_j \left(a_i \hat{c}_{ij} + \int_\Gamma q^* \hat{c}_j \, d\Gamma - \int_\Gamma c^* \hat{q}_j \, d\Gamma \right) \qquad (5.11$$

$$\text{where} \qquad \hat{q}_j = \frac{\partial \hat{c}_j}{\partial n}, \qquad q^* = \frac{\partial c^*}{\partial n}, \qquad q = \frac{\partial c}{\partial n}$$

The q's are the normal derivatives as defined above and n is the unit outward normal to the boundary. After considering all the N boundary elements, equation (5.11) can be written as:

$$a_i c_i + \sum_{k=1}^{N} \int_{\Gamma_k} q^* c \, d\Gamma - \sum_{k=1}^{N} \int_{\Gamma_k} c^* q \, d\Gamma =$$

$$\sum_{j=1}^{N+L} \phi_j \left[a_i \hat{c}_{ij} + \sum_{k=1}^{N} \int_{\Gamma_k} q^* \hat{c}_j \, d\Gamma - \sum_{k=1}^{N} \int_{\Gamma_k} c^* \hat{q}_j \, d\Gamma \right] \qquad (5.12)$$

5.1.2. Boundary Element Discretization

It is customary in the boundary element method to discretize the boundary of the domain into elements of finite length. Several element types may be used in this approach depending on the location of the nodes on the element (e.g., at the middle of the element (constant), at the ends of the element (linear) or at the ends and middle of the element (quadratic)), (Figure 5.2). In this work linear elements are employed.
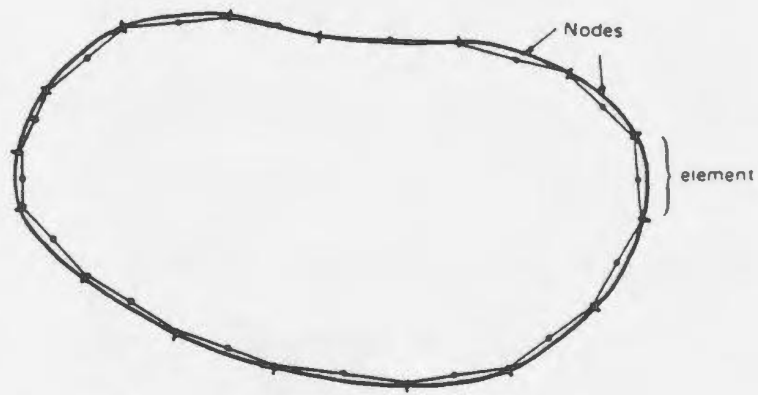
(a) Constant Elements
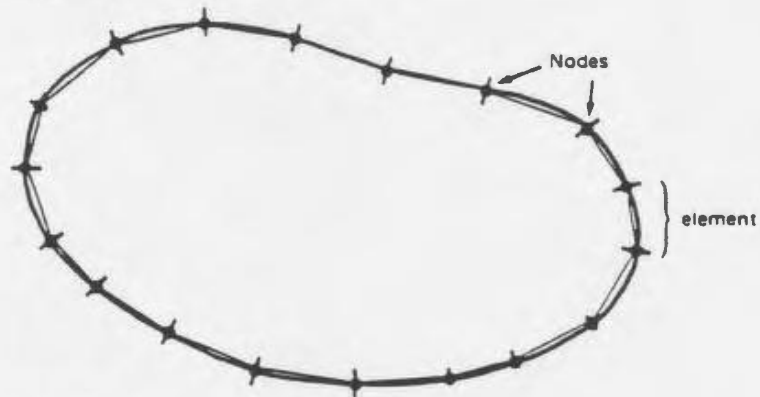
(b) Linear Elements
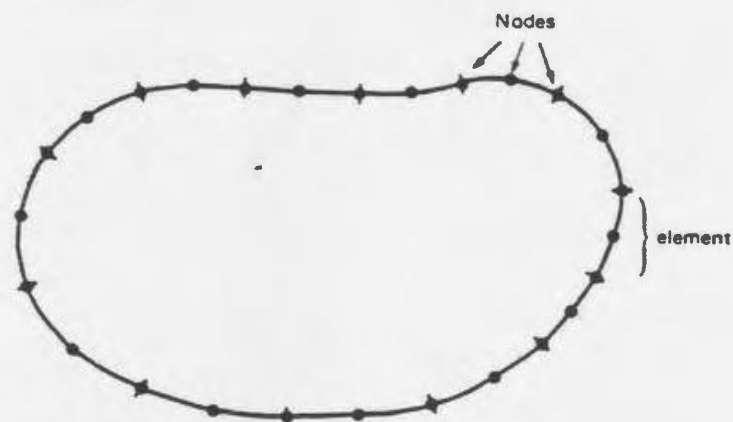
(c) Quadratic Elements

Figure 5.2: Different types of elements used in the boundary element discretization (after Brebbia and Dominguez 1992)

In the BEM analysis for the present work, linear elements are employed. The concentration c and its normal derivative are linear functions over the element and their values are defined in terms of their nodal values. Two linear interpolation functions (Ψ_1 and Ψ_2) are defined in a local coordinates system (Figure 5.3) to relate the variation of c and q over an element j (say)

$$c(\eta) = \psi_1 c_j + \psi_2 c_{j+1} = [\psi_1 \ \psi_2] \begin{bmatrix} c_j \\ c_{j+1} \end{bmatrix} \qquad (5.13)$$

$$q(\eta) = \psi_1 q_j + \psi_2 q_{j+1} = [\psi_1 \ \psi_2] \begin{bmatrix} q_j \\ q_{j+1} \end{bmatrix} \qquad (5.14)$$

where the two interpolation functions are defined as

$$\begin{aligned} \psi_1 &= 1-\eta \\ \psi_2 &= \eta \qquad\qquad (5.15) \\ 0 &\leq \eta \leq 1 \end{aligned}$$

where η is a local dimensionless distance variable defined over each element and takes the values of 0 to 1 as one traverses the element in a counter-clockwise direction. These variables are represented in the Figure 5.3 below.
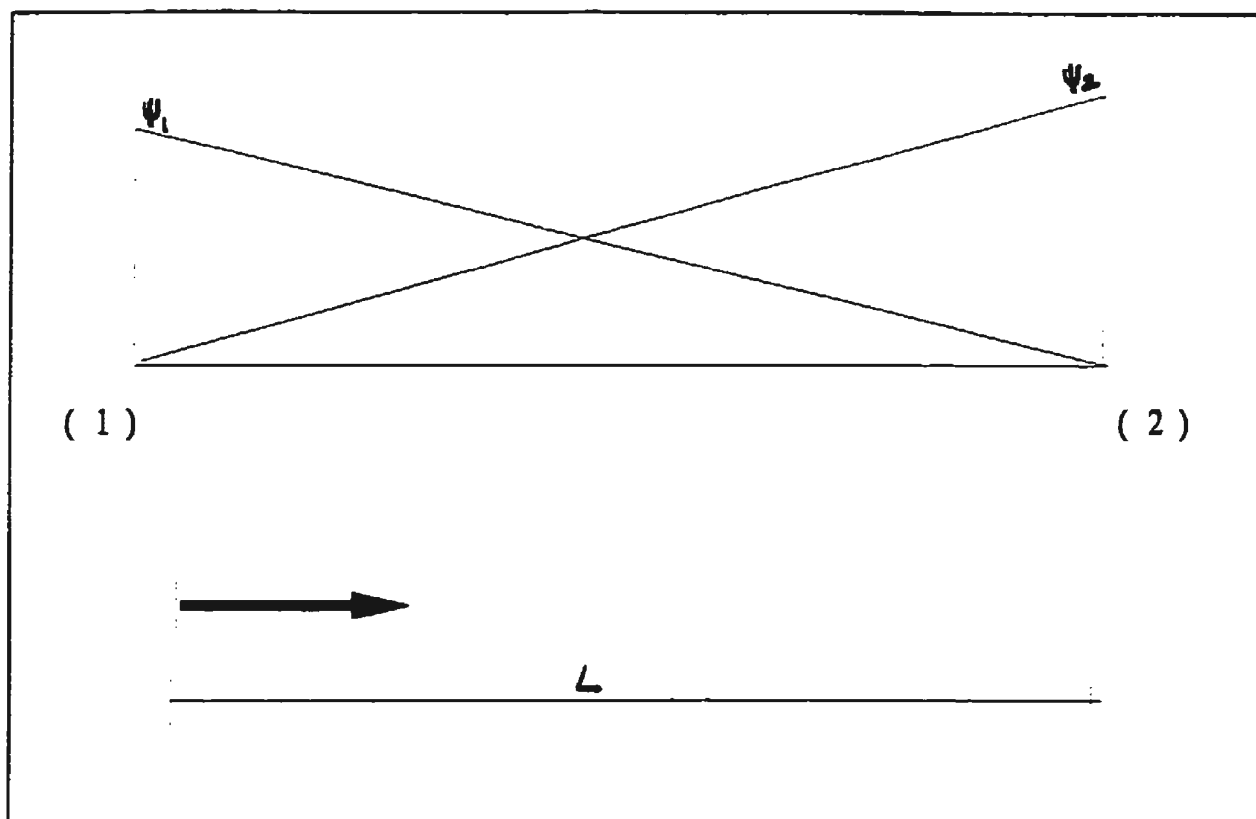
Figure 5.3   Local coordinate system used in linear element

Introducing equation (5.13) into equation (5.12), the integrals in equation (5.12) can be modified to become,

$$\int_{\Gamma_j} cq^* d\Gamma = \int_{\Gamma_j} [\psi_1 \psi_2] q^* d\Gamma \begin{bmatrix} c_j \\ c_{j+1} \end{bmatrix} = \begin{bmatrix} h^1_{ij} & h^2_{ij} \end{bmatrix} \begin{bmatrix} c_j \\ c_{j+1} \end{bmatrix}$$

$$\text{where, } h^1_{ij} = \int_{\Gamma_j} \psi_1 q^*$$

$$h^2_{ij} = \int_{\Gamma_j} \psi_2 q^*$$

(5.16)

Recall that c^* and q^* are functions of x_i. In the boundary element method, the values of h^k_{ij} are termed influence coefficients and they define the link between the point i under consideration and a particular node k of an element j in an anticlockwise direction. The integrals in equation (5.12) involving q can be transformed by using (5.14) to become

$$\int_{\Gamma_j} qc^* d\Gamma = \int_{\Gamma_j} [\psi_1 \psi_2] c^* d\Gamma \begin{bmatrix} q_j \\ q_{j+1} \end{bmatrix} = \begin{bmatrix} g^1_{ij} & g^2_{ij} \end{bmatrix} \begin{bmatrix} q_j \\ q_{j+1} \end{bmatrix}$$

$$\text{where, } g^1_{ij} = \int_{\Gamma_j} \psi_1 c^*$$

(5.17)

$$g^2_{ij} = \int_{\Gamma_j} \psi_2 c^*$$

Upon using equation (51.6) and equation (5.17) in the left hand side (LHS) of equation (5.12) it follows that

$$a_i c_i + \sum_{j=1}^{N} \begin{pmatrix} h^1_{ij} & h^2_{ij} \end{pmatrix} \begin{bmatrix} c_j \\ c_{j+1} \end{bmatrix} - \sum_{j=1}^{N} \begin{pmatrix} g^1_{ij} & g^2_{ij} \end{pmatrix} \begin{bmatrix} q_j \\ q_{j+1} \end{bmatrix} = Z$$

(5.18)

where Z represents the right hand side (RHS) of equation (5.12) and can be simplified as:

$$a_i c_i + \sum_{j=1}^{N} H_{ij} c_j - \sum_{j=i}^{N} G_{ij} q_j = Z \qquad (5.19)$$

where H_{ij} is equal to the h_{ij} term of the element (j) plus the h_{ij} term of the element (j-1). At any particular node i, the nodal coefficients are determined by considering the contributions of the two adjoining elements (j-1) and (j). The first term on the left hand side of equation (5.19) is usually combined in the H_{ij} term as follows

$$\sum_{j=1}^{N} \bar{H}_{ij} c_j - \sum_{j=i}^{N} G_{ij} q_j = Z$$

$$\bar{H}_{ij} = H_{ij} + a_i \text{ for } i = j \qquad (5.20)$$

$$\bar{H}_{ij} = H_{ij} \text{ for } i \neq j$$

The value of a_i is equal to ½, for constant elements where the boundary is assumed to be smooth (Brebbia and Dominguez 1992). However for other types of boundaries or other elements the authors have derived an expression which is standard in the BEM to evaluate a_i as, $a_i = (\theta/2\pi)$ where θ is the internal angle of the corner in radians. Alternatively a_i may be determined implicitly following the procedure proposed by Brebbia and Dominguez (1992).

5.1.3 Dealing with Unequal Fluxes at the Boundary

When the boundary is discretized into elements a geometric discontinuity occurs. Usually a unique value of the potential (e.g., concentration c) is prescribed such that c_2 of element j and c_1 of element j+1 are the same. However this may not be valid for the flux q, especially at the corners of the boundary where different values of flux on either side of a node may occur. Brebbia and Dominguez (1992) suggested an approach for handling two fluxes at a nodal point by specifying two values of fluxes at each nodal point and then arranging the fluxes in a 2N array. This procedure allows for two different values to be specified at corners. Equation (5.20) can now be written as:

$$\sum_{j=1}^{N} \bar{H}_{ij}c_j - \sum_{j=i}^{2N} G_{ij}q_j - Z \qquad (5.21)$$

When all the collocation points of j=1,...,N are considered, the resulting equation can be represented in matrix form as;

$$\bar{H}c - Gq - Z \qquad (5.22)$$

where G is a matrix of size N X 2N.

By applying the discretization procedure to the DRM formulation using the same linear interpolation functions, equation (5.12) can be written as:

$$a_i c_i + \sum_{k=1}^{N} H_{ik} C_k - \sum_{k=1}^{N} G_{ik} q_k = \sum_{j=1}^{N+L} \phi_j \left[a_i \hat{c}_{ij} + \sum_{k=1}^{N} H_{ik} \hat{C}_{kj} - \sum_{k=1}^{N} G_{ik} \hat{q}_{kj} \right] \qquad (5.23)$$

The DRM values of $\hat{c}$ and $\hat{q}$ are always known whenever the approximation function F_j is defined therefore their variation within a boundary are not approximated. As a result the same H and G matrices are used on the right hand side as approximate values with reasonable accuracy and more efficiency (Partridge et al. 1992). Since L denotes the number of internal nodes, q is not defined for i greater than N. The above equation can be written in the BEM matrix form as:

$$\bar{H}c - Gq = \sum_{j=1}^{N+L} \phi_j (\bar{H}\hat{c} - G\hat{q}) \qquad (5.24)$$

Over the summation from 1 to N+L, the vectors c_j and q_j correspond to the columns of the matrices c and q respectively and hence equation (5.23) can be written as:

$$\bar{H}c - Gq - (\bar{H}\hat{c} - G\hat{q})\phi \qquad (5.25)$$

5.1.4 The DRM Parameters F, ϕ, $\hat{c}$ and $\hat{q}$

It is recalled from the previous approximation of b that,

$$b \simeq \sum_{j-1}^{N+L} \phi_j \, F_j \qquad (5.26)$$

Now, if the values of b are defined at all the N+L nodes, ϕ and F can be defined at these points too. To evaluate ϕ, $\hat{c}$, and $\hat{q}$, the function F must be defined. Nardini and Brebbia (1982) proposed the distance function r used in the fundamental solution as the best approximation for F. The following definitions for F_j were proposed

(1) $F_j = r_j$

(2) $F_j = 1 + r_j$

(3) $F_j = 1 + r_j + r_j^2$

(4) $F_j = 1 + r_j + r_j^2 + r_j^3$ etc.

There is no restriction in using any of these definitions or a combination thereof except that the derivative of F_j must not be singular. However, comparative studies by Partridge and Brebbia (1990), Partridge and Brebbia (1992) and recently by Eldho (1996) have shown that, the linear approximation in the form $F_j = 1 + r_j$ is the simplest and also gives the most accurate results. When F_j is defined, the values of ϕ can then be determined by collocating b over all the N+L boundary and internal nodes to obtain a set of equations which in matrix form as

$$b - F\phi \qquad (5.27)$$

where each column of the F matrix consist of the vector F_j. It can now be seen that the matrix F depends on geometric data only and neither the equation type or boundary condition influence its values. The value of ϕ can then be obtained by inverting matrix F and multiplying by b to obtain

$$\phi - F^{-1}b \qquad (5.28)$$

If b is a known function then ϕ can be obtained directly otherwise it is solved iteratively. Similarly once F is defined, the DRM parameters $\hat{c}$ and $\hat{q}$ can be determined using the relationship defined earlier by equation (5.8). In the sections to follow details of the derivation of these parameters will be given when the DRM approach is applied to the solution of the solute transport equation.

5.2 DRM Formulation for the Solute Transport Equation.

5.2.1 Transformation of Governing Equations

The dual reciprocity method described above is general and can be applied to a variety of problems. However, the ease of its application depends on the ability to transform the governing equation under consideration to a form amenable for application. The equation governing the 2-D solute transport in a saturated porous subsurface medium is reproduced here for ease of reference as:

$$\frac{\partial}{\partial x}\left[D_x \frac{\partial c}{\partial x}\right] + \frac{\partial}{\partial y}\left[D_y \frac{\partial c}{\partial y}\right] - V_x \frac{\partial c}{\partial x} - V_y \frac{\partial c}{\partial y} - R\lambda c + Q = R\frac{\partial c}{\partial t} \tag{5.29}$$

where the parameters are as defined earlier. In solute transport analysis, the coefficient of hydrodynamic dispersion is a function of flow direction therefore even in an isotropic homogeneous medium, D_x may not be equal to D_y. In the application of the DRM approach to problems of this nature Partridge and Brebbia (1990), Partridge et al. (1992) have suggested an approach that involves the differentiation of the approximation function F. For example when dealing with an equation involving a product of two function and/or non-linear terms such as

$$\nabla^2 u - b - E(x,y)\frac{\partial u}{\partial x}$$

<div align="right">(5.30)</div>

Partridge and Brebbia (1990) approximated the right hand side as:

$$\frac{\partial u}{\partial x} - \frac{\partial F}{\partial x}F^{-1}u$$

<div align="right">(5.31)</div>

Where the governing equation expresses an anisotropy, as in the case of equation (5.29), such an approach requires the second derivative of F_j. The first problem is that the simplest and most accurate definition of $F_j = 1 + r_j$ cannot be employed since its second derivative is singular when $r=0$. It has also been shown (Zhu and Zhang 1994) that the differentiation of the distance function r in order to associate non-linear terms such as the advective terms in equation (5.29) results in singularities at collocation points. These singularities sometimes lead to large numerical errors reducing the accuracy of the DRM approach. Zhu and Zhang (1994) proposed an approach to avoid this but, their method is more cumbersome and does not produce corresponding improvements over the traditional DRM approach. Moreover their transformation is only valid if the coefficients of the non-linear terms such as E(x,y) in equation (5.30) are continuous functions in the domain. Amoah et al. (1996) proposed an approach to circumvent such problems in the application of DRM to this class of partial differential equations. Their

method employed simple transformations to avoid the differentiation of the approximation function. This was successfully applied to theoretical problems in solute transport analysis. In this work we slightly modify the procedure followed by Amoah et al. (1996) to improve the computational efficiency and extend it for analysis of practical field problems. First the anisotropy is removed by writing the ADE in the form of:

$$\frac{\partial^2 c}{\partial x_1^2} + \frac{\partial^2 c}{\partial y_1^2} - \frac{V_x}{D_x}\frac{\partial c}{\partial x_1} - \left[\frac{V_y}{D_x}\sqrt{\frac{D_x}{D_y}}\right]\frac{\partial c}{\partial y_1} + R\frac{\lambda c}{D_x} + \frac{Q}{D_x} = \frac{R}{D_x}\frac{\partial c}{\partial t} \tag{5.32}$$

where the following coordinate transformations have been employed

$$y_1 = y\sqrt{\frac{D_x}{D_y}} \quad , \qquad x_1 = x \, , \tag{5.33}$$

and D_x and D_y are constant. Furthermore by letting

$$c = \mu(x_1)\bar{c}(x_1, y_1, t) \tag{5.34}$$

appropriate expressions for the terms in equation (5.32) can be derived for example,

$$\frac{\partial^2 c}{\partial x_1^2} = \bar{c}\frac{\partial^2 \mu}{\partial x_1^2} + \mu\frac{\partial^2 \bar{c}}{\partial x_1^2} + 2\frac{\partial \bar{c}}{\partial x_1}\frac{\partial \mu}{\partial x_1} \tag{5.35}$$

By writing

$$\frac{d\mu}{dx_1} = \mu' \ , \quad \frac{d^2\mu}{dx_1^2} = \mu'' \tag{5.36}$$

and considering a uniform flow field in the x-direction with constant V_x and $(V_y=0)$, equation (5.32) can be written as:

$$\frac{R}{D_x}\mu\frac{\partial \bar{c}}{\partial t} = \mu\nabla^2\bar{c} + \bar{c}\mu'' + 2\mu'\frac{\partial \bar{c}}{\partial x_1} - \hat{V}_x\left[\mu'\ \bar{c}+\frac{\partial \bar{c}}{\partial x_1}\mu\right] - \frac{R}{D_x}\mu\lambda\bar{c} + \frac{Q}{D_x} \tag{5.37}$$

where

$$\hat{V}_x = \frac{v_x}{D_x} \tag{5.38}$$

The value of μ is sought such that

$$\left[2\mu' - \mu\hat{V}_x \right]\frac{\partial \bar{c}}{\partial x_1} = 0 \tag{5.39}$$

and then

$$\frac{\mu'}{\mu} - \frac{(\hat{V}_x)}{2} = \mu_0 \tag{5.40}$$

Rearranging and integrating both sides gives:

$$\mu = e^{\mu_0 x_1} \tag{5.41}$$

Dividing through equation (5.37) by μ and noting that

$$\frac{\mu^{\prime\prime}}{\mu} = \mu_0^2 \qquad (5.42)$$

results in the expression

$$\frac{R}{D_x}\frac{\partial \bar{c}}{\partial t} = \nabla^2\bar{c} + \mu_0^2\bar{c} + 2\mu_0\frac{\partial \bar{c}}{\partial x_1} - 2\mu_0\left[\mu_0\ \bar{c} + \frac{\partial \bar{c}}{\partial x_1}\right] - \frac{R\lambda\bar{c}}{D_x} - Q'$$

$$(5.43)$$

$$\text{where} \qquad Q' = \frac{Q}{\mu D_x}$$

which simplifies to:

$$\nabla^2\bar{c} - \mu_0^2\ \bar{c} = \frac{R}{D_x}\frac{\partial \bar{c}}{\partial t} - \frac{R\lambda\bar{c}}{D_x} - Q' \qquad (5.44)$$

5.2.3 Application of DRM to the Transformed Equation

Equation (5.44) can be described as a modified form of the Helmholtz equation which is still a nonhomogeneous, nonlinear equation. In the conventional BEM analysis, a fundamental solution for this equation must be derived in order to carry out the boundary only solution. The

derivation of fundamental solution and its implementation in the BEM process can be very tedious. However, the dual reciprocity method allows the use of any suitable fundamental solutions to be employed and therefore the simplest form corresponding to the Laplace equation will be used here. Equation (5.44) is then treated as a Poisson type equation and written in the form:

$$\nabla^2 \bar{c} = b\left(\bar{c}, x_1, y_1, t\right) \qquad (5.45)$$

where

$$b = \mu_0^2\, \bar{c} + \frac{R}{D_x}\frac{\partial \bar{c}}{\partial t} - \frac{R\lambda \bar{c}}{D_x} - Q' \qquad (5.46)$$

Applying the dual reciprocity BEM formulation already described and collocation over N boundary nodes and L internal nodes results in an equation of the form

$$a_i c_i + \sum_{k=1}^{N} H_{ik}\bar{c}_k - \sum_{k=1}^{N} G_{ik} q_k = \sum_{j=1}^{N+L} \phi_j \left[a_i \bar{c} + \sum_{k=1}^{N} H_{ik}\bar{c}_{kj} - \sum_{k=1}^{N} G_{ik}\hat{q}_{kj} \right] \qquad (5.47)$$

This simplifies to the usual DRM-BEM equation:

$$\overline{H}\overline{c} - Gq = \sum_{j=1}^{N+L} \left(\overline{H}\overline{c}_j - G\hat{q}_j\right)\phi_j \qquad (5.48)$$

and can further be written in the conventional form as:

$$\overline{H}\overline{c} - Gq = \left(\overline{H}\overline{c} - G\hat{q}\right)\phi \qquad (5.49)$$

5.2.4 Evaluation of the DRM Parameters F, ϕ, $\hat{c}$ and $\hat{q}$

The series of transformations allows the use of the simplest definition of $F_j = 1 + r_j$ in the determination of the required parameters. Now r_j is the usual distance function given as:

$$r_j = \sqrt{(x - x_j)^2 + (y - y_j)^2} \qquad (5.50)$$

Now recall that the relationship between the particular solution $\hat{c}(r)$ and the approximation function F can be written as:

$$\nabla^2\hat{c} = \frac{d^2\hat{c}}{dr^2} + \frac{1}{r}\frac{d\hat{c}}{dr} = F = 1+r \qquad (5.51)$$

This can also be written as:

$$\nabla^2\hat{c} = \frac{dg}{dr} + \frac{1}{r}g = 1+r$$

$$\text{where} \quad g = \frac{d\hat{c}}{dr} \qquad (5.52)$$

Equation (5.52) is a linear differential equation with integration factor r and a solution given as:

$$rg = r\frac{d\hat{c}}{dr} = \int r(1+r)dr = \frac{r^2}{2} + \frac{r^3}{3} \qquad (5.53)$$

From this we can deduce that

$$\frac{d\hat{c}}{dr} = \frac{r}{2} + \frac{r^2}{3} \qquad (5.54)$$

and

$$\hat{c} = \frac{r^2}{4} + \frac{r^3}{9} \qquad (5.55)$$

The normal derivative is evaluated by considering that

$$\frac{\partial \hat{c}}{\partial n} = \frac{\partial \hat{c}}{\partial x}\frac{\partial x}{\partial n} + \frac{\partial \hat{c}}{\partial y}\frac{\partial y}{\partial n} = \frac{\partial \hat{c}}{\partial x}n_x + \frac{\partial \hat{c}}{\partial y}n_y \qquad (5.56)$$

where n_x and n_y are the direction cosines of x and y respectively. Consider also that

$$\frac{\partial \hat{c}}{\partial x} = \frac{\partial \hat{c}}{\partial r}\frac{\partial r}{\partial x} = \left[\frac{r}{2}+\frac{r^2}{3}\right]\left[\frac{x-x_j}{r}\right] \qquad (5.57)$$

therefore

$$\hat{q} = \frac{\partial \hat{c}}{\partial n} = \left[\frac{1}{2}+\frac{r_j}{3}\right]\left[(x-x_j)n_x+(y-y_j)n_y\right] \qquad (5.58)$$

5.2.5 Evaluation of the F Matrix

With these definitions in place, the matrix F is constructed by considering the values of b at the boundary and internal nodes 1,2,3,......N+L of the domain under consideration. At all the collocation points the following equations can be deduced;

$$b_1 = F_{11}\phi_1 + F_{12}\phi_2 + F_{13}\phi_3 + \ldots F_{1N+L}\phi_{N+L}$$

$$b_2 = F_{21}\phi_1 + F_{22}\phi_2 + F_{23}\phi_3 + \ldots F_{2N+L}\phi_{N+L}$$

$$b_3 = F_{31}\phi_1 + F_{32}\phi_2 + F_{33}\phi_3 + \ldots F_{3N+L}\phi_{N+L}$$

$$\ldots = \ldots\ldots\ldots\ldots\ldots\ldots\ldots\ldots\ldots\ldots\ldots\ldots$$

$$\ldots = \ldots\ldots\ldots\ldots\ldots\ldots\ldots\ldots\ldots\ldots\ldots\ldots$$

$$b_{N+L} = F_{(N+L)1}\phi_{N+L} + \ldots\ldots\ldots\ldots + F_{N+L}\phi_{N+L}$$

(5.59)

which can be put in a matrix form as:

$$
\begin{bmatrix} b_1 \\ b_2 \\ b_3 \\ \cdot \\ \cdot \\ \cdot \\ b_{N+L} \end{bmatrix}
=
\begin{bmatrix}
F_{11} & F_{12} & F_{13} & \cdot & \cdot & \cdot & F_{1N+L} \\
F_{21} & F_{22} & F_{23} & \cdot & \cdot & \cdot & F_{2N+L} \\
F_{31} & \cdot & \cdot & \cdot & \cdot & \cdot & F_{3N+L} \\
\cdot & \cdot & \cdot & \cdot & \cdot & \cdot & \cdot \\
\cdot & \cdot & \cdot & \cdot & \cdot & \cdot & \cdot \\
\cdot & \cdot & \cdot & \cdot & \cdot & \cdot & \cdot \\
\cdot & \cdot & \cdot & \cdot & \cdot & \cdot & F_{(N+L)N+L}
\end{bmatrix}
\begin{bmatrix} \phi_1 \\ \phi_2 \\ \phi_3 \\ \cdot \\ \cdot \\ \cdot \\ \phi_{N+L} \end{bmatrix}
$$

(5.60)

and can be written as

$$B = F\Phi$$

(5.61)

Now the matrix F is symmetric of size $(N+L) \times (N+L)$ with each of the F_{ij} terms being a function of F_j at point i and evaluated by taking the distance between points i and j such that, for example,

$$f_{12} = f_2 = 1+\sqrt{(x_1-x_2)^2+(y_1-y_2)^2}$$
$$f_{34} = f_4 = 1+\sqrt{(x_3-x_4)^2+(y_3-y_4)^2}$$

(5.62)

The vector B has components corresponding to the nodal values of b. Thus if b is known, the value of Φ can be calculated in a straight forward manner. However, in the present case where b is an unknown function of (c,x,y,t), the value of Φ cannot be explicitly determined but has to be expressed in terms of F and B and then solved iteratively. Therefore by substituting in equation (5.28) in equation (5.49) we have,

$$H\bar{c}-Gq = (H\bar{c}-Gq)F^{-1}B$$

(5.63)

Recalling the expression for b from equation (5.46) and substituting in equation (5.63) gives

$$\bar{H}\bar{c}-Gq \;-\; (\bar{H}\bar{c}-G\hat{q})F^{-1}\left[\mu_0^2\tilde{c}+\frac{R}{D_x}\frac{\partial\bar{c}}{\partial t}-\frac{R\lambda\tilde{c}}{D_x}-Q'\right] \tag{5.64}$$

This is simplified as

$$[\bar{H}\bar{c}-Gq] \;-\; \mu_1^2\,P\tilde{c}\;+P\left[\frac{R}{D_x}\frac{\partial\bar{c}}{\partial t}\right]-PQ' \tag{5.65}$$

where the matrix P is given as:

$$P \;-\; (\bar{H}\bar{c}-G\hat{q})\,F^{-1} \tag{5.66}$$

and

$$\mu_1^2 \;-\; \mu_0^2-\frac{R\lambda}{D_x} \tag{5.67}$$

5.2.6 Time Integration

The time derivative term is evaluated by using a simple finite difference approximation of the change in concentration with time as:

$$\frac{\partial c}{\partial t} \approx \frac{c_i - c_{i-1}}{\Delta t} \tag{5.68}$$

Assuming a linear variation of the concentration and its normal derivatives within any time step, a dimensionless variable ω, to locate c and q within any time interval t_i and t_{i+1} as:

$$c = (1-\omega_c)c_i + \omega_c \ c_{i+1} \tag{5.69}$$

$$q = (1-\omega_q)q_i + \omega_q \ q_{i+1} \tag{5.70}$$
$$0 \leq \omega \leq 1$$

When ω takes the value of 0.5, the approximation becomes the Crank-Nicholson central difference approach which is unconditionally stable. Reasonable accuracy has been reported in the literature with values of $\omega_c = 0.5$ and $\omega_q = 1.0$ in similar analysis (Partridge et al. 1992, Eldho 1996). Using these values in the above equations and substituting the results in equation (5.65), we have

$$0.5\bar{H} \ (c_1 + c_0) - Gq_1 - \mu_1^2 P \ (c_1 + c_0) + \frac{R}{D_x} \frac{Pc_1}{\Delta t} - \frac{R}{D_x} \frac{Pc_0}{\Delta t} - PQ' \tag{5.71}$$

and by rearranging and grouping terms together we have

$$\left[\bar{H}-\mu_1{}^2P-\frac{R}{D_x}\frac{2P}{\Delta t}\right]c_1-2Gq_1 = \left[\mu_1{}^2P-\bar{H}-\frac{R}{D_x}\frac{2P}{\Delta t}\right]c_0-2PQ' \qquad (5.72)$$

This is the dual reciprocity boundary element equation required to be evaluated for the problem at hand. Now at each node, there are three unknowns initially which are the potential c_j, the flux on either side of the nodal point $q_j{}^2$ and $q_j{}^1$. However by applying the boundary conditions, any two will be specified leaving only one unknown. For example, in a Dirichlet type boundary condition the concentration is set to the prescribed value for that element. A similar operation is performed for a Neuman or Cauchy type boundary condition. The known values are then taken to the right hand side to obtain an N x N system of equations which in the matrix form is written as:

$$Ax = y_1+y_2 \qquad (5.73)$$

The arrangement of the above matrix is done following the approach of Partridge et al. (1992). Whenever c_1 is unknown the column represented by the first term on the left hand side is retained in the same column of matrix A. If however c_1 is known it is multiplied and transferred to the right hand side and added to vector y_1. If q is unknown, the column of -2G is retained in A. The vector y_2 will contain the terms involving c_0 in equation (5.72), therefore

this vector will be computed at each time step when c_i moves to c_{i+1}. The vector x therefore will contain the N values of c and q at the boundary and L values of c at interior points.

5.2.7 Computation of Interior Values

The interior values are computed on the nodes represented from $N+1$ to $N+L$. Equation (5.47) is used in this regard from which is obtained an equation of the form:

$$c_i = \sum_{k=1}^{N} H_{ik}\bar{c}_k - \sum_{k=1}^{N} G_{ik}q_k + \sum_{j=1}^{N+L} \phi_j \left[\bar{c}_{ij} + \sum_{k=1}^{N} H_{ik}\bar{c}_{kj} - \sum_{k=1}^{N} G_{ik}\hat{q}_{kj} \right] \qquad (5.74)$$

This is rearranged to produce a similar matrix equation of the form

$$c_I = Gq - Hc + \phi[H\hat{c} - G\hat{Q}] + \hat{c}\phi \qquad (5.75)$$

where c_I is a vector of the interior values of c. In the DRM approach the interior values are computed alongside the boundary values by including L number of interior nodes such that the size of the DRM matrix is $N+L \times N+L$, where N is the number of boundary nodes.

5.3 Evaluation of the Integrals

5.3.1 Regular Integrals

For two dimensional BEM analysis, regular Gaussian quadrature formulas are usually employed to integrate over all the one-dimensional elements except the ones corresponding to source points. Each integral is written as:

$$\int_{-1}^{1} f(\xi)d(\xi) = \sum_{i=1}^{i=N} f(\xi)w_i \qquad (5.76)$$

The evaluation of the integrals involved in the H and G matrices is done by first recalling that the fundamental solution for Laplace's equation is employed (equation 5.5 a). As a result of the transformations employed, the fundamental solution will become in the transformed domain as:

$$c^* = \frac{1}{2\pi\sqrt{D_y/D_x}}\ln\left(\frac{1}{r}\right) \qquad (5.77)$$

The H and G matrices are evaluated as follows:

$$H_{ij} = \int_{\Gamma_j} q^* d\Gamma = \frac{l_j}{2}\sum_{k=1}^{N} q_k^* w_k \qquad (5.78)$$

and

$$G_{ij} = \int_{\Gamma_j} c^* d\Gamma = \frac{l_j}{2} \sum_{k=1}^{N} c_k^* w_k \tag{5.79}$$

where l_j is the length of an element j and w_k is the Gaussian weight associated with the integration point x_k. Using a ten point Gaussian integration and employing the transformed fundamental solution, the G_{ij} term of an element at a collocation point is evaluated as:

$$G_{ij} = \frac{L_j}{4\pi\sqrt{D_y/D_x}} \sum_{k=1}^{10} \ln(\frac{1}{r_k}) w_k \tag{5.80}$$

where k is the Gaussian integration point, r_k is the distance between the collocation point, (x_i, y_i) and the Gaussian integration point (x_k, y_k). Similarly, where (x_0, y_0), (x_1, y_1) are the local coordinates of the end points of an element j,

$$H_{ij} = \frac{L_j}{4\pi\sqrt{D_y/D_x}} \sum_{k=1}^{10} \frac{d}{dn} \left[\ln\frac{1}{r_k} \right] w_k$$

$$= \frac{L_j}{4\pi\sqrt{D_y/D_x}} \sum_{k=1}^{10} -\frac{1}{r_k} \left[\frac{\partial r}{\partial x} n_x + \frac{\partial r}{\partial y} n_y \right] w_k \tag{5.81}$$

$$= \frac{L}{4\pi\sqrt{D_y/D_x}} \sum_{k=1}^{10} -\frac{1}{r_k} \left[\left[\frac{(x_k - x_i)}{r_k} \frac{(y_1 - y_0)}{L} \right] + \left[\frac{(y_k - y_i)}{r_k} \frac{(x_0 - x_1)}{L} \right] \right] w_k$$

5.3.2 Integrals with Singularities

A difficulty in using the Gaussian integration arises at the source points. As the source is applied at designated points in turn, on two occasions, the integrals are unbounded as a result of singularities in the kernel terms when the node at which the source is applied coincides with the node at which the influence is integrated (nodes $i=j$). This singularity in the potential and flux kernels results in improper integrals involving $\ln(x)$ and $1/x$. Several approaches have been suggested to carefully handle this by using an analytical solution for simple elements and hybrid quadrature schemes for some complicated ones. For quadratic and higher order elements in two and three dimensional problems with log singularities, the Gaussian quadrature formula is modified to the form:

$$I = \int_0^1 \ln(\frac{1}{x})f(x)dx = \sum_{k=1}^{N} w_k f(x_k) \tag{5.82}$$

where N is the number of log quadrature points, x_k are the location of these points with weights w_k. However for lower order elements like the linear ones used in this analysis it is most efficient and accurate to use analytical integration. Consider the integration over the elements shown below.
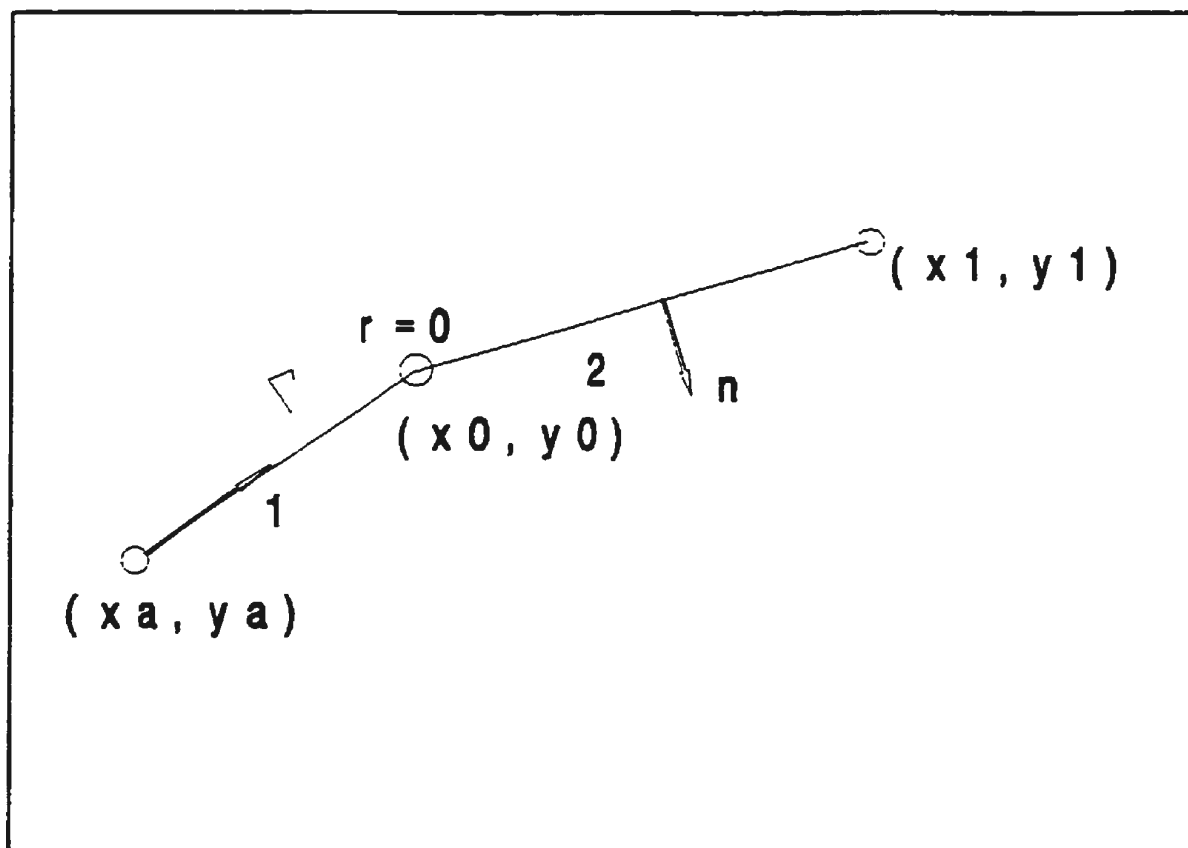
Figure 5.4: Integration over linear elements

The value of r is zero at the points (x_0, y_0) and (x_1, y_1). For a linear variation of c over an element, we recall that:

$$c = (1-\eta)c_0 + \eta c_1 \tag{5.83}$$

and

$$q = (1-\eta)q_0 + \eta q_1 \tag{5.84}$$

It is required to evaluate the integrals such as

$$\int_\Gamma c^* = [(1-\eta)c_0 + \eta\, c_1] d\Gamma$$
$$\text{where } c^* = -\frac{1}{2\pi}\ln(r) \tag{5.85}$$

Now for a general element (say)

$$x = (1-\eta)x_0 + \eta x_1 \tag{5.86}$$

and

$$y = (1-\eta)y_0 + \eta y_1 \tag{5.87}$$

therefore

$$x - x_0 = \eta(x_1 - x_0) \tag{5.88}$$

$$y - y_0 = \eta(y_1 - y_0) \tag{5.89}$$

and hence

$$r = \sqrt{\eta^2[(x_1 - x_0)^2 + (y_1 - y_0)^2]} = \eta L \tag{5.90}$$

where L is the length of the element . Similarly

$$d\Gamma = \sqrt{dx^2 + dy^2} = \sqrt{d\eta^2[(x_1 - x_0)^2 + (y_1 - y_0)^2]} = L \, d\eta \tag{5.91}$$

Now let

$$I_1 = \int_\Gamma c^* d\Gamma = -\frac{1}{2\pi} \int_0^1 \ln(\eta L) L \, d\eta$$

$$= -\frac{1}{2\pi} \int_0^L \ln(z) \, dz \tag{5.92}$$

where, $z = \eta L$

therefore

$$I_1 = \int_\Gamma c^* d\Gamma = -\frac{L}{2\pi}(1-\ln L) \tag{5.93}$$

Let

$$I_2 = \int_\Gamma \eta c^* d\Gamma = -\frac{1}{2\pi}\int_0^L \eta\ln(\eta L)L \ d\eta$$
$$= -\frac{1}{2\pi}\int_0^L \frac{z}{L}\ln(z) \ dz \tag{5.94}$$

Therefore

$$I_2 = \int_\Gamma \eta c^* d\Gamma = -\frac{L}{8\pi}(1-2\ln L) \tag{5.95}$$

hence

$$\int_\Gamma (1-\eta)c^* d\Gamma = \frac{L}{2\pi}(1-\ln L)-\frac{L}{8\pi}(1-2\ln L)$$
$$= \frac{L}{8\pi}(3-2\ln L) \tag{5.96}$$

Similarly when the analysis is carried out over a preceding element away from (x,y) and towards (x_0,y_0), the analytical integration formula is evaluated as follows:

$$x = (1-\eta)x_a + \eta x_0$$
$$y = (1-\eta)y_a + \eta y_0$$

(5.97)

from this we obtain

$$r = \sqrt{(1-\eta^2)[(x_a-x_0)^2+(y_a-y_0)^2]} = (1-\eta)L$$

(5.98)

Now

$$\int_\Gamma \psi_2 c^* d\Gamma = \int_0^1 (1-\eta)c^* d\Gamma$$

(5.99)

$$\int_0^1 c^* d\Gamma = -\frac{1}{2\pi}\int_0^L \ln[(1-\eta)L] \; L \; d\eta$$

$$= -\frac{1}{2\pi}\int_0^L \ln(z)dz$$

(5.100)

$$= \frac{L}{2\pi}(1-\ln L)$$

where $z = (1-\eta)L$

Similarly,

$$\int_\Gamma \eta c^* \, d\Gamma = -\frac{1}{2\pi} \int_0^L \eta \ln[(1-\eta)L] \, L \, d\eta$$

$$= -\frac{1}{2\pi} \int_0^L \left[1 - \frac{z}{L}\right] \ln(z) \, dz \qquad (5.101)$$

$$= -\frac{L}{2\pi}\left[(\ln L - 1) - \frac{1}{4}(2\ln L - 1)\right]$$

$$= \frac{L}{8\pi}(3 - 2\ln L)$$

Hence

$$\int_\Gamma (1-\eta)c^* \, d\Gamma = \frac{L}{2\pi}(1 - \ln L) - \frac{L}{8\pi}(3 - 2\ln L)$$

$$= \frac{L}{4\pi}(\frac{1}{2} - \ln L) \qquad (5.102)$$

Therefore in general, considering a point (x_0, y_0) connecting any two elements j and $j-1$, the two analytical integration formulas that will be used to evaluate the coefficients g_{ii} for those parts of elements which includes singularity are:

$$g_{ii,e1} = -\frac{1}{2\pi} \int_{\Gamma_j} \psi_1 \ln(r) d\Gamma = \frac{L}{8\pi}(3 - 2\ln L)$$

$$\qquad (5.103)$$

$$g_{ii,e2} = -\frac{1}{2\pi} \int_{\Gamma_j} \psi_2 \ln(r) d\Gamma = \frac{L}{4\pi}(\frac{1}{2} - \ln L)$$

The integrals in H_{ii} evaluated along the elements with singularity are determined as:

$$H_{ii} - \int_{\Gamma_i} q^* d\Gamma - \int_{\Gamma_i} \frac{\partial c^*}{\partial n} - \int_{\Gamma_i} \frac{\partial c^*}{\partial r} \frac{\partial r}{\partial n} d\Gamma \qquad (5.104)$$

but

$$\frac{\partial r}{\partial n} - \frac{\partial r}{\partial x} n_x + \frac{\partial r}{\partial y} n_y$$

$$- \left[\frac{x_1 - x_0}{L} \right] (y_1 - y_0) + \left[\frac{y_0 - y_1}{L} \right] (x_0 - x_1) - 0 \qquad (5.105)$$

Hence the H_{ii} terms are zero, ie.

$$H_{ii} - \int_{\Gamma_i} q^* d\Gamma \equiv 0 \quad \text{on} \quad \Gamma_i \qquad (5.106)$$

5.4 Summary of the Boundary Element Formulation

In this chapter a background of the dual reciprocity method (DRM) has been provided. A DRM formulation of the solute transport equation is developed which uses series of transformations and mathematical manipulations to transform the advection-dispersion equation into a modified Helmholtz equation. The dual reciprocity method is employed to carry the nonhomogeneous terms to the boundary for a boundary only formulation. This avoids the differentiation of the approximation function F_j which is the conventional DRM approach proposed by Partridge and Brebbia (1990) for the solution of such types of problems. We believe this approach of avoiding singularities at collocation points improves the accuracy and is also less cumbersome than the procedure of Zhu and Zhang (1994).

Chapter 6

Verification and Benchmarking of the DRBEM Model

6.1 Introduction

Verification and benchmarking are very important test procedures to enhance reliability and confidence in a numerical model. There are no standard testing procedures for numerical models. However, in this chapter the DRBEM model will be tested by following some well accepted procedures proposed in the literature. Huyakorn et al. (1984) examined the quality of numerical models and their applicability to specific problems and proposed three levels of quality control procedures pertaining to model utility and three additional levels on model applicability. The procedures for ensuring model utility are, (i) validation of the mathematical basis of a numerical model by comparing its output with known analytical solutions to specific problems; (ii) benchmarking the efficiency of the model in solving problems by comparison with the performance of other numerical models; (iii) verification of the applicability of the model to various categories by successful simulation of observed field data. The model

applicability test procedures include: (i) a critical review of the problem conceptualization to ensure that the modelling effort considers all physical, chemical and biological processes that affect the problem; (ii) an evaluation of the specifics of the model's application, e.g., appropriateness of the boundary conditions, grid design and time step; and (iii) an appraisal of the match between mathematical sophistication of the model and the temporal and spatial resolution of data.

By following the definition of Huyakorn et al. (1984) the numerical model will be verified by checking the accuracy of the computational algorithm used to solve the governing equations and its implementation into computer code. The model is therefore applied to simplified but realistic problems for which analytical solutions are available. During the verification process the sensitivity of the model to input parameters, the time and space discretizations are evaluated. The effects of temporal and spatial grid design are evaluated based on the grid Peclet and Courant number criteria. The grid Peclet number, P_e, and Courant number C_r are defined as (Roache 1982, Daus and Frind 1985):

$$P_e = \frac{\Delta x}{\alpha_L} \qquad (6.1)$$

$$C_r = \frac{|V| \Delta t}{\Delta x} \qquad (6.2)$$

where, Δx is the grid spacing in the x-direction and Δt is the time step. The grid Courant number controls the errors due to the discrete approximation of the time derivative while the grid Peclet number controls oscillations due to spatial discretization. P_e also serve as a measure of the relative magnitude of the advection and dispersion during the mass transport process.

6.2 Verification of the Model

Four problems have been considered in the verification of the model. One heat transport problem and three contaminant transport problems are considered, each representing a different way by which contaminant is introduced into the aquifer. The contaminant transport problems are (1) continuous migration of contaminants from a patch source, (2) continuous migration from a point source, (3) instantaneous or pulse release of contaminant from a point source. All of these problems have well developed analytical solutions and codes (e.g., Javandel et al. 1984, Huyakorn et al. 1984, Beljin 1988). Different aquifer and grid parameters are employed for each problem. The aquifer is assumed to be of uniform thickness and relatively thin to allow complete mixing of solute over the entire thickness. Groundwater flow velocity is assumed to be uniform in the longitudinal direction. A zero initial concentration is assumed throughout the domain. It is also assumed that the rate of injection and mixing is such that the density and viscosity of the ambient groundwater is not altered. The effects of molecular diffusion are assumed to be negligible in all cases during the hydrodynamic dispersion process. A rectangular

domain defined in the Cartesian plane is considered. The domain dimensions, spatial and temporal discretizations are different for each type of problem selected so that the overall results will demonstrate the efficiency of the boundary element model for different applications. For each of the problem types, details of parameters used and the analytical solution given in the literature will be provided for completeness. The average error between the results from the analytical solution and that of the numerical model, is quantified by using the root mean square error (RMSE) criteria (Anderson and Woessner 1992). This is given as:

$$\text{RMSE} = \left[\frac{1}{n} \sum_{i=1}^{i=n} \left(c_a - c_m \right)_i^2 \right]^{1/2} \qquad (6.3)$$

where, c_a's represent the concentration values obtained from the analytical or exact solution, the c_m's are the values obtained from numerical solution and n is the number of values computed.

6.2.1 Verification Problem I: Heat Diffusion in a Square Plate

The first verification problem involves heat transport through a square plate (3 m x 3 m). Although this problem does not relate to contaminant transport it was meant to check the accuracy of the new approach of using transformations. This problem has been solved by the traditional DRBEM approach involving the differentiation of the approximation function by Partridge et al. (1992). A computer implementation of the approach (which is later referred to as Partridge's approach) has been verified by the analytical solution. The only reason for using this problem is to verify the accuracy and efficiency of our new procedure of avoiding the differentiation of the approximation function used in the DRM. The initial temperature of the plate was 30°C and then it was cooled by the application of thermal shock (u=0°C all over the boundary). The values D_x and D_y and were specified as 4.0 m²/s and 1.0 m²/s respectively. The computer program to implement our new approach was modified to solve this problem. The results of the temperature distribution at specified nodes are compared with those of Partridge (1992) and the analytical solution in Table 6.1 below. The results in Table 6.1 show the improved accuracy of the present approach of avoiding the differentiation of the approximation function and confirms the findings of Zhu and Zhang (1993).

Table 6.1: Comparison of Present work with Partridge's approach for heat diffusion problem

x (m)	y (m)	DRM-Partridge's approach (Temp (°C))	DRM-Present work (Temp (°C))	Analytical (Temp (°C))
2.4	2.4	0.024	0.021	0.020
2.4	1.5	0.041	0.036	0.036
1.8	1.8	0.064	0.056	0.055
1.8	1.5	0.067	0.059	0.058
1.5	1.5	0.071	0.062	0.061

6.2.2 Verification Problem II: Migration of Contaminant from a Patch Source

The second verification problem concerns the migration of a contaminant from a finite length strip source in a two dimensional space (patch source). In practice, this may be in the form of the migration of contaminant from a rectangular strip of surface impoundment lying perpendicular to the direction of groundwater flow (Figure 6.1). It is assumed that contaminant reaches the aquifer and creates a constant concentration c_0 in the area beneath the impoundment. The problem is to estimate the concentration distribution in the aquifer at different times after the leakage has started and also to delineate the extent of aquifer contamination at these times. A similar type of problem has been considered by Javandel et al (1984) to test the accuracy of an analytical model. Sudicky (1989) also considered a patch source problem to verify a Laplace transform Galerkin finite element model. This problem is selected to demonstrate the accuracy of the DRBEM in handling large contrasts between longitudinal and transverse dispersivities. Therefore dispersivity ratios (transverse/longitudinal) of 1/10, 1/20, which are realistic in practical field cases are used. An analytical solution for the patch source problem as described above was given by Clearly and Ungs (1978) as:

$$c(x,y,t) = \frac{c_o x}{4(\pi D_x)^{1/2}} \exp\left(\frac{|V|x}{2D_x} - \alpha t\right) \cdot$$

$$\int_{-0}^{t/R} \exp\left[-\left(\lambda R - \alpha R + \frac{v^2}{4D_x}\right)\tau - \frac{x^2}{4D_x\tau}\right]\tau^{-3/2} \cdot \quad (6.4)$$

$$\left(\operatorname{erf}[\frac{a-y}{2(D_y\tau)^{1/2}}] + \operatorname{erf}[\frac{a+y}{2(D_y\tau)^{1/2}}]\right)d\tau$$

The computer implementation of the above solution was given by Javandel et al. (1984) for the following initial condition (t=0) and boundary condition:

$$c = c_o e^{-\alpha t}, \quad x=0, \quad -a \le y \le +a, \quad t=0$$

$$\quad (6.5)$$

$$c = 0, \quad x=0, \quad y > +a, \quad y < -a$$
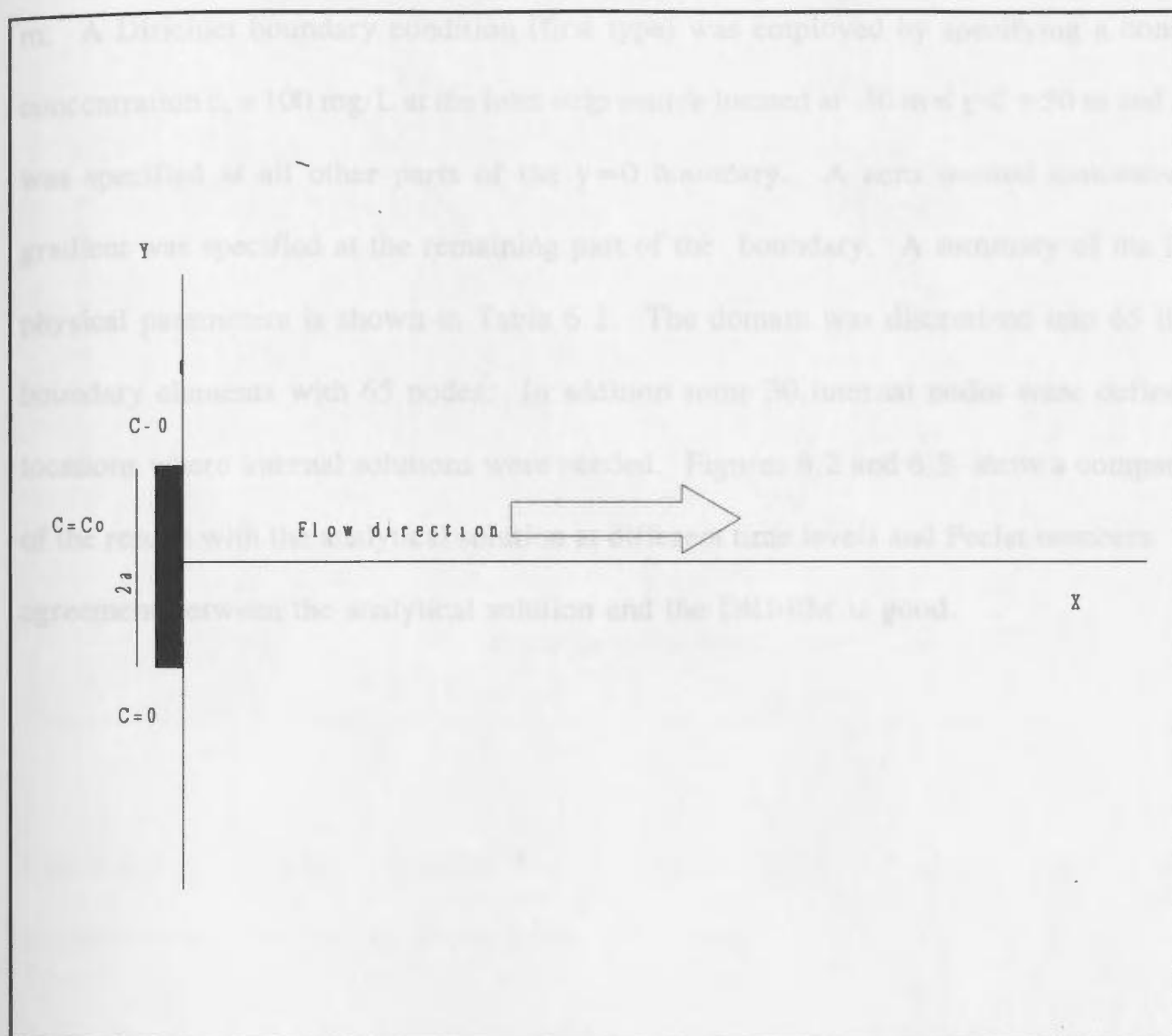
Figure 6.1 Contaminant migration form a patch source

A boundary element solution was obtained for this problem by considering a rectangular domain defined in the Cartesian plane by the lines $y = 100$ m, $y = -100$ m, $x = 0$, $x = 1600$ m. A Dirichlet boundary condition (first type) was employed by specifying a constant concentration $c_o = 100$ mg/L at the inlet strip source located at -50 m $< y < +50$ m and $c = 0$ was specified at all other parts of the $y = 0$ boundary. A zero normal concentration gradient was specified at the remaining part of the boundary. A summary of the input physical parameters is shown in Table 6.2. The domain was discretized into 65 linear boundary elements with 65 nodes. In addition some 30 internal nodes were defined at locations where internal solutions were needed. Figures 6.2 and 6.3 show a comparison of the results with the analytical solution at different time levels and Peclet numbers. The agreement between the analytical solution and the DRBEM is good.
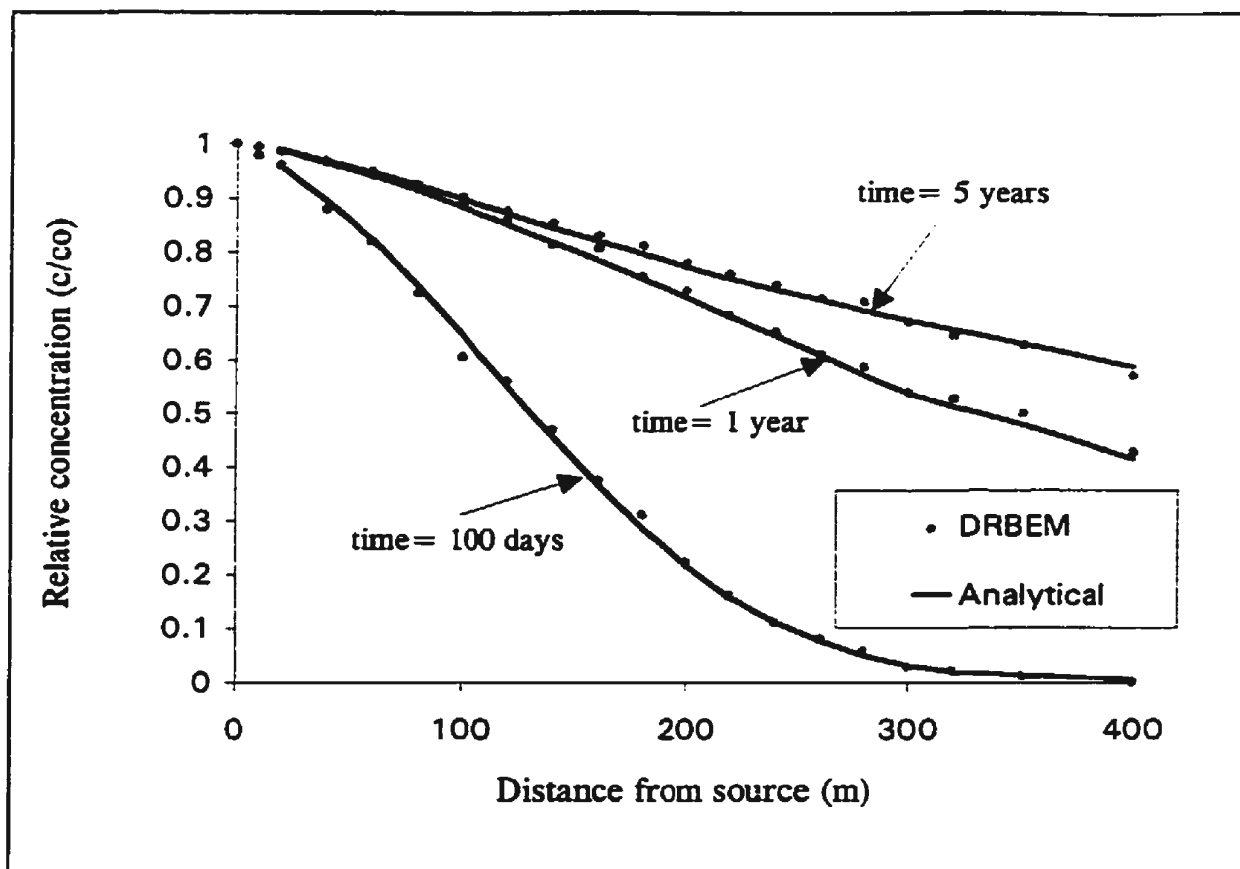
Figure 6.2 Comparison of DRBEM and analytical results for a patch source problem (concentration profile along plume centre line, y=0)
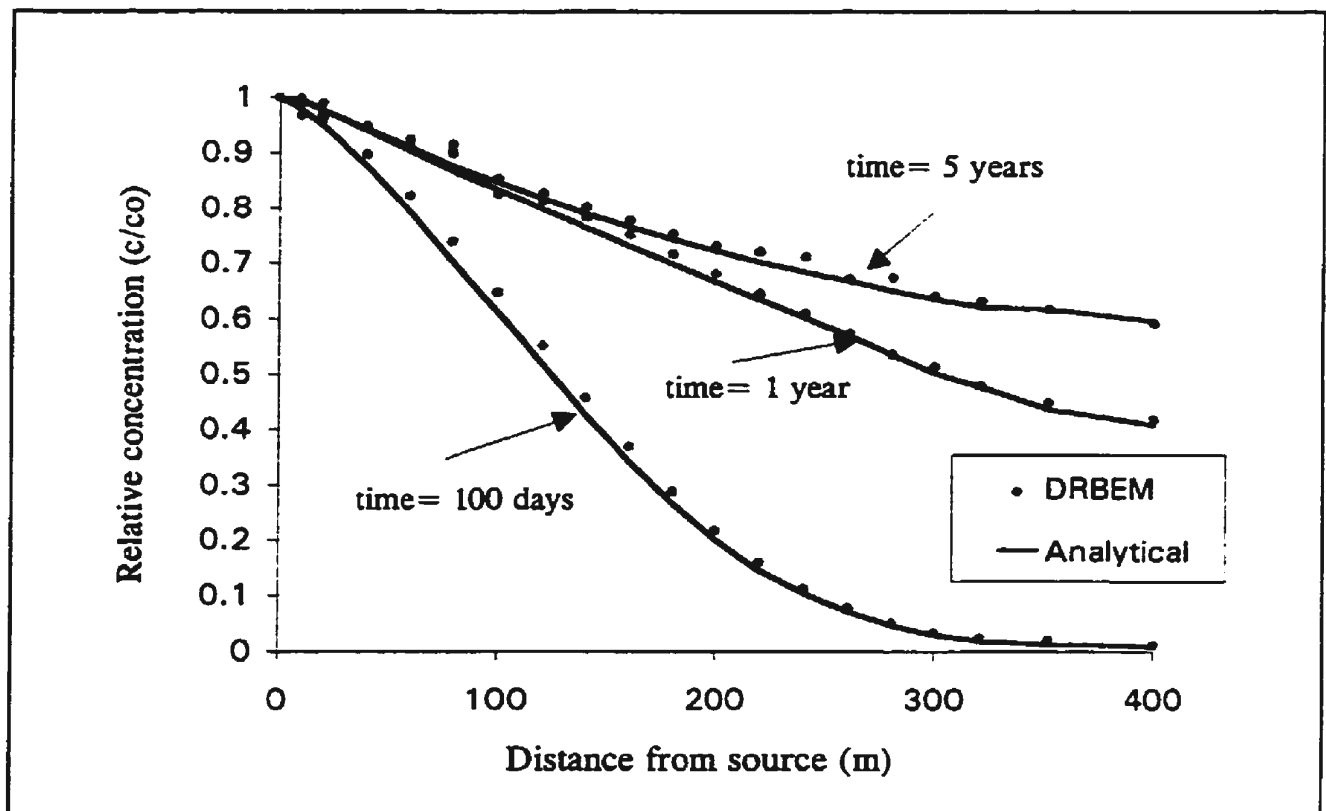
Figure 6.3 Comparison of DRBEM and analytical results for a patch source problem (concentration profile along line y=20 m)

6.2.3 Verification Problem III: Continuous Release of Contaminant from a Point Source

The third verification problem involves continuous leakage of contaminant from a point source. In practice this may occur in the form of a continuous injection of solute into a well or leakage of contaminant from a small industrial waste pit or sump. The contaminant plume will develop and spread in both longitudinal and lateral directions due to advection and dispersion. The nature of the plume is usually in the form shown in Figure 6.4. The analytical solution for this problem was provided by Wilson and Miller, (1978), Hunt (1978) as:

$$c(x,y,t) = \frac{M'}{4\pi\epsilon\sqrt{D_x D_y}} \, \exp(x/B) \, W(u, \frac{r}{B})$$

$$(6.6)$$

$$\text{where, } B = \frac{2D_x}{|V|} \, , \quad u = \frac{r^2}{4\gamma D_x t} \, , \quad r = \left[\left(x^2 + \frac{D_x y^2}{D_y} \right) \gamma \right]^{1/2} \, , \quad \gamma = 1 + \frac{2B\lambda}{|V|}$$

M' is the mass injection rate of contaminant per unit thickness of aquifer, lambda is the decay coefficient (1/T), W(u, r/B) is the leaky well function described by Hantush (1956) and Wilson and Miller (1978).
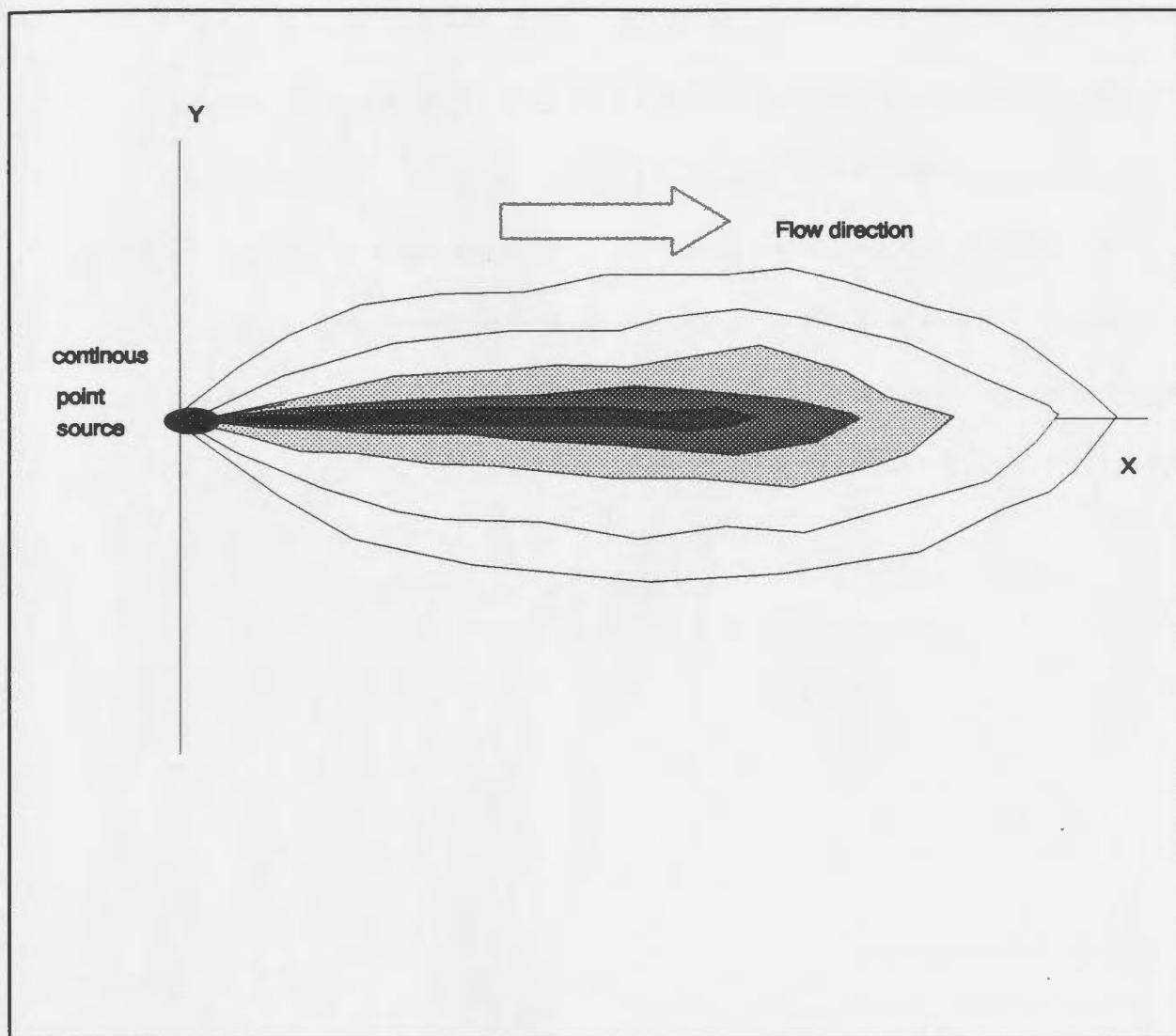
Figure 6.4: Continuous release of contaminant from a point source

The Boundary element model was verified for this problem and the results compared with the analytical solution. The domain for this problem was defined by the lines x=0, x=360 m, y=20 m, and y=-20 m. The input parameters for this problem are summarized in Table 6.2. The boundary of the domain was discretized into 40 linear boundary elements. In addition 30 internal nodes were defined at locations where internal solutions were required. The boundary condition at the contaminant source was considered by specifying a mass injection rate at a source node located at x=0, y=0. Concentration values were computed along the plume centre line at other locations in the transverse direction. Figure 6.5 shows the results from the boundary element method compared with the analytical solution. A good agreement between these two results can be observed.
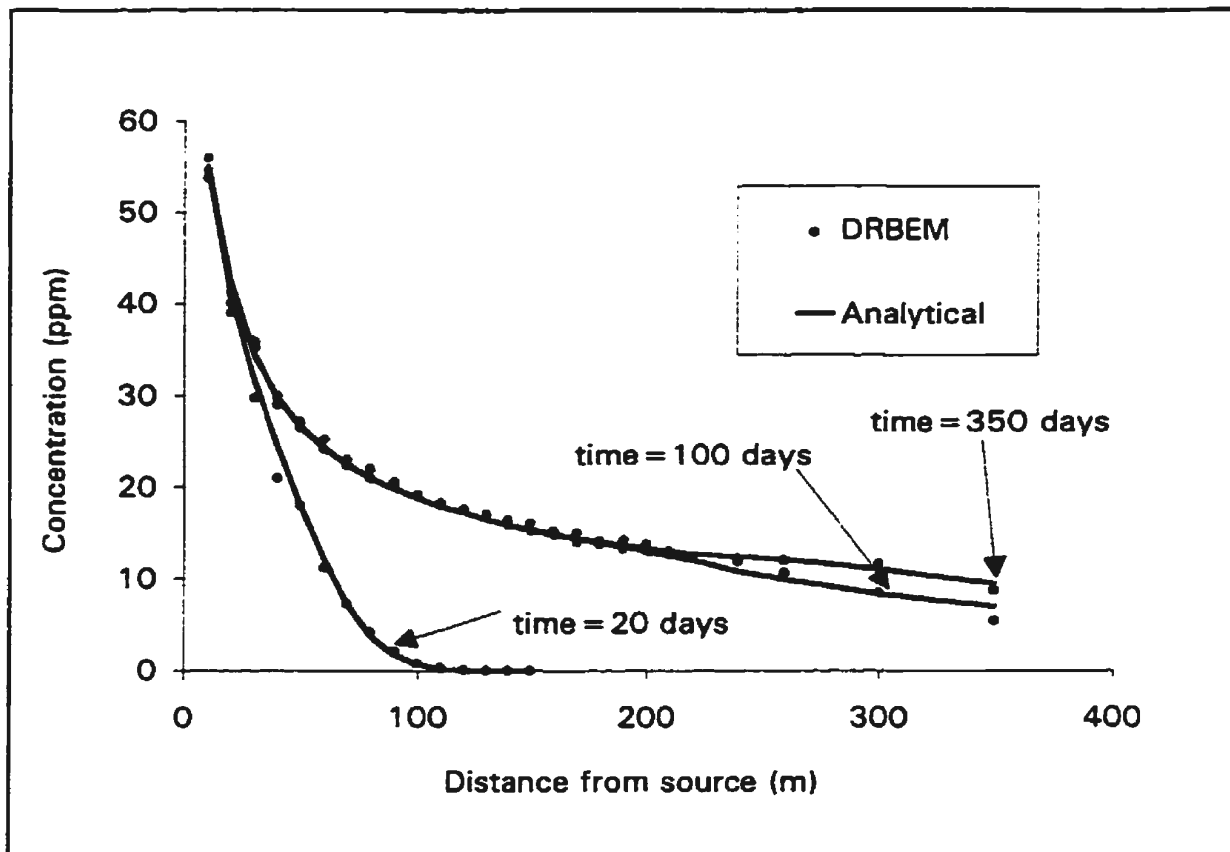
Figure 6.5 Comparison of DRBEM with analytical results for a continuous point source

problem (concentration profile along plume centre line y=0)

6.2.4 Verification Problem IV: Instantaneous Release of Contaminant from a Point Source

The fourth verification problem involves a pulse or instantaneous release of contaminant from a point source. In a practical sense this may happen in the form of a contaminant spill or an injection of a tracer solution into a well for a short period of time as used in field tracer test studies. While a continuous contaminant plume develops from a continuous point source, in the case of an instantaneous point source, a plug develops (Fetter 1993) and advects in the flow direction and spread out with time. This is accompanied by a continuous reduction in the peak concentration. At any time t, the peak concentration will be located at the centre of the plug where $y = 0$ (centre line) and $x = v_x t$ as shown in Figure 6.6. An analytical solution for this type of problem was provided by Wilson and Miller (1978).

$$c(x,y,t) = \frac{M}{4\pi \epsilon t \sqrt{D_x D_y}} \exp\left[-\frac{(x - |V|t)^2}{4D_x t} - \frac{y^2}{4D_y t} - \lambda t\right] \qquad (6.7)$$
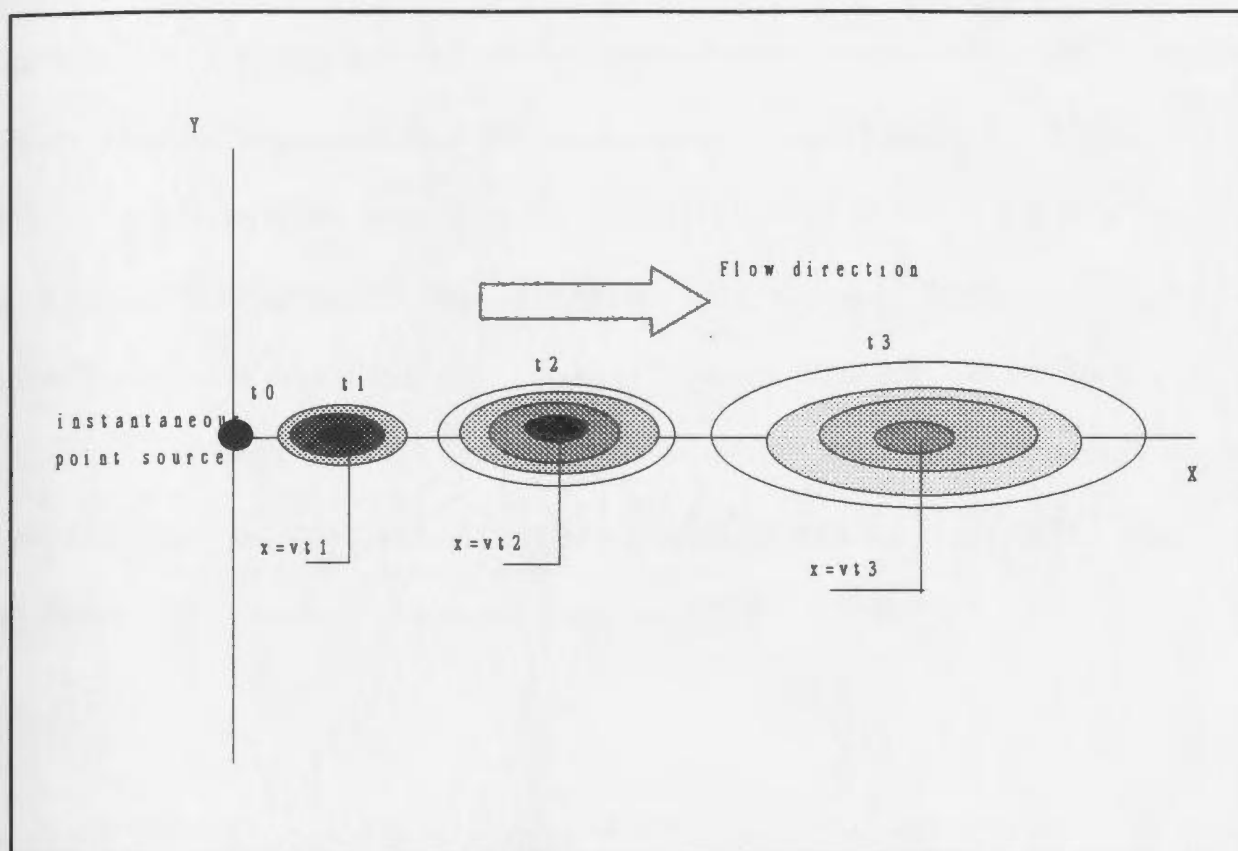
Figure 6.6: Contaminant migration from an instantaneous point source.

The purpose of this verification problem is to test the ability of the DRBEM model to trace the location of the advective front and the magnitude of the concentration at that point in time. The solution approach employed by the DRBEM is similar to that of the continuous point source described above except that an instantaneous solute mass per unit aquifer thickness was specified at the source boundary node located at $x=0$ and $y=0$. The domain for this problem was defined by the lines $x=0$, $x=120$ m, $y=10$ m and $y=-10$ m. The physical parameters used as input are summarized in Table 6.1. The boundary of the domain was discretized into 40 linear elements connected by 40 nodes and some internal nodes were also defined at locations of interest. The concentration values computed were compared with the analytical solution obtained by using PLUME2D (Van der Heijde 1993) and the results are shown in Figures 6.7 and 6.8
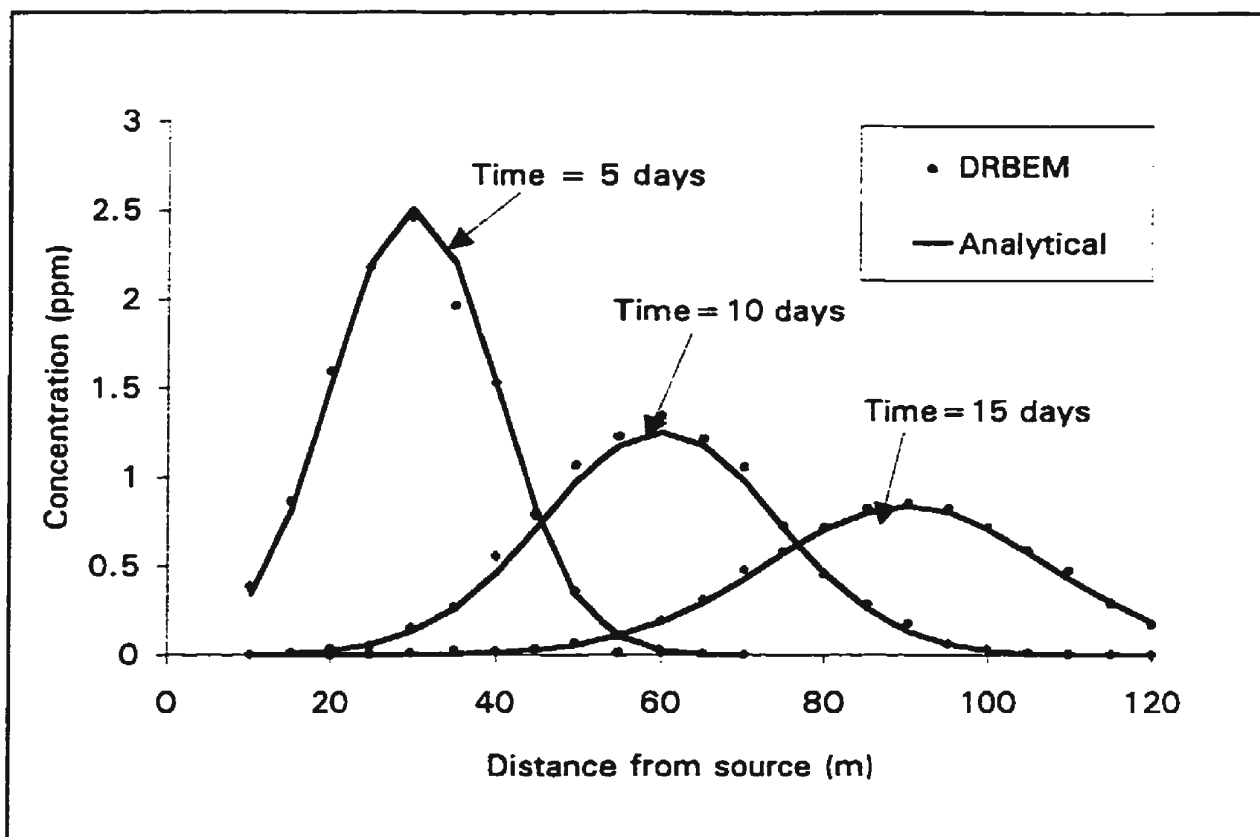
Figure 6.7 Comparison of DRBEM with analytical results of concentration profile for an

instantaneous point source problem (along plume centre line y=0 m)
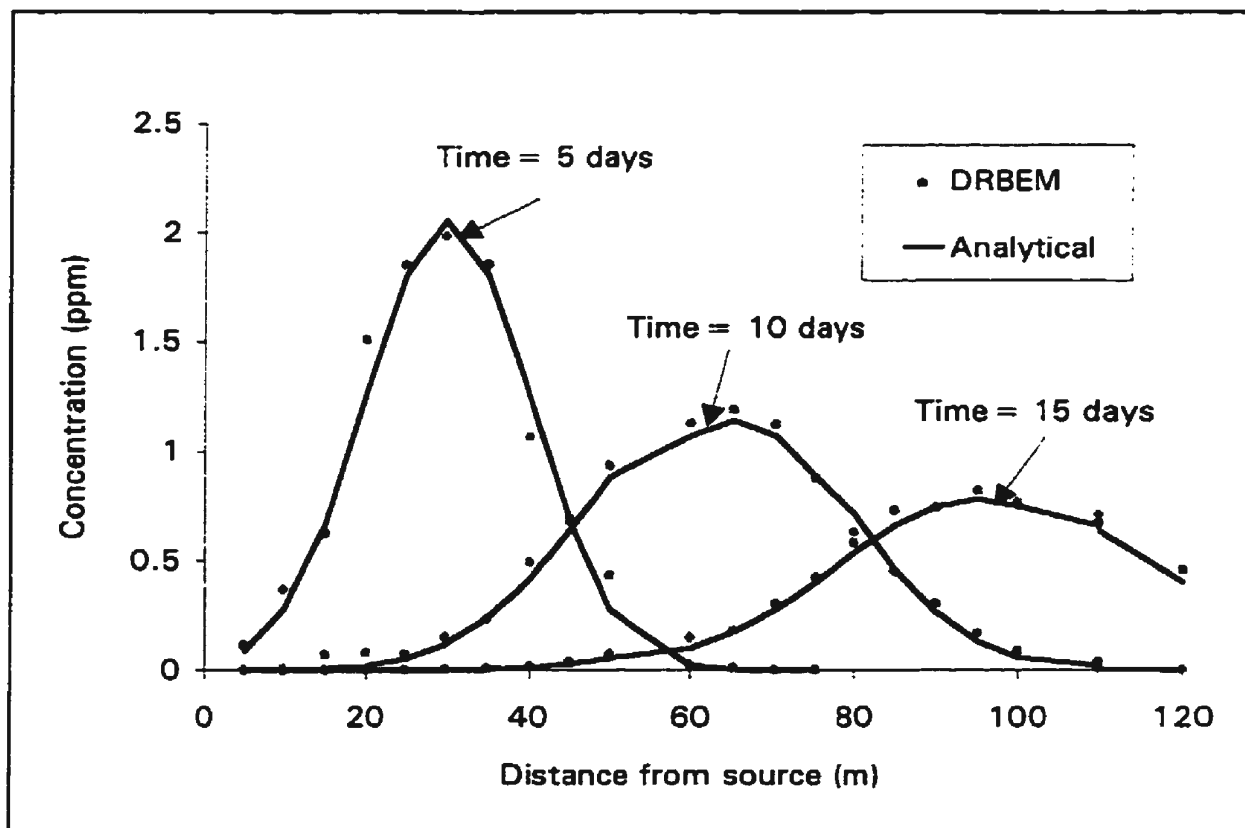
Figure 6.8 Comparison of DRBEM with analytical results of concentration profile for an instantaneous point source problem (along line y=4.0 m)

Table 6.2: Parameters used for verification problems

Parameter	Patch source Value	Continuous point source Value	Instantaneous point source Value
Seepage velocity	1.0 m/day	4.0 m/day	6.0 m/day
Porosity	0.25	0.35	0.30
Longitudinal dispersivity (α_L)	25 m	3.0 m	2.67 m
Transverse dispersivity (α_T)	2.5 m	0.75 m	.33 m
Aquifer saturated thickness	8.0 m	10.0 m	10.0 m
Point source strength	-	23.59 kg/day	-
Concentration at source	100 mg/l	-	-
Solute mass per aquifer thickness	-	-	3.5 kg/m
Grid spacing (m)	$\Delta x = 25$ m $\Delta y = 10$ m	$\Delta x = 30$ m, $\Delta y = 10$ m	$\Delta x = 5$ m, $\Delta y = 2$ m
Time	100 days, 1yr, 5yrs	20,350 days	5,10,15, 30 days
Grid Peclet number (P_e)	1.0	10.0	3.0
Courant number (C_r)	0.75	0.67	0.6

6.3 Benchmarking with Other Numerical Techniques

The performance of the DRBEM model relative to other numerical solution techniques has been investigated. Huyakorn et al. (1984) and Beljin (1988) have proposed two problems that are used to compare the performance of numerical models. These problems have been solved and the results compared with that of the three most popular numerical solution techniques: finite element method (FEM), the method of characteristics (MOC) and the random walk (RNDWK).

The first of these problems describes continuous release of contaminant from a point source into a homogeneous, non-leaky aquifer. The domain of this problem is defined by the lines $x=0$, $x=1380$ m, $y=120$ m and $y=-120$ m. The spatial and temporal discretization employed by Huyakorn et al., (1984) was used for proper comparison. The model consisted of DRBEM technique employed 65 linear boundary elements connected by 65 nodes. The source node was located at $x=0$, $y=0$. The concentrations along the plume centre line $y=0$ were computed by DRBEM and the other numerical schemes and the results compared. The program was executed for 28 time steps with a time step value of 100 days. Figure 6.9 shows the results from these different numerical techniques.
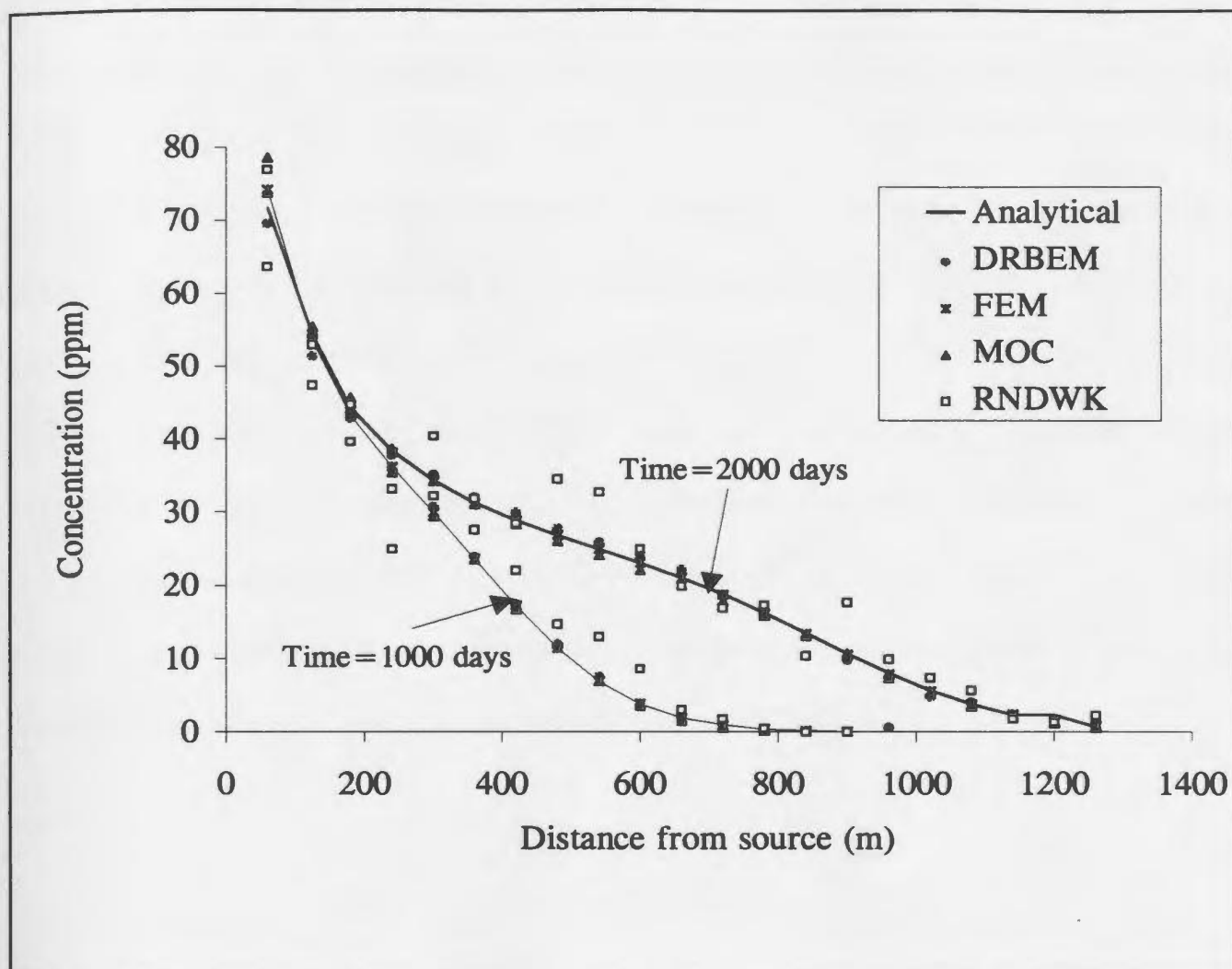
Figure 6.9: Comparison of DRBEM with other numerical solution schemes (concentration distribution at plume centre line for a continuous point source problem)

The second problem involves an instantaneous release from a point source. The domain of this problem was also defined by the lines $x=0$, $x=150$ m, $y=15$ m, and $y=-15$ m. This problem originally proposed by Huyakorn et al. (1984) was also adopted by Beljin (1988) to compare FEM, MOC and random walk models. All three numerical models considered symmetry and modelled half of the domain. By using a nodal spacing of $\Delta x = \Delta y = 5$ meters the FEM used 480 rectangular elements and 539 nodes; the MOC and random walk grids consisted of 19 rows and 40 columns. To obtain concentration values, MOC and random walk used 6000 and 2400 particles respectively. By using the same spatial discretization the DRBEM used 45 linear boundary element with 45 boundary nodes and 30 internal nodes. Concentration distributions and locations of the advective front were computed at three different times and the results are shown in Figures 6.10 and 6.11. Values of the physical input parameters are shown in Table 6.3.
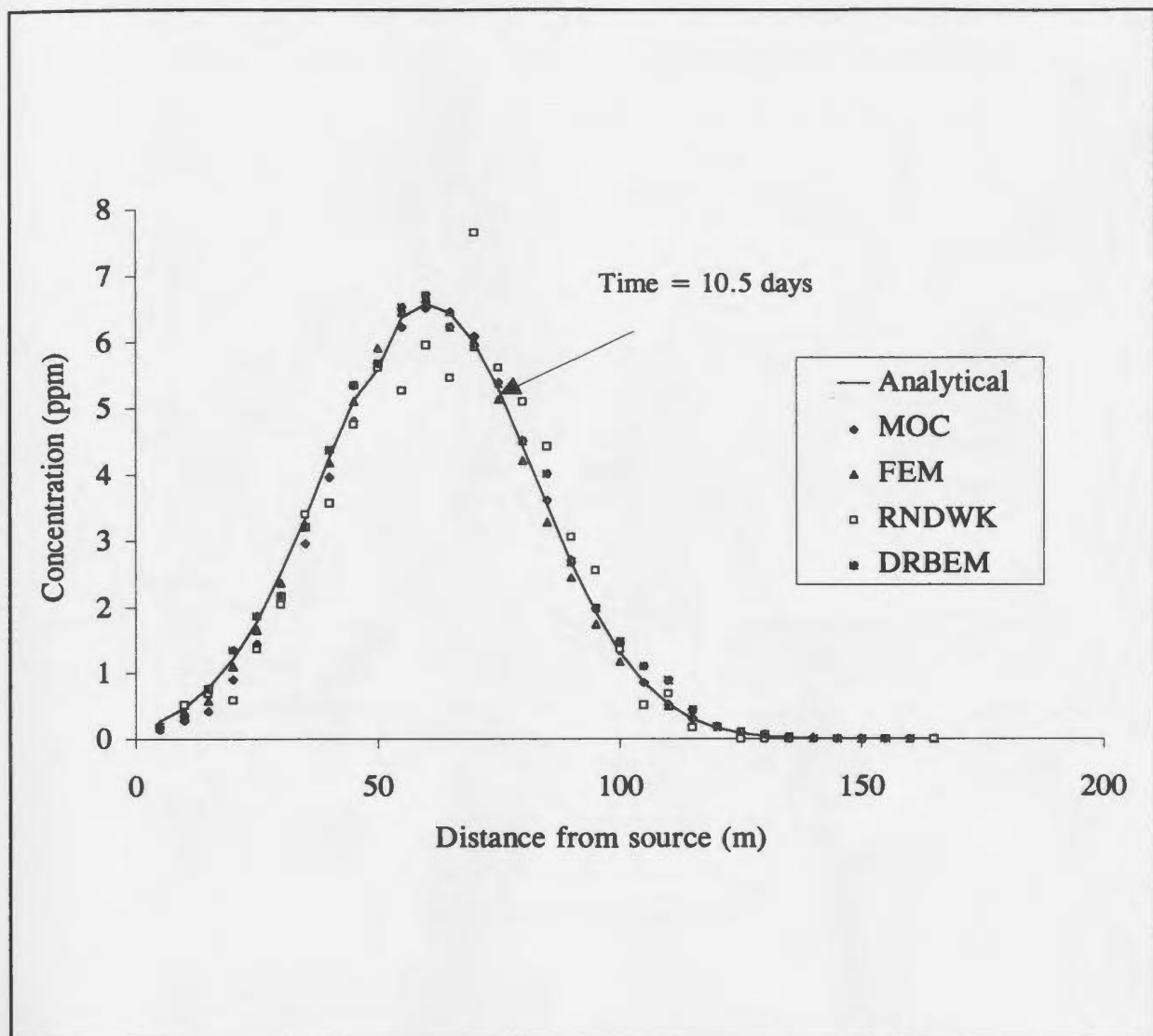
Figure 6.10: Comparison of DRBEM with other numerical solution schemes (concentrations along plume centre line for an instantaneous point source problem, time = 10.5 days)
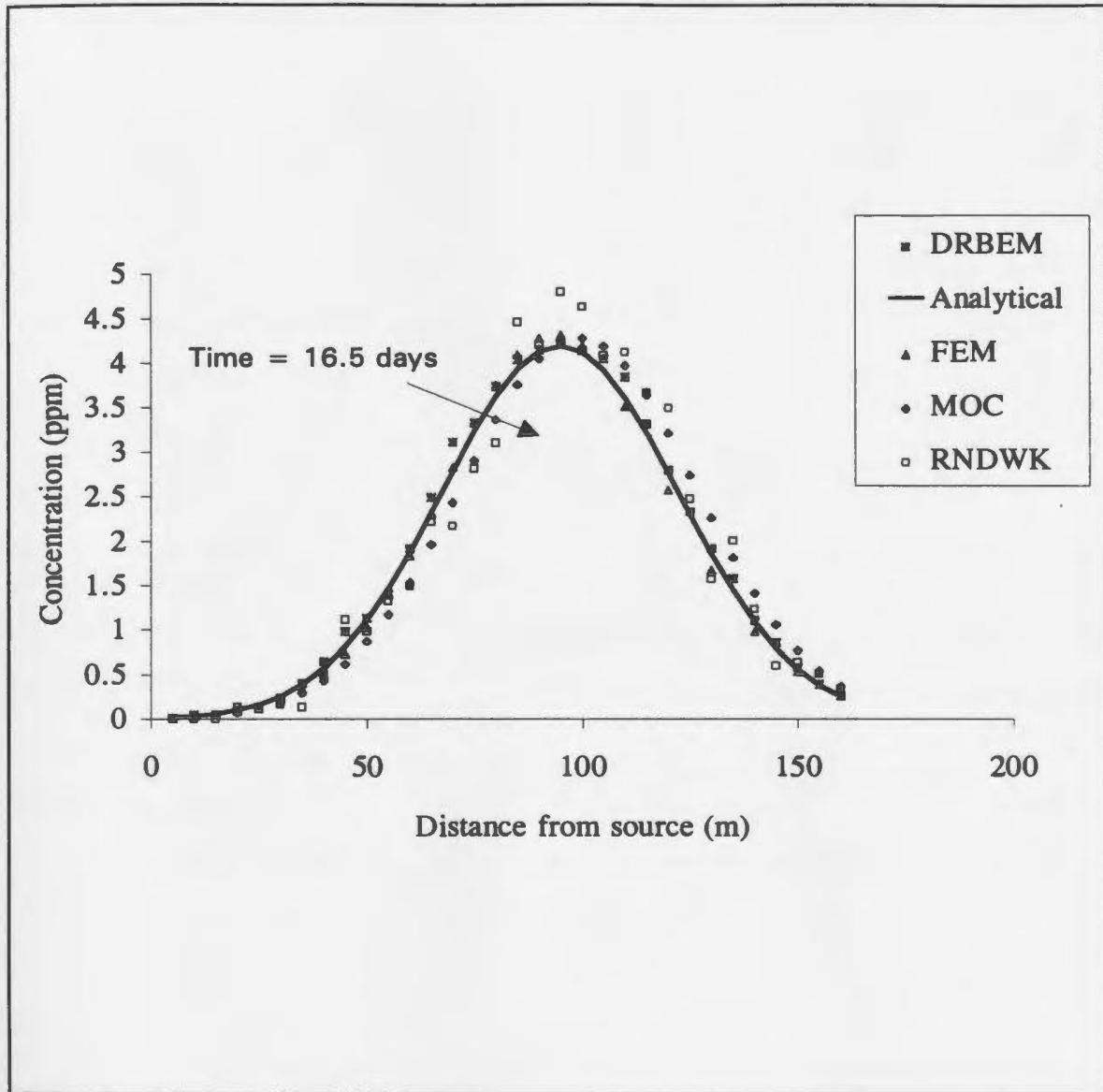
Figure 6.11: Comparison of DRBEM results with other numerical solution schemes for (concentrations along plume centre line for an instantaneous point source problem, time=16.5 days).

Table 6.3: Parameters used for benchmark problems (adapted from Beljin, 1988)

Parameter	Continuous point source Value	Instantaneous point source Value
Seepage velocity	0.460 m/day	5.71 m/day
Porosity	0.35	0.35
Longitudinal dispersivity (α_L)	21.3 m	4.0 m
Transverse dispersivity (α_T)	4.27 m	1.0 m
Aquifer saturated thickness	33.5 m	33.5 m
Point source strength	23.59 kg/day	-
Solute mass per unit aquifer thickness	-	3.5 kg/m
Grid spacing	$\Delta x = 60$ m, $\Delta y = 30$ m	$\Delta x = 5$ m, $\Delta y = 5$ m
Time (t)	1000, 2000, 2800 days	4.0,10.50,16.50 days
Grid Peclet number (P_e)	2.91	1.25
Courant number (C_r)	0.76	0.60

6.4 Summary of Model Verification

In this chapter we have verified and benchmarked the dual reciprocity boundary element numerical model with various contaminant transport problems. The potential of the dual reciprocity method in solute transport analysis has been confirmed with the three major contaminant transport problem types. High accuracy and good agreement between the DRBEM results and the analytical results were achieved at Peclet numbers as high as 12.0 and Courant numbers up to 0.75 for the patch source problem. Accurate values at such Peclet number can only be achieved with a particle tracking method. The efficiency of the method has been demonstrated with two benchmark problems. By using the same spatial and temporal discretization to solve an instantaneous solute release problem, the DRBEM approach achieved accurate results with fewer elements and nodes compared with the other numerical solution techniques (156 boundary elements DRBEM, 485 rectangular elements and 546 nodes with the FEM, 19 rows, 40 columns and 6000 particles with the MOC, and 19 rows, 40 columns and 2500 particles with the random walk). It was found that the DRBEM requires the least computational effort and input data preparation. The results (tabulated data) from the verification and benchmarking problems are shown in Appendix C (Tables C1 to C10).

Chapter 7

Model Calibration and Sensitivity Analysis

7.1 Introduction

This chapter presents the calibration of the numerical model by using information obtained from the site investigations described in the previous chapters. The field applicability of the DRBEM model and also the optimal aquifer parameters that are deemed representative for solute transport simulation in these types of aquifers are presented. The main difficulty involved in model calibration of this type is the correct interpretation of the database and site conditions which are often associated with a certain degree of uncertainty due to sparsity of data and measurement error. In many field studies and particularly in this work, the data density is low for the interpolation of concentration isolines or for the computation of spatial moments at a level accurate enough for calibration and validation. The alternative approach (Ptak and Schmid 1996, Thorbjarnason and Mackay 1997) that is followed in this work is to compare effective breakthrough curve parameters, estimated individually from each numerically simulated results and measured breakthrough curves. The various sections in this chapter present the conceptual model and simulation domain,

calibration procedures, the qualitative and quantitative evaluation of results and sensitivity analysis of the individual parameters.

7.2 Assumptions on Model Calibration

In the calibration of groundwater flow and transport models the complexity of the field system necessitates several assumptions and simplifications to be made. Although such assumptions reduce the correctness of the modelled system, they render the problem more tractable for analysis, interpretation and simulation. The following assumptions have therefore been made with respect to this calibration: (i) Flow in the incompressible aquifer is in the horizontal plane in the longitudinal and transverse lateral directions (two dimensional flow). Thus the concentrations can be viewed as an average over the thickness of the aquifer. (ii) Darcy's law is valid and flow is controlled by a hydraulic gradient. (iii) The temperature gradients and the tracer concentrations do no affect the density and viscosity of the groundwater or the distribution of velocities in the domain under consideration. (iv) Porosity is uniform in space and constant with time. (v) The effects of molecular diffusion is negligible. (vi) The medium is isotropic with respect to dispersivity hence only the two major components of dispersivity (longitudinal and transversal) are involved.

7.3 The Conceptual Model, Simulation Domain and Boundary Conditions

7.3.1 The Conceptual Model

Although it is possible that flow in fractured rock aquifers such as the type found at the experimental site can occur exclusively in discrete fractures, the field investigations have suggested that the bulk movement of contaminants can be approximated using an equivalent porous media concept (Amoah and Morin 1996b). Therefore the calibration is done by the computer implementation of the classical advection dispersion equation for porous media flow. However the input parameters are derived from the information obtained from site characterization and groundwater quality data during tracer tests in the fractured aquifer.

7.3.2 Simulation Domain and Boundary Conditions

Due to insufficient information on the regional groundwater flow and also the spatial scale of the test it was decided to use local boundaries related to the tracer test area. The difficulty involved in the use of local boundaries is how to define them to be conceptually and numerically suitable for accurate results. The procedure for boundary conditions was simplified by the orientation of the Cartesian coordinate axes (x and y) in the average

groundwater flow direction observed during site monitoring period. This direction also coincided with the trajectory of the tracer plume. The domain boundary was defined to cover a wider area than necessary and made to coincide with well defined local topographical features so that reasonable boundary conditions could be defined. In the boundary element method one has an option to prescribe at a point on the boundary either the potential (concentration) or its derivative (solute flux) while the other is computed. Therefore by defining a bigger domain we can specify a zero concentration at all parts of the boundary where physical evidence suggest no tracer appearance. Alternatively we can also specify a zero solute fluxes at these portions of the boundary.

7.3.3 Source Boundary Condition

The domain boundary was defined to pass through the deep injection well (well #31). This well was used as the source boundary node which was also defined as the origin (0,0) of the Cartesian coordinate system. An instantaneous solute mass per unit aquifer thickness (M_o) was specified at this node. If the mass (M) is unknown it can be computed as:

$$M_o = \frac{Q\,c_o\,t_i}{\Lambda} \qquad (7.1)$$

where, Q is the volumetric tracer injection rate (L^3/t) , c_o is the concentration of the tracer solution (M/L^3), t_i is the period for tracer injection (T), Λ is the aquifer thickness

(L), M_0 is the solute mass per aquifer thickness (M/L). In this work, the total mass injected was known to be 160 g (tracer test phase II). The aquifer was considered as confined with a uniform thickness over the domain. Therefore the thickness (A) remained one of the initially unknown parameters. However an initial value of 3.6 m estimated by Gale (1993) near the site was used at the beginning of the simulation.

7.4 Model Calibration Procedure

7.4.1 Introduction

In this section we shall define model calibration as the process of varying parameters until an acceptable match is obtained between measured and calculated values. Generally there are two ways of achieving calibration (Anderson and Woessner 1992): (i) manual trial and error selection of parameters; (ii) automated approach.

In the manual trial and error technique, parameter values are initially assigned to each node or element in the grid. The parameters are then manually varied during a sequential model run until a reasonable match between a predetermined target and model results are obtained. Where some parameters are known with reasonable confidence they may be varied slightly or not varied at all. A major disadvantage is the time consuming nature and the effort involved which is required to achieve reasonable results. It is found that

nonuniqueness of solution may occur when different combinations of parameters yield essentially the same results.

The automated approach usually employs statistical techniques that quantify uncertainty in parameter estimates. The method is usually faster and claimed to be more reliable than the manual approach. However, Sampler et al. (1990) made a comparative analysis and observed that the automated technique may not necessarily be superior to the manual approach in terms of accuracy but its advantage lies rather in the speed and avoidance of most time consuming and frustrating part of the modelling process. The automated approach also can produce nonunique results. In this work we shall employ the manual approach in spite of its time consuming nature in order to obtain practical insight into sensitivity and parameter behaviour.

7.4.2 Calibration for Effective Transport Parameters

One of the main aims of the model calibration is to obtain optimal representative values of parameters for transport analysis. Because of the heterogeneity and the uncertainties associated with the parameters obtained for input, it is clear that one cannot reasonably expect to predict the concentration distribution exactly at any point in the domain and in particular at the points where the monitoring wells are located. The initial values of input parameters such as velocity and dispersivity were estimated from tracer test data by using the analytical method of Zou and Parr (1993). These values were used as start values for

the simulation. Thus, by assuming a uniform groundwater flow in the direction observed during the tracer tests, these initial values were varied within practical limits. During the first batch of sequential runs a zero concentration was specified at the boundaries except at the source node. Then in another batch of sequential runs, a zero solute flux was specified. Several sequential model runs were performed by adjusting the main transport parameters, longitudinal dispersivity (α_L), transverse dispersivity (α_T), average linear velocity ($|V|$) and aquifer thickness (A). Tracer transport velocities were considered to be known with a reasonable certainty and therefore they were varied within a small range observed from the tracer tests.

A criteria was established for the assessment of model performance against observed data by using the sum of squares error function which was defined by the root mean square error (RMSE). This quantitative criteria has been found very suitable for solute transport simulations and has been widely employed by many workers including Anderson and Woessner (1992), Moltyaner et al. (1993) and Zheng and Bennett (1995). The sum of squares function was computed by using the square of residuals (r^2) between the simulated and measured concentrations. The values of the parameters with minimum RMSE were considered to be the optimal values. Table 7.1 shows a typical example of calibration results for two different values of longitudinal dispersivity, and how the RMSEs were computed. Several examples of parameter variations and their RMSE are shown in Appendix D. A qualitative approach for determining a good match between observed and simulated results was also employed (Voss and Knopman 1989). This was done by

plotting the simulated results against the experimental results on a scatter diagram. The narrower the scatter around the 45° line, the better is the match. Figures 7.1 and 7.2 show typical scatter plots of simulated against observed concentrations by using different values of dispersivities. After several sequential model runs and a quantitative analysis of the results the effective transport parameters were estimated and these are shown in Table 7.2. Some of the results are compared with experimental data in Figures 7.3 to 7.11.

Table 7.1: Typical example of experimental and calibrated results and their root mean square error for a parameter (longitudinal dispersivity) in observation well #30

Time	Experiment	DRBEM			
(days)	Conc (ppm) (a)	Conc (ppm) (b) $\alpha_L=5.5$	residual $(a-b)^2$	Conc(ppm) (c) $\alpha_L=4.4$	$(a-c)^2$
2	1.06359	1.96708	0.81631	1.93384	0.75734
3	1.76067	1.61051	0.02255	1.67665	0.00706
5	1.13737	0.94611	0.03658	1.04423	0.00867
7	0.34899	0.56225	0.04548	0.63176	0.07995
9	0.13802	0.34705	0.04369	0.38976	0.06337
12	0.21783	0.17953	0.001467	0.19821	0.000385
16	0.3338	0.08271	0.00244	0.08721	0.00291
19	0.04866	0.04846	3.96E-08	0.04955	7.02E-07
23	0.01236	0.02541	0.00017	0.02454	0.000148
28	0.00876	0.01214	1.4E-05	0.01084	4.32E-06
35	0.00455	0.00479	5.9 E-06	0.00377	6.02E-07
42	0.00299	0.02059	0.00031	0.00143	2.42E-06
56	0.000364	0.00429	4.17 E-07	0.00024	1.15E-05
61	0.00248	0.00024	5.01 E-06	0.00018	5.31E-06
89	0.00112	0.000187	9.37 E-07	5.61E-05	1.13E-06
107	0.00095	0.000146	3.88 E-05	5.34E-05	8.11E-07
129	0.00025	0.000135	4.32 E-07	5.02E-05	7.14E-07
163	0.00011	0.000117	5.27 E-06	4.95E-06	5.67E-06
183	0.00008	0.000102	1.10 E-06	4.38E-06	1.18E-06
		RMSE	**0.231055**		**0.487401**
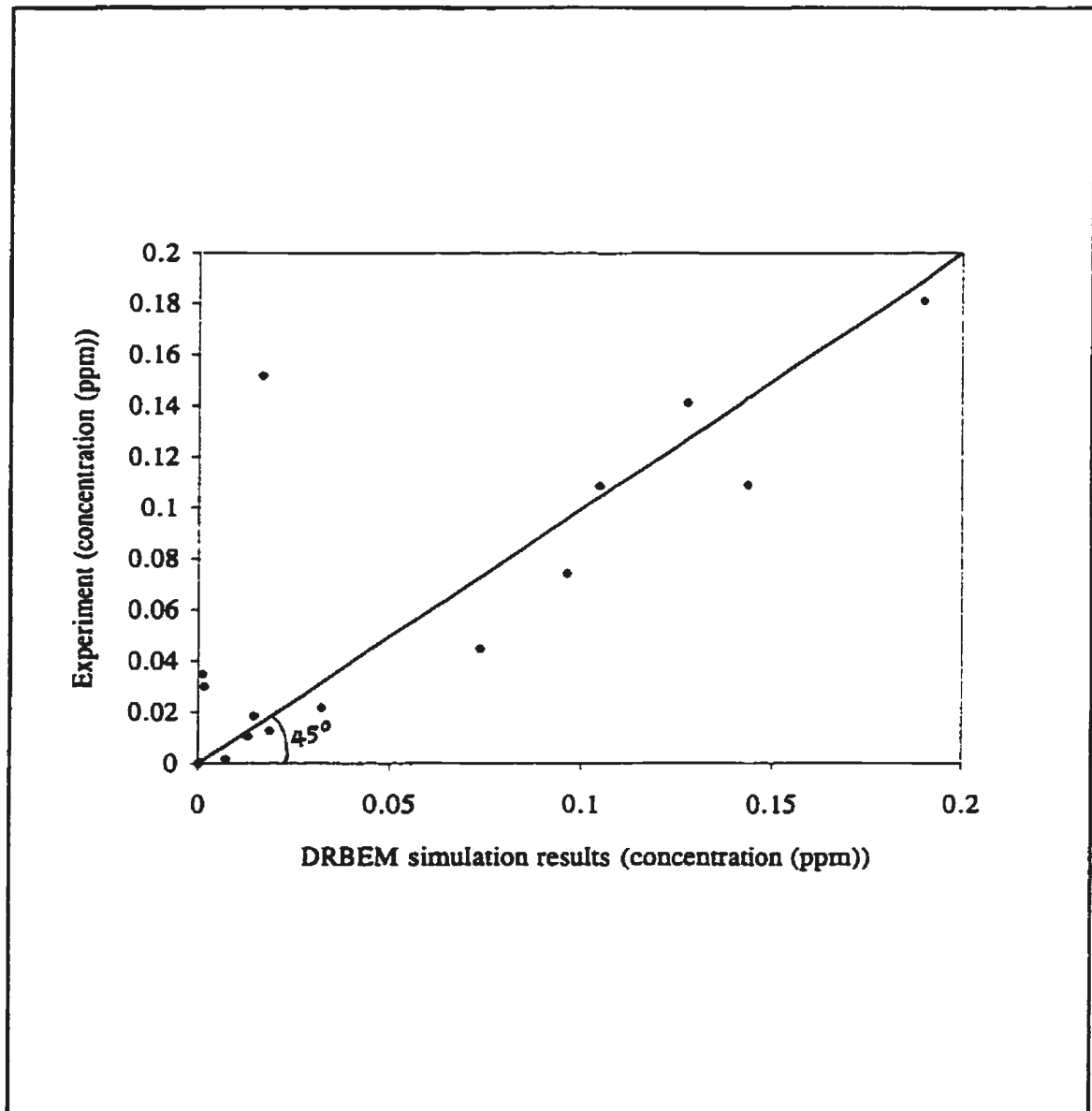
Figure 7.1: Scatter diagram showing qualitative measure of goodness of fit between experimental and simulated results for α_T =0.345 m
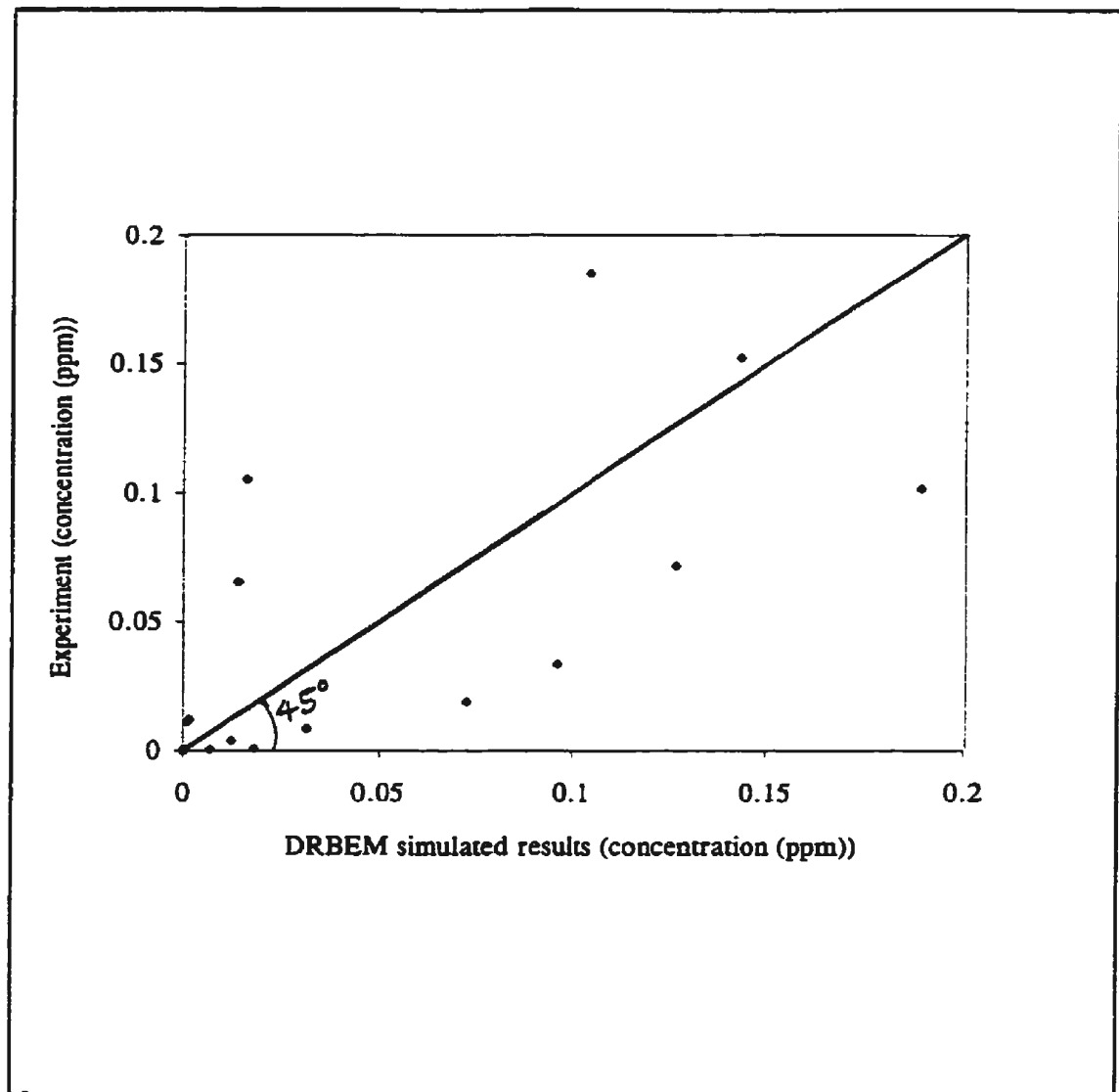
Figure 7.2: Scatter diagram showing qualitative measure of goodness of fit between experimental and simulated results for α_T =0.69 m

Table 7.2: Optimal range of aquifer parameters obtained from calibration

parameter	optimal range	effective mean value
longitudinal dispersivity (α_L)	5.0-6.5 m^2/day	5.52 m^2/day
transverse dispersivity (α_T)	0.3 - 0.5 m^2/day	0.35 m^2/day
effective porosity (ϵ)	0.01 - 0.025	0.015
average linear velocity ($|V|$)	1.3 - 1.7 m/day	1.5 m/day
aquifer thickness (Λ)	5.0 - 7.0 m	6.5.0 m
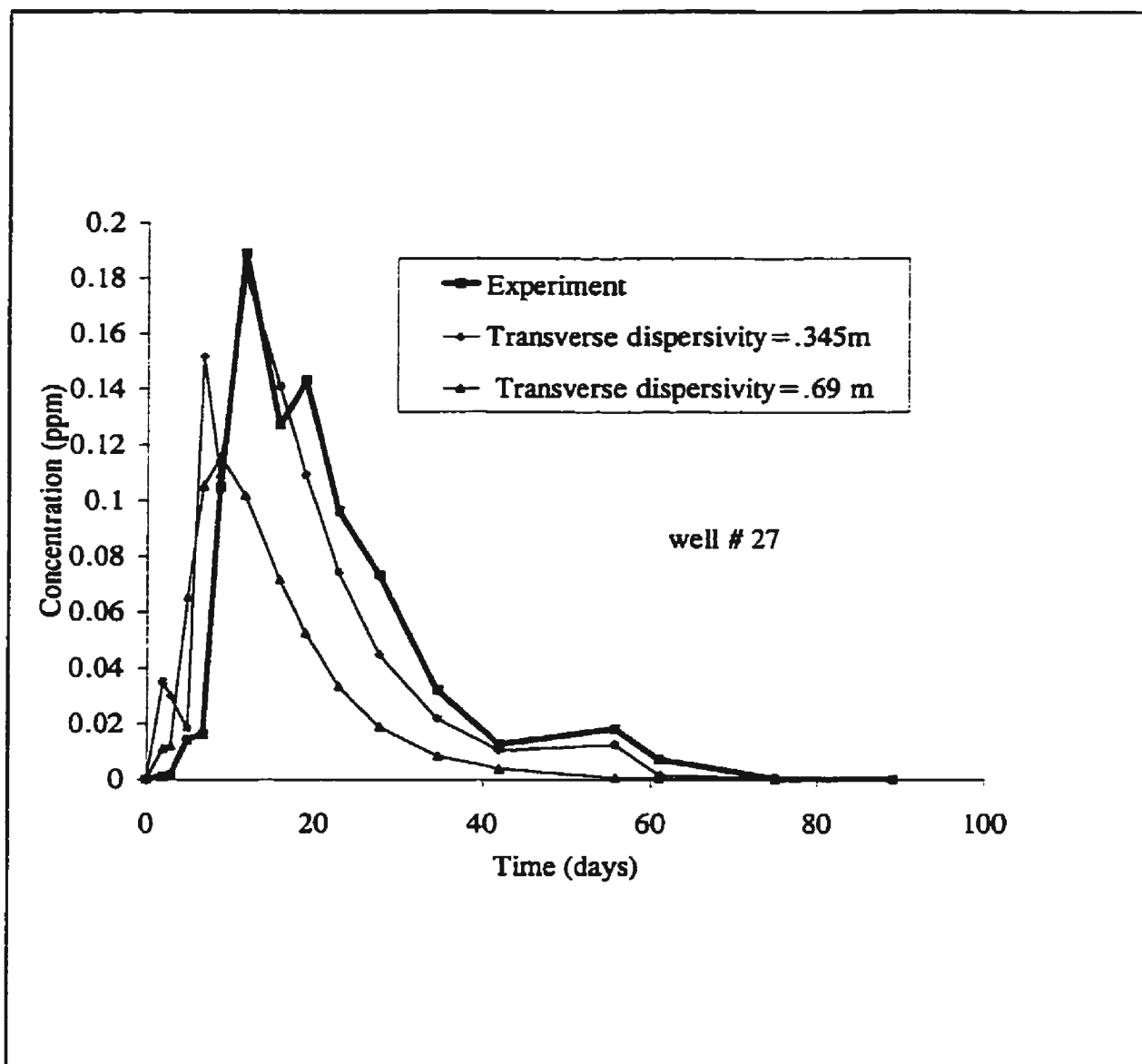
Figure 7.3: Comparison of numerically simulated and experimental results of concentration

at well #27 located 24 m from source-Effects of transverse dispersivity
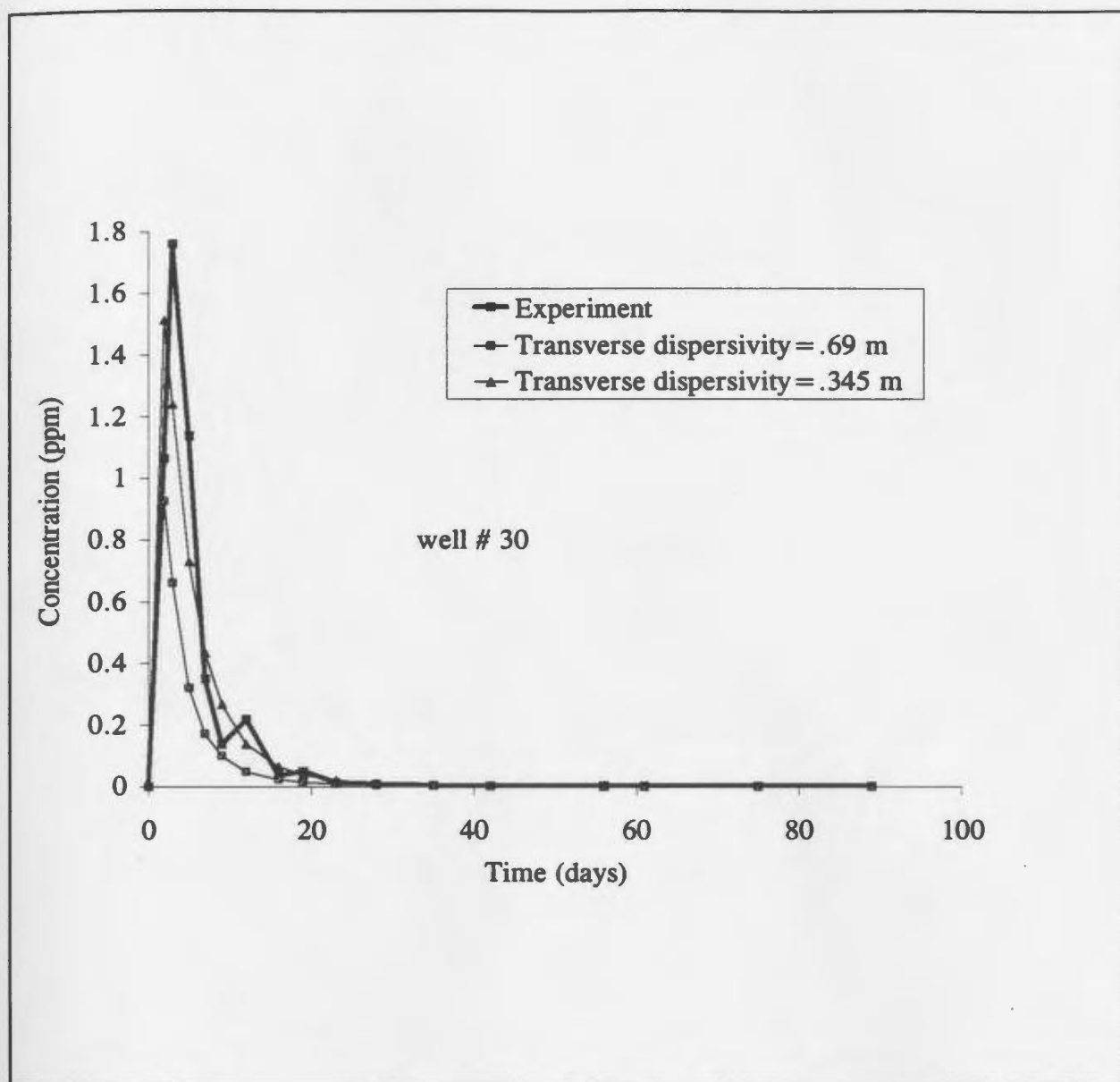
Figure 7.4: Comparison of numerically simulated and experimental results of concentration at well #30 located 7.9 m from source-Effects of transverse dispersivity
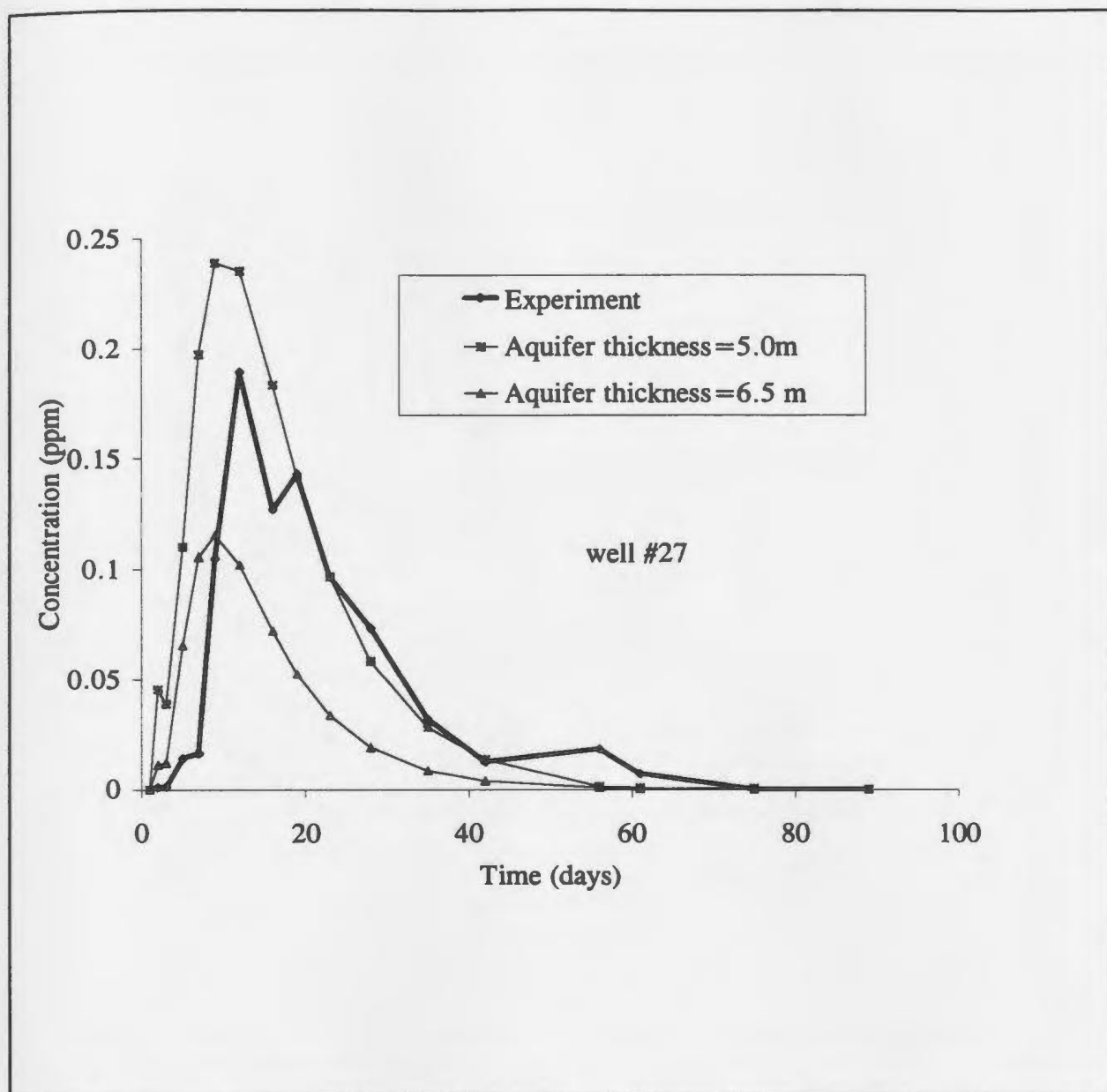
Figure 7.5: Comparison of numerically simulated and experimental results of concentration

at well #27 located 24 m from source-Effects aquifer thickness
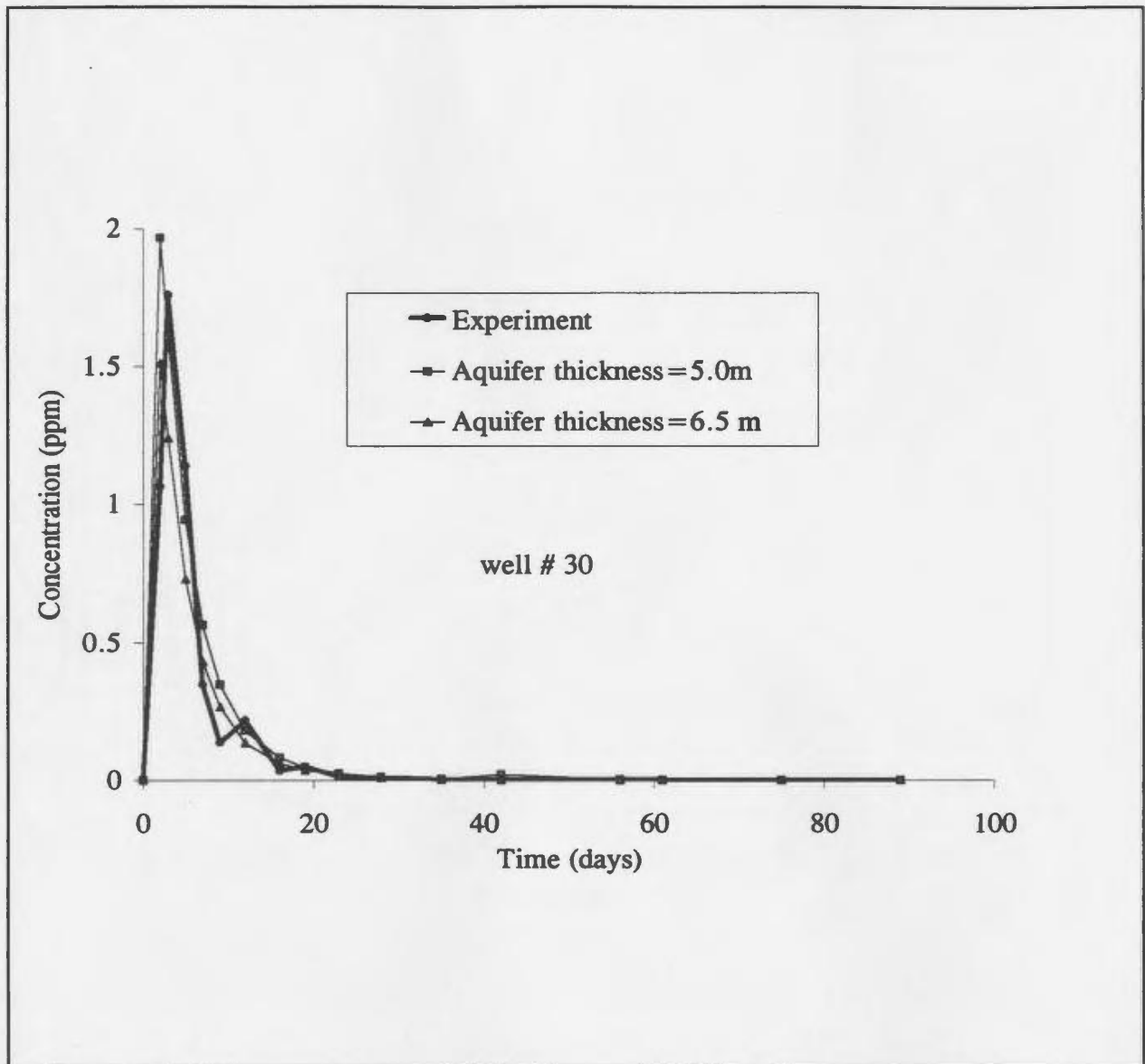
Figure 7.6: Comparison of numerically simulated and experimental results of concentration at well #30 located 7.9 m from source-Effects of aquifer thickness
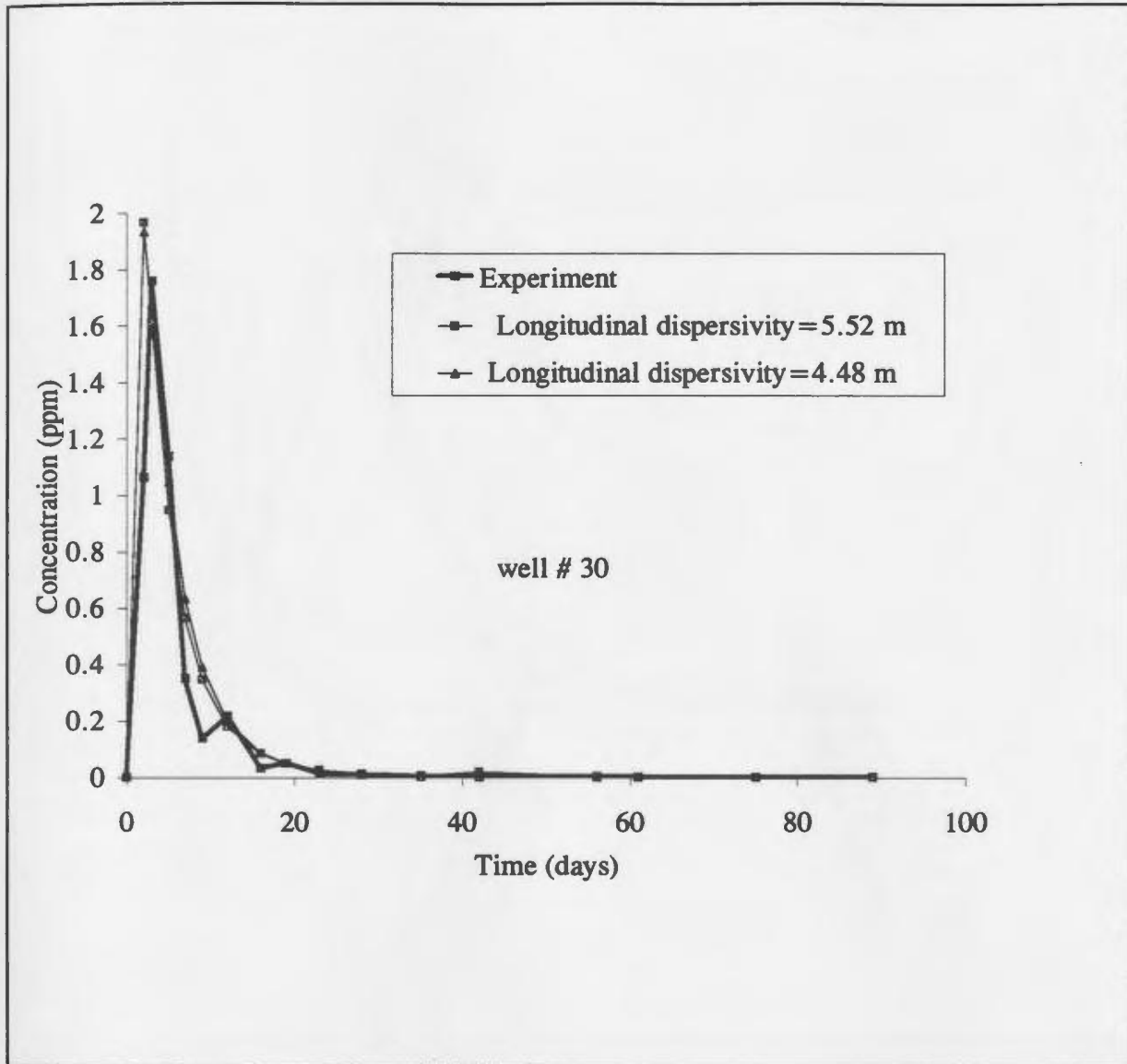
Figure 7.7: Comparison of numerically simulated and experimental results of concentration at well #30 (7.9 m from source),(effects of longitudinal dispersivity).
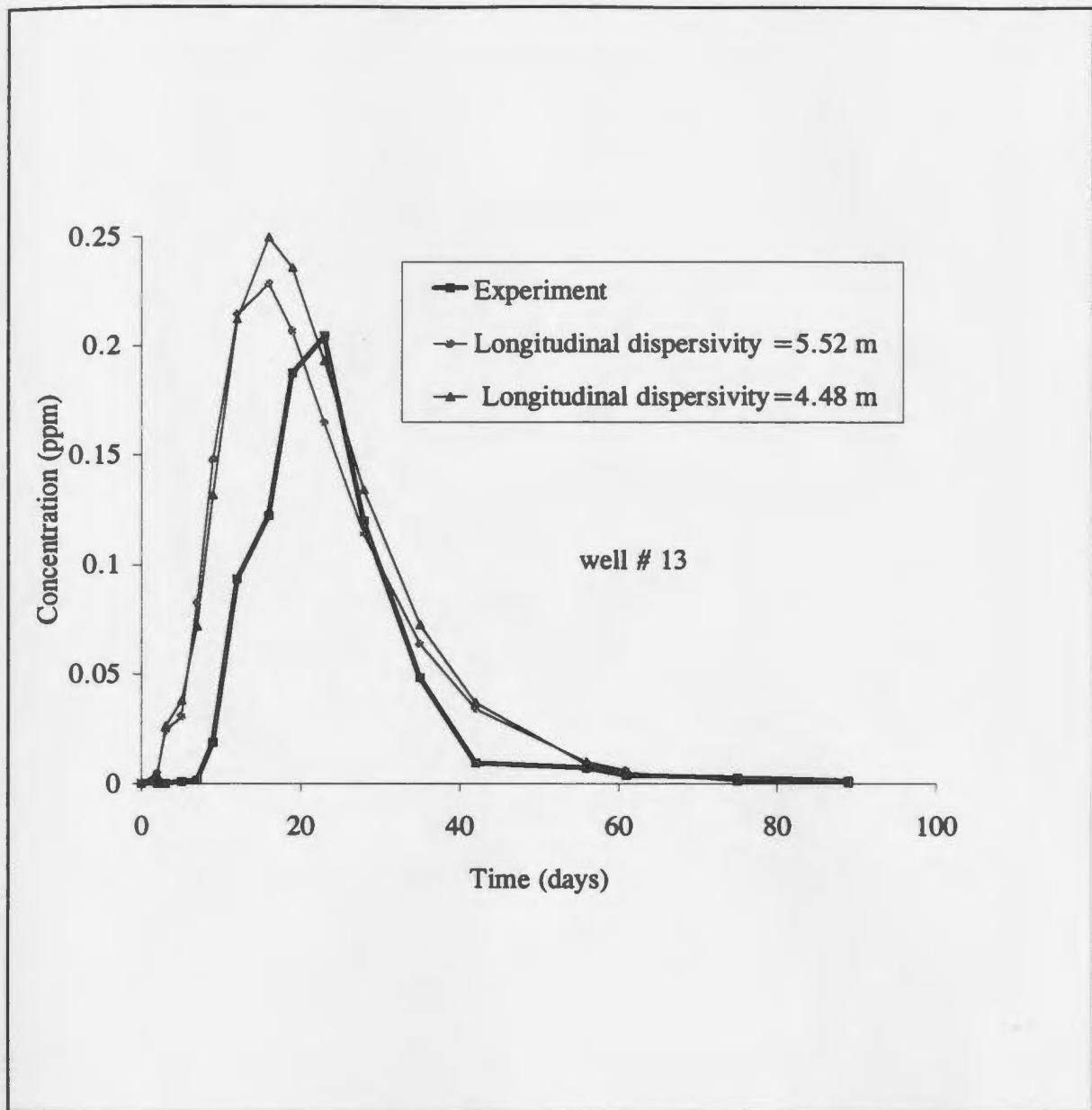
Figure 7.8: Comparison of numerically simulated and experimental results of concentration

at well #13 (35 m from source),(effects of longitudinal dispersivity).
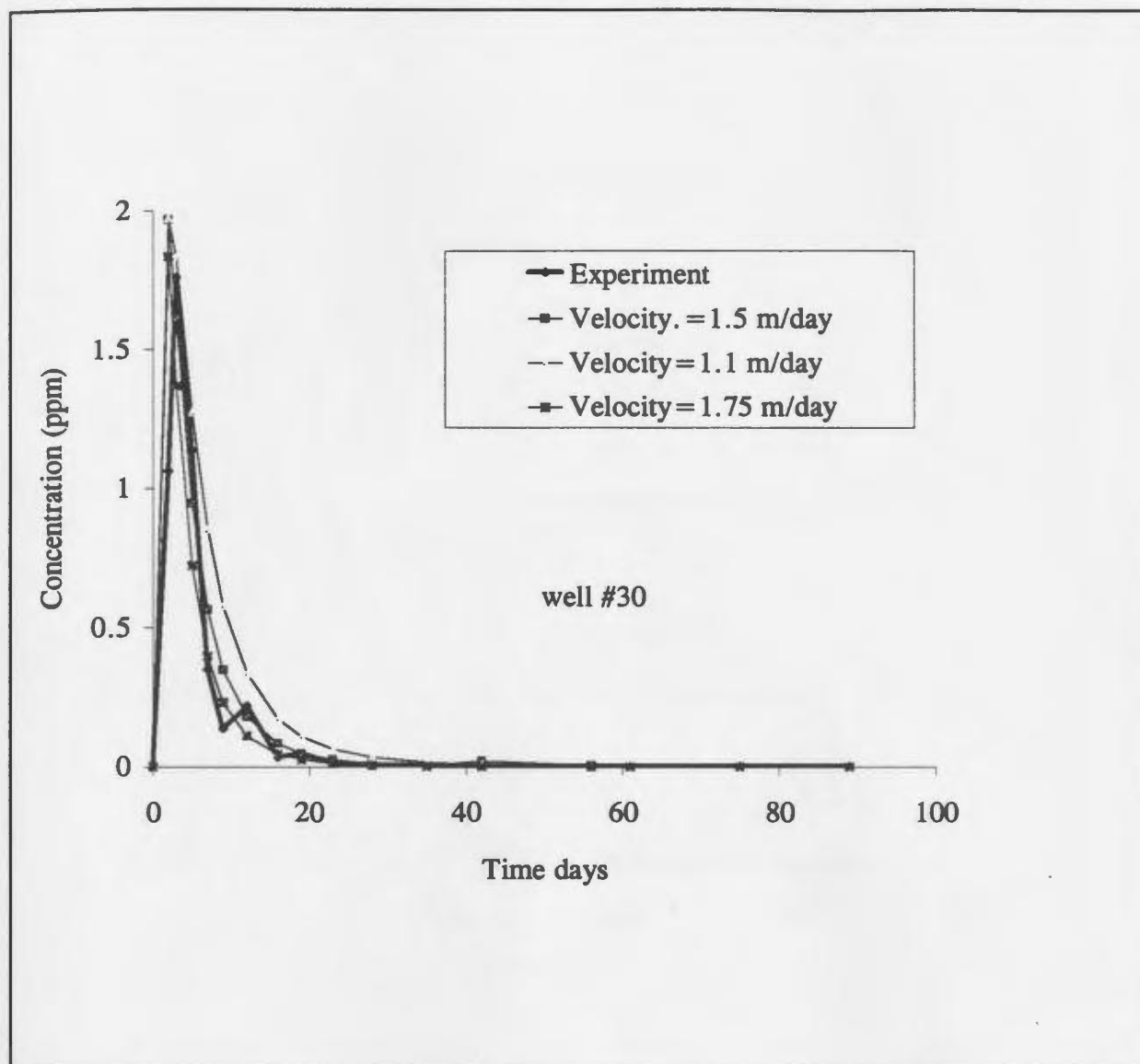
Figure 7.9: Comparison of numerically simulated and experimental results of concentration at well #30 located 7.9 m from source-Effects of velocity
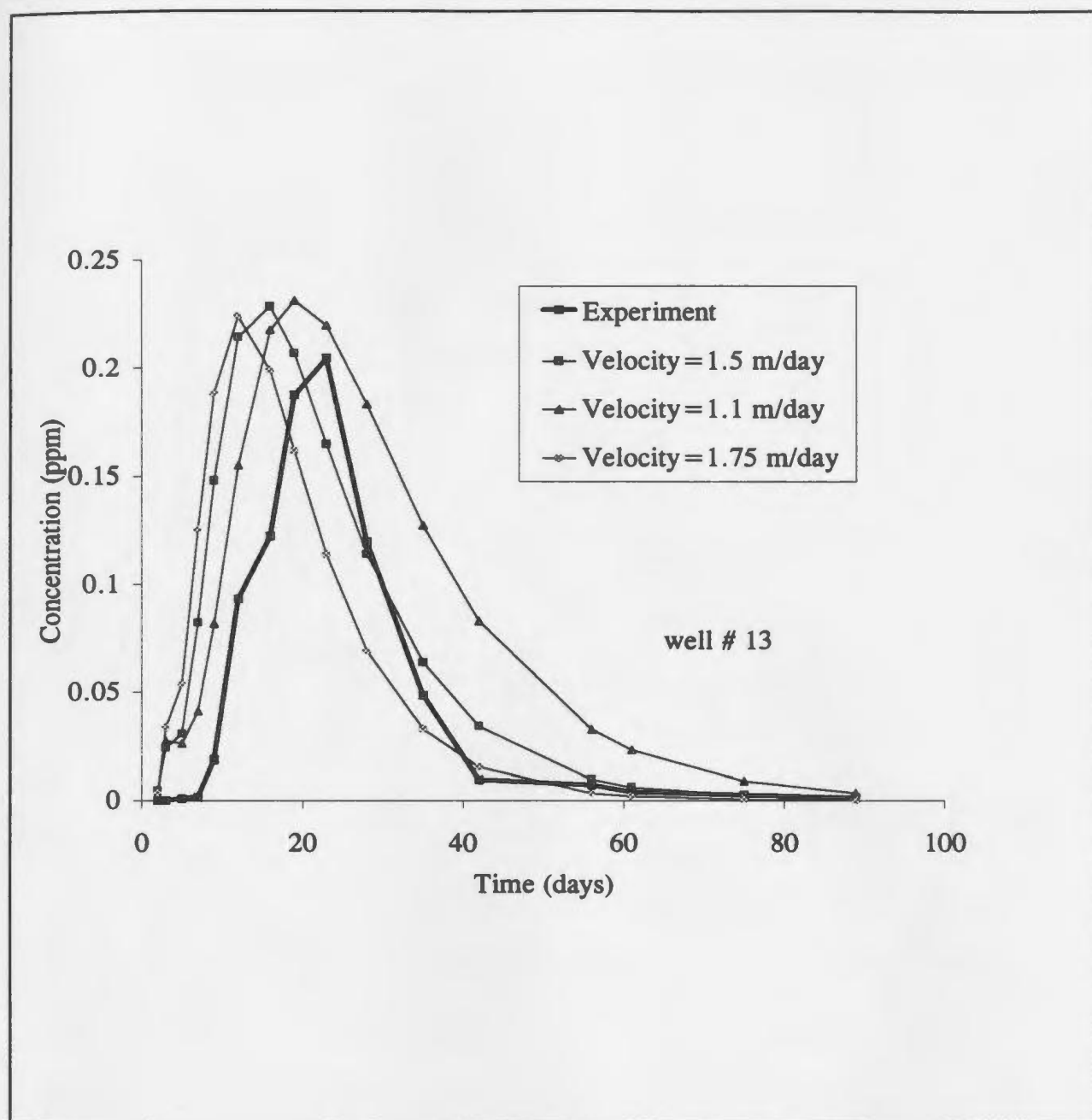
Figure 7.10: Comparison of numerically simulated and experimental results of concentration at well #13 located 35 m from source-Effects of velocity
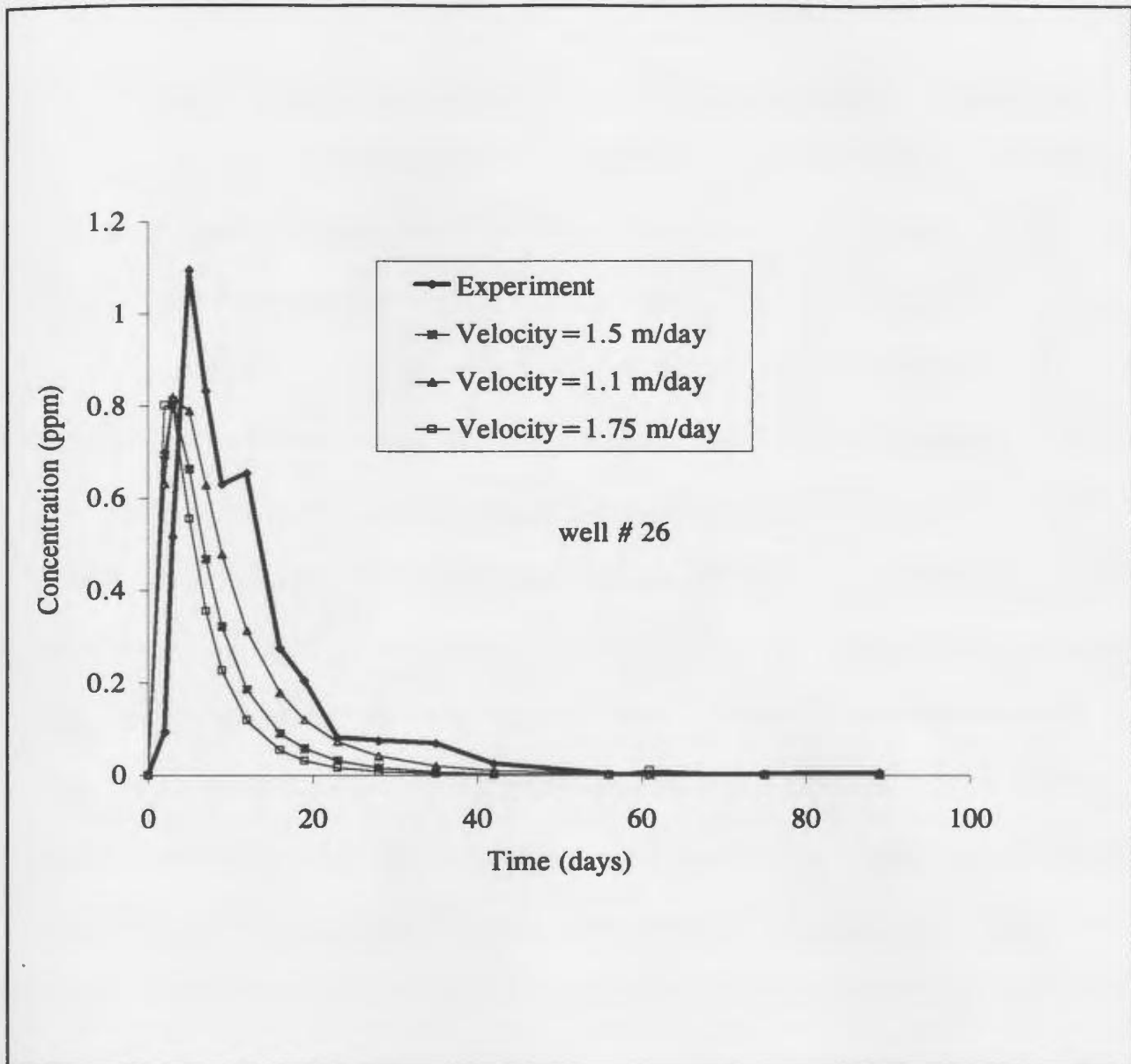
Figure 7.11: Comparison of numerically simulated and experimental results of concentration at well #26 located 10.5 m from source-Effects of velocity

7.4.3 Observations from Simulation Results

During the model runs it was observed that the parameters have different effects on the simulated concentrations and hence the breakthrough curves. Small values of aquifer thickness result in higher concentration values all over the domain. This was not surprising since the aquifer thickness influences the source concentration at the injection point. Sensitivities of velocities are due to the fact that different velocities produce different arrival times which result in different levels of concentrations at a particular location in space and in time. Such velocities also influence the magnitude of dispersion coefficient. The effect of an incorrect estimate of velocity on concentration prediction increases as one moves away from the source. It was also observed that as longitudinal dispersivity increases, the concentration levels reduce in general but, with a more significant reduction in the maximum concentration at a particular location in time. This results in the slope of the breakthrough curve being gentler. It became obvious that the different influences that these parameters have on the simulated breakthrough curves make it difficult to estimate more than one parameter at a time by just comparing the simulated results with that of the tracer test results experiment. Therefore many trial runs were performed for each parameter and verified by several combinations of different parameters.

7.4.4 Backcalculation of Effective Aquifer Parameters

The information obtained from the numerically simulated results are used to estimate some important aquifer parameters and compared with those estimated from in situ and tracer tests. Transmittivity (T) values from aquifer pumping data from a well close to the test area were analyzed by Jacob's and Theis' methods to obtain a value of 2.42 m^2/s (Gale, 1993). By using the value of aquifer thickness which combined with other parameters to qive a close match between numerically simulated and experimental results (optimal aquifer thickness, $\Lambda = 6.5$ m), a bulk hydraulic conductivity (K) value of 0.321 m/day was computed from the relation $K = T/\Lambda$. Furthermore, this K value was combined with the optimal value for the average linear velocity ($|V|$) of 1.5 m/day and the hydraulic gradient (I) of 0.08, to estimate effective porosity (ϵ) value of 0.017. This compares with the bulk hydraulic conductivity of 0.224 m/day obtained from in situ tests and effective porosity value of 0.014 obtained by combining both in situ and tracer tests.

7.5 Sensitivity Analysis

From Figures 7.3 to 7.11, one can evaluate qualitatively the effect of changes in the various parameters on the concentration levels. However the task to determine which of these parameters is most sensitive becomes more complicated or difficult especially in this case where different parameters have different effects on the simulated breakthrough curves. A quantitative approach which provides more insight on the sensitivities of the individual parameters is presented in this section.

McElwee (1982) was among the earlier workers to propose a suitable quantitative approach for evaluating sensitivities of solute transport parameters by defining a sensitivity coefficient. Mathematically the sensitivity of a model dependent variable to a model input parameter is defined as (McElwee 1982):

$$X_{i,k} = \frac{\partial y_i}{\partial a_k} \qquad (7.2)$$

where $X_{i,k}$ is termed the sensitivity coefficient of the model dependent variable y with respect to the kth parameter a_k at the ith observation. Equation (7.2) can be normalized by the parameter value so that the sensitivity coefficient with respect to any parameter is in the same unit as that for the dependent variable in the form:

$$X_{i,k} = \frac{\partial y_i}{\partial a_k / a_k} \tag{7.3}$$

The normalized form is convenient for comparing sensitivity coefficients among different parameters and types of dependent variable in a form given (Zheng and Bennett 1995). The sensitivity coefficient with respect to a particular parameter can then be estimated by making a small variation in the parameter while keeping all the others constant as:

$$X_{i,k} = \frac{\partial y_i}{\partial a_k / a_k} \approx \frac{y_i(a_k + \Delta a_k) - y_i(a_k)}{\Delta a_k / a_k} \tag{7.4}$$

where a_k is the parameter value for the base case, Δa_k is a small change in the parameter and $y(a_k)$ and $y(a_k + \Delta a_k)$ are the values of the dependent variable obtained for the base case and for the perturbed parameter case respectively. The sensitivity coefficients defined by equation (7.4) measure the sensitivity of the model response at a particular point to a given parameter. Zheng and Bennett (1995) proposed an extension of this technique that can be used to define a single sensitivity for a group of observation wells by employing statistical analysis which involves the sum of squares error function. In the normalized form this is given as (Zheng and Bennett 1995):

$$X_k = \frac{\partial S}{\partial a_k / a_k} \approx \frac{S(a_k + \Delta a_k) - S(a_k)}{\Delta a_k / a_k} \tag{7.5}$$

where X_k is the group normalized sensitivity coefficient, ∂S is the change in the sum-of-squares error function from base case $S(a_k)$ to the case $S(a_k + \Delta a_k)$ due to change in parameter a_k. To compute the sensitivity coefficient for a given parameter using this approach, a base case is selected and the S value (RMSE) is calculated from the measured concentration (say) at various times and/or observation points. The base parameter a_k is then varied by a factor Δa_k while keeping all remaining parameters constant and the S value is calculated under the new parameter set. Then equation (7.5) can be used to compute the sensitivity coefficients. The optimal values obtained from sequential model runs (Table 7.1) were used as the base $S(a_k)$ and then the parameters were varied one after the other to obtain their RMSEs which were then used in equation (7.5). By following this approach sensitivity coefficients have been computed for various solute transport parameters.

It was observed from the quantitative values and graphical representations that aquifer thickness and average velocity had the highest sensitivity coefficients followed by the dispersivities. Changes in the magnitudes of these parameters led to a more than corresponding impacts in the concentration distribution in space. The specification made at the boundary (specified concentration or specified solute flux) gave the least sensitivity

coefficient. This was not surprising for this work because, by defining a bigger domain than necessary, the effects of specifying either the concentration or the solute flux on the boundary were reduced. Therefore the lower sensitivity coefficient computed here may be only applicable under such conditions and needs to be investigated further. The sensitivity coefficients for the individual parameters are shown in Figure 7.13.
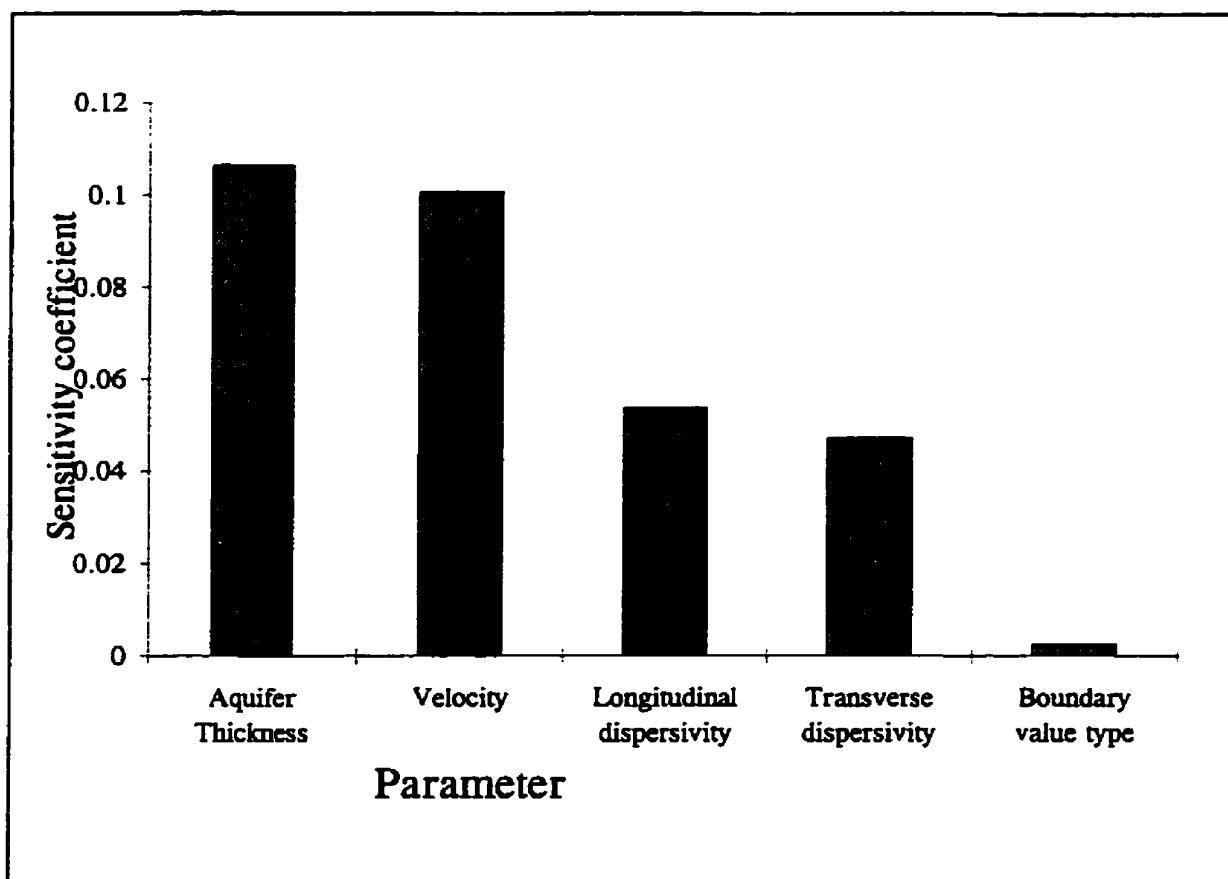
Figure 7.13: Sensitivity coefficients for solute transport modelling parameters

7.6 Uncertainties Associated with Calibration Results

The main uncertainties associated with the model calibration results may be classified into conceptual uncertainty and measurement errors. The classical equation has been employed to model the solute transport in this aquifer by using the continuum (equivalent porous media) approach. Although detailed site experimental studies suggested the appropriateness of this approach, the limited spatial scale of the test highly influence the validity of this concept beyond the test area or in other nearby aquifers. Such uncertainty is difficult to discuss since this is the first time this type of investigation has been conducted in Newfoundland and hence no previous data exist for comparison. From the results of the field in situ tests and tracer experiments, parameter uncertainties that may be attributed to heterogeneity of formation properties and fracture properties were observed. For example, variations in tracer arrival rates and velocities, dispersivities, hydraulic gradients, hydraulic conductivities etc. were recognized. Tracer breakthrough curves were all characterized by steep fronts and long trailing tails indicating some form of non-Fickian dispersion. However, since it was impossible to characterize heterogenieties especially those resulting from fracture properties, deterministic analysis which require mean values of input parameters has been employed.

Another source of uncertainty involves measurement accuracy. Although several quality control measures were adopted during the sampling and measurement times, the results are still prone to errors due to sampling frequency, sample storage, accuracy of measuring

equipment, data transformation etc. The effects of all these sources of errors directly influence the accuracy of the simulated results since the parameters have been derived based on the closeness of fit between experimental and simulated results.

7.7 Summary of Model Calibration

This chapter has presented the application of the boundary element model to an actual field case. The information obtained from several months of groundwater monitoring, in situ hydraulic test and natural gradient tracer tests has been used to simulate solute transport in this type of fractured aquifer. After several sequential runs of the boundary element code, optimal aquifer parameters were estimated. The effects of changes of various solute transport parameters on the spatial and temporal distribution of concentrations were evaluated qualitatively by using graphical methods and quantitatively by using sensitivity analysis. Some of the results (tabulated data) from these analyses are shown in appendix D, Table D1 to Table D17. Sensitivity coefficients computed indicate that the choice of aquifer thickness and average linear velocity have the highest effects on the simulated concentration levels. This implies that the major inherent parameters of average linear velocity such as hydraulic conductivity and effective porosity which are usually not known with high degree of certainty should be estimated carefully by combining several approaches as used in this work. When a larger domain is defined, specifying either the solute flux or the concentration at the boundary did not have any significant effect on the accuracy of the results. It was observed that several uncertainties caused by the inability

to characterize in detail the heterogeneities produced by the fracture properties made it difficult to get an excellent match between simulated and experimental results. However all such uncertainties are typical of the application of numerical techniques in field situations.

Chapter 8

Summary and Conclusions

8.1 Summary and Conclusions for the Work

In this thesis, a detailed review of the literature on the mechanisms and theory underlying solute transport in both porous and fractured formations have been conducted. The various numerical solution techniques employed for the implementation of the governing equations have also been reviewed. Review of previous work indicates a need for more studies in this area of research. It was found that comparatively few field studies have been conducted in fractured formations and therefore, the major theoretical concepts (equivalent porous medium, discrete fracture and channel flow) proposed for solute transport analysis in such aquifers have not been examined for field applications. It was also observed that, although numerical modelling of solute transport has advanced over the past decade, the inherent limitations of the commonly used numerical solution techniques and the lack of available data have impeded progress.

To address the problem of data limitation and conceptual understanding, a field study has been performed. Our goal was to investigate contaminant migration patterns in the type of fractured bedrock aquifer found in the St. John's area. This site specific information

would then be used to develop and test a boundary element model for solute transport.

To obtain detailed understanding of the hydraulic characteristics of the aquifer at the test site we performed several in situ tests for hydraulic conductivity and monitored groundwater levels and flow directions over a two year period. Two natural gradient tracer experiments were performed to examine the theoretical concept applicable for solute transport analysis in this aquifer. The tracer tests also provided data for solute transport parameters which complemented those obtained from hydraulic conductivity tests and groundwater monitoring. Since the primary objective was to examine the physical transport mechanisms in the bedrock aquifer most of the attention was focused on the analysis of conservative solutes. The information obtained was used to develop a numerical model for solute transport analysis. The results of the field study presented herein may be summarized as follows:

Hydraulic conductivities in the underlying fractured bedrock across the site vary within three orders of magnitude (10^{-4} to 10^{-7} cm/s) and were found to follow a lognormal distribution. Between the years 1994 and 1995, hydraulic heads and gradients exhibited some temporal and spatial variability. Although the hydraulic heads fluctuated according to the seasonal variation of precipitation, they did not have significant variation in the hydraulic gradients and groundwater flow directions. The hydraulic gradients were found to follow normal distribution. Due to the higher scale of variability of the hydraulic conductivities compared to other parameters, they were considered to be the major source

of uncertainty in solute transport analysis in the fractured bedrock. Therefore the difficulty in precisely characterizing the hydraulic structure should be recognized in the design of field studies for aquifer contamination in this area.

Results from the tracer tests revealed that tracer migration rate in the glacial till is about three times faster than those in the fractured bedrock. Longitudinal and transport dispersivity values were also found to be larger in the glacial till. However tracer migration direction and the spreading pattern in the glacial till and in the bedrock were found to be similar. A unique observation was that contaminant migration in the overlying till tends to be confined to this layer. This was noted when dye tracers injected in the overlying till were not measured in any of the bedrock wells downstream. This observation suggests that at least in the short term and in certain areas there is limited exchange of fluid (hydraulic communication) between these two media.

In both tests performed in the bedrock, tracers were detected in all the wells downstream in the direction of groundwater flow. This was accompanied by a spatial spreading both in the longitudinal and transverse directions similar to that observed in the glacial till. There was no evidence of channel flow. It was deduced from the tracer migration patterns that the bedrock fracture density and inter-connectivity are very high. Therefore the representation of this formation at the scale of individual fractures (discrete fracture concept) was impossible. Hence an equivalent porous medium conceptualization (continuum approach) was proposed for solute transport analysis in the aquifer. Solute

transport parameters for the bedrock aquifer were also estimated from the tracer test data. The concentration profiles for the wells in the bedrock were found to be non-Gaussian probably due to the heterogeneity of the aquifer material.

To demonstrate the applicability of a numerical model for solute transport analysis a boundary element model was developed based on the practical information obtained from the field experiments. A new approach in the application of the dual reciprocity boundary element method has been proposed and a computer code was written to implement the idea. The numerical model has been verified with good agreement, by comparing the results with the analytical solutions for three theoretical problems of subsurface solute transport. Numerical results show that the DRBEM model is capable of handling the dual nature of the advection-dispersion equation by achieving reasonable accuracy for Peclet numbers ranging from 0.5 to 12.0.

The results from our new approach also show that avoiding the differentiation of the approximation function F_j leads to increased accuracy and improved computational efficiency. These were observed by comparing the numerical results from the present work with those from the conventional DRBEM approach. Furthermore, the numerical model was benchmarked by comparing the results with those from other numerical solution techniques (FEM, MOC, Random Walk) for two solute transport problems proposed in the literature. The efficiency of the DRBEM was demonstrated by using fewer elements than other techniques to achieve results of comparable accuracy. This is a major

advantage of the DRBEM model in terms of a significant reduction in input data preparation, computational efficiency and modelling effort.

The DRBEM model was applied to the field case for calibration. Numerically simulated breakthrough curves were compared with those from the tracer experiment. Effective mean macroscopic solute transport parameters which gave a reasonable match between numerical and experimental breakthrough curves were obtained and assumed to represent the bulk effective mean parameters for the aquifer at the test site. The DRBEM model was found to be flexible since only the boundary of the domain had to be modelled.

A sensitivity analysis was performed to examine the effects of the various input parameters on the concentration levels. The effects were quantified by computing sensitivity coefficients for the various parameters. Results show that aquifer thickness and average linear velocity have the greatest influence on simulated concentration levels in space and in time. Longitudinal and transverse dispersivities were also found to have a significant influence. This means that parameters such as hydraulic conductivity and effective porosity which determine solute transport velocity need to be determined carefully. For fractured aquifers such as those found at the experimental site the fracture characteristics influence the spatial variability of hydraulic conductivity and bulk effective porosities. It is thus extremely important to characterize them in detail by various field tests as employed in this work.

8.2 Recommendations For Further Study

The present work has provided preliminary insights into the contaminant transport mechanisms in a typical aquifer found in Newfoundland. Since the field tracer experiments are the first of their kind in this type of aquifer, further field studies are needed to verify the findings outlined in this work. Moreover, in the field of numerical modelling of contaminant transport the boundary element method has not been widely used especially for practical field studies. The efforts made in this study points to the need for further investigation of this numerical technique for field application. Some findings from this work which require attention for further investigation may be outline as follows:

The limited hydraulic communication between the overlying glacial till and the underlying fractured bedrock needs to be investigated further to examine how the till influences the recharge to the bedrock and hence the susceptibility of the bedrock aquifer to contamination from solutes moving through the till.

It is important that several large scale and long term tracer tests be conducted at different sites around St. John's to examine the validity of the equivalent porous medium concept which was very critical for accurate analysis by the numerical model.

The extent of fracturing, fracture orientations and degree of interconnectivity were deduced based on the tracer spreading and appearance in the wells. However, more

sophisticated methods such as geophysical techniques will provide further insights to the actual characteristics of the fractures which may influence fluid flow.

Although tracer breakthrough curves suggested some form of non-Fickian transport, the analysis has been performed by assuming Fickian type dispersion. This needs to be further investigated by tracer experiments to determine the scale dependence of dispersivity in this type of aquifer. Furthermore, since dispersion phenomena are sensitive to fracture characteristics, more field studies on other sites will enhance the understanding.

The dual reciprocity boundary element model has proved efficient and accurate in both theoretical and practical field problems. What remains to be determined is the robustness of the model when applied to a wide range of sites. This points to the need of further elaborate tracer tests performed in various sites to validate the model.

The DRBEM model has been developed for isotropic homogeneous media for a 2-D case. However, simulation of solute transport in this fractured aquifer for a 3-D case will fully account for fracture interconnectivity in all directions and therefore improve the results.

REFERENCES

Abelin, H., Birgersson, L., Gidlund, J., and Neretnieks, I. 1991. *A Large Scale Flow and Tracer Experiment in Granite. 1 Experimental Design and Flow Distribution.* Water Resources Research, **27**(12): 3101-3117

Amoah N., and Morin P. 1996a *In Situ Assessment of Groundwater Flow Parameters for Contaminant Transport Modelling.* Proceedings, 49th Canadian Geotechnical Conference, St. John's Newfoundland. pp. 801-808.

Amoah N., Morin P., and Sabin G. 1996b. *Analysis of Solute Transport Through Saturated Porous Aquifer Using Dual Reciprocity Boundary Element Method,* BEM XVIII, Editors, C. A. Brebbia, J. B. Martins, M. H. Aliabadi and N. Haie, Computational Mechanics Publication, Southampton, UK. pp. 619-628.

Amoah N., and Morin P. 1996. *A Natural Gradient Tracer Test to Evaluate Solute Transport Mechanisms in Saturated Fractured Porous Aquifer.* Proceedings, 49th Canadian Geotechnical Conference, St. John's Newfoundland. pp. 481-488.

Anderson, M. P. 1979. *Using Models to Simulate the Movement of Contaminants Through Groundwater Systems,* CRC Critical Review on Environmental Control, **9**: 97-156.

Anderson M. P., and Woessner, W. W. 1992. *Applied Groundwater Modelling, Simulation of Flow and Advective Transport.* Academic Press, Sand Diego, 381 pp.

Bachmat, Y. and Bear J. 1964. *The General Equation of Hydrodynamic Dispersion,* J. of Geophysical. Research, **68**(12): 2561-2567

Batterson, M. J. 1984. *Surficial Geology of the Waterford River Basin, St. John's Newfoundland. Urban Hydrology of the Waterford River Basin.* Technical Report T-1. Newfoundland Department of Environment, Water Resources Division, 22 pp.

Barenblatt, G. I., Zehletov, I. P., and Kochina, I. N., 1960. *Basic Concepts in the Theory of Seepage of Homogeneous Liquids in Fissured Rocks.* PMM, Soviet Appl. Math. Mech., **24**(5): 852-864.

Bear, J. 1972. *Dynamics of Fluid in Porous Media.* Elsevier, New York, 567 pp.

Bear, J. 1979. *Hydraulic of Groundwater.* McGraw-Hill, New York, 764 pp.

Bedient, P. G., Rifai, H. S., and Newell, C. J. 1994. *Groundwater Contamination, Transport and Remediation,* Prentice Hall, Englewood Cliffs, NJ. 541 pp.

Beljin, M. S. 1985. *Analytical Modelling of Solute Transport, Practical Application of Groundwater Model,* NWWA Conference, Columbus, Ohio, August 19-20.

Beljin, M. S. 1988. *Testing and Validation of Models for Simulating Solute Transport in Groundwater, Code intercomparison and Evaluation of Validation Methodology.* GWMI 88-11, International Groundwater Modelling Center, Holcomb Research Institute, Butler University, Indianapolis, Indiana 46208, USA.

Berkowitz, B., Bear, J. and Braester, C. 1988. *Continuum Models for Contaminant Transport in Fractured Formations.* Water Resources Research, 24(8): 1225-1236.

Bibby, R. 1981. *Mass Transport of Solutes in Dual Porosity Media,* Water Resources Research, 17(4): 1075-1081.

Boggs, J. M., Young, S. C., Beard, L. M., Gelhar, L. W., Rehfeldt, K. R., and Adams, E. E. 1992. *Field Study of Dispersion in a Heterogeneous Aquifer 1. Overview and Site Description.* Water Resources Research, 28(12): 3281-3291.

Brebbia, C. A., and Wrobel, L. C. 1987. *Non-Linear Transient Thermal Analysis Using the Dual Reciprocity Method, In BETECH/87,* Computational Mechanics Publications, Southampton.

Brebbia, C. A., and Dominguez, J. 1992. *Boundary Element, An Introductory Course,* 2nd Ed., Computational Mechanics Publications, McGraw-Hill Book Company., 314 pp.

Bredehoeft, J. D., and Pinder, G. F. 1973. *Mass transport in Flowing Groundwater.* Water Resources Research, 9(1): 194-210.

Celia, M.A., Russel, T. F., Herrera, I., and Ewing, R. E. 1990. *An Euleriain-Lagrangian Localized Adjoint Method for Advection-Diffusion Equation.* Advances in Water Resources, 13(4) pp. 187-206.

Chapuis, R. P., Pare, J. J., and Lavallee, J. G. 1981. *In Situ Variable Head Permeability Tests.* Proceedings, Xth ICSMFE, Stockholm 1:401-406.

Cheng, A. H-D, and Lafe O. E. 1991. *Boundary Integral Solution for Stochastic Groundwater Flow.* Water Resources Research, 27(2): 231-242.

Chiang, C. Y., Wheeler, M. F., and Bedient, P. B. 1989. *A Modified Method of Characteristics Technique and Mixed Finite Element Method for Simulation of Groundwater Transport.* Water Resources Research, 25(7): 1541- 1549.

Cleary, R. W., and Ungs. M. J. 1978. *Groundwater Pollution and Hydrology, Mathematical Models and Computer Programs.* Rep. 78-WR-15. Water Resources

Program, Princeton University, Princeton, New Jersey.

Dagan, G. 1967. *Linearized Solution of Free Surface Groundwater Flow with Uniform Recharge.* Journal of Geophysical Research, **72**: 1183-1193.

Daus, A. D., and Frind, E. O. 1985. *An Alternating Direction Galerkin Technique for Simulation of Contaminant Transport in Complex Groundwater Systems.* Water Resources Research **21**(5): 653-64

Domenico, P.A. and Schwartz, F. W. 1990. *Physical and Chemical Hydrogeology.* John Wiley and Sons, New York, 824 pp.

Dominie, K., 1992, *A Report on Provincial Waste Disposal Sites and Waste Management Practices,* Dept. of Environment and Lands, Gov't of Newfoundland and Labrador, pp 6.

Eldho, T. I. 1996. *A Sensitivity Study of Transient Groundwater Flow Using Dual Reciprocity Boundary Element Method,* BEM XVIII, Editors, C. A. Brebbia, J. B. Martins, M. H. Aliabadi and N. Haie, Computational Mechanics Publication, Southampton, UK. pp. 637-646.

El Harrouni, K., Brebbia, C. A., and Ingber, M. S. 1992. *Dual Reciprocity Boundary Element for Heterogenous Porous Media.* BETECH VII. Ed. C. A. Brebbia and M.S. Ingber. Computational Mechanics Publications, Southampton, UK. pp. 151-159.

Fetter, C. W., 1988. *Applied Hydrogeology,* 2nd ed. Merrill Publ Co., Columbus, Ohio.

Fetter, C. W., 1993., *Contaminant Hydrogeology*, Macmillan Publishing Co., New York

Freeze, R. A. , and Cherry, J. A., 1979. *Groundwater.* Prentice-Hall, Englewood Cliffs, NJ, 604 pp.

Freyberg, D. L. 1986. *A Natural Gradient Experiment on Solute Transport in a Sand Aquifer. 2, Spatial Moment and Advection and the Dispersion of Nonreactive Tracers.* Water resources Research, **22**(13): 2031-2046.

Fodgen, A., Landman, K. A., and White, L. R. 1988. *Contaminant Transport in fractured Porous Media, Steady State Solution by Boundary Integral Method.* Water Resources Research, **24**(8): 1384-1396.

Gale, J. E., 1973. Personal Communication

Gale, J. E., Francis, R. M., King, A. F., and Rogerson, R. J. 1984. *1984 Hydrogeology of the Avalon Peninsula area.* Water Resources Report 2-6, Groundwater Series. Newfoundland and Labrador Dept. of Environment, Water Resources Division, 165p, .

Gardner, Jr., A. O., Peaceman, D. W., and Pozzi, Jr., A. L. 1964. *Numerical Calculations of Multidimensional miscible displacement by the Method of Characteristics.* Society of Petroleum Eng. J., 6(2): 175-182.

Gaspar E. 1987a. *Modern Trends in Tracer Hydrology, Vol 1,* CRC Press Inc. Boca, FL

Gaspar E. 1987a. *Modern Trends in Tracer Hydrology, Vol 2,* CRC Press Inc. Boca, FL

Gelhar, L. W. and Axness, C. L. 1983. *Three Dimensional Stochastic Analysis of Macrodispersion in Aquifers.* Water Resources Research, 19(1): 161-189.

Gelhar, L. W., Mantaglou, A., Welty, C., and Rehfeldt, K. R. 1985. *A Review of Field Scale Physical Solute transport in Saturated and Unsaturated Porous Media.* EPRI-Report, EA 4190, Electric Power Resources Institute. Pal Alto, California. USA.

Gelhar, L.W., Welty, C and Rehfeldt, K.R. 1992. *A Critical Review of Data on Field Scale Dispersion in Aquifers.* Water Resources Research 28(7): 1955-1974

Gerabedian, S. P., LeBlanc, D. R., Gelhar, L. W., and Celia, M. A. 1991. *Large Scale Natural Gradient Tracer Test in Sand and Gravel, Cape cod, Massachussets, 2.* Analysis of Tracer Moments for Nonreactive Tracer. Water Resources Research, 27(5): 911-924.

Grisak, G. E., and Pickens, J. F. 1980. *Solute Transport through Fractured Media 1, The Effects of Matrix diffusion,* Water Resources research, 16(4): 731-739.

Grisak, G. E., and Pickens, J. F. 1981. *Analytical Solution for Transport Through Fractured Media with Matrix Diffusion.* Journal of Hydrology, Vol. 5, pp. 719-730.

Guzzwell, G. K. 1996. *A Hydrogeological and Geophysical Assessment of a Contaminant Plume Emanating From the Terra Nova Regional Waste Disposal Site.* Master of Science Thesis, Department of Earth Science, Memorial University of Newfoundland, St. John's, Newfoundland, Canada, 193 pp.

Haie, N., Martins, J. B., and Veloso da Veiga E. 1993. *Application of the Dual Reciprocity Boundary Element Method (DRM) to Groundwater Pollution.* BETECH VIII, Editors, C. A. Brebbia, and P. H. Pina, Computational Mechanics Publication, Southampton, UK. pp. 37-46.

Haie, N., Machado, G. J., Fortunas, F. C., Teixeira, J. C., and Martins, J. B. 1996. *Comparison of BEM, FEM, and FDM for the Solution of Some Engineering Problems.* BEM XVIII, Editors, C. A. Brebbia, J. B. Martins, M. H. Aliabadi and N. Haie, Computational Mechanics Publication, Southampton, UK. pp. 193-202.

Hamilton, D. A. 1982. *Groundwater Modelling: Selection, Testing and Use.* Michigan

Department of Natural Resources, Water Management Division, 199 pp.

Hantush, M. S. 1956. *Analysis of Data from Pumping Tests in Leaky Aquifers*. Trans. American Geophysical Union, Vol. 37 pp. 702-714.

Healy, R. W., and Russel, T. F. 1992. *Solution of the Advection-Dispersion Equation by a Finite-Volume Eulerian-Lagrangian Local Adjoint Method*. Numerical Method in Water Resources Vol. 1. pp 33-39. Computational Methods in Water Resources IX, Editors. T.F Russel, R.E. Ewing, C.A. Brebbia, W.G. Gray and G.F. Pinder, Computaional Mechanics Publication. Elsevier Applied Science.

Henderson E.P. 1972. *Surficial Geology of the Avalon Peninsula*, Newfoundland Geological Survey of Canada, Memoir 368, 121 pp.

Heringa, P. K. 1981. *Soils of the Avalon Peninsula*, Newfoundland Report No. #, Newfoundland Soil Survey, Research Branch, Agriculture Canada, St. John's, Newfoundland, 117 pp.

Hunt, B. W. 1978. *Dispersive Sources in uniform groundwater flow*, Journal of Hydraulics Division, ASCE, Vol. 104, pp. 75-85.

Huyakorn, P. S., Mercer, J. W., and Lester, B. H. 1983. *An Efficient Finite Element Technique for Modelling Transport in Fractured Porous Media 1. Single Species Transport*. Water Resources research, 19(3): 841-854.

Huyakorn, P. S., Kretschek, A. G., Broome, R. W., Mercer, J. W., and Lester, B. H. 1984. *Testing and Validation of Models for Simulating Solute Transport in Groundwater, Development, Evaluation and Comparison of Benchmark Techniques*, GWMI-84, International Groundwater Modelling Center, Holcomb Research Institute, Butler University, Indianapolis, Indiana, 46208, USA.

Ingber, S. M. and Phan-Thien, N. 1992. *A Boundary Element Approach for Parabolic Differential Equations Using a Class of Particular Solutions*. Applied Mathematical Modelling, **16**: 124-132.

Ivany, P. A. 1994. *Site Characterization, Design, Construction and Management of a Field Experiment to Assess Groundwater Contamination by Agricultural Waste Management Practices*. MSc. Thesis, Memorial University of Newfoundland, Department of Earth Sciences, Canada.

Javandel, I., Doughty, C., and Tsang, C. F. 1984. *Groundwater Transport: Handbook of Mathematical Models*. Water Resources Monograph, 10. American Geophysical Union. 227 pp.

Jiao, J. J. 1993. Data Analyses Methods for Determining Two-Dimensional Dispersive Parameters. Groundwater, **31**(1): 57-62.

King A. F. 1984. *Geology of the Waterford River basin, St. John's, Newfoundland.* Urban Hydrology of the Waterford River Basin Technical Report T-2. Newfoundland Department of Environment, Water Resources Div, 25 pp.

King, A. F. 1986. *Geology of the St. John's Area, Newfoundland.* Current Research, Newfoundland Department of Mines and Energy, Mineral Development Division, Report 86(1): 209-218.

King, A. F. 1990. *Geology of the St. John's Area,* Geological Survey Branch, Newfoundland Department of Mines and Energy, Report 90(2): 88 pp.

Koch, D.H., and Prickett, T.A. 1993. *RAND3D, A Three Dimensional Ground Water Solute Transport Model, User's Manual.* Engineering Technologies Associates, Inc., Ellicot City, MD.

Konikow, L. F., and Bredehoeft, J. D. 1978. *Computer Model of Two Dimensional Solute Transport and Dispersion in Groundwater.* U. S. Geological Survey Water Resources Investigations Book 7, Chapter C2, pp 90.

Lafe, O. E., Liggett, J. A. and Liu, P. L-F. 1981. *BIEM Solution to Combinations of Leaky Layered, Confined, Unconfined, Nonisotropic Aquifers.* Water Resource Research, **17**(5): 1431-1443.

LeBlanc, D. R., Garabedian, S. P., Hess, K. M., Gelhar, L. W., Quadri, R. P., Stollenwerk, K. G., and Wood, W. W. 1991. *Large Scale Natural Gradient Tracer Test in Sand and Gravel, Cape Cod, Massachusetts 1. Experimental Design and Observed Tracer Movement.* Water Resources Research, **27**(5): 895-910.

Leo C. J. and Booker, J. R. 1993. *Boundary Element Analysis of Contaminant Transport in Fractured Porous Media.,* International Journal for Numerical and Analytical Methods in Geomechanics. **17**(7): 471-492.

Lennon, G. P., Liu, P. L-F, and Liggett, J. A. 1979a. *Boundary Integral Solution to Axisymetric Potential Flows 1, Basic Formulation,* Water Resources Research, **15**(5): 1102-1106.

Lennon, G. P., Liu, P. L-F, and Liggett, J. A. 1979b. *Boundary Integral Solution to Axisymetric Potential Flows 2,* Recharge and Well Problems in Porous Media, Water Resources Research, **15**(5): 1107-1115.

Lennon, G. P., Liu, P. L-F, and Liggett, J. A. 1980. *Boundary Integral Solution for*

Three Dimensional Darcy Flow. Water Resources Research, **16**(4): 1715-1723.

Ligget, J. A. 1977. *Location of Free Surface in Porous Media.* Journal of Hydraulic Division, American Society of civil Engineers, **103** (HY4): 353-365.

Liggett, J. A. and Liu, L-F. 1983. *The Boundary Integral Equation Method for Porous Media Flow*, Allen and Unwin, London.

Liu, P. L-F, and Liggett, J. A. 1978. *An Efficient Numerical Method for Two-Dimensional Steady Groundwater Problems,* Water Resources Research, **14**(3): 385-390.

Mackay, D. M, Freyberg, D. L. Roberts, P. V., and Cherry, J. A. 1986. *A Natural Gradient Experiment on Solute Transport in a Sand Aquifer 1. Approach and Overview of Plume Movement.*, Water Resources Research, **22**(13): 2017-2029.

Masumoto, T., Tanaka, M., and Fujii, H. 1990. *Transient Analysis of Scalar Wave Equation Using Boundary Element Method Based on a Time-Stepping Scheme.* Topics in Engineering, Vol. 7, Advances in BEM in Japan and U.S.A. pp. 203-217.

McDonald, M. G., and Harbaugh, A. W. 1988. *A Modular Three Dimensional Finite Difference Groundwater Flow Model.* U. S. Geological Survey Techniques of Water resources Investigations, Book 6, 586 pp.

McElwee, C. D., 1982, *Sensitivity Analysis and the Groundwater Inverse Problems.* Ground Water, **20**(6): 723-735.

Moltyaner, G. I., Klukas, M. H.,, Wills, C. A., and Killey, R. W. D. 1993. *Numerical Simulation of Twin Lake Natural Gradient Tracer Tests: A Comparison of Methods.* Water Resources Research, **29**(10): 3433-3452.

Murray, C. R. and Reeves, E. B. 1977. *Estimated Use of Water in the United States,* 1975, U. S. Geological Survey Circular 765, 39 pp.

Nardini, D. and Brebbia, C. A. 1982. *A New Approach to Free Vibration Analysis Using Boundary Elements,* In Boundary Element Methods in Engineering (ed., C. A., Brebbia), Springer-Verlag, Berlin and New York.

Neretnieks, I., Eriksen, T., and Tahtinen, P. 1982. *Tracer Movement in a Single Fissure in Granitic Rock: Some Experimental Results and their Interpretation*, Water Resources Research 18(4): 849-858.

Neretnieks, I. 1987. *Channelling Effects in Flow and Transport in Fractured Rocks, Some Recent Observations and Models,* GEOVAL-87, International Symposium, Swed. Nuclear Insp., Stockholm.

Neville, C. J. 1994. *Compilation of Analytical Solutions for Solute Transport in Uniform Flow.* S. S. Papadopoulos & Associates, Inc. Bethesda, MD.

Noorishad, J., Tsang, P., Perrochet, P. and Musy, A. 1992. *A Perspective on the numerical Solution of Convection-Dominated Transport Problems: A Price to Pay for the Easy Way Out.* Water Resources Research, 28(2): 551-561.

Novakowski, K. S. and Lapcevic, P. A. 1994. *Field Measurement of Radial Solute Transport in Fractured rocks.* Water Resources Research, 30(1): 37-44.

Novakowski, K. S. and Lapcevic, P. A. 1996. *Field Measurement of Radial Solute Transport in Fractured rocks.* Hydrogeology, 4(3): 84-93.

Nowak, A. J. and Brebbia C. A., 1989, *The Multiple Reciprocity Method-A New Approach for Transforming BEM Domain Integrals to the Boundary, Engineering Analysis with Boundary Elements,* 6(3): 164-167.

Ogata, A., and Banks, R.B. 1961. *A Solution of Differential Equation of longitudinal Dispersion in Porous Media.* U. S. Geological Survey, Professional Paper 411-A.

Palmer, C. D., and Johnson, R. L. 1989. *Physical processes Controlling the Fate of Transport of Contaminants in the Aqueous Phase,* EPA/625/4-89/019, Seminar Publication, Transport and Fate of Contaminants in the Subsurface.

Partridge, P. W., and Brebbia, C. A. 1990. Computer *Implementation of the Dual Reciprocity Method for the Solution of General field Problems.* Communications in Applied Numerical Methods, 6(2): 83-92.

Partridge, P. W., Brebbia, C. A. and Wrobel, L. C. 1992. *Dual Reciprocity Boundary Element Method.* Computational Mechanics Publications, Elsevier Applied Science, London, New York. 276 pp.

Pankov, J.F., Johnson, R. L. Hewetson, J. P., and Cherry, J. A. 1986. *An evaluation of Contaminant Migration Patterns at Two Waste Disposal Sites on Fractured Porous Media in Terms of the Equivalent Porous Medium (EPM) Model.* Journal of Contaminant Hydrology, 1: 65-76.

Pinder, G. F., and Cooper, H. H., Jr. 1970. *A Numerical Technique for Calculating the Transient Position of the Saltwater Front.* Water resources Research, 6(3): 875- 882.

Prickett, T. A., and Lonnquist, C. G. 1971. *Selected Digital Computer Models for Groundwater Resource Evaluations.* Bulletin 55, Illinois State Water Survey, Champaign,

Prickett, T. A., Naymik, T. G., and Lonnquist, C. G. 1981. *A Random Walk Solute*

Transport Model for Selected Groundwater Quality Evaluations. Bulletin 65, Illinois State Water Survey, Champaign, IL..

Ptak, T. and Schmid, G. 1996. *Dual tracer Transport Experiment in a Physically and Chemically Heterogeneous Porous Aquifer: Effective Transport Parameters and Spatial Variability.* Journal of Hydrology, **183**: 117-138.

Rasmusson, A. and Neretnieks, I. 1986. *Radionuclide Transport in Fast Channels in Crystalline Rock.* Water Resources Research, **22**(8): 1247-1256.

Raven,, K. G., Novakowski, K.S. and Lapcevic, P. A. 1988. *Interpretation of Tracer Test of a Single Fracture Using a Transient Solute Storage Model.* Water Resources Research, **24**(12): 2019-2036.

Roache, P. J. 1982. *Computational Fluid Dynamics.* Hermosa Publishers, Albuquerque, New Mexico. 446 pp.

Robinson, J. W. 1985. *Groundwater in the Waterford River Basin.* Urban Hydrology Study of the Waterford River Basin, 134 pp.

Romm, E. S. 1966. *Flow Characteristics of Fractured Rocks*, Nedra, Moscow, 283 pp.

Rowe, R. K., and Booker, J. R. 1988. *A Semi-analytical Model for Contaminant Transport in a Regular Three Dimensional Fractured Network: Conservative Contaminants.* International Journal for Numerical Methods in Geomechanics **13**:531-550

Rowe, R. K., and Booker, J. R. 1990. *Contaminant Migration in Regular Three Dimensional Fractured Network: Reactive Contaminants.* International Journal for Numerical Methods in Geomechanics **14**:401-425

Sampler J., Carrera G., Garlaza G., and Medina A. 1990. *Application of an Automatic Calibration Technique to Modelling an Alluvial Aquifer,* In: Calibration and Reliability in Groundwater Modelling (K. Kovar, ed.) IAHS publication 195, pp. 87-96.

Sauty, J. P. 1980. *An Analysis of Hydrodispersive Transfer in Aquifers.* Water Resources Research, **16**(1): 145-158.

Schwartz, F. W. and Smith L. 1988. *A continuum Approach for Modelling Mass Transport in Fractured Media.* Water Resources Research, **24**(8): 1360-1372.

Scheidegger, A. E. 1961. *General Theory of Dispersion in Porous Media.* J. Geophysical Research, **66**(10): 3273-3278.

Sophocleous, M. A., Heidari, M. and McElwee, C. D. 1982. *Water Quality Modelling of the Equus Beds Aquifer in South-Central Kansas*. The Kansas Water Resources Research Institute, Lawrence, Kansas. 68 pp.

Sutton, P. A. and Barker, J. F. 1985. *Migration and Attenuation of Selected Organic in a Sandy aquifer.* Groundwater 23:10-16

Smart P. L. and Laidlaw, I. M. S. 1977. *An Evaluation of Some Fluorescent Dyes for Water Tracing,* Water Resources Research, 13(1): 15-33.

Sudicky, E. A., and Frind, E. O. 1982. *Contaminant Transport Through Fractured Porous Media: Analytical Solution for a System of Parallel Fractures.* Water Resources Research, 18(6): 1634-1642.

Sudicky, E. A., Cherry, J. A., and Frind, E. O. 1983. *Migration of Contaminants in Groundwater at a Landfill: A Case Study 4. A Natural-Gradient Dispersion Test.* Journal of Hydrology, 63: 81-108.

Sudicky, E. A., 1986, *A Natural Gradient Experiment on Solute Transport in Sandy Aquifer, Spatial Variability of Hydraulic Conductivity and its Role in the Dispersion the Process,* Water Resources Research, 22(13): 2069-2082.

Sudicky, E. A., 1989, *The Laplace Transform Galerkin Technique: A Time Continuous Finite Element Theory and Application to Mass Transport in Groundwater.* Water Resources Research, 25(8): 1833-1846.

Sutton, P. A., and Barker, J. F. 1985, *Migration and Attenuation of Selected Organics in a Sandy Aquifer- A Natural Gradient Experiment.* Groundwater, 23(1): 10-16.

Taigbenu, A. E., 1985, *A New Boundary Element Formulation for Groundwater Flow.* Ph.D. Dissertation, Cornell University, U.S.A. pp. 265.

Taigbenu, A., and Ligget, J. A., 1986, *An Integral Solution for the Diffusion-Advection Equation.* Water Resources Research, 22(8): 1237-1246.

Tang, D. H., Frind, E. O. and Sudicky, E. A. 1981. *Contaminant Transport in fractured Porous Media: Analytic Solution for Single Fracture.* Water Res Research 17(3): 555-564.

Thorbjarnarson, K. and Mackay, D. M. 1997. *A field Test of Tracer Transport and Organic Contaminant Elution in a Stratified Aquifer at the Rocky Mountain Arsenal (Denver, Colorado, USA.).* Journal of Contaminant Hydrology, 24: 287-312.

Tsang, Y., and Tsang, C. F. 1987. *Channel Model of Flow Through Fractured Media*, Water Resources Research, 23(3): 467-480.

Tsang, Y., and Tsang, C. F. 1989. *Flow Channelling in a Single Fractured as a Two-Dimensional Strongly Heterogeneous Permeable Medium*, Water Resources Research, 25(9): 2076-2080.

Tsang, Y., and Tsang, C. F., and Hale, V. F. 1991. *Tracer Transport in Fractures, Analysis of Field Data Based on a Variable-Aperture Channel Model*. Water Resources Research 25(9): 3095-3106.

Tsang, Y., and Tsang, C. F. Neretnieks, I., Moreno, L. 1988. *Flow and Tracer Transport in Fractured Media, A Variable Aperture Channel Model and its Properties*, Water Resources Research, 24(12): 2049-2060.

Van Genuchten, M. Th. and Alves. 1982. *Analytical Solutions of the One-Dimensional Convective-Disperrsive Solute Transport Equation*. U. S. Salinity Laboratory, U. S. Department of Agriculture, Riverside, CA.

Van der Heijde, P. K. M. 1994. *Groundwater Modelling Software Catalogue, 1994 Edition*, International Groundwater Modelling Center, Colorado School of Mines, Golden, CO 80401, USA.

Van der Heijde, P. K. M. 1993. *PLUME2D, Two-Dimensional Solution for Transport of a Non-Conservative Tracer in Groundwater.* International Groundwater Modelling Center, Colorado School of Mines, Golden, CO 80401, USA.

Voss, C. I. 1984. *A Finite Element Simulation Model for Saturated-Unsaturated, Fluid-Density-Dependent Groundwater Flow with Energy Transport or Chemically Reactive Single Species Solute Transport*. U. S. Geological Survey, Reston, Virginia. 409 pp.

Voss, C. I., and Knopman, D. S., 1989. Strong Classical one-dimensional descriptions of field solute transport exist. *In Proc. Conf. on Solving Ground Water Problems with Models*. National Water wells Association, Dublin, OH.

Walton, W. C. 1989. *Numerical Groundwater Modelling*. Lewis Publishers Inc. 272 pp

Wang, H. F., and Anderson, M. P. 1984. *Introduction to Groundwater Modelling-Finite Difference and Finite Element Methods*. W. H. Freeman and Co, San Francisco, 230 pp.

Wang, H. Q., Crampton, N., Huberson, S. and Garnier, J. M. 1987. *A Linear Graphical Method for Determining Hydro-dispersive Characteristics in Tracer Experiments with Instantaneous injection*. Journal of Hydrology, 95: 143-154.

Wilson, J. L., and Miller, P. J. 1978. *Two-Dimensional Plume in Uniform Groundwater Flow*. Journal of the Hydraulics Division, ASCE, HY4: 503-514.

Witherspoon, P.A., Wang, J. S. Y, Iwai, K. and Gale, J. E. 1980. *Validity of Cubic Law for Fluid Flow in a Deformable Fracture*, Water Resources Research, 16(6): 1016-1024.

Wrobel, L. C., Brebbia, C. A., and Nardini, D., 1986. *The Dual Reciprocity Boundary Element Formulation for Transient Heat Conduction*, In Finite Elements in Water Resources VI, Computational Mechanics Publications, Southampton and Springer-Verlag, Berlin and New York.

Wrobel, L. C., and Brebbia, C. A. 1987. *The Dual Reciprocity Boundary Element Formulation for Non-Linear Diffusion Problems*. Computer Methods in Applied Mech and Engineering. 65: 147-164

Yeh, G. T. 1990. *A Lagrangian-Eulerian Method with Zoomable Hidden Fine-mesh Approach for Solving Advection Dispersion Equations*. Water Resources Research, 26(6): pp. 1133-1144.

Yeh, G. T., Chang, J. R., and Short, T. E. 1992. *A exact Peak Capturing and Oscillation-free Scheme to Solve Advection-Dispersion Transport Equations*. Water Resources Research, 28(11): 2937-2951.

Zheng, C., 1990. MT3D, *A Modular Three Dimensional Transport Model for Simulation of Advection Dispersion and Chemical Reaction of Contaminants in Groundwater Systems*. Report to the U. S. Environmental Protection Agency, Ada, OK, 170 pp.

Zheng, C., 1992. *MT3D Version 1.8 Documentation and User's Guide*. S. S. Papadopoulos & Associates, Inc. Bethesda, MD.

Zheng, C., 1993. *Extension of the Method of Characteristics for Simulation of Solute Transport in Three Dimensions*. Ground Water, 26(6): 734-742.

Zheng, C. and Bennett, G. D., 1995. *Applied Contaminant Transport Modelling: Theory and Practice*. Van Nostrand Reinhold, 115 Fifth Avenue, New York, NY 10003. 440 pp.

Zheng, C., and Bennett, G. D., 1996. ZBSOFT, *A Collection of Groundwater Modelling and Utility Software to Accompany Applied Contaminant Transport Modelling*, Personal Communication.

Zheng, C., and Bennett, G. D. 1996. MT3, *Groundwater Modelling and Utility Software Manual*. Personal Communication.

Zhu, S. and Zhang, Y. 1994. *Improvement in Dual Reciprocity Boundary Element Method for Equations with Convective Terms.* Communications in Numerical Methods in Engineering (10) 361-371

Zou, S. and Parr, A.., 1994. *Two Dimensional Dispersivity Estimation Using Tracer Experiment Data.* Groundwater 32(3): 367-373.

APPENDICES

Appendix A

Summary of in situ tests results

Table A1: Summary of Hydraulic Conductivities

Well #	Hydraulic conductivity (cm/s)	Well #	Hydraulic conductivity (cm/s)
5	1.9×10^{-5}	14	1.0×10^{-4}
7	3.8×10^{-7}	16	4.0×10^{-4}
9	4.7×10^{-5}	19	1.3×10^{-5}
11	3.8×10^{-4}	31	8.9×10^{-4}
21	7.7×10^{-4}	13	1.1×10^{-5}
23	4.5×10^{-6}	27	4.9×10^{-4}
30	2.0×10^{-5}	25	9.4×10^{-5}
26	1.4×10^{-3}		
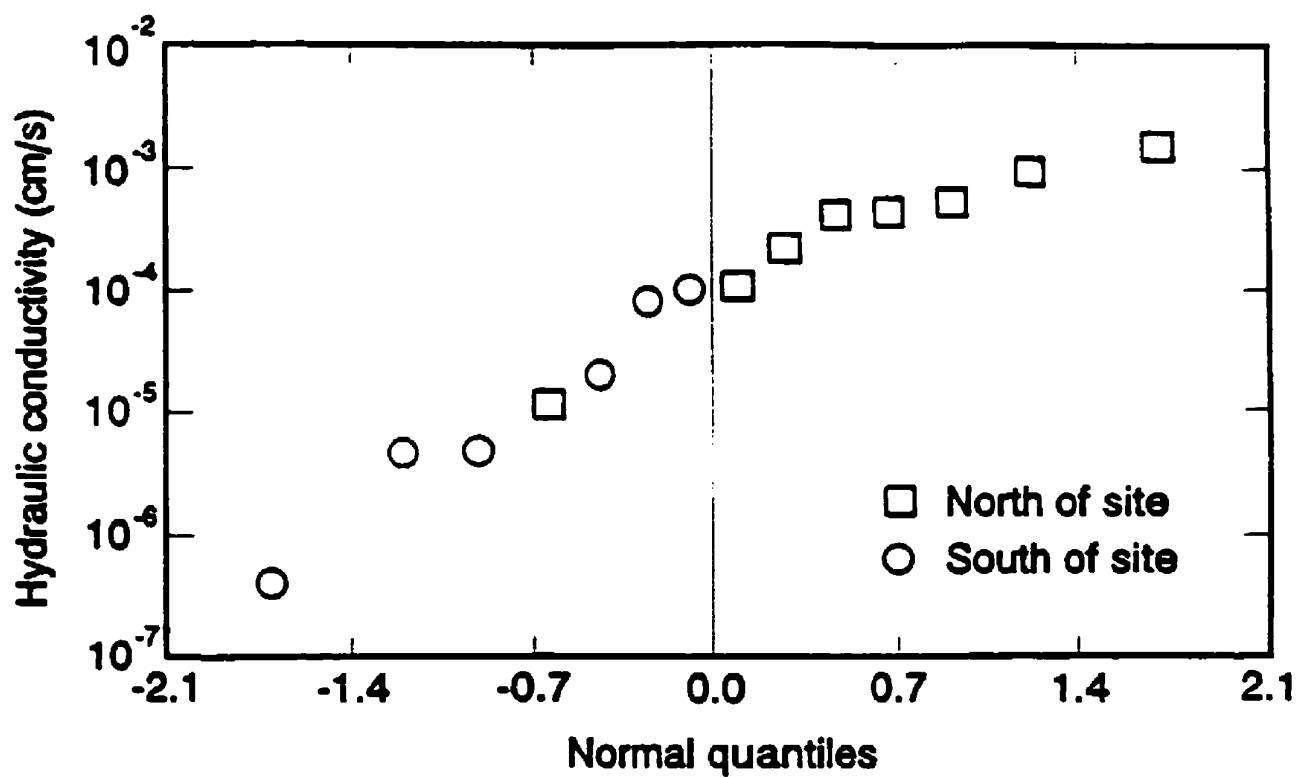
Figure A1.1: Probability plots of hydraulic conductivity data (after Amoah and Morin, 1996)

Table A2: Hydraulic Head (m) distribution (October 1994–November 1995)

Date	well #26 GL=96.8	well #27 GL=95.8	well #28 GL=95.9	well #30 GL=97.0	well #31 GL=97.6	well #13 GL=94.8
31-Oct 94	94.61	92.87	92.84	94.62	94.85	93.22
2-Nov 94	94.57	92.32	92.33	94.59	94.87	92.68
4-Nov 94	94.63	92.47	92.44	94.61	94.86	92.71
8-Nov 94	94.60	92.5	92.51	94.62	94.93	92.78
14-Nov 94	94.62	92.62	92.62	94.67	94.90	93.02
18-Nov 94	94.51	92.47	92.45	94.56	94.84	92.77
2-Dec 94	94.29	91.52	91.67	94.34	94.66	92.08
15-Dec 94	94.51	92.40	92.36	94.54	94.78	92.91
28-Dec 94	94.63	92.60	91.66	94.65	94.81	92.81
15-Feb 95	94.00	91.44	91.65	94.01	94.35	92.01
27-Feb 95	94.09	91.51	91.89	94.18	94.58	92.12
31-Mar 95	94.82	92.98	91.96	94.86	95.09	93.28
25-Apr 95	94.27	91.79	91.77	94.27	94.61	92.28
12-May 95	93.18	91.5	91.68	94.21	94.56	91.87
4-Jul 95	93.75	91.32	91.54	93.80	94.18	90.85
17-Jul 95	93.70	91.39	91.69	93.69	94.17	90.92
24-Jul 95	93.65	91.36	9,971	93.70	94.15	90.90
9-Jul 95	93.52	91.38	91.72	93.58	94.07	90.85
16-Jul 95	93.51	91.41	91.71	93.52	94.05	90.82
23-Jul 95	93.46	91.39	91.69	93.49	94.01	90.81
30-Jul 95	94.42	91.38	91.71	93.41	94.00	90.80
14-Sep 95	94.20	91.48	91.70	94.28	94.50	91.38
28-Sep 95	94.12	91.47	91.76	94.19	94.51	91.59
12-Oct 95	94.20	91.49	91.77	94.27	94.50	91.49
1-Nov 95	94.28	91.52	91.49	94.33	94.57	91.82

Note: GL=ground level elevation (m)

Table A2: (cont'd): Hydraulic Head (m) distribution (October 1994-November 1995)

Date	well #14 GL=96.5	well #16 GL=97.3	well #15 GL=96.5	well #29 GL=96.8	well #32 GL=97.9
31-Oct 94	94.45	94.62	94.43	94.56	94.93
2-Nov 94	94.41	94.64	94.40	94.48	94.99
4-Nov 94	94.45	94/68	94.45	94.53	94.98
8-Nov 94	94.46	94.57	94.47	94.55	95.05
14-Nov 94	94.47	94.70	94.46	94.60	95.04
18-Nov 94	94.37	94.63	94.34	94.48	94.99
2-Dec 94	94.16	94.39	94.17	94.23	94.80
15-Dec 94	94.34	94.56	94.33	94.40	95.03
28-Dec 94	94.39	94.43	94.23	94.53	95.17
15-Feb 95	94.08	94.16	94.07	94.91	94.69
27-Feb 95	94.21	94.27	94.19	94.11	94.89
31-Mar 95	94.62	94.91	94.61	94.75	95.30
25-Apr 95	94.10	94.38	94.08	94.19	94.86
12-May 95	94.03	94.30	94.05	94.13	94.78
4-Jul 95	93.69	93.91	93.70	93.65	dry
17-Jul 95	93.57	93.82	93.62	dry	dry
24-Jul 95	93.55	93.75	dry	dry	dry
9-Aug 95	93.46	93.67	dry	dry	dry
16-Aug 95	93.39	93.33	dry	dry	dry
23-Aug 95	93.35	93.59	dry	dry	dry
30-Aug 95	93.27	93.55	dry	dry	dry
14-Sep 95	94.10	94.30	NA	NA	NA
28-Sep 95	94.03	94.21	NA	NA	NA
12-Oct 95	94.08	94.29	NA	NA	NA
1-Nov 95	94.20	94.38	NA	NA	NA

Note GL= ground level elevation (m), NA= No measurement

Table A3: Hydraulic gradients (well # 30 as reference),October 1994-November 1995)

Date	well #26	well #27	well #28	well #30	well #13	well #14	well #16
31-Oct 94	0.0229	0.0801	0.0775	0.0288	0.0478	0.0246	0.0576
2-Nov 94	0.0287	0.1032	0.0979	0.0350	0.0643	0.0283	0.0575
4-Nov 94	0.0220	0.0967	0.0933	0.0313	0.0631	0.0252	0.0450
8-Nov 94	0.0316	0.0983	0.0932	0.0387	0.0631	0.0289	0.0900
18-Nov 94	0.0316	0.0959	0.0921	0.0350	0.0607	0.0289	0.0525
2-Dec 94	0.0354	0.1271	0.1153	0.0400	0.0757	0.0307	0.0675
15-Dec 94	0.0258	0.0963	0.0933	0.0300	0.5492	0.0271	0.0550
28-Dec 94	0.0172	0.0894	0.0829	0.0201	0.0587	0.0258	0.0950
15-Feb 95	0.0335	0.1178	0.1041	0.0425	0.0687	0.0166	0.0475
27-Feb 95	0.0469	0.1242	0.1037	0.0500	0.0722	0.0228	0.0775
31-Mar 95	0.0258	0.0854	0.0821	0.0287	0.0532	0.0289	0.0450
25-Apr 95	0.0325	0.1141	0.1095	0.0425	0.0684	0.0314	0.0575
12-May 95	0.0364	0.1238	0.1111	0.0438	0.0790	0.0326	0.0650
4-Jul 95	0.0412	0.1157	0.1018	0.0475	0.0778	0.0301	0.0675
24-Jul 95	0.0478	0.1129	0.0937	0.0575	0.0945	0.0369	0.1000
9-Aug 95	0.0526	0.1089	0.0906	0.0613	0.0946	0.0375	0.1001
16-Aug 95	0.0517	0.1068	0.0902	0.0663	0.0948	0.0406	0.1801
23-Aug 95	0.0526	0.1060	0.0895	0.0651	0.0937	0.0406	0.1050
30-Aug 95	0.0555	0.1060	0.0887	0.0738	0.0940	0.0449	0.1125
14-Sep 95	0.0287	0.1222	0.1079	0.0275	0.0916	0.0246	0.0501
28-Sep 95	0.0373	0.1230	0.1061	0.0401	0.0857	0.0295	0.0750
12-Oct 95	0.0287	0.1218	0.1053	0.0288	0.0884	0.0258	0.0525
1-Nov 95	0.0275	0.1234	0.1187	0.0300	0.0807	0.0228	0.0475
Arith mean	0.0354	0.1082	0.0973	0.0421	0.0759	0.0299	0.0736
CV	0.3065	0.1250	0.1095	0.3454	0.2152	0.2194	0.4153
Geo. mean	0.0338	0.1073	0.0968	0.0399	0.0742	0.0293	0.0689

Appendix A2

Box plot of hydraulic gradient data for selected wells

well

0.0180   0.0240   0.0300   0.0360   0.0420

well

0.050   0.075   0.100   0.125   0.150   0.175

well

0.020   0.040   0.060   0.080   0.100   0.120

well2

| 0.0210 | 0.0280 | 0.0350 | 0.0420 | 0.0490 | 0.0560 |

well

| 0.080 | 0.090 | 0.100 | 0.110 | 0.120 | 0.130 |

well

| 0.020 | 0.030 | 0.040 | 0.050 | 0.060 | 0.070 |
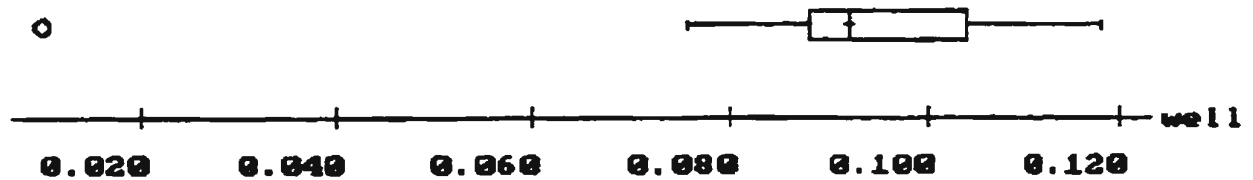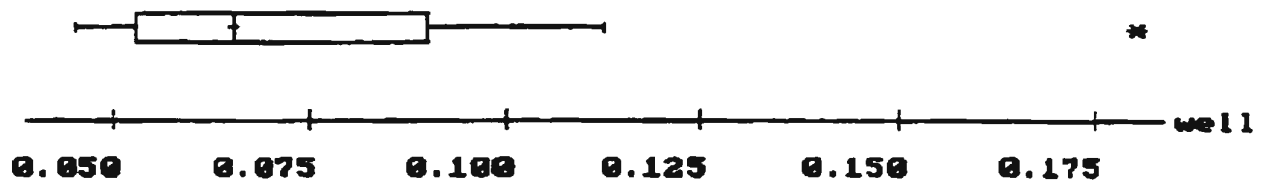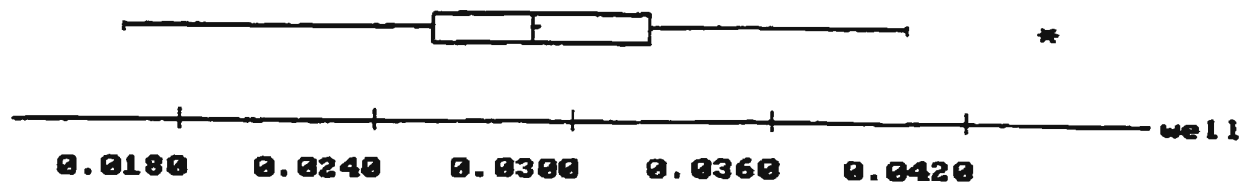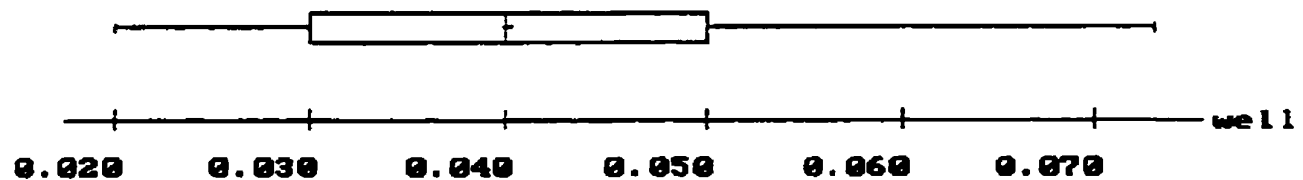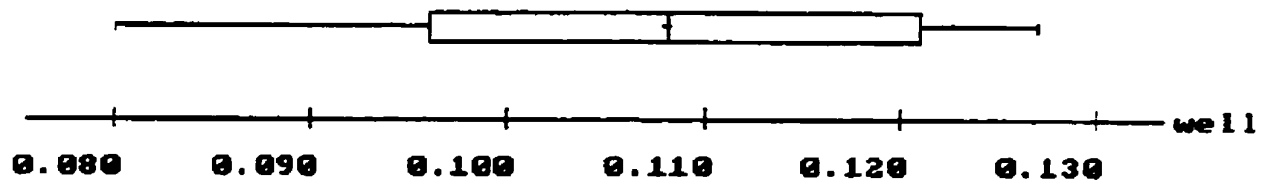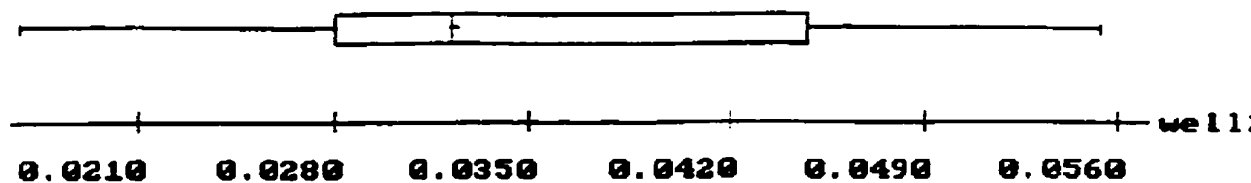
Appendix A3

Probability plot of hydraulic gradients data for selected wells
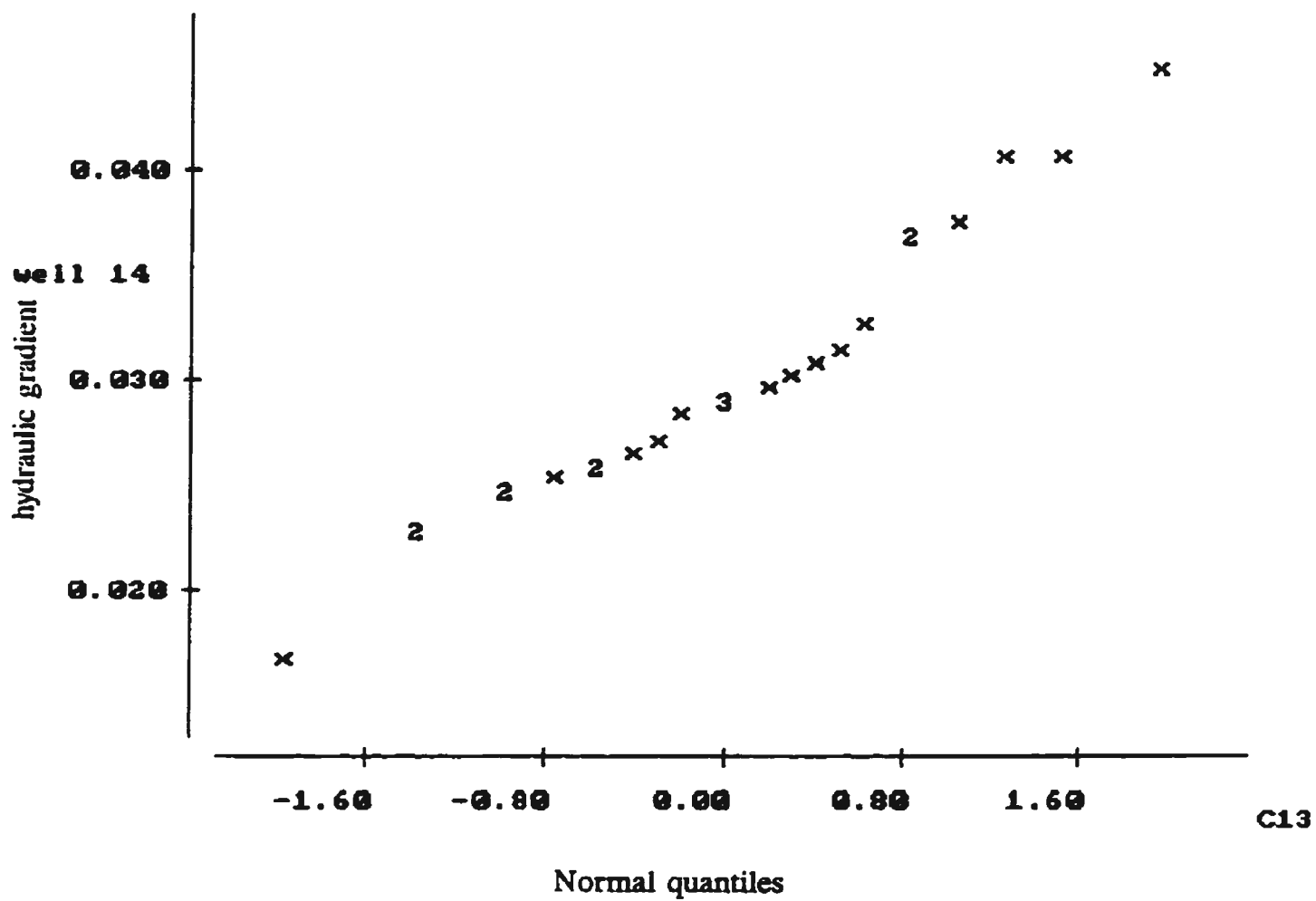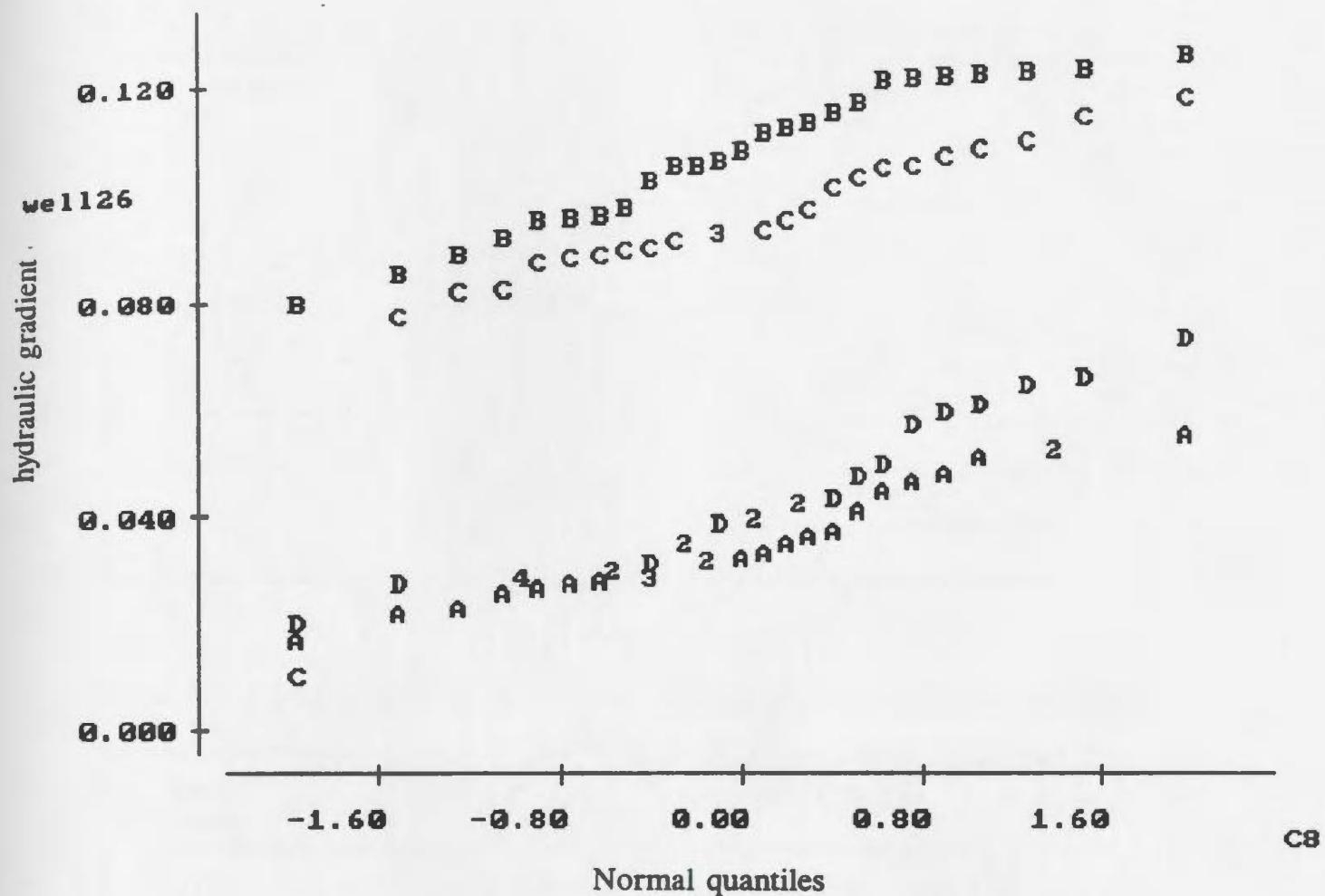
A = well26   vs. C8   C = well 28   vs. C10
B = well 27   vs. C9   D = well 30   vs. C11

Table A4: Summary of hydraulic heads observed during 1994-1995 period

Well #	Ground Surface Elevation(m)	Mean Hydraulic Head (m)	Range (m)
31	97.6	94.5	1.09
26	96.8	94.2	1.40
27	95.8	91.1	1.66
28	95.9	92.1	1.42
30	97.0	94.2	1.45
13	94.8	92.0	2.48
14	96.5	94.1	2.19
16	97.3	94.2	1.36

Table A5: Background concentration of selected compounds in site groundwater

Chemical Parameter	Range of Values	Chemical Parameter	Range of Values
Orthophosphate	1.0-3.2 mg/l	Total Hardness	48.0-231.0 mg/l
Nitrate	0-26.40 mg/l	Magnesium Hardness	6.0-267.0 mg/l
Ammonia Nitrogen	0-2.20 mg/l	Calcium Hardness	40-270 mg/l
Chloride	18-40 mg/l	Sodium Fluorescein	0.0 mg/l
pH	6.0-8.40	Lithium	0.0 mg/l
Conductance	0.2-0.50 mS/cm	Bromide	0.0 mg/l
Total Dissolved Solids	0.08-0.25 mg/l	Amino G Acid	0.0

Table A6: Generic and Alternative Names, Maximum Excitation and Emission of Tracer Dyes (after, Smart and Laidlaw, 1977)

Name of Dye	Colour Index	Generic Name	Alternative Names	Max. Excitation	Max. Emiss
Blue Dyes					
Amino G acid			7-amino 1,3naphtalene disulphonic acid	355	445
Photine CU		fluorescent Brightener 15		345	435
Green Dyes					
Uranine	45350	acid yellow 73	fluorescein LT, Sodium fluorescein	490	520
Lissamine FF	56205	acid yellow 7	Lissamine yellow FF, Brilliant Sulpho-flavine FF, Brilliant acid yellow 8G	420	515
Pyranine	59040	solvent green 7	pyranine, D&C Green 8	455	455
Orange Dyes					
Rhodamine B	45170			555	580
Rhodamine Wt				555	580
Sulpho rhodamineB	45100		Pontacyl brilliant pink B, Lissamine Red 4B, Kitton rhodamine B, Acid rhodamine B	565	590

Appendix B

Data for Tracer Test Phase II (Concentration in ppm)

Table B.1: Temporal and spatial distribution of concentration from tracer test phase II

Time (days)	well#30 conc (ppm)	well # 27 conc (ppm)	well #13 conc (ppm)	well #26 conc (ppm)	well #14 conc (ppm)	well #16 conc (ppm)
1	0.062745	0.000000	0.000000	0.025089	0.000000	0.000000
1.5	0.042735	0.000000	0.000000	0.139403	0.000000	0.006515
2	1.063586	0.001112	0.000010	0.093248	0.005386	0.009919
3	1.760672	0.001545	0.000010	0.516484	0.006508	0.012619
5	1.137367	0.014271	0.000915	1.094354	0.042123	0.018234
7	0.348989	0.016242	0.001506	0.832258	0.053120	0.021025
9	0.138017	0.104702	0.018592	0.629842	0.143642	0.022375
12	0.217829	0.189254	0.093211	0.653713	0.249710	0.023877
16	0.033327	0.127152	0.12222	0.274295	0.160610	0.021628
19	0.048657	0.143248	0.187329	0.204741	0.042532	0.019327
23	0.012363	0.096233	0.20458	0.080921	0.013040	0.012434
28	0.008756	0.073178	0.119716	0.074721	0.011217	0.011683
35	0.004554	0.031832	0.048305	0.068281	0.019751	0.009484
42	0.002985	0.012701	0.009266	0.024434	0.015378	0.006098
56	0.003639	0.018273	0.006917	0.002018	0.015661	0.005004
61	0.002482	0.007171	0.003639	0.001545	0.011504	0.004534
75	0.002482	0.000205	0.002482	0.002753	0.007198	0.004061
89	0.001121	0.000186	0.001112	0.004857	0.001436	0.003486
107	0.000954	0.000637	0.000399	0.000677	0.004022	0.000352
129	0.000248	0.000176	0.000915	0.000479	0.000448	0.000310
163	0.000115	0.000281	0.000319	0.000319	0.000436	0.000283
183	0.000796	0.000253	0.000241	0.000283	0.000034	0.000199

Appendix B1

Box plots of concentration data for selected wells
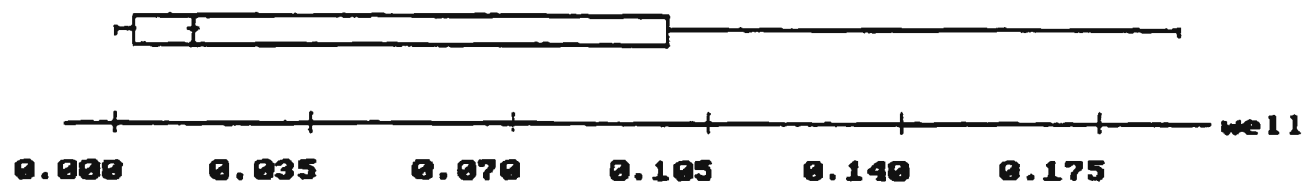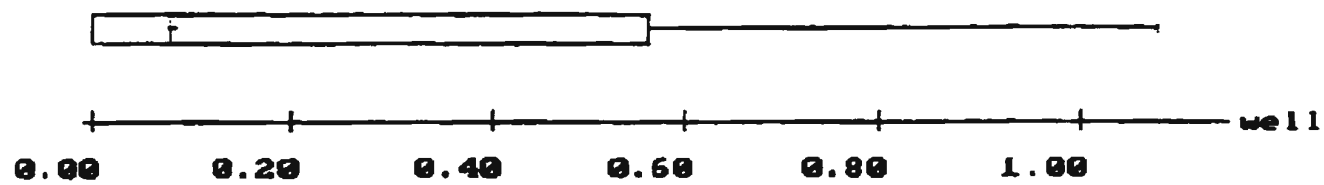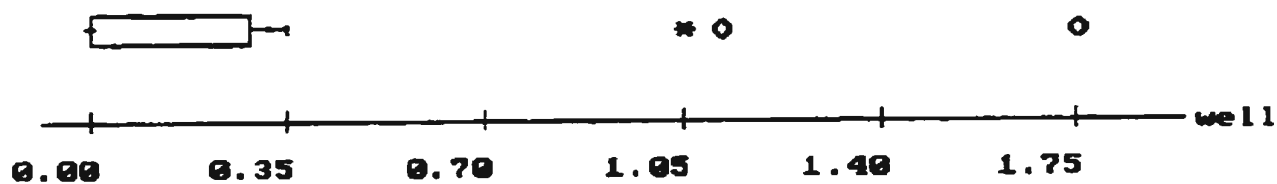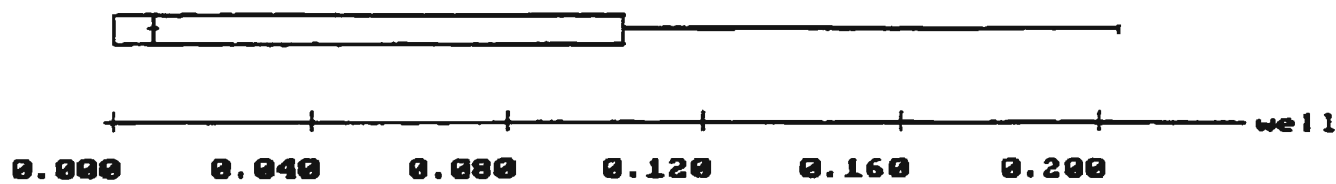
Appendix B2

Probability plot for concentration data for selected wells
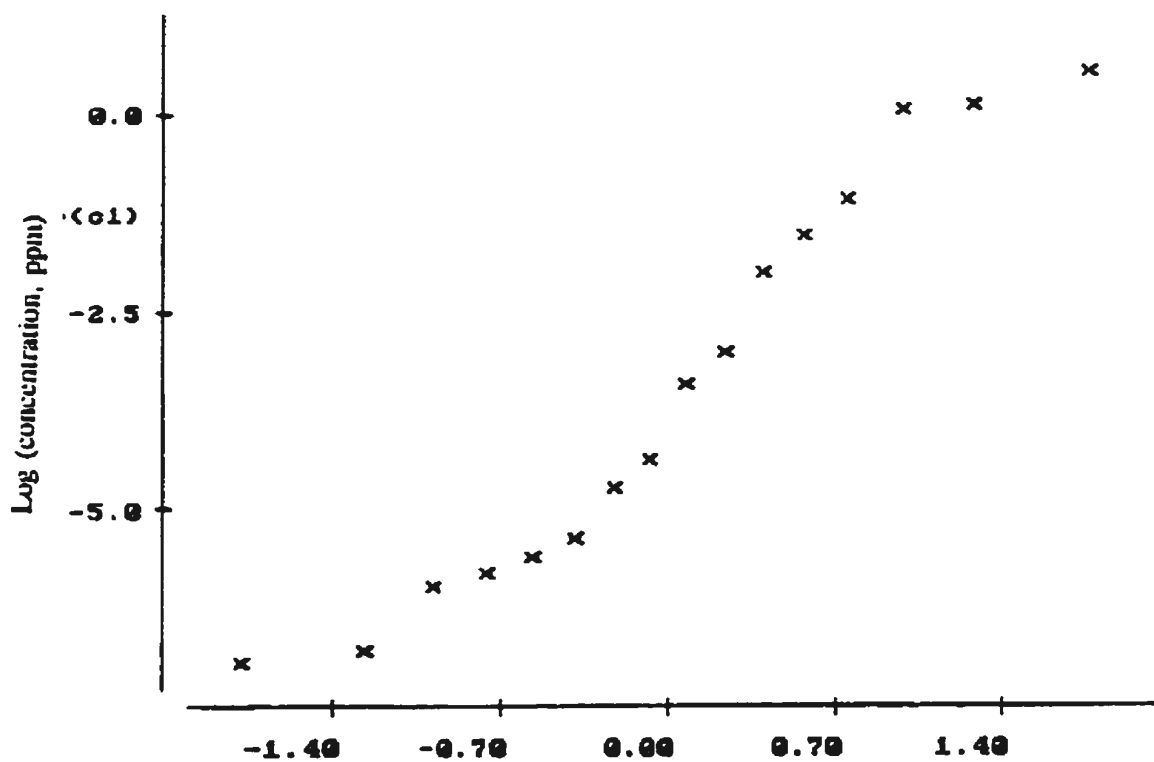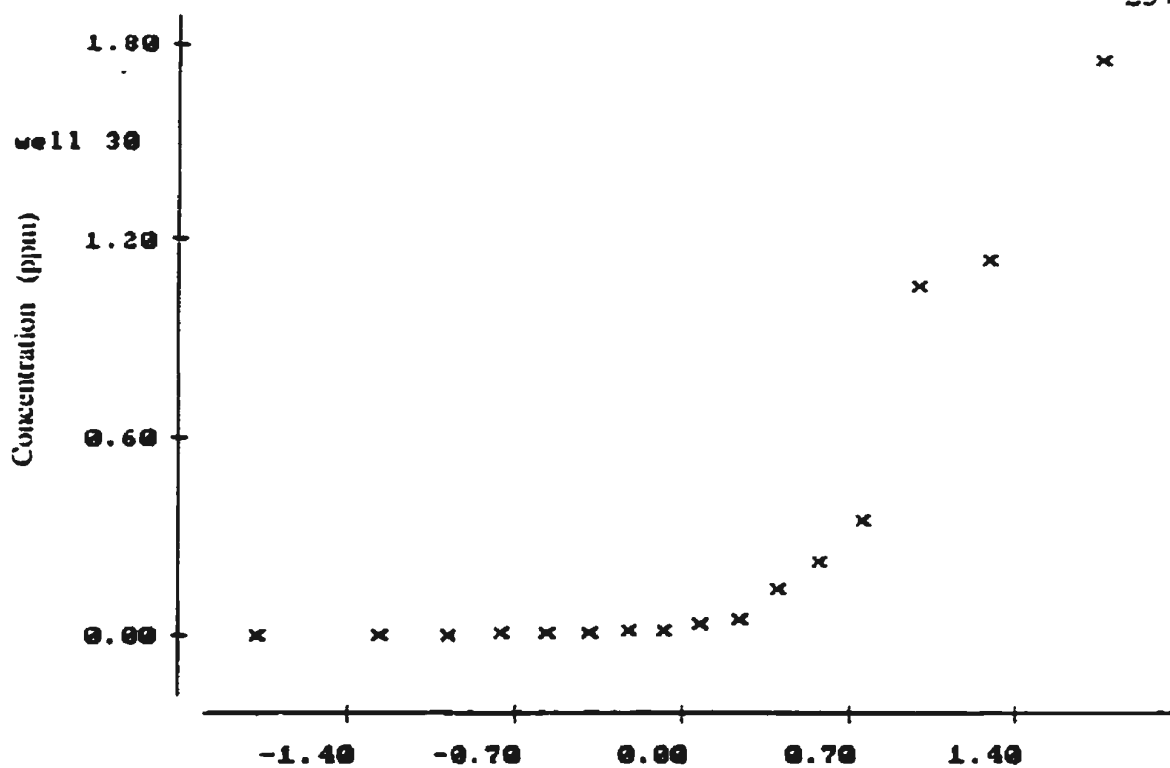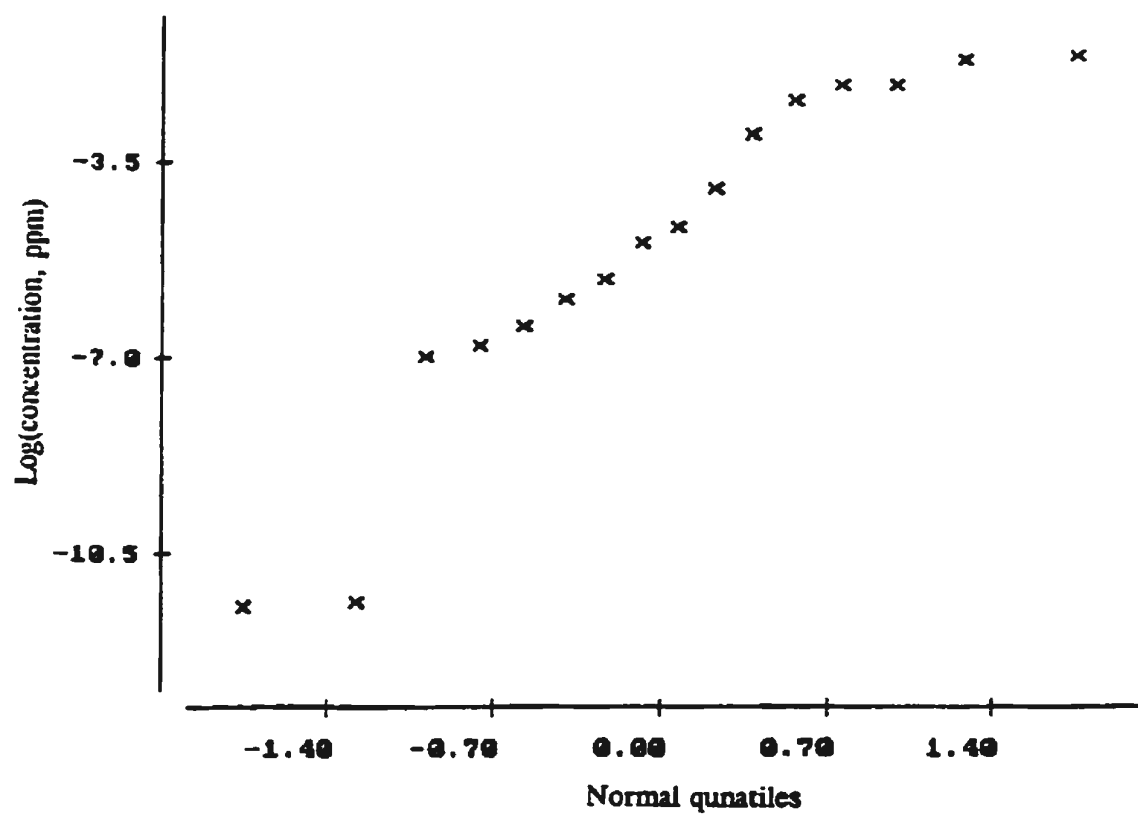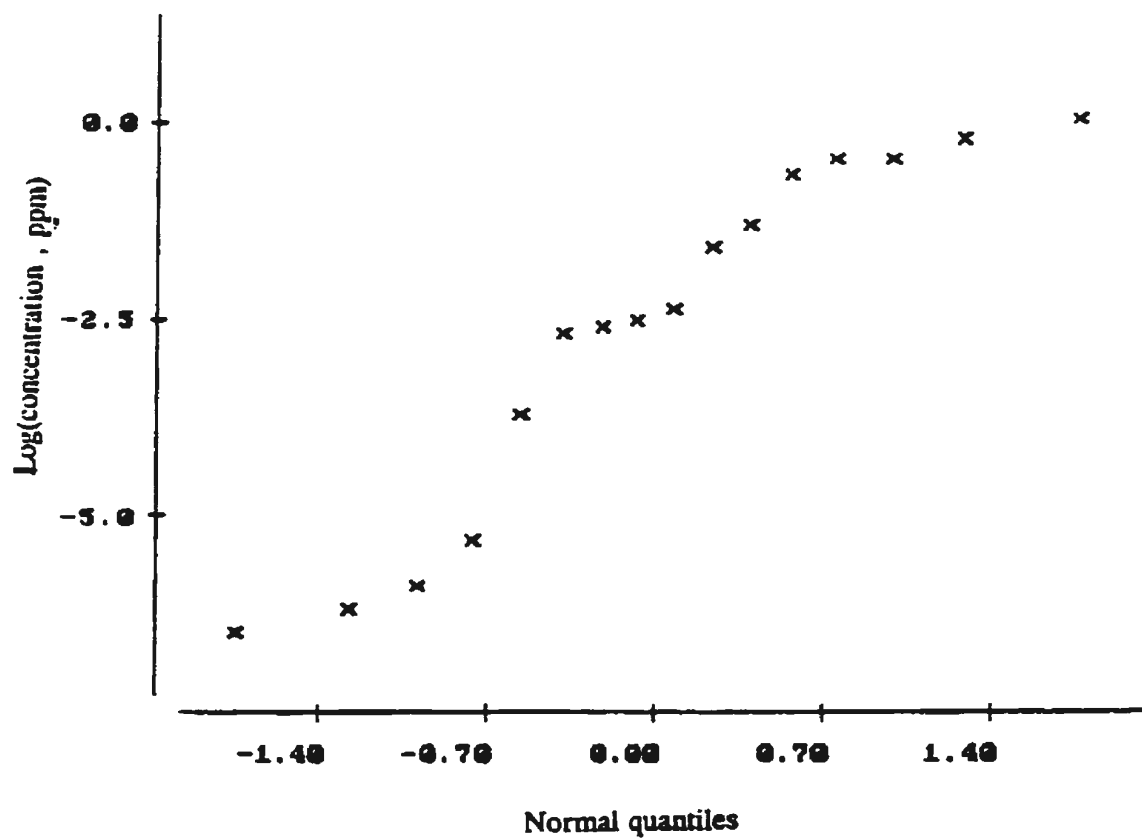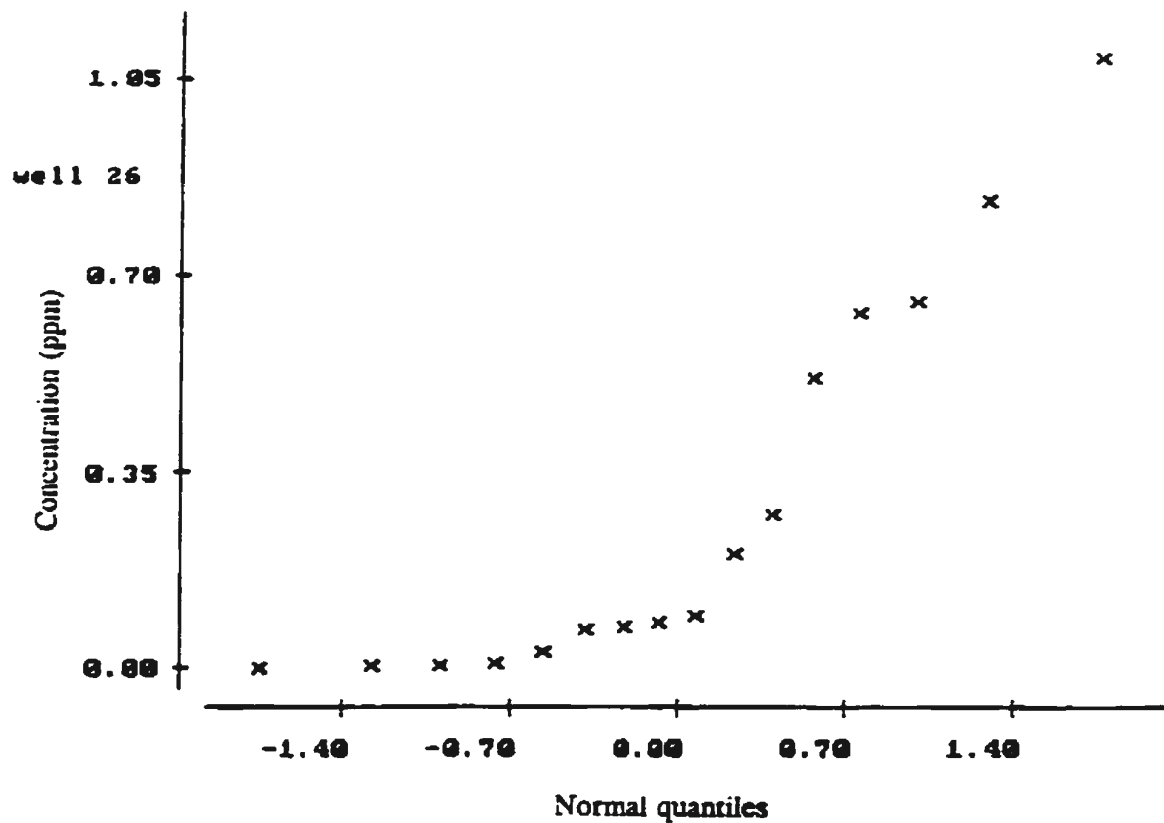
Appendix C

Results from numerical model verification and benchmarking

Table C1:   Results from verification Problem II: Contaminant migration from a patch source. Relative concentration (C/Co) distribution along plume center line (y=0) at different times after leakage has started (Comparison of Analytical and DRBEM results)

Distance from source (m)	100 days		1 year		5 years	
	DRBEM	Analytical	DRBEM	Analytical	DRBEM	Analytical
0	1	1	1	1	1	1
10	0.977832	0.96492	0.99356	0.98979	0.9941941	0.99563
20	0.96155	0.95919	0.98522	0.98868	0.98672	0.99014
40	0.87823	0.89598	0.96567	0.96514	0.96874	0.996864
60	0.81995	0.82312	0.94261	0.94152	0.94791	0.94778
80	0.72352	0.73861	0.91675	0.91402	0.92472	0.92394
100	0.60559	0.64642	0.88911	0.88388	0.90035	0.89844
120	0.55962	0.55094	0.86098	0.85192	0.87575	0.87227
140	0.46861	0.45662	0.81312	0.81874	0.85225	0.84616
160	0.37534	0.36753	0.80734	0.78476	0.83064	0.82064
180	0.31157	0.28694	0.75516	0.75021	0.81276	0.79705
200	0.22336	0.21706	0.72878	0.71522	0.78018	0.77258
220	0.16112	0.15895	0.68129	0.67987	0.75889	0.75034
240	0.11138	0.11257	0.64976	0.64417	0.73863	0.72934
260	0.08007	0.07705	0.60871	0.60815	0.71191	0.70957
280	0.05844	0.05094	0.58783	0.57188	0.70692	0.69097
300	0.029156	0.03251	0.53863	0.53542	0.66988	0.67349
320	0.021671	0.02001	0.52761	0.51989	0.64582	0.65705
350	0.011186	0.014052	0.50004	0.47903	0.62861	0.63022
400	0.001581	0.00659	0.42751	0.41514	0.57014	0.58793

Table C2: Results from verification Problem II (cont'd): Contaminant migration from a patch source (cont'd). Relative concentration (C/Co) distribution along (y=20 m) at different times after leakage has started (Comparison of Analytical and DRBEM results)

Distance from source (m)	100 days		1 year		5 years	
	DRBEM	Analytical	DRBEM	Analytical	DRBEM	Analytical
0	1	1	1	1	1	1
10	0.96739	0.97901	0.98998	0.99656	0.99683	0.99373
20	0.95919	0.94929	0.98868	0.97672	0.96864	0.97812
40	0.89598	0.87546	0.94514	0.93978	0.94778	0.94316
60	0.82312	0.79396	0.91152	0.90408	0.92394	0.91013
80	0.73862	0.70432	0.91402	0.86753	0.89844	0.87709
100	0.64642	0.61068	0.82388	0.83169	0.85227	0.84574
120	0.55094	0.51674	0.81192	0.79699	0.82616	0.81663
140	0.45662	0.42597	0.78187	0.76334	0.80064	0.78982
160	0.36753	0.34151	0.75021	0.73046	0.77605	0.76509
180	0.28694	0.26587	0.71522	0.69805	0.75058	0.74229
200	0.21706	0.2007	0.67987	0.66582	0.73034	0.72119
220	0.15895	0.14675	0.64417	0.63355	0.71934	0.70159
240	0.11257	0.10382	0.60815	0.60101	0.70957	0.68333
260	0.07705	0.07101	0.57188	0.56835	0.67097	0.66628
280	0.05094	0.04692	0.53542	0.53528	0.67349	0.65031
300	0.03251	0.02993	0.51268	0.50194	0.64003	0.63531
320	0.02296	0.01842	0.47816	0.47684	0.62981	0.62123
350	0.02017	0.01328	0.44856	0.43679	0.61584	0.61571
400	0.01107	0.009897	0.41806	0.40896	0.59093	0.59519

Table C3: Results from verification Problem III: Continuous migration of contaminant from a point source. Concentration distribution along plume center line (y=0 m) at different times after leakage has started (Comparison of Analytical and DRBEM results-concentrations in ppm)

Distance from source (m)	20 days		100 days		350 days	
	DRBEM	Analytical	DRBEM	Analytical	DRBEM	Analytical
10	53.7652	54.430	55.963	55.117	54.623	55.102
20	39.0376	40.613	40.022	42.162	41.037	42.165
30	29.7277	31.431	35.198	34.319	35.846	34.321
40	21.0244	24.451	28.995	27.718	29.856	29.720
50	17.9991	18.022	26.456	26.626	27.097	26.627
60	11.1928	12.124	24.091	24.310	25.171	24.311
70	7.2364	7.283	22.344	22.526	23.012	22.526
80	4.1534	3.821	20.938	21.007	21.988	21.009
90	2.0879	1.690	19.995	19.805	20.519	19.808
100	0.7018	0.638	19.086	18.841	19.093	18.845
110	0.2568	0.202	18.214	17.903	18.339	17.903
120	0.0592	0.053	17.523	17.210	17.423	17.212
130	0.0145	0.012	17.012	16.501	16.767	16.502
140	0.0019	0.002	16.415	15.911	15.825	15.910
150	0.00035	0.0003	16.041	15.312	15.134	15.402
160			15.184	14.814	14.745	14.903
180			14.068	13.901	13.712	14.026
200			13.746	13.202	12.964	13.307
220			12.196	12.001	12.438	12.754
240			11.851	10.865	12.285	12.407
260			10.604	9.925	11.963	12.109
300			8.429	8.32	11.625	11.069
350			5.424	7.013	8.683	9.539

Table C4: Results from verification Problem IV: Instantaneous release of contaminant from a point source. Concentration distribution along plume center line (y=0 m) at different times after leakage has started (Comparison of Analytical and DRBEM results-concentrations in ppm)

Distance form source (m)	5 days		10 days		15 days	
	DRBEM	Analytical	DRBEM	Analytical	DRBEM	Analytical
10	0.38332	0.34153	0.00162	0.00245	0.00110	0.00016
15	0.85987	0.81651	0.01083	0.00802	0.00994	0.00624
20	1.59136	1.52012	0.03246	0.02311	0.00150	0.00024
25	2.18408	2.21061	0.05193	0.05901	0.00291	0.00074
30	2.46189	2.51270	0.15041	0.13323	0.00904	0.00215
35	1.96019	2.21583	0.26626	0.26435	0.01967	0.00546
40	1.52618	1.52091	0.55199	0.46201	0.02134	0.01312
45	0.79644	0.81653	0.78158	0.715390	0.03319	0.02882
50	0.35596	0.34153	1.06665	0.97704	0.06702	0.05841
55	0.10928	0.11105	1.22881	1.18030	0.01313	0.10901
60	0.02511	0.02810	1.33906	1.25002	0.19013	0.18734
65	0.00452	0.00555	1.21389	1.1803	0.3088	0.29604
70	0.00072	0.00085	1.05568	0.97736	0.47823	0.43312
75			0.72394	0.71539	0.58023	0.57503
80			0.45634	0.46201	0.71801	0.70808
85			0.28503	0.26435	0.82390	0.80221
90			0.17995	0.13310	0.85387	0.83623
95			0.06009	0.05932	0.82128	0.80207
100			0.02892	0.02311	0.71856	0.70815
105			0.01083	0.00802	0.59037	0.57503
110			0.00279	0.00245	0.47372	0.43312
115			0.00002	0.00066	0.28612	0.29604
120			0.00011	0.00016	0.17285	0.18734

Table C5: Results from verification Problem IV: (cont'd): Instantaneous release of contaminant from a point source. Concentration distribution along (y =4.0 m) at different times after leakage has started (Comparison of Analytical and DRBEM results-concentrations in ppm)

Distance from source (m)	5 days		10 days		15 days	
	DRBEM	Analytical	DRBEM	Analytical	DRBEM	Analytical
5	0.11457	0.09091	0.00076	0.00059	0.00015	0.00047
10	0.36641	0.27903	0.00684	0.00222	0.00025	0.00018
15	0.62032	0.66921	0.06959	0.00726	0.00027	0.00067
20	1.50774	1.27334	0.08048	0.02104	0.00165	0.00022
25	1.85156	1.81103	0.07336	0.05342	0.00132	0.00069
30	1.98301	2.06421	0.15013	0.12304	.00318	0.00196
35	1.85153	1.81103	0.2317	0.23902	0.00823	0.00511
40	1.06622	1.25011	0.49106	0.41843	0.01748	0.01224
45	0.68754	0.66922	0.67965	0.64210	0.03908	0.02691
50	0.43215	0.27903	0.93354	0.88432	0.07348	0.05467
60	0.02430	0.02340	1.12975	1.07010	0.14862	0.10203
65	0.00839	0.00455	1.18593	1.14432	0.18026	0.17553
70	0.00253	0.00071	1.12143	1.07010	0.30729	0.27771
75	0.00196	0.00010	0.87531	0.88432	0.42429	0.40229
80			0.63154	0.71503	0.58005	0.53816
85			0.45119	0.46201	0.73159	0.66210
90			0.30751	0.26441	0.74312	0.75507
95			0.16831	0.13302	0.81946	0.78222
100			0.08743	0.05901	0.76807	0.75002
110			0.03867	0.02261	0.70890	0.66221
115			0.00957	0.00782	0.67231	0.63802
120			0.00611	0.00239	0.45676	0.40231

Table C6: Comparison of DRBEM results with those obtained by using FEM, MOC and Random walk (Beljin, 1988) for a **continuous point source** problem proposed by Huyakorn et., 1984. (**time=1000 days** after tracer injection, **concentrations in ppm**)

Distance from source (m)	DRBEM	Analytical	FEM	MOC	Random walk
60	69.5359	71.66	74.221	78.611	76.900
125	51.3866	53.89	53.440	55.420	52.900
180	42.7637	43.33	43.254	43.530	44.700
240	35.9186	36.17	36.222	35.390	24.900
300	30.6957	30.01	29.942	29.400	32.200
360	23.8106	23.91	23.583	23.470	27.500
420	17.3647	17.78	17.220	16.620	21.900
480	11.8287	12.03	11.451	11.970	14.600
540	7.5166	7.26	6.906	6.930	12.900
600	3.7494	3.85	3.792	3.520	8.590
660	2.0155	1.77	1.915	1.490	3.010
720	1.0891	0.70	0.901	0.550	1.720
780	0.2370	0.24	0.401	0.180	0.430
840	0.1319	0.07	0.169	0.050	0.000
900	0.0836	0.02	0.689	0.010	0.000

Table C7: Comparison of DRBEM results with those obtained by using FEM, MOC and Random walk (Beljin, 1988) for a **continuous point source** problem proposed by Huyakorn et., 1984. **(time=2000 days** after tracer injection, **concentrations in ppm)**

Distance from source (m)	DRBEM	Analytical	FEM	MOC	Random walk
60	69.455	71.660	74.260	73.780	63.600
125	51.402	54.300	53.650	54.830	47.300
180	43.268	44.330	43.980	45.630	39.600
240	37.754	38.390	38.160	38.630	33.100
300	35.086	34.310	34.170	34.250	40.400
360	31.967	31.280	31.190	31.050	31.800
420	29.976	28.860	28.820	28.250	28.400
480	27.714	26.790	26.810	26.000	34.400
540	25.756	24.900	24.940	24.020	32.700
600	24.242	23.000	23.050	22.020	24.900
660	22.137	20.970	20.990	19.970	19.800
720	18.608	18.710	18.670	17.710	16.800
780	16.077	16.190	16.070	15.790	17.200
840	13.085	13.480	13.280	13.070	10.300
900	9.765	10710	10.470	10.630	17.600
960	7.320	8.060	7.841	7.330	9.880
1020	4.708	5.710	5.557	5.210	7.300
1080	3.994	3.790	3.724	3.480	5.590
1140	2.372	2.350	2.361	2.120	1.720
1200	1.729	2.350	1.418	1.170	1.290
1260	0.827	0.720	0.808	0.590	2.150

Table C8: Comparison of DRBEM results with those obtained by using FEM, MOC and Random walk (Beljin, 1988) for a **continuous point source** problem proposed by Huyakorn et., 1984. (**time=2800 days** after tracer injection, **concentrations in ppm**)

Distance from source (m)	DRBEM	Analytical	FEM	MOC	Random walk
60	69.899	71.660	74.260	83.190	71.800
125	53.172	54.300	53.650	57.550	51.100
180	43.239	44.340	43.980	46.570	39.100
240	37.729	38.400	38.170	38.480	37.400
300	35.064	34.340	34.190	33.530	36.500
360	31.945	31.350	31.230	30.420	24.900
420	30.002	29.020	28.930	27.980	25.800
480	28.921	27.140	27.080	26.060	25.800
540	26.872	25.580	25.530	24.510	26.200
600	24.871	24.240	24.210	23.230	28.800
660	23.578	23.070	23.050	22.080	17.200
720	22.438	22.000	22.000	20.990	28.400
780	21.760	20.980	21.000	19.960	16.800
840	20.816	19.950	19.990	18.920	18.000
900	17.895	18.860	19.800	17.860	22.800
960	17.284	17.650	17.680	16.670	18.900
1020	15.812	16.270	16.280	15.320	15.900
1080	14.660	14.710	14.670	13.870	17.600
1140	12.311	12.970	12.880	12.240	13.800
1200	11.672	11.100	10.970	10.420	8.590
1260	10.001	9.180	9.021	8.600	10.700
1320	8.532	7.300	7.146	6.780	6.020
1380	5.444	5.560	5.440	5.120	7.300
1440	3.217	4.050	3.973	3.530	4.300

Table C9: Comparison of DRBEM results with those obtained by using FEM, MOC and Random walk (Beljin, 1988) for **instantaneous point source** problem proposed by Huyakorn et., 1984. (**time=10.5 days** after tracer injection, **concentrations in ppm**)

Distance from source (m)	DRBEM	Analytical	FEM	MOC	Random walk
5	0.1830	0.2726	0.230	0.140	0.170
10	0.3487	0.4714	0.400	0.280	0.510
15	0.7622	0.7740	0.570	0.420	0.680
20	1.3527	1.2069	1.090	0.900	0.580
25	1.8655	1.7872	1.650	1.440	1.360
30	2.1690	2.5133	2.370	2.150	2.040
35	3.2079	3.3567	3.230	2.960	3.400
40	4.3667	4.2573	4.180	3.960	3.570
45	5.3519	5.1279	5.110	4.810	4.760
50	5.6796	5.5865	5.910	5.630	5.610
55	6.5254	6.3718	6.450	6.230	5.270
60	6.7064	6.5733	6.650	6.520	5.950
65	6.2277	6.4399	6.460	6.460	5.460
70	5.9494	5.9916	5.930	6.090	7.650
75	5.3743	5.2940	5.130	5.390	5.610
80	4.5034	4.4421	4.210	4.520	5.100
85	4.0106	3.5398	3.280	3.610	4.420
90	2.6730	2.6788	2.440	2.710	3.060
100	1.4723	1.3139	1.170	1.330	1.360
110	0.8775	0.5242	0.500	0.520	0.680
120	0.1785	0.1701	0.190	0.180	0.170
130	0.0653	0.0449	0.070	0.050	0.000
140	0.0068	0.0096	0.020	0.010	0.000
160	0.0000	0.0002	0.000	0.000	0.000

Table C10: Comparison of DRBEM results with those obtained by using FEM, MOC and Random walk (Beljin, 1988) for **instantaneous point source** problem proposed by Huyakorn et., al. 1984. (**time=16.5 days** after tracer injection, **concentrations in ppm**))

Distance from source (m)	DRBEM	Analytical	FEM	MOC	Random walk
5	0.0089	0.0206	0.010	0.010	0.000
10	0.0454	0.0366	0.030	0.020	0.000
20	0.0509	0.0630	0.050	0.040	0.000
25	0.0983	0.1049	0.080	0.070	0.130
30	0.1166	0.1690	0.130	0.110	0.130
35	0.2318	0.2634	0.210	0.180	0.170
40	0.4006	0.3972	0.330	0.290	0.130
45	0.6455	0.5796	0.500	0.430	0.510
50	0.9779	0.8182	0.730	0.620	1.110
55	1.1276	1.1176	1.020	0.870	0.980
60	1.4004	1.4771	1.390	1.170	1.320
65	1.9093	1.8890	1.830	1.530	1.490
70	2.4870	2.3371	2.310	1.960	2.210
75	3.1069	2.7980	2.820	2.430	2.170
80	3.3286	3.2412	3.320	2.900	2.810
85	3.7332	3.6327	3.750	3.360	3.100
90	4.0375	3.9396	4.090	3.760	4.460
100	4.1533	4.1338	4.280	4.050	4.210
110	4.1353	4.1230	4.190	4.280	4.630
120	3.8403	3.6040	3.510	3.970	4.120
130	2.7947	2.7614	2.570	3.210	3.490
140	1.9153	1.8543	1.670	2.260	1.570
150	1.1038	1.0914	0.980	1.410	1.230
160	0.2588	0.2546	0.260	0.370	0.340

Appendix D

Results from Numerical Model Calibration

Table D1: Effects of change in longitudinal dispersivity (α_L) on BEM simulated results of temporal distribution of **concentration (ppm)** in **(Well # 30)**, porosity = 0.015, aquifer thickness = 5.0 m, α_T = 0.345, average velocity = 1.5 m/day

Time (days)	Experimental results	DRBEM (α_L=5.52 m^2/day)	DRBEM (α_L= 4.48 m^2/day)
2	1.063586	1.967084	1.933841
3	1.760672	1.610519	1.676652
5	1.137367	0.946108	1.044225
7	0.348989	0.562250	0.631758
9	0.138017	0.347058	0.389762
12	0.217829	0.179526	0.198209
16	0.033277	0.082711	0.087205
19	0.048657	0.048458	0.049495
23	0.012363	0.025410	0.02454
28	0.008756	0.012136	0.010835
35	0.004554	0.004797	0.003778
42	0.002985	0.020588	0.001439
56	0.003639	0.004285	0.000241
61	0.002482	0.000243	0.000183
75	0.001120	0.000110	5.61E-05
89	0.000954	0.000879	5.34E-06
RMSE		**0.263089**	**0.239775**

Table D2: Effects of change in average velocity on BEM simulated results of temporal distribution of **concentration (ppm)** in **(Well # 30)**, porosity = 0.015, α_L = 5.52 m²/day, α_T = 0.345 m²/day, aquifer thickness = 5.0 m

Time (days)	Experimental results	DRBEM (Velocity = 1.1 m/day	DRBEM (Velocity = 1.5 m/day)	DRBEM (Velocity = 1.75 m/day)
2	1.063586	1.971540	1.967084	1.833377
3	1.760672	1.832988	1.610519	1.370152
5	1.137367	1.273937	0.946108	0.721522
7	0.348989	0.851167	0.562256	0.396749
9	0.138017	0.575990	0.347058	0.229831
12	0.217829	0.333460	0.179526	0.109832
16	0.033277	0.172309	0.082711	0.045978
19	0.048657	0.109643	0.048458	0.025536
23	0.012363	0.062876	0.025412	0.012426
28	0.008756	0.033328	0.012136	0.005485
35	0.004554	0.014862	0.004797	0.001912
42	0.002985	0.007143	0.002058	0.007262
56	0.003639	0.001963	0.004285	0.000161
61	0.002482	0.012142	0.000243	0.000118
75	0.001120	0.000417	0.000156	5.72E-05
89	0.000954	0.000162	0.000147	3.01E-05
RMSE		**0.288536**	**0.246097**	**0.242529**

Table D3: Effects of change in aquifer thickness on BEM simulated results of temporal distribution of **concentration (ppm)** in **(Well #30)**, porosity = 0.105, $\alpha_L = 5.52$ m²/day, $\alpha_T = 0.345$ m²/day, average velocity = 1.5 m/day

Time (days)	Experimental results	DRBEM (Aquifer thickness = 5.0 m)	DRBEM (Aquifer thickness = 6.5 m)
2	1.063586	1.967084	1.511636
3	1.760672	1.610519	1.238546
5	1.137367	0.942108	0.727581
7	0.348989	0.562250	0.432118
9	0.138017	0.347058	0.266512
12	0.217829	0.179526	0.137868
16	0.033277	0.082711	0.063976
19	0.048657	0.048458	0.037197
23	0.012363	0.025411	0.019509
28	0.008756	0.012136	0.009352
35	0.004554	0.004797	0.003694
42	0.002985	0.020588	0.001552
56	0.003639	0.004285	0.000303
61	0.002482	0.000243	0.000177
75	0.001120	0.000186	7.72E-05
89	0.000954	0.000158	3.98E-05
RMSE		**0.246293**	**0.204977**

Table D4:   Effects of change in aquifer thickness on BEM simulated results of temporal distribution of **concentration (ppm)** in (**Well #27**), porosity = 0.105, α_L=5.52 m^2/day, α_T=0.345 m^2/day, average velocity=1.5 m/day

Time (days)	Experimental results	DRBEM (Aquifer thickness =5.0 m)	DRBEM (Aquifer thickness =6.5 m)
2	0.000115	0.045072	0.011118
3	0.001542	0.038592	0.012170
5	0.014277	0.109858	0.065371
7	0.016244	0.197145	0.105351
9	0.104702	0.23881	0.115473
12	0.189250	0.235153	0.101768
16	0.127151	0.183348	0.071712
19	0.143248	0.141639	0.052345
23	0.096231	0.096504	0.033551
28	0.073178	0.058066	0.018937
35	0.031832	0.028178	0.008508
42	0.012720	0.013717	0.003882
56	0.018272	0.001449	0.000858
61	0.007171	0.000897	0.000512
75	0.000201	0.000476	0.000119
89	0.000186	0.000121	3.02E-05
RMSE		**0.065662**	**0.048553**

Table D5: Effects of change in aquifer thickness on BEM simulated results of temporal distribution of **concentration (ppm)** in **(Well #27)**, porosity$=0.105$, $\alpha_L=5.52$ m^2/day, $\alpha_T=0.345$ m^2/day, average velocity$=1.5$ m/day

Time (days)	Experimental results	DRBEM (Aquifer thickness =5.0 m)	DRBEM (Aquifer thickness =6.5 m)
2	0.000115	0.045072	0.011118
3	0.001542	0.038592	0.012170
5	0.014277	0.109858	0.065371
7	0.016244	0.197145	0.105351
9	0.104702	0.23881	0.115473
12	0.189250	0.235153	0.101768
16	0.127151	0.183348	0.071712
19	0.143248	0.141639	0.052345
23	0.096231	0.096504	0.033551
28	0.073178	0.058066	0.018937
35	0.031832	0.028178	0.008508
42	0.012720	0.013717	0.003882
56	0.018272	0.001449	0.000858
61	0.007171	0.000897	0.000512
75	0.000201	0.000476	0.000119
89	0.000186	0.000121	3.02E-05
RMSE		**0.065662**	**0.048553**

Table D6: Effects of change in velocity on BEM simulated results of temporal distribution of concentration (ppm) in (Well #26), porosity= 0.015, α_L=5.52 m²/day, α_T=0.345 m²/day, aquifer thickness =5.0 m

Time (days)	Experimental results	DRBEM (Velocity = 1.1 m/day)	DRBEM (Velocity = 1.5 m/day)	BEM (Velocity = 1.75 m/day)
2	0.093248	0.631504	0.693861	0.799991
3	0.516484	0.818735	0.811759	0.799789
5	1.094354	0.788070	0.662421	0.555192
7	0.832258	0.628646	0.467278	0.354776
9	0.629841	0.478296	0.321623	0.226618
12	0.653711	0.311972	0.185296	0.119295
16	0.274295	0.178025	0.090311	0.054253
19	0.204741	0.120112	0.057439	0.031406
23	0.080901	0.072596	0.031488	0.015921
28	0.074721	0.040448	0.015690	0.007302
35	0.068281	0.018896	0.006411	0.002643
42	0.024431	0.009404	0.002732	0.000986
56	0.002018	0.002611	0.000618	0.000205
61	0.001545	0.001661	0.000356	0.0001486
75	0.002753	0.000519	0.000276	7.73E-05
89	0.004857	0.000165	0.000195	2.74E-05
RMSE		**0.26785**	**0.20562**	**0.32004**

Table D7: Effects of change in longitudinal dispersivity (α_L) on BEM simulated results of temporal distribution of **concentration (ppm)** in (**Well #26**), porosity = 0.015, average velocity = 1.5 m/day, α_T = 0.345 m^2/day, aquifer thickness = 5.0 m

Time (days)	Experimental results	DRBEM (α_L = 5.52 m^2/day)	DRBEM (α_L = 4.48 m^2/day)
2	0.093248	0.693861	0.613513
3	0.516484	0.811759	0.838421
5	1.094354	0.662421	0.733631
7	0.832258	0.467278	0.530951
9	0.629841	0.321632	0.368361
12	0.653711	0.185296	0.210818
16	0.274295	0.090312	0.102473
19	0.204741	0.057439	0.061167
23	0.080901	0.031488	0.031762
28	0.074721	0.015692	0.014872
35	0.068281	0.006411	0.005443
42	0.024431	0.002732	0.002146
56	0.002018	0.001618	0.000382
61	0.001545	0.000856	0.000195
75	0.002753	0.000301	5.88E-05
89	0.004857	0.000264	2.44E-05
RMSE		**0.286343**	**0.239842**

Table D8: Effects of change in longitudinal dispersivity (α_L) on BEM simulated results of temporal distribution of **concentration (ppm)** in (**Well # 13**), porosity = 0.015, average velocity = 1.5 m/day, α_T = 0.345 m²/day, aquifer thickness = 5.0 m

Time (days)	Experimental results	DRBEM (α_L = 5.52 m²/day)	DRBEM (α_L = 4.48 m²/day)
2	0.000001	0.000451	0.000371
3	0.000001	0.002407	0.002634
5	0.000915	0.030725	0.037915
7	0.001506	0.082206	0.071789
9	0.018590	0.147932	0.131632
12	0.093211	0.214130	0.212169
16	0.122231	0.228291	0.249617
19	0.018732	0.206719	0.235720
23	0.204580	0.016448	0.192809
28	0.119716	0.113983	0.134091
35	0.048305	0.063604	0.072458
42	0.009266	0.034213	0.036735
56	0.006917	0.009635	0.008874
61	0.003639	0.006078	0.005172
75	0.002482	0.002045	0.001181
89	0.001112	0.000671	0.000314
RMSE		**0.061822**	**0.058209**

Table D9: Effects of change in velocity on BEM simulated results of temporal distribution of **concentration (ppm)** in (**Well #13**), porosity = 0.015, velocity = 1.5 m/day, α_L = 5.52 m^2/day, α_T = 0.345 m^2/day, aquifer thickness = 5.0 m

Time (days)	Experimental results	DRBEM (velocity = 1.1 m/day)	DRBEM (velocity = 1.5 m/day)	DRBEM (velocity = 1.75 m/day)
2	0.000001	0.002091	0.002508	0.003343
3	0.000001	0.002734	0.002407	0.003350
5	0.000915	0.026023	0.030725	0.053667
7	0.001506	0.041156	0.082206	0.125192
9	0.018590	0.081768	0.147931	0.188012
12	0.093211	0.154708	0.214180	0.223841
16	0.122231	0.217428	0.228291	0.198643
19	0.018732	0.231116	0.206672	0.161483
23	0.204580	0.219558	0.164482	0.113832
28	0.119716	0.183077	0.113983	0.069179
35	0.048305	0.127084	0.063604	0.032832
42	0.009266	0.082877	0.034213	0.015247
56	0.006917	0.032622	0.009635	0.003281
61	0.003639	0.023142	0.006078	0.001929
75	0.002482	0.008805	0.002415	0.000465
89	0.001112	0.003355	0.001161	0.000134
RMSE		**0.049157**	**0.057828**	**0.071844**

Table D10: Effects of change in longitudinal dispersivity (α_L) on DRBEM simulation results of spatial distribution of **concentration (ppm)**, average velocity=1.5 m/day, aquifer thickness=5.0 m, porosity=0.015, α_T=0.345 m²/day, **time=7 days** after tracer injection

Well #	Experimental results	α_L=5.52 m²/day	α_L=4.48 m²/day
30	0.34899	0.562250	0.631764
14	0.45312	0.573672	0.618487
27	0.02624	0.197146	0.202634
28	0.10562	0.298335	0.271191
13	0.00151	0.082206	0.071789
26	0.30914	0.467278	0.530951
RMSE		**0.062232**	**0.078171**

Table D11: Effects of change in longitudinal dispersivity (α_L) on DRBEM simulation results of spatial distribution of concentration (ppm), average velocity=1.5 m/day, aquifer thickness=6.5 m, effective porosity=0.015, α_T=0.345 m²/day, **time=7 days** after tracer injection

Well #	Experimental results	α_L=5.52 m²/day	α_L=4.48 m²/day
30	0.34899	0.432118	0.170292
14	0.45312	0.441068	0.222511
27	0.02624	0.151648	0.105351
28	0.10562	0.220929	0.124937
13	0.00151	0.062917	0.368174
26	0.30914	0.359403	0.178316
RMSE		**0.035083**	**0.082208**

Table D12: Effects of change in velocity on DRBEM simulation results of spatial distribution of **concentration (ppm)**, $\alpha_L = 5.52$ m^2/day, aquifer thickness$=5.0$ m, porosity$=0.015$, $\alpha_T = 0.345$ m^2/day, **time$=7$ days** after tracer injection

Well #	Experimental results	Velocity$=1.5$ m/day	Velocity$=1.75$ m/day
30	0.34899	0.562250	0.396749
14	0.45312	0.573672	0.831472
27	0.02624	0.197146	0.222358
28	0.10562	0.298335	0.322314
13	0.00151	0.082206	0.125191
26	0.30914	0.467278	0.354776
RMSE		**0.066224**	**0.083042**

Table D13: Effects of change in aquifer thickness on DRBEM simulation results of spatial distribution of **concentration (ppm)**, average velocity$=1.5$ m/day, $\alpha_L = 5.52$ m^2/day, porosity$=0.015$, $\alpha_T = 0.345$ m^2/day, **time$=7$ days** after tracer injection

Well #	Experimental results	Aquifer thickness $=5.0$ m	Aquifer thickness $=6.5$ m
30	0.34899	0.562251	0.432118
14	0.45312	0.577367	0.441068
27	0.02624	0.197142	0.151648
28	0.10562	0.298335	0.222903
13	0.00151	0.082206	0.062917
26	0.30914	0.467228	0.359403
RMSE		**0.066411**	**0.034495**

Table 14: Effects of change in longitudinal dispersivity (α_L) on DRBEM simulation results of spatial distribution of **concentration (ppm)**, average velocity=1.5 m/day, aquifer thickness=5.0 m, effective porosity=0.015, α_T=0.345 m^2/day, **time=23 days** after tracer injection

Well #	Experimental results	α_L=4.48 m^2/day	α_L=5.52 m^2/day
30	0.0123606	0.024541	0.025410
14	0.021326	0.070618	0.064852
27	0.043061	0.112824	0.096504
28	0.105624	0.141870	0.122057
13	0.204586	0.192809	0.164482
26	0.008145	0.031762	0.031488
RMSE		**0.016206**	**0.014287**

Table D15: Effects of change in transverse dispersivity (α_T) on DRBEM simulation results of spatial distribution of **concentration (ppm)**, average velocity=1.5 m/day, aquifer thickness=5.0 m, effective porosity=0.015, α_L=5.52 m^2/day, **time=23 days** after tracer injection

Well #	Experimental results	α_T=0.345 m^2/day	α_T=0.69 m^2/day
30	0.0123606	0.019509	0.006686
14	0.021326	0.049808	0.019588
27	0.043061	0.014197	0.033521
28	0.105624	0.093810	0.039765
13	0.204586	0.126386	0.056483
26	0.008145	0.024180	0.009221
RMSE		**0.015101**	**0.027079**

Table D16: Effects of change in average velocity on DRBEM simulation results of spatial distribution of **concentration** **(ppm)** α_T=0.345 m^2/day, aquifer thickness=6.5 m, porosity=0.015, α_L= 5.52 m^2/day, **time=23 days** after tracer injection

Well #	Experimental results	Velocity = 1.5 m/day	Velocity = 1.75 m/day
30	0.0123606	0.025412	0.012426
14	0.021326	0.064852	0.034572
27	0.043061	0.096504	0.058313
28	0.105624	0.122057	0.731831
13	0.204586	0.164481	0.113802
26	0.008145	0.031488	0.015923
	RMSE	**0.014287**	**0.105521**

Table D17: Effects of change in aquifer thickness on DRBEM simulation results of spatial distribution of **concentration** **(ppm)**, average velocity=1.5 m/day, α_L=5.52 m^2/day, porosity=0.015, α_T= 0.345 m^2/day, **time=23 days** after tracer injection

Well #	Experimental results	aquifer thickness =5.0 m	aquifer thickness =6.5 m
30	0.0123606	0.025411	0.019509
14	0.021326	0.064852	0.049808
27	0.043061	0.096504	0.074197
28	0.105624	0.122057	0.009385
13	0.204586	0.164482	0.126386
26	0.008145	0.031488	0.024182
	RMSE	**0.014286**	**0.015226**